

NASA SP-7037 (317)

May 1995

p 89

AERONAUTICAL ENGINEERING

(NASA-SP-7037(317)) AERONAUTICAL
ENGINEERING: A CONTINUING
BIBLIOGRAPHY WITH INDEXES
(SUPPLEMENT 317) (NASA) 89 p

N95-25798

Unclass

00/01 0048298

A CONTINUING BIBLIOGRAPHY WITH INDEXES



National Aeronautics and
Space Administration

Scientific and Technical
Information Office

The NASA STI Office ... in Profile

Since its founding, NASA has been dedicated to the advancement of aeronautics and space science. The NASA Scientific and Technical Information (STI) Office plays a key part in helping NASA maintain this important role.

The NASA STI Office provides access to the NASA STI Database, the largest collection of aeronautical and space science STI in the world. The Office is also NASA's institutional mechanism for disseminating the results of its research and development activities.

Specialized services that help round out the Office's diverse offerings include creating custom thesauri, translating material to or from 34 foreign languages, building customized databases, organizing and publishing research results ... even providing videos.

For more information about the NASA STI Office, you can:

- **Phone** the NASA Access Help Desk at (301) 621-0390
- **Fax** your question to the NASA Access Help Desk at (301) 621-0134
- **E-mail** your question via the **Internet** to help@sti.nasa.gov
- **Write** to:

NASA Access Help Desk
NASA Center for AeroSpace Information
800 Elkridge Landing Road
Linthicum Heights, MD 21090-2934

NASA SP-7037 (317)

May 1995

AERONAUTICAL ENGINEERING

A CONTINUING BIBLIOGRAPHY WITH INDEXES



National Aeronautics and Space Administration
Scientific and Technical Information Office
Washington, DC

1995

This publication was prepared by the NASA Center for AeroSpace Information,
800 Elkridge Landing Road, Linthicum Heights, MD 21090-2934, (301) 621-0390.

INTRODUCTION

This issue of *Aeronautical Engineering — A Continuing Bibliography with Indexes* (NASA SP-7037) lists 224 reports, journal articles, and other documents recently announced in the NASA STI Database.

Accession numbers cited in this issue include:

<i>Scientific and Technical Aerospace Reports (STAR)</i> (N-10000 Series)	N95-19506 — N95-19882
Open Literature (A-60000 Series)	A95-65816 — A95-69893

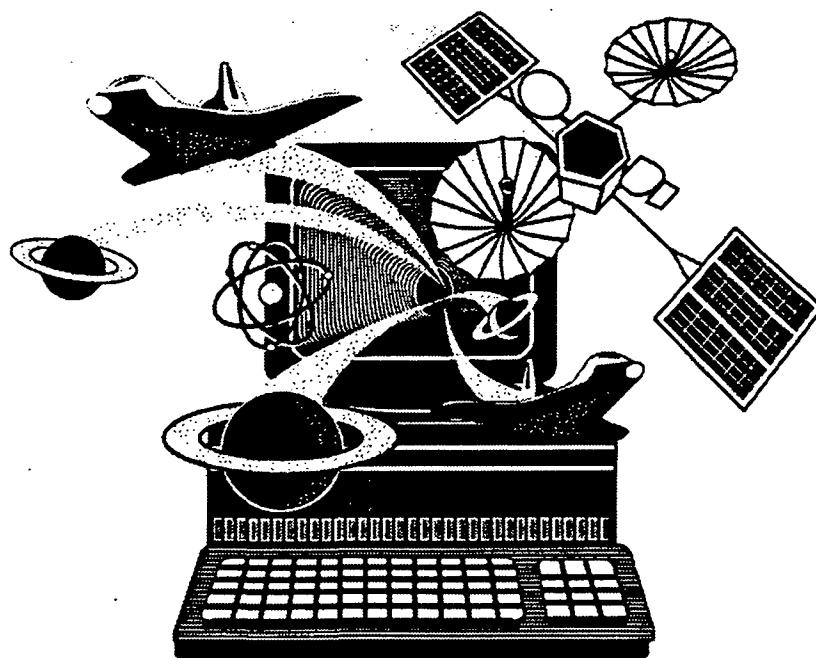
The coverage includes documents on the engineering and theoretical aspects of design, construction, evaluation, testing, operation, and performance of aircraft (including aircraft engines) and associated components, equipment, and systems. It also includes research and development in aerodynamics, aeronautics, and ground support equipment for aeronautical vehicles.

Each entry in the publication consists of a standard bibliographic citation accompanied, in most cases, by an abstract. The listing of the entries is arranged by the first nine *STAR* specific categories and the remaining *STAR* major categories. This arrangement offers the user the most advantageous breakdown for individual objectives. The citations include the original accession numbers from the respective announcement journals.

Seven indexes—subject, personal author, corporate source, foreign technology, contract number, report number, and accession number—are included.

A cumulative index for 1995 will be published in early 1996.

The NASA CASI price code table, addresses of organizations, and document availability information are located at the back of this issue.



SCAN Goes Electronic!

If you have NASA Mail or if you can access the Internet, you can get biweekly issues of *SCAN* delivered to your desk—top absolutely free!

Electronic SCAN takes advantage of computer technology to alert you to the latest aerospace-related, worldwide scientific and technical information that has been published.

No more waiting while the paper copy is printed and mailed to you. You can review *Electronic SCAN* the same day it is released! And you get all 191—or any combination of—subject areas of announcements with abstracts to browse at your leisure. When you locate a publication of interest, you can print the announcement or electronically add it to your publication order list.

Electronic SCAN

Timely
Flexible
Complete
Free!

For instant access via Internet:

<ftp.sti.nasa.gov>
<gopher.sti.nasa.gov>
listserv@sti.nasa.gov

For additional information:

e-mail: help@sti.nasa.gov
scan@sti.nasa.gov

(Enter this address on the "To" line. Leave the subject line blank and send. You will receive an automatic reply with instructions in minutes.)

Phone: (301) 621-0390 Fax: (301) 621-0134

Write: NASA Access Help Desk
NASA STI Office
NASA Center for AeroSpace Information
800 Elkridge Landing Road
Linthicum Heights, MD 21090-2934



National Aeronautics and
Space Administration
Scientific and Technical
Information Office

TABLE OF CONTENTS

Category 01	Aeronautics	179
Category 02	Aerodynamics Includes aerodynamics of bodies, combinations, wings, rotors, and control surfaces; and internal flow in ducts and turbomachinery.	181
Category 03	Air Transportation and Safety Includes passenger and cargo air transport operations; and aircraft accidents.	188
Category 04	Aircraft Communications and Navigation Includes digital and voice communication with aircraft; air navigation systems (satellite and ground based); and air traffic control.	189
Category 05	Aircraft Design, Testing and Performance Includes aircraft simulation technology.	191
Category 06	Aircraft Instrumentation Includes cockpit and cabin display devices; and flight instruments.	194
Category 07	Aircraft Propulsion and Power Includes prime propulsion systems and systems components, e.g., gas turbine engines and compressors; and onboard auxiliary power plants for aircraft.	195
Category 08	Aircraft Stability and Control Includes aircraft handling qualities; piloting; flight controls; and autopilots.	203
Category 09	Research and Support Facilities (Air) Includes airports, hangars and runways; aircraft repair and overhaul facilities; wind tunnels; shock tubes; and aircraft engine test stands.	204
Category 10	Astronautics Includes astronautics (general); astrodynamics; ground support systems and facilities (space); launch vehicles and space vehicles; space transportation; space communications, spacecraft communications, command and tracking; spacecraft design, testing and performance; spacecraft instrumentation; and spacecraft propulsion and power.	204
Category 11	Chemistry and Materials Includes chemistry and materials (general); composite materials; inorganic and physical chemistry; metallic materials; nonmetallic materials; propellants and fuels; and materials processing.	205
Category 12	Engineering Includes engineering (general); communications and radar; electronics and electri- cal engineering; fluid mechanics and heat transfer; instrumentation and photogra- phy; lasers and masers; mechanical engineering; quality assurance and reliability; and structural mechanics.	207

Category 13 Geosciences	212
Includes geosciences (general); earth resources and remote sensing; energy production and conversion; environment pollution; geophysics; meteorology and climatology; and oceanography.	
Category 14 Life Sciences	N.A.
Includes life sciences (general); aerospace medicine; behavioral sciences; man/system technology and life support; and space biology.	
Category 15 Mathematical and Computer Sciences	217
Includes mathematical and computer sciences (general); computer operations and hardware; computer programming and software; computer systems; cybernetics; numerical analysis; statistics and probability; systems analysis; and theoretical mathematics.	
Category 16 Physics	218
Includes physics (general); acoustics; atomic and molecular physics; nuclear and high-energy; optics; plasma physics; solid-state physics; and thermodynamics and statistical physics.	
Category 17 Social Sciences	N.A.
Includes social sciences (general); administration and management; documentation and information science; economics and cost analysis; law, political science, and space policy; and urban technology and transportation.	
Category 18 Space Sciences	218
Includes space sciences (general); astronomy; astrophysics; lunar and planetary exploration; solar physics; and space radiation.	
Category 19 General	N.A.

Subject Index	A-1
Personal Author Index	B-1
Corporate Source Index	C-1
Foreign Technology Index	D-1
Contract Number Index	E-1
Report Number Index	F-1
Accession Number Index	G-1
Appendix	APP-1

TYPICAL REPORT CITATION AND ABSTRACT

NASA SPONSORED

↓
ON MICROFICHE

ACCESSION NUMBER → N95-10318*# Dow Chemical Co., Midland, MI. ← CORPORATE SOURCE
 TITLE → NOVEL MATRIX RESINS FOR COMPOSITES FOR AIRCRAFT
 PRIMARY STRUCTURES, PHASE 1 Final Report, Apr. 1989 -
 Mar. 1992
 AUTHORS → EDMUND P. WOO, P. M. PUCKETT, S. MAYNARD, M. T. BISHOP,
 K. J. BRUZA, J. P. GODSCHALX, AND M. J. MULLINS Aug. 1992 ← PUBLICATION DATE
 164 p
 CONTRACT NUMBERS → (Contracts NAS1-18841; RTOP 510-02-11-02)
 REPORT NUMBERS → (NASA-CR-189657; NAS 1.26:189657) Avail: CASI HCA08/MFA02 ← AVAILABILITY AND
 PRICE CODE

The objective of the contract is the development of matrix resins with improved processability and properties for composites for primarily aircraft structures. To this end, several resins/systems were identified for subsonic and supersonic applications. For subsonic aircraft, a series of epoxy resins suitable for RTM and powder prepreg was shown to give composites with about 40 ksi compressive strength after impact (CAI) and 200 F/wet mechanical performance. For supersonic applications, a thermoplastic toughened cyanate prepreg system has demonstrated excellent resistance to heat aging at 360 F for 4000 hours, 40 ksi CAI and useful mechanical properties at greater than or equal to 310 F. An AB-BCB-maleimide resin was identified as a leading candidate for the HSCT. Composite panels fabricated by RTM show CAI of approximately 50 ksi, 350 F/wet performance and excellent retention of mechanical properties after aging at 400 F for 4000 hours. Author

TYPICAL JOURNAL ARTICLE CITATION AND ABSTRACT

NASA SPONSORED

↓

ACCESSION NUMBER → A95-60192* National Aeronautics and Space Administration. Ames. ← CORPORATE SOURCE
 Research Center, Moffett Field, CA.
 TITLE → AERODYNAMIC INTERACTIONS BETWEEN A ROTOR AND
 WING IN HOVER
 AUTHORS → FORT F. FELKER NASA. Ames Research Center, Moffett Field, ← AUTHOR'S AFFILIATION
 CA, US and JEFFREY S. LIGHT NASA. Ames Research Center,
 Moffett Field, CA, US Journal of the American Helicopter Society ← JOURNAL TITLE
 PUBLICATION DATE → 2 Jun. 1986 p. 53-61
 REPORT NUMBER → (HTN-94-00714) Copyright

An experimental investigation of rotor/wing aerodynamic interactions in hover is described. The investigation consisted of both a large-scale and a small-scale test. A 0.658-scale V-22 rotor and wing was used in the large-scale test. Wing download, wing surface pressure, rotor performance, and rotor downwash data from the large-scale test are presented. A small-scale experiment was conducted to determine how changes in the rotor/wing geometry affected the aerodynamic interactions. These geometry variations included the distance between the rotor and wing, wing incidence angle, wing flap angle, rotor rotation direction, and configurations both with the rotor axis at the tip of the wing (tilt rotor configuration) and with the rotor axis at the center of the wing (compound helicopter configuration). Author (Herner)

AERONAUTICAL ENGINEERING

A Continuing Bibliography (Suppl. 317)

May 1995

01

AERONAUTICS (GENERAL)

A95-68172

LIFT ANALYSIS OF A VARIABLE CAMBER FOIL USING THE DISCRETE VORTEX-BLOB METHOD

B. J. MACLEAN Univ. of Utah, Salt Lake City, UT and R. A. DECKER
AIAA Journal (ISSN 0001-1452) vol. 32, no. 7 July 1994 p. 1525-1527 refs

(BTN-94-EIX94441386623) Copyright

The paper presents the use of a discrete vortex-blob method to compare lift performance between fixed and variable camber NACA 0012 foils at a Reynolds number of 1×10^6 for incompressible flow in two dimensions. The vortex method provides a natural and numerically efficient description of eddies and the vorticity they carry. Since a large number of discrete vortex blobs are used to produce a vorticity field in a Lagrangian reference frame, the method becomes grid free and allows modeling of unsteady flows even around multielement bodies of arbitrary shape in nonuniform motion or rotation. EI

A95-68181

NUMERICAL COMPUTATIONS OF SUPERSONIC BASE FLOW WITH SPECIAL EMPHASIS ON TURBULENCE MODELING

JUBARAJ SAHU US Army Research Lab., Aberdeen Proving Ground, MD AIAA Journal (ISSN 0001-1452) vol. 32, no. 7 July 1994 p. 1547-1549 refs

(BTN-94-EIX94441386632) Copyright

A zonal, implicit, time-marching Navier-Stokes computational technique has been used to compute the turbulent supersonic base flow over a cylindrical afterbody. Flowfield computations have been performed using two algebraic models and a turbulence model. Comparison of both the mean and turbulence quantities have been made with the available experimental data. Computed base pressure distributions have been compared with the measured base pressures. EI

A95-68216

EXPERIMENTAL STUDY OF THREE-DIMENSIONAL SEPARATION [ETUDE EXPERIMENTALE DU DECOLLEMENT TRIDIMENSIONNEL]

D. BARBERIS ONERA, Chatillon (France) Recherche Aerospatiale (ISSN 0034-1223) no. 2 1994 p. 85-102 In FRENCH
(BTN-94-EIX94441385752) Copyright

Three-dimensional separation is studied by considering the flow past a large scale model consisting of a half prolate ellipsoid extended by a circular cylinder ending in a flat base at 45 deg with respect to the cylinder axis. The flow past the model, including boundary-layer and vortical structures, is investigated in great detail by using a three-component LDV system and three-hole pressure probes actuated by a displacement system installed inside the model. This last device allows probing the separating 3-D boundary layer very close to the surface. We observed how a boundary layer evolves as it gradually shears into a vortex rollup and then into an organized vortex. When skewing of the boundary layer grows, the difference of direction between velocity

gradient vector and shear stress vector increases. For this type of flow, turbulence models based on the assumption of isotropic turbulent viscosity are inadequate for numerical modelization. Author (EI)

A95-68258

MAINTENANCE REQUIREMENTS FOR A SUPERSONIC TRANSPORT

STUART BIRCH Aerospace Engineering (Warrendale, Pennsylvania) (ISSN 0736-2536) vol. 14, no. 1 January-February 1994 p. 39-42

(BTN-95-EIX95031502751) Copyright

The paper discusses maintenance requirements for a supersonic transport. Maintenance demands of these transports vary widely and recently, there has been an increasing focus on the need for improved maintainability. The Concorde has become the world's only regularly scheduled passenger services and has been dedicated a maintenance support unit where all major maintenance is carried out. With such a complex airplane, maintenance hours for the Concorde is considerably longer than those for a Boeing 747. Maintainability levels must be kept level to those of a subsonic aircraft and components must be more accessible. EI

A95-68350

RELIABILITY AND MAINTAINABILITY

THOMAS J. HOWARD Wright Lab. and JOHN P. LAVERDURE Aerospace Engineering (Warrendale, Pennsylvania) (ISSN 0736-2536) vol. 14, no. 9 September 1994 p. 13-15

(BTN-95-EIX95042477109) Copyright

The US Department of Defense (DOD) and the airline industry have collaborated to address the issues of common or dual-use technologies, reliability improvements, and reductions in maintainability requirements, with the ultimate aim of reducing costs and improving operations. Dual-use systems are those which have both military and commercial applications such as the GPS. This collaborative effort examines the concerns identified by the airlines and determines if the DOD has developed, or could develop, a technology to solve these problems. Because the airlines and DOD both try to reduce support costs, many reliability and maintainability issues can be addressed under dual use. The specific issues are presented. EI

A95-68351

NOISE AND VIBRATION CONTROL

LINDA F. TREGO Aerospace Engineering (Warrendale, Pennsylvania) (ISSN 0736-2536) vol. 14, no. 9 September 1994 p. 10-12
(BTN-95-EIX95042477108) Copyright

Lord Corp has developed a combination of three technologies to help solve problems of aircraft cabin noise and vibration. Lord's NVX systems combine active and passive noise and vibration control techniques to increase cabin comfort to levels previously unattainable. The technologies are distinguished by the actuators and sensors used for control. Active noise control uses microphones to detect cabin sound, and speakers to eliminate it. Active structural control uses inertial actuators which monitor and control the vibration of the fuselage which, in turn, reduces noise. Active isolation control includes active mounts which control noise and vibration at

ABSTRACTS

01 AERONAUTICS (GENERAL)

the interface between disturbance sources and the fuselage. Microphones and accelerometers are used to monitor noise and vibration in both active isolation control and active structural control. EI

A95-68394

USAF AGING AIRCRAFT PROGRAM

JOHN W. LINCOLN and WILLIAM R. ELLIOTT Aerospace Engineering (Warrendale, Pennsylvania) (ISSN 0736-2536) vol. 14, no. 10 October 1994 p. 11-13
(BTN-95-EIX95072498878) Copyright

The US Air Force has used its Aircraft Structural Integrity Program (ASIP) for the past 35 yrs to maintain safe and economical operation of aging aircraft but the program has undergone modifications to meet more demanding standards. Originally using a reliability-based or 'safe-life' approach to establish the operational life of an aircraft, ASIP saw its shortcomings when several incidents of service breakdown occurred. To address the shortcomings of the safe-life approach, a fundamental change was made in terms of design, qualification, and inspection of aircraft. Improved reliability and damage-tolerance approaches emerged as main considerations. EI

A95-68395

NATIONAL AEROSPACE PLANE: TECHNOLOGY TRANSFER

ANON Aerospace Engineering (Warrendale, Pennsylvania) (ISSN 0736-2536) vol. 14, no. 10 October 1994 p. 15-19
(BTN-95-EIX95072498879) Copyright

The development of advanced, high-strength materials from the concluded National AeroSpace Plane program has been applied to other projects, including the Tomahawk missile launcher and the Boeing 777. The titanium-based-alloy materials feature reduced weight, while exhibiting such characteristics as the ability to maintain strength and toughness at high temperatures, significant resistance to corrosion in salt-water environments, and excellent ability to be cold-formed and rolled into thin sheets. EI

A95-68396

FUTURE SSTS A EUROPEAN APPROACH

PHILIPPE POISSON-QUINTON ONERA Aerospace America (ISSN 0740-722X) vol. 32, no. 9 September 1994 p. 38-43
(BTN-95-EIX95072419883) Copyright

Recent studies in the U.S., Europe, and Japan indicate significant market potential for a new high-capacity supersonic transport (SST) linking the world's major cities. This SST could be economically viable and environmentally acceptable, provided investments are made to acquire the required technologies. The SST would fly over the Atlantic, the Pacific, and desert areas, covering about 80% of the most attractive routes, where supersonic flight (with its propagated boom) is allowed. The article discusses a joint European Supersonic Research Program that will cover materials, aerodynamics, systems, and engine integration for a reference configuration. The aircraft is expected to reach operational status by 2005-10. EI

A95-68398

PUTTING THE ACSYNT ON AIRCRAFT DESIGN

ARVID MYKLEBUST ACSY and PAUL GEHAUSEN Aerospace America (ISSN 0740-722X) vol. 32, no. 9 September 1994 p. 26-30
(BTN-95-EIX95072419881) Copyright

Aircraft conceptual design today is based largely on dimensional layout and semiempirical methods used by separate discipline groups. The most time consuming aspect of design is transferring the geometrical model into a form the various discipline analyses can use. One approach, designed to ensure manageable growth of large parametric feature-based computer-aided aircraft concep-

tual design tools, is based on experience with ACSYNT (aircraft synthesis). EI

A95-69215

DEVELOPMENT OF AN EFFICIENT INVERSE METHOD FOR SUPERSONIC AND HYPERSONIC BODY DESIGN

JAEWOO LEE Virginia Polytechnic Inst and State Univ, Blacksburg, VA, United States and W. H. MASON Journal of Spacecraft and Rockets (ISSN 0022-4650) vol. 31, no. 3 May-June 1994 p. 400-405
(BTN-95-EIX95041503784) Copyright

An efficient inverse method for supersonic and moderate hypersonic axisymmetric body design is developed for the Euler equations. Numerous surface pressure-body geometry rules are examined to obtain an inverse procedure that is robust, yet demonstrates fast convergence. Each rule is analyzed and examined numerically within the inverse calculation routine for supersonic ($M(\text{sub infinity}) = 3.0$) and moderate hypersonic ($M(\text{sub infinity}) = 6.28$) speeds. Based on the analysis, a new method to obtain rapid, reliable convergence is presented. Example results are given for several demanding cases: a hypersonic minimum drag body and several bodies derived from specification of extreme target pressure distributions. The new method requires slightly more than twice the CPU time of a direct calculation. Author (EI)

A95-69216

MINIMUM-DRAG AXISYMMETRIC BODIES IN THE SUPERSONIC/HYPERSO- NIC FLOW REGIMES

W. H. MASON Virginia Polytechnic Inst and State Univ, Blacksburg, VA, United States and JAEWOO LEE Journal of Spacecraft and Rockets (ISSN 0022-4650) vol. 31, no. 3 May-June 1994 p. 406-413
(BTN-95-EIX95041503785) Copyright

A study of minimum-drag body shapes was conducted over a Mach range from 3 to 12. Numerical results show that power-law bodies result in low-drag shapes, where the power $n = 0.69$ ($l/d = 3$) or $n = 0.70$ ($l/d = 5$) shapes have lower drag than theoretical minimum results ($n = 0.75$ or 0.66 , depending on the particular form of the theory). To evaluate the results, a numerical analysis was made, including viscous effects and the effect of a gas model. None of these considerations altered the conclusions. The Hayes minimum-drag body was analyzed and had a higher drag than the optimum power-law body. Author (EI)

A95-69230* National Aeronautics and Space Administration. Hugh L. Dryden Flight Research Facility, Edwards, CA.

FLIGHT EXPERIENCE WITH LIGHTWEIGHT, LOW-POWER MINIATURIZED INSTRUMENTATION SYSTEMS

PHILIP J. HAMORY and JAMES E. MURRAY Journal of Aircraft (ISSN 0021-8669) vol. 31, no. 5 September-October 1994 p. 1016-1021 refs
(BTN-95-EIX95062487522) Copyright

Engineers at the NASA Dryden Flight Research Facility (NASA-Dryden) have conducted two flight research programs with lightweight, low-power miniaturized instrumentation systems built around commercial data loggers. One program quantified the performance of a radio-controlled model airplane. The other program was a laminar boundary-layer transition experiment on a manned sailplane. The purpose of this article is to report NASA-Dryden personnel's flight experience with the miniaturized instrumentation systems used on these two programs. This article will describe the data loggers, the sensors, and the hardware and software developed to complete the systems. It also describes how the systems were used and covers the challenges encountered to make them work. Examples of raw data and derived results will be shown as well. For some flight research applications where miniaturized instrumentation is a requirement, the authors conclude that commercially available data loggers and sensors are viable alternatives. In fact, the data loggers and sensors make it possible to gather research-quality data in a timely and cost-effective manner. Author (EI)

AERODYNAMICS

Includes aerodynamics of bodies, combinations, wings, rotors, and control surfaces; and internal flow in ducts and turbomachinery.

A95-66276

**BALLOON TECHNOLOGY AND OBSERVATIONS;
SYMPOSIUM P3 OF THE COSPAR PLENARY MEETING,
29TH, WASHINGTON, DC, AUG. 28-SEPT. 5, 1992**

W. RIEDLER, editor Austrian Academy of Sciences, Graz, Austria
and K. M. TORKAR, editor Austrian Academy of Sciences, Graz,
Austria *Advances in Space Research* (ISSN 0273-1177) vol. 14,
no. 2 February 1994 212 p.
(HTN-95-70250) Copyright

The prime purpose of this meeting was to review current developments in technical aspects related to scientific ballooning. A second goal was the promotion of interdisciplinary contact between space and atmospheric physicists, astronomers and other scientists who consider balloons as platforms for their instruments, balloon designers concentrating on the technical development of balloons in all aspects, and organizers of long duration, often multi-national or even planetary balloon campaigns. There were sessions on balloon design, including materials and analysis techniques, applications for scientific ballooning, national balloon programs, long-duration flights with emphasis on both polar regions, and balloons on other planets. Among the many highlights were reports on remarkable improvements of balloon materials, new techniques for material and stress analysis and balloon engineering, novel instrument designs, mainly in the field of X-ray astronomy, and long duration flights over Antarctica. For individual titles, see A95-66277 through A95-66307.

Hemer

A95-66277

**FRENCH CONTRIBUTION TO NEW BALLOON DESIGNS
AND MATERIALS**

A. SOUBRIER Centre National d'Etudes Spatiales, Toulouse,
France Balloon technology and observations; Symposium P3 of
the COSPAR Plenary Meeting, 29th, Washington, DC, Aug. 28-
Sept. 5, 1992. A95-66276 *Advances in Space Research* (ISSN
0273-1177) vol. 14, no. 2 February 1994 p. (2)5-(2)12
Copyright

Research and development are permanent concerns in the French Balloon activity. One of the most significant improvements took place in the mid 80's in the field of materials, where linear low density polyethylenes demonstrated outstanding qualities at very low temperature, and allowed balloons to renew with success after the gap of the years 1985-86. Successful flights have since then been achieved under very cold temperatures, either in tropical or arctic zones, with very large and heavily loaded balloons. Significant steps have equally been achieved in balloon design, thanks to a new approach using the finite elements method. Because of its versatility, this method allows a very precise design of any shaped envelope (spherical, cylindrical, natural or else) with any type of appendix (belt, polar load, sleeve or else).

Author (Hemer)

A95-66282

**THEORETICAL AND ACTUAL PERFORMANCE OF A LONG
DURATION SUPERPRESSURE BALLOON MADE FROM A
BIAXIALLY ORIENTED NYLON-6 FILM**

T. LEW Winzen International, Inc., San Antonio, TX, US, L. SEELY
Winzen International, Inc., Sulphur Springs, TX, US, and R. RAI
Winzen International, Inc., San Antonio, TX, US Balloon technology
and observations; Symposium P3 of the COSPAR Plenary Meeting,
29th, Washington, DC, Aug. 28-Sept. 5, 1992. A95-66276 *Advances
in Space Research* (ISSN 0273-1177) vol. 14, no. 2 February 1994
p. (2)35-(2)38
Copyright

This paper summarizes the information gained during Winzen's program to develop a practical long duration superpressure balloon

capable of carrying a 22.7 kilogram payload at 36.6 kilometers for a over a year. The material used for this Superpressure Stratospheric Vehicle (SSV) is biaxially oriented nylon-6. An allowable design stress as a function of temperature has been developed. A cold temperature creep model for the nylon-6 has been developed. Permeability of nylon-6 to helium has been measured and the results indicate that this material is an excellent gas barrier, especially at cold temperatures. The transmissivity and reflectivity of this biaxially oriented nylon-6 has also been measured. A balloon prototype made with a pressure sensitive adhesive tape has been fabricated and successfully flown.

Author (Hemer)

A95-66285* National Aeronautics and Space Administration.
Wallops Flight Center, Wallops Island, VA.

**A COMPARATIVE STUDY OF INTERNALLY AND
EXTERNALLY CAPPED BALLOONS USING SMALL SCALE
TEST BALLOONS**

DOUGLAS P. BELL NASA, Wallops Flight Facility, Wallops Island,
VA, US Balloon technology and observations; Symposium P3 of the
COSPAR Plenary Meeting, 29th, Washington, DC, Aug. 28-Sept. 5,
1992. A95-66276 *Advances in Space Research* (ISSN 0273-1177)
vol. 14, no. 2 February 1994 p. (2)49-(2)52
Copyright

Caps have been used to structurally reinforce scientific research balloons since the late 1950's. The scientific research balloons used by the National Aeronautics and Space Administration (NASA) use internal caps. A NASA cap placement specification does not exist since no empirical information exists concerning cap placement. To develop a cap placement specification, NASA has completed two in-hangar inflation tests comparing the structural contributions of internal caps and external caps. The tests used small scale test balloons designed to develop the highest possible stresses within the constraints of the hangar and balloon materials. An externally capped test balloon and an internally capped test balloon were designed, built, inflated and simulated to determine the structural contributions and benefits of each. The results of the tests and simulations are presented.

Author (Hemer)

A95-66296* National Aeronautics and Space Administration.
Wallops Flight Center, Wallops Island, VA.

STATUS OF THE NASA BALLOON PROGRAM

H. C. NEEDLEMAN NASA, Wallops Flight Facility, Wallops Island,
VA, US Balloon technology and observations; Symposium P3 of the
COSPAR Plenary Meeting, 29th, Washington, DC, Aug. 28-Sept. 5,
1992. A95-66276 *Advances in Space Research* (ISSN 0273-1177)
vol. 14, no. 2 February 1994 p. (2)129-(2)135
Copyright

The U.S. National Aeronautics and Space Administration (NASA) Balloon Program has been highly successful since recovering from the catastrophic balloon failure problems of the early to mid 1980s. Balloons have continued to perform at unprecedented success rates. The comprehensive research and development (R&D) effort has continued with advances being made across the spectrum of balloon related disciplines. The long duration balloon project will be transitioning from a development effort to an operational capability this year. Recently, emphasis has been placed on the development and implementation of new support systems and facilities. A new permanent launch facility at Fort Sumner, New Mexico has been established. New ground station support equipment is being implemented, and a new heavy load launch vehicle is scheduled to be implemented in 1992. The progress, status and future plans for these and other aspects of the NASA program will be presented.

Author (Hemer)

A95-66297* National Aeronautics and Space Administration.
Wallops Flight Center, Wallops Island, VA.

OVERVIEW OF THE NASA BALLOON R&D PROGRAM

I. STEVE SMITH, JR. NASA, Wallops Flight Facility, Wallops Island,
VA, US Balloon technology and observations; Symposium P3 of the
COSPAR Plenary Meeting, 29th, Washington, DC, Aug. 28-Sept. 5,
1992. A95-66276 *Advances in Space Research* (ISSN 0273-1177)

vol. 14, no. 2 February 1994 p. (2)137-(2)146

Copyright

The catastrophic balloon failure during the first half of the 1980's identified the need for a comprehensive and continuing balloon research and development (R&D) commitment by NASA. Technical understanding was lacking in many of the disciplines and processes associated with scientific ballooning. A comprehensive balloon R&D plan was developed in 1986 and implemented in 1987. The objectives were to develop the understanding of balloon system performance, limitations, and failure mechanisms. The program consisted of five major technical areas: structures, performance and analysis, materials, chemistry and processing, and quality control. Research activities have been conducted at NASA/Goddard Space Flight Center (GSFC)-Wallops Flight Facility (WFF), other NASA centers and government facilities, universities, and the balloon manufacturers. Several new and increased capabilities and resources have resulted from this activity. The findings, capabilities, and plan of the balloon R&D program are presented.

Author (Herner)

A95-66303

THE JOINT RUSSIAN-BRASIL RESEARCH ON BALLOONS

N. A. BUIVUN Institute of Meteorology, Brasil, V. I. LAPSHIN Commission on Balloon Research, Moscow, Russia, L. L. LAZUTIN Commission on Balloon Research, Moscow, Russia, I. M. MARTIN Campinas Univ., Brasil, S. I. NIKOLSKY Commission on Balloon Research, Moscow, Russia, YU. I. STOKHOV Commission on Balloon Research, Moscow, Russia, A. JR. TURTELLY Campinas Univ., Brasil, and M. I. FRADKIN Commission on Balloon Research, Moscow, Russia Balloon technology and observations; Symposium P3 of the COSPAR Plenary Meeting, 29th, Washington, DC, Aug. 28-Sept. 5, 1992. A95-66276 Advances in Space Research (ISSN 0273-1177) vol. 14, no. 2 February 1994 p. (2)175

Copyright

A brief report on the joint Russian-Brazilian research on balloons in the Brazilian magnetic anomaly region is given. The scientific program is discussed too. The Russian-Brazilian joint research on balloons began in 1988. Since that time two balloon campaigns (in 1989 and 1991, respectively) including several launches of large balloons (180,000 cu m volume) and small ones (180,000 cu m volume) with scientific instruments installed on the balloons were performed. The launches had been made in the Brazil magnetic anomaly region. Several organizations participated in this work: from the Russian side - P.N. Lebedev Physical Institute and Polar Geophysical Institute, Russian Academy of Sciences, Moscow University and Moscow Engineering and Physical Institute; from Brazilian side - Campinas University and Bauru Meteorological Institute. From 1988 until 1991 the regular measurement of ionizing radiation in the atmosphere in Campinas was done. For this measurements small rubber balloons were used. Author (Herner)

A95-66304

A PROGRAM FOR SCIENTIFIC AND APPLIED INVESTIGATIONS USING AEROSTAT COMPLEXES

B. BONEV Space Research Institute, Sofia, Bulgaria, P. PETROV Space Research Institute, Sofia, Bulgaria, V. S. DJEPA-PETROVA Space Research Institute, Sofia, Bulgaria, N. NIKOLOV Space Research Institute, Sofia, Bulgaria, S. HOTIMSKII Russian Academy of Sciences, Moscow, Russia, B. LEVSHUK Russian Academy of Sciences, Moscow, Russia, and V. LAPSHIN Russian Academy of Sciences, Moscow, Russia Balloon technology and observations; Symposium P3 of the COSPAR Plenary Meeting, 29th, Washington, DC, Aug. 28-Sept. 5, 1992. A95-66276 Advances in Space Research (ISSN 0273-1177) vol. 14, no. 2 February 1994 p. (2)177-(2)179

Copyright

The programs for research work using aerostats will lead to the solution of a wide range of scientific problems in the field of astronomy, aeronomy, meteorology and remote sensing of the Earth. They include a number of experiments concerning applied ecology, navigation, aerostats and space equipments, etc. Author (Herner)

A95-67332

ROTATING KIRCHHOFF METHOD FOR THREE-DIMENSIONAL TRANSONIC BLADE-VORTEX INTERACTION HOVER NOISE

YU XUE Univ. of Minnesota, Minneapolis, MN and A. S. LYRINTZIS AIAA Journal (ISSN 0001-1452) vol. 32, no. 7 July 1994 p. 1350-1359 refs

(BTN-94-EIX94441386601) Copyright

Three-dimensional transonic blade-vortex interaction (BVI) noise is studied numerically. The unsteady transonic full-potential rotor (FPR) code is used for the simulation of the transonic BVI near-field flow. The rotating Kirchhoff method is used for the extension to the acoustic far field. Two rotating Kirchhoff formulations are developed for the three-dimensional BIV far-field noise prediction. The first formulation (Morino's method) is for an observer rotating with the blade. This allows the direct comparison with computational fluid dynamics results. The second formulation (Farassat's method) is for a stationary observer and allows a direct comparison with acoustic experiments. Test results are presented in this paper for a rotating point source and a transonic high-speed impulsive (HSI) noise prediction. The results for a parallel vortex line interacting with a nonlifting hovering rotor are presented and various cases are shown. The understanding of the three-dimensional transonic BVI noise mechanisms and directivity are discussed here.

Author (EI)

A95-67335

SUPERSONIC AND HYPERSONIC SHOCK/BOUNDARY-LAYER INTERACTION DATABASE

GARY S. SETTLES Pennsylvania State Univ., University Park, PA and LORI J. DODSON AIAA Journal (ISSN 0001-1452) vol. 32, no. 7 July 1994 p. 1377-1383 refs

(BTN-94-EIX94441386604) Copyright

An assessment is given of existing shock wave/turbulent boundary-layer interaction experiments having sufficient quality to guide turbulence modeling and code validation efforts. Although the focus of this work is hypersonic, experiments at Mach numbers as low as 3 were considered. The principal means of identifying candidate studies was a computerized search of the AIAA Aerospace Database. Several hundred candidate studies were examined and over 100 of these were subjected to a rigorous set of acceptance criteria for inclusion in the database. Nineteen experiments were found to meet these criteria, of which only seven were in the hypersonic regime (M greater than 5).

Author (EI)

A95-67336

LINEAR DISTURBANCES IN HYPERSONIC, CHEMICALLY REACTING SHOCK LAYERS

GREG STUCKERT Arizona State Univ., Tempe, AZ and HELEN L. REED AIAA Journal (ISSN 0001-1452) vol. 32, no. 7 July 1994 p. 1384-1393 refs

(BTN-94-EIX94441386605) Copyright

The effects of equilibrium- and nonequilibrium-air chemical reactions on the linear stability of a Mach 25, 10-deg half-angle sharp-cone shock layer are investigated. First, the basic state is computed using the parabolized Navier-Stokes equations with a shock-fitting scheme. This eliminates spurious numerical oscillations that could adversely affect the stability analysis. Spatial stability analyses are then described for three different approximations of the physics: perfect gas, air in local chemical equilibrium, and air in chemical nonequilibrium. It is shown in both the equilibrium- and nonequilibrium-air calculations that the second mode of Mack is shifted to lower frequencies. This is attributed to the increase in the size of the region of relative supersonic flow due to the lower speeds of sound in the relatively cooler boundary layers. Finally, in the equilibrium air calculations, modes that travel supersonically relative to the inviscid region of the shock layer are shown to exist. These modes are a superposition of incoming and outgoing disturbances whose magnitude oscillates with the distance normal to the wall in the inviscid region of the shock layer. This oscillatory behavior is possible only because the shock standoff distance is finite.

Author (EI)

A95-67337

BEHAVIOR OF THE JOHNSON-KING TURBULENCE MODEL IN AXISYMMETRIC SUPERSONIC FLOWS

YASUO NOGUCHI Univ. of Salford, Salford (United Kingdom) and
TOSHIMASA SHIRATORI AIAA Journal (ISSN 0001-1452) vol. 32,
no. 7 July 1994 p. 1394-1398 refs
(BTN-94-EIX94441386606) Copyright

A series of systematic tests are carried out on the Johnson-King turbulence model (JKM) for applied compressible aerodynamics. Two-dimensional flows with a moderate adverse pressure gradient and without separation at various Mach numbers are used for the tests. The results are compared with the Baldwin-Lomax model (BLM) as well as the measurements. The agreement of the results of both models and the measured data becomes poorer at higher Mach numbers. Overall, the performance of the JKM is slightly better than BLM except with respect to the prediction of the skin friction coefficient. The ordinary differential equation (ODE) in the JKM is effective in improving the prediction. However, the effects of the ODE are not as significant as in flows with separation. Use of the JKM even in nonseparated flows may improve accuracy of prediction, which has not been clearly established before this work.

Author (EI)

A95-67347

AEROELASTIC STABILITY OF HINGELESS ROTOR BLADE IN HOVER USING LARGE DEFLECTION THEORY

MAENG HYU CHO Korea Advanced Inst. of Science and
Technology, Taejeon (Korea, Republic of) and IN LEE AIAA Journal
(ISSN 0001-1452) vol. 32, no. 7 July 1994 p. 1472-1477 refs
(BTN-94-EIX94441386616) Copyright

The coupled flap-lag-torsion aeroelastic stability of a hingeless rotor blade in hover is investigated using finite elements based on large deflection beam theory. The finite element equations of motion for beams undergoing arbitrary large displacements and rotations, but small strains, are obtained from Hamilton's principle. The stability boundary is calculated assuming blade motions to be small perturbations about the nonlinear steady equilibrium deflections, which are obtained through an iterative Newton-Raphson method. The p-k modal flutter analysis based on coupled rotating natural modes is used. Various unsteady two-dimensional strip theories are used to evaluate the aerodynamic loads. The sensitivity of the stability boundary to these aerodynamic assumptions is examined. Numerical results of the steady deflections and stability boundaries are presented for some representative blade configurations and also compared with those given in previous moderate deflection type theories.

Author (EI)

A95-67828

ASPECTS OF VORTEX BREAKDOWN

JEAN M. DELERY ONERA, Chatillon, France Progress in
Aerospace Sciences (ISSN 0376-0421) vol. 30, no. 1 March 1994
p. 1-59 Research sponsored by French Ministry of Defense
(HTN-95-A0001) Copyright

Vortex breakdown is of primary importance in many situations met in aeronautical as well as extra-aeronautical applications. During the past 40 years, this problem has been the subject of a large number of investigations, both in the experimental and theoretical domains. This article presents an overview of some of the results obtained by these studies. Carefully executed visualizations and velocity measurements have allowed a clear description of the field associated with breakdown. These experiments executed in a vortex tube, where the vortex is confined, or in arrangements where it is free, show that the existence of a stagnation point forming on the center-line of the vortical structure is a distinctive feature of breakdown. Different types of breakdown (spiral and bubble types) seem to exist, however this point is subject to controversy. At the same time, the vortex undergoes a brutal dilatation with the generation of large-scale fluctuations. Similar features are observed when the breakdown occurs over a delta wing. The two main parameters influencing the phenomenon are the adverse pressure gradient to which the vortex is submitted and its swirl intensity which cannot go

beyond a critical value. The most popular theories for vortex breakdown belong to four main classes: the quasi-cylindrical approach and analogy to boundary layer separation, solution of the axisymmetric Navier-Stokes equations, the concept of the critical state and hydrodynamic instabilities. More advanced models, based on the bifurcation theory or using a direct numerical simulation of the problem have also been developed. In most, the obtained results are in good agreement with experimental observations, but the predictive capability of these theories is still limited. Author (Herner)

A95-67829

KINETIC THEORY IN AEROTHERMODYNAMICS

M. N. KOGAN TsAGI, Moscow, Russia Progress in Aero-
space Sciences (ISSN 0376-0421) vol. 29, no. 4 December 1992
p. 271-354
(HTN-95-A0002) Copyright

Aerothermodynamics is a branch of gas dynamics which is usually considered for continuum media. But many problems of gas dynamics cannot be solved and even properly understood in the framework of continuum media, and cannot be described on the macroscopic level. The aim of this review is to consider some problems of a continuum flow regime which cannot be solved without regarding the gas as a collection of molecules. Some of these problems are important for aerothermodynamics today. Others open up new ways, new possibilities and new questions.

Author (Herner)

A95-67830

SHOCK LAYERS AND BOUNDARY LAYERS IN HYPERSONIC FLOWS

J. COUSTEIX CERT, Toulouse, France, D. ARNAL CERT,
Toulouse, France, B. AUPOIX CERT, Toulouse, France, J. PH.
BRAZIER CERT, Toulouse, France, and A. LAFON CERT,
Toulouse, France Progress in Aerospace Sciences (ISSN 0376-
0421) vol. 30, no. 2 June 1994 p. 95-212
(HTN-95-A0003) Copyright

This paper presents an overview of the physical and numerical aspects of flows encountered around a vehicle in hypersonic flight. These problems are typically related to the reentry phase of a space shuttle into the atmosphere. Nonetheless, it is believed that the material given here is a good background for other applications. Compared with the standard aerodynamic problems on an aircraft in transonic or supersonic flight, hypersonic flows are characterized by a much higher level of energy. The high temperature of the flow can lead to thermochemical non-equilibrium, with chemical reactions and vibrational relaxation. These effects are of prime importance in the evaluation of the heating of the body and they may affect general flow features, including the wall pressure. Basic elements are discussed to understand the physics of these phenomena. Applications are given in the framework of boundary layer calculations and of numerical solutions of the Navier-Stokes equations. In the front of the vehicle, a strong bow shock wave forms and the boundary layer is fed by a rational flow. A discussion is given concerning how a boundary layer theory can account for these effects. At lower altitudes, the velocity of the flow remains large, the Reynolds number increases and the flow becomes turbulent. In this context, laminar transition and turbulence modeling are discussed.

Author (Herner)

A95-68173

DESIGN AND OPERATION OF A SUPERSONIC ANNULAR FLOW FACILITY

K. E. WILLIAMS Univ. of Washington, Seattle, WA, F. B. GESSNER,
and G. J. HARLOFF AIAA Journal (ISSN 0001-1452) vol. 32,
no. 7 July 1994 p. 1528-1531 refs
(BTN-94-EIX94441386624) Copyright

Several important issues have been addressed relating to shock-free, supersonic turbulent flow in an annular duct. By properly designing the flow components upstream of the duct and choosing an appropriate boundary layer trip location, it has been shown that an experimental flow can be generated for which the inner and outer

02 AERODYNAMICS

wall boundary layers are fully turbulent, with the near-wall flow in local equilibrium at all streamwise locations along the duct. By initiating the computations in the plenum chamber and prescribing the Baldwin-Lomax turbulence model, excellent agreement is possible between experimental and numerical flows. EI

A95-68174

MODEL FOR COMPRESSIBLE TURBULENCE IN HYPERSONIC WALL BOUNDARY AND HIGH-SPEED MIXING LAYERS

RODNEY D. W. BOWERSOX Air Force Inst. of Technology, OH and
JOSEPH A. SCHETZ AIAA Journal (ISSN 0001-1452) vol. 32,
no. 7 July 1994 p. 1531-1533 refs
(BTN-94-EIX94441386625) Copyright

The effects of numerically including the compressible apparent mass terms in all of the conservation equations were assessed. A straightforward gradient transport analysis was applied to model the apparent mass term. This new formulation was incorporated into a modern Navier-Stokes computational fluid dynamics code. The compressible apparent mass mixing length extension (CAMMLE) model as well as other popular models were numerically tested against experimental data. The numerical results showed that compressible turbulence terms are important for hypersonic wall boundary layers and high-density gradient flows. EI

A95-68180

ADAPTIVE COMPUTATIONS OF FLOW AROUND A DELTA WING WITH VORTEX BREAKDOWN

DAVID L. MODIANO Massachusetts Inst. of Technology, Cambridge, MA and EARLL M. MURMAN AIAA Journal (ISSN 0001-1452) vol. 32, no. 7 July 1994 p. 1545-1547 refs
(BTN-94-EIX94441386631) Copyright

An adaptive mesh Euler solver was used to simulate the flow over a sharp edged delta wing. Adaptation enables the normal force to be well predicted at high range of angle of attack in the presence of vortex breakdown. The position of breakdown is in reasonable agreement with experimental measurements. Vortex breakdown is predicted to primarily exhibit the spiral form, which is typically observed in delta wing experiments. EI

A95-68195

INFLUENCE OF INJECTANT MACH NUMBER AND TEMPERATURE ON SUPERSONIC FILM COOLING

K. A. JUHANY California Inst. of Technology, Pasadena, CA, M. L. HUNT, and J. M. SIVO Journal of Thermophysics and Heat Transfer (ISSN 0887-8722) vol. 8, no. 1 January-March 1994 p. 59-67 refs
(BTN-94-EIX94441386686) Copyright

The current work is an experimental investigation of the dependence of film cooling effectiveness on the injection Mach number, velocity, and mass flux. The freestream Mach number is 2.4, and the injection Mach numbers range from 1.2 to 2.2 for both air and helium injection. The adiabatic wall temperature is measured directly. The injection velocity and mass flux are varied by changing the total temperature and Mach number while maintaining matched pressure conditions between the injected flow and that of the freestream. The total temperature of the freestream is 295 K, and for the injection it ranges from 215-390 K. The results indicate an increase in film cooling effectiveness as the injection rate is increased. With the exception of heated helium runs, larger injection Mach numbers slightly increase the effective cooling length per mass injection rate. The results for helium injection indicate an increase in effectiveness as compared to that for air injection. Heated injection, with the injectant to freestream velocity ratios greater than 1, exhibit a rise in wall temperature downstream of the slot resulting in effectiveness values greater than 1. The experimental results are also compared with earlier studies in the literature. Author (EI)

A95-68218

PHENOMENOLOGICAL DESCRIPTION AND SIMPLIFIED MODELLING OF THE VORTEX WAKE ISSUING FROM A JET

IN A CROSSFLOW

L. JACQUIN ONERA, Chatillon (France) Recherche Aerospatiale (ISSN 0034-1223) no. 2 1994 p. 117-133 refs
(BTN-94-EIX94441385754) Copyright

The basic physical mechanisms of a jet in a crossflow are first reviewed, and then a simplified method based on an analogy with a wing wake is discussed for modeling this kind of flow. Author (EI)

A95-68219

TIP VORTEX ON A SWEEPED WING. MEAN FLOW AND UNSTEADY PHENOMENA [TOURBILLON D'APEX SUR UNE AILE EN FLECHE. ECOULEMENT MOYEN ET PHENOMENES INSTATIONNAIRES]

J. TENSI URA CNRS, Futuroscope (France) Recherche Aerospatiale (ISSN 0034-1223) no. 2 1994 p. 135-151 In FRENCH refs
(BTN-94-EIX94441385755) Copyright

To gain a better understanding of scrolling of vortex sheets around a swept wing in incompressible state, the ENSMA Aerodynamics Laboratory in Poitiers conducted a series of wind tunnel tests over several years that provided interesting results, in particular concerning fluctuations in the upper surface separation and reattachment. These results give valuable data for apprehending the corresponding instabilities of the vortex that interfere with turbulence. Author (EI)

A95-68220

ON WAVE-FRONT CURVATURE IN LINEAR STABILITY THEORY

G. SCHRAUF Deutsche Aerospace Airbus, Bremen (Germany) Recherche Aerospatiale (ISSN 0034-1223) no. 2 1994 p. 153-158 refs
(BTN-94-EIX94441385756) Copyright

A potential confusion regarding the signs of the wave-front curvature terms $m_{(sub\ 12)}$, $m_{(sub\ 21)}$ in the linear stability equations is resolved. It is shown that these terms, although denoted by Stuart, Malik, and the author with the same symbols, have different geometrical meanings depending on the underlying coordinate systems. Author (EI)

A95-68353

TWISTING SMARTLY IN THE WIND

MOISHE GARFINKLE Drexel Univ., Philadelphia, PA Aerospace America (ISSN 0740-722X) vol. 32, no. 7 July 1994 p. 18-20 (BTN-95-EIX95041503093) Copyright

The author considers ways of controlling an airplane wing box beam under steady flight conditions. He considers active control of fiber-composite box beams by embedding miniature piezoelectric crystal actuators between laminates within the fiber-composite structure, but the practical application of active control to smart structures is severely restricted. Investigators are examining whether it would be possible to so tailor a fiber-composite wing box-beam that the desired twist-bend coupling could arise intrinsically from the fiber architecture itself, resulting in passive control. This solution requires the construction of a continuous-fiber antisymmetric box beam that has a balanced stacking sequence, but there are obstacles to such a construction. To circumvent them, a novel architecture has been developed wherein two ordinarily wound antisymmetric, balanced stacking sequence box beams with opposite direction windings are stacked upon one another. EI

A95-68355

WAVERIDERS WITH FINLETS

X. HE Univ. of Oklahoma, Norman, OK, M. L. RASMUSSEN, and R. A. COX Journal of Aircraft (ISSN 0021-8669) vol. 31, no. 5 September-October 1994 p. 1135-1142 refs
(BTN-95-EIX95062487541) Copyright

A generalized analytical method for designing waverider shapes is presented. Waverider configurations that incorporate finlets are of primary interest. These finlets resemble fins on conventional aircraft and might imaginably be used as control surfaces. The design method-

ology determines the waverider shape by alternatively specifying the planform shape, the freestream-surface trailing-edge shape, the compression-surface trailing-edge shape, or various combinations of the three. A wide variety of shapes is presented, and the aerodynamic properties are calculated by means of hypersonic small-disturbance theory. The effects of finlets are used to shift the c.p. aft and to improve static stability. The results are novel, and the analysis is readily usable for a variety of design studies. Author (EI)

A95-68357

EXPERIMENTAL INVESTIGATIONS ON LIMIT CYCLE WING ROCK OF SLENDER WINGS

ANDREW S. ARENA, JR. Oklahoma State Univ., Stillwater, OK and ROBERT C. NELSON Journal of Aircraft (ISSN 0021-8669) vol. 31, no. 5 September-October 1994 p. 1148-1155 refs (BTN-95-EIX95062487543) Copyright

The phenomena of wing rock of a delta wing with 80-deg sweep has been investigated through a comprehensive series of experiments. Two unique experimental apparatus have been developed for the investigation. A free-to-roll system was developed using an air-bearing spindle that allowed the isolation of applied torques due to the flowfield. An unsteady pressure acquisition system was also developed in order to measure the unsteady surface pressure distributions acting on the wing during wing rock motion. Experimental measurements include motion characteristics obtained from motion history plots, static and dynamic flow visualization of vortex position and vortex breakdown, static surface flow visualization, and steady and unsteady surface pressure distributions. Correlation using the different sources of data provides insight into mechanisms that are most likely to cause the wing rock motion. Author (EI)

A95-68358

AERODYNAMIC EFFECTS OF DELTA PLANFORM TIP SAILS ON WING PERFORMANCE

LANCE W. TRAUB Univ. of the Witwatersrand, Johannesburg (South Africa) Journal of Aircraft (ISSN 0021-8669) vol. 31, no. 5 September-October 1994 p. 1156-1159 refs (BTN-95-EIX95062487544) Copyright

An experimental investigation was conducted to establish the effects of delta planform tip sails (DPTSs) on a planar rectangular wing. The DPTS is a small wingtip-mounted device analogous to a conventional tip sail, but with a slender planform. It is suggested that using a sharp-edged, slender tip device may alleviate some of the design complexities (e.g., twist and camber) associated with keeping attached flow on winglets and tip sails. The results indicate that performance improvements can be obtained with DPTSs. Increases in the wing lift curve slope, maximum lift coefficient and, for some configurations, the Oswald efficiency factor were obtained compared to the basic wing. Increasing the DPTS leading-edge sweep angle and taper ratio resulted in an increase in the wing's Oswald efficiency factor. Author (EI)

A95-68359

APPLICATION OF CIRCULATION CONTROL TO ADVANCED SUBSONIC TRANSPORT AIRCRAFT. PART 1: AIRFOIL DEVELOPMENT

ROBERT J. ENGLAR Georgia Tech. Research Inst., Atlanta, GA, MARILYN J. SMITH, SEAN M. KELLEY, and RICHARD C. ROVER, III Journal of Aircraft (ISSN 0021-8669) vol. 31, no. 5 September-October 1994 p. 1160-1168 refs (BTN-95-EIX95062487545) Copyright

An experimental/analytical research program was undertaken to develop advanced versions of circulation control wing (CCW) blown high-lift airfoils, and to address specific issues related to their application to subsonic transport aircraft. The primary goal was to determine the feasibility and potential of these pneumatic airfoils to increase high-lift system performance in the terminal area while reducing system complexity. A four-phase program was completed, including (1) experimental development and evaluation of advanced CCW high-lift configurations, (2) development of effective pneumatic leading-edge devices, (3) computational evaluation of CCW airfoil designs plus high-lift and cruise capabilities, and (4) investigation

of the terminal-area performance of transport aircraft employing these airfoils. The first three phases of this program are described in Part 1 of this article. Applications to the high-lift and control systems of advanced subsonic transport aircraft and resulting performance are discussed in the continuation of this article, Part 2. Experimental lift coefficient values approaching 8.0 at zero incidence and low blowing rates were demonstrated by two-dimensional CCW configurations that promised minimal degradation of the airfoil's performance during cruise. These results and experimental/CFD methods are presented. Author (EI)

A95-68360

APPLICATION OF CIRCULATION CONTROL TO ADVANCED SUBSONIC TRANSPORT AIRCRAFT. PART 2: TRANSPORT APPLICATION

ROBERT J. ENGLAR Georgia Tech. Research Inst., Atlanta, GA, MARILYN J. SMITH, SEAN M. KELLEY, and RICHARD C. ROVER, III Journal of Aircraft (ISSN 0021-8669) vol. 31, no. 5 September-October 1994 p. 1169-1177 refs (BTN-95-EIX95062487546) Copyright

An experimental/analytical research program was undertaken to develop advanced versions of circulation control wing (CCW) airfoils and to address specific issues related to the application of these blown high-lift devices to subsonic transport aircraft. The primary goal was to determine the feasibility and potential of these pneumatic configurations to increase high-lift system performance in the terminal area while reducing system complexity and aircraft noise. A four-phase program was completed, including (1) experimental development and evaluation of advanced CCW high-lift configurations; (2) development of effective pneumatic leading-edge devices; (3) computational evaluation of CCW airfoil designs plus high-lift and cruise capabilities; and (4) the investigation of the terminal-area performance of transport aircraft employing these airfoils. The first three phases were presented in Part 1 of this article. This segment, Part 2, describes the fourth phase of the program. Experimental lift coefficient values approaching 8.0 at zero incidence were demonstrated by two-dimensional CCW configurations and were reported in Part 1. These were used to predict 70-80% reductions in takeoff and landing distances for a three-dimensional advanced subsonic transport configuration employing a simplified pneumatic high-lift system. These results and the methodology used to obtain them are presented. Author (EI)

A95-68366

INTERFERENCE BETWEEN TANKER WING WAKE WITH ROLL-UP AND RECEIVER AIRCRAFT

A. W. BLOY Univ. of Manchester, Manchester (United Kingdom) and M. G. WEST Journal of Aircraft (ISSN 0021-8669) vol. 31, no. 5 September-October 1994 p. 1214-1216 refs (BTN-95-EIX95062487552) Copyright

A model of wing wake roll-up was developed and applied to the problem of the lateral aerodynamic interference between tanker and receiver aircraft during air-to-air refueling. For the configuration considered, the wake roll-up gives a tip vortex strength at the receiver wing position that is 42.5% of the circulation at the tanker wing centerline. From the downwash and sidewash distributions the receiver rolling moments due to sideways and bank displacements were calculated. Compared with predictions from a flat vortex sheet model of the wing wake, the predictions from the wake roll-up model indicated significantly higher values of the receiver rolling moment due to sideways displacement derivative. For the configuration considered, the effect of roll-up on the receiver rolling moment due to bank derivative was negligible. EI

A95-68368* National Aeronautics and Space Administration, Langley Research Center, Hampton, VA.

PASSIVE POROSITY WITH FREE AND FIXED SEPARATION ON A TANGENT-OGIVE FOREBODY

RICHARD M. WOOD NASA, Langley Research Center, Hampton, VA, DANIEL W. BANKS, and STEVEN X. S. BAUER Journal of Aircraft (ISSN 0021-8669) vol. 31, no. 5 September-October 1994 p. 1219-1221 refs

(BTN-95-EIX95062487554) Copyright

Despite the extensive experimental and computational data base in the literature on passive porosity, no clear explanation of the governing flow physics exists. It is theorized that the positive porosity concept modifies the external pressure loading by allowing communication between high- and low-pressure regions on the external surface. This study determines the dominant flow phenomena that govern the effectiveness of passive porosity. It aims to assess the contribution of each phenomenon as related to a porous slender axisymmetric forebody. To assess the influence of the mass transfer and pressure equalization phenomena on the effectiveness of passive porosity on slender axisymmetric forebodies, strakes were attached to the 5.0-caliber solid and porous forebodies to force crossflow separation. Longitudinal force and moment data were obtained at a Mach number of 0.1 over an angle-of-attack range of 0 to 55 deg. EI

A95-68369

VORTICAL FLOW STRUCTURE NEAR THE F/A-18 LEX AT HIGH INCIDENCE

B. H. K. LEE Univ. of Ottawa, Ottawa, Ontario and N. R. VALERIO Journal of Aircraft (ISSN 0021-8669) vol. 31, no. 5 September-October 1994 p. 1221-1223 refs (BTN-95-EIX95062487555) Copyright

An attempt was made to provide further insight into the complex vortical flow structure generated by the leading-edge extension (LEX) and fence, through a study of the topology of the surface skin friction lines. Various angles of attack were investigated. LEX surface flow visualization and LEX off-surface flow topology near the end of the fence, both at $M = 0.6$ and $\alpha = 30$ deg, are described. EI

A95-68372* National Aeronautics and Space Administration. Ames Research Center, Moffett Field, CA.

EFFECT OF GROUND AND CEILING PLANES ON SHAPE OF ENERGIZED WAKES

VERNON J. ROSSOW NASA. Ames Research Center, Moffett Field, CA Journal of Aircraft (ISSN 0021-8669) vol. 31, no. 5 September-October 1994 p. 1227-1231 refs (BTN-95-EIX95062487558) Copyright

Results are presented from an investigation of the structure of energized wakes in the presence of ground or ceiling planes when powered-lift devices are tested at zero and low wind tunnel velocities. Solutions are presented to indicate how the presence of a nearby ground plane causes the energized wake to constrict less than when in free space. In contrast, another set of solutions indicate that the presence of a ceiling plane enhances wake construction so that the wake width is even smaller than when in free space. Hence, a ground plane tends to reduce the chance for interaction between the wake and the energizing elements, while a nearby ceiling plane tends to increase the likelihood for interference. EI

A95-69232

NUMERICAL SIMULATION OF STEADY AND UNSTEADY, VORTICITY-DOMINATED AERODYNAMIC INTERFERENCE

JAMAL M. ELZEBDA Virginia Polytechnic Inst and State Univ, Blacksburg, VA, DEAN T. MOOK, and ALI H. NAYFEH Journal of Aircraft (ISSN 0021-8669) vol. 31, no. 5 September-October 1994 p. 1031-1036 refs (BTN-95-EIX95062487524) Copyright

The problem of modeling steady and unsteady aerodynamic interference is discussed. A configuration resembling the X-29 is used as an example. The general unsteady vortex-lattice method is used to model the flowfield. By considering the components operating alone and as members of the complete configuration, we demonstrate the importance of accurately simulating the wakes of the upstream components. The wakes of the canards as well as the canards themselves have a strong negative influence on the lift generated by the main wing; the main wing has a positive influence on the lift generated by the canards. The forward sweep of the main wing tends to focus the generated upwash in the vicinity of the

canards. It is shown that the maximum influence of the vorticity shed from the canards does not develop until the shed vorticity convects downstream directly over the main wing. The general unsteady vortex-lattice method appears to be a reasonably accurate model of closely coupled, vorticity-dominated flowfields as long as the lines of the separation are known and vortex bursting does not occur near the wings. Author (EI)

A95-69234* National Aeronautics and Space Administration. Ames Research Center, Moffett Field, CA.

NUMERICAL SIMULATION OF INCIDENCE AND SWEEP EFFECTS ON DELTA WING VORTEX BREAKDOWN

J. A. EKATERINARIS and LEWIS B. SCHIFF Journal of Aircraft (ISSN 0021-8669) vol. 31, no. 5 September-October 1994 p. 1043-1049 refs

(BTN-95-EIX95062487526) Copyright

The structure of the vortical flowfield over delta wings at high angles of attack was investigated. Three-dimensional Navier-Stokes numerical simulations were carried out to predict the complex leeward-side flowfield characteristics, including leading-edge separation, secondary separation, and vortex breakdown. Flows over a 75- and a 63-deg sweep delta wing with sharp leading edges were investigated and compared with available experimental data. The effect of variation of circumferential grid resolution grid resolution in the vicinity of the wing leading edge on the accuracy of the solutions was addressed. Furthermore, the effect of turbulence modeling on the solutions was investigated. The effects of variation of angle of attack on the computed vortical flow structure for the 75-deg sweep delta wing were examined. At moderate angles of attack no vortex breakdown was observed. When a critical angle of attack was reached, bubble-type vortex breakdown was found. With further increase in angle of attack, a change from bubble-type breakdown to spiral-type vortex breakdown was predicted by the numerical solution. The effects of variation of sweep angle and freestream Mach number were addressed with the solutions on a 63-deg sweep delta wing. Author (EI)

A95-69235

ANALYSIS OF AN OSCILLATING JOUKOWSKI AIRFOIL WITH SURFACE SUCTION AND MOVING VORTICES

CHYN-SHAN CHIU China Junior Coll of Technology, Taipei (Taiwan, Province of China) Journal of Aircraft (ISSN 0021-8669) vol. 31, no. 5 September-October 1994 p. 1050-1056 refs (BTN-95-EIX95062487527) Copyright

An attempt is made to enhance the beneficial effects of the trapped vortex by increasing its lingering period on the upper surface of a Joukowski airfoil in oscillating motions. Studies are made on the stability of a trapped free vortex when perturbed away from its equilibrium position with a finite displacement, and on the lingering period of the trapped free vortex in the upper vicinity of the airfoil. The computational results show that a proper combination of oscillation and suction might be an efficient method for trapping a free vortex to generate high lift on an airfoil. It is found that the trailing-edge suction position is more effective in capturing a free vortex for a longer lingering time and the lift increment directly dependent on the strength of the trapped vortex. This result may provide an explanation of the high lift generated by a dragonfly whose back wings are found to flap in a flow containing vortices shed from the front wings. Author (EI)

A95-69238

AERODYNAMIC SENSITIVITY COEFFICIENTS USING THE THREE-DIMENSIONAL FULL POTENTIAL EQUATION

HESHAM M. EL-BANNA Texas A&M Univ., College Station, TX and LELAND A. CARLSON Journal of Aircraft (ISSN 0021-8669) vol. 31, no. 5 September-October 1994 p. 1071-1077 refs (BTN-95-EIX95062487530) Copyright

The quasianalytical (QA) approach is applied to the three-dimensional full potential equation to compute wing aerodynamic sensitivity coefficients in the transonic regime. Symbolic manipulation is used and is crucial in reducing the effort associated with

obtaining sensitivity equations, and the large sensitivity system is solved using sparse solver routines such as the iterative conjugate gradient method. The results obtained are almost identical to those obtained by the finite difference (FD) approach and indicate that obtaining the sensitivity derivatives using the QA approach is more efficient than computing the derivatives by the FD method, especially as the number of design variables increases. It is concluded that the QA method is an efficient and accurate approach for obtaining transonic aerodynamic sensitivity coefficients in three dimensions. Author (EI)

A95-69239

PRELIMINARY ASSESSMENT OF TUNNEL WALL INTERFERENCE IN THE NDA CRYOGENIC WIND TUNNEL

YUTAKA YAMAGUCHI National Defense Academy, Kanagawa (Japan), MASAHIRO YOROZU, TADASHI SAKAUE, and TERUO SAITO Journal of Aircraft (ISSN 0021-8669) vol. 31, no. 5 September-October 1994 p. 1078-1083 refs (BTN-95-EIX95062487531) Copyright

As the second stage of a preliminary cryogenic airfoil testing program, the test section interference of the National Defense Academy cryogenic tunnel was evaluated. A R4 airfoil model, which has the chord length of 12 cm and the aspect ratio of 0.5, was tested in the range of Mach number 0.5 to 0.75, and that of Reynolds number 7×10^6 (exp 6) to about 1.1×10^7 (exp 7). The experimental results were corrected with empirical wall interference correction methods, the Barnwell-Sewall method for sidewall boundary layers, and the Blackwell method for the top and bottom walls. This preliminary evaluation showed that the sidewall boundary layers dominate the tunnel wall interference of the present cryogenic tunnel, and there may be some possibility of utilizing the tunnel for performing two-dimensional airfoil tests if more precise wall interference parameters are obtained. Author (EI)

A95-69240

COMPARISON OF ELECTROSTATIC AND AERODYNAMIC FORCES DURING PARACHUTE OPENING

M. HORENSTEIN Boston Univ., Boston, MA and N. ROBERTS Journal of Aircraft (ISSN 0021-8669) vol. 31, no. 5 September-October 1994 p. 1084-1088 refs (BTN-95-EIX95062487532) Copyright

The work reported here seeks to determine the conditions, if any, under which electrostatic effects become comparable to aerodynamic forces during parachute opening. A simple Bernoulli model is used to estimate the principal aerodynamic forces during the early stages of inflation. The electrostatic forces during this period are found by computing the Coulomb attraction between two folds of parachute cloth charged to opposite polarity. These attractive Coulomb forces produce an inward 'electrostatic tension' that acts to oppose the outwardly directed tension caused by the Bernoulli pressure. The investigation involves theoretical analysis, small-scale wind-tunnel tests, and extrapolations to full-size parachutes. Our present estimates suggest that aerodynamic forces are two to three orders of magnitude larger than electrostatic forces for typical levels of air velocity and charge density. Typical levels of charge density are defined as those easily obtained in the laboratory via the process of triboelectrification (creation of static charge by friction). Author (EI)

A95-69244

STATE-SPACE REPRESENTATION OF AERODYNAMIC CHARACTERISTICS OF AN AIRCRAFT AT HIGH ANGLES OF ATTACK

M. GOMAN Central Aerohydrodynamic Inst., Moscow (Russia) and A. KHRABROV Journal of Aircraft (ISSN 0021-8669) vol. 31, no. 5 September-October 1994 p. 1109-1115 refs (BTN-95-EIX95062487536) Copyright

Mathematical modeling of unsteady aerodynamic forces and moments plays an important role in aircraft dynamics investigation and stability analysis at high angles of attack. In this article the state-

space representation of aerodynamic forces and moments for unsteady aircraft motion is proposed. Consideration of separated flow about an airfoil and flow with vortex breakdown about a slender delta wing gives the base for mathematical modeling using internal variables describing the flow state. Coordinates of separation points or vortex breakdown can be taken, e.g., as internal state-space variables. These variables are governed by some differential equations. Within the framework of the proposed mathematical model it is possible to achieve good agreement with different experimental data obtained in water and wind tunnels. These high angle-of-attack experimental results demonstrate considerable dependence of aerodynamic loads on motion time history. Author (EI)

A95-69245

AERODYNAMIC CHARACTERISTICS OF STRAKE VORTEX FLAPS ON A STRAKE-WING CONFIGURATION

LANCE W. TRAUB Univ of the Witwatersrand, Johannesburg (South Africa) and JUAN VANDERMERWE Journal of Aircraft (ISSN 0021-8669) vol. 31, no. 5 September-October 1994 p. 1116-1120 refs (BTN-95-EIX95062487537) Copyright

The effects of strake vortex flaps (SVFs), determined experimentally, on the aerodynamic characteristics of a strake-wing configuration are presented. SVFs may improve cruise performance over that of a planar strake by partially unloading the strake and generating a thrust component. The magnitude of the nose-up pitching moment may also be reduced by unloading the strakes. The use of SVFs as lateral control devices is also investigated. The results indicate that cruise performance is improved for all vortex flap deflection angles compared to planar strakes, with minimal or no concomitant penalty at high lift coefficients. Positive pitching moment is also substantially reduced. Differentially deflected strakes appear to be capable of generating significant rolling moments at high angles of attack. Author (EI)

A95-69247

RADIAL REEFING METHOD FOR ACCELERATED AND CONTROLLED PARACHUTE OPENING

CALVIN K. LEE US Army Natick Research, Natick, MA Journal of Aircraft (ISSN 0021-8669) vol. 31, no. 5 September-October 1994 p. 1124-1129 refs (BTN-95-EIX95062487539) Copyright

Future Army airdrop systems will require aerial insertion of cargo and personnel from low altitudes to minimize ground-fire hazards. A radial reefing method was developed as a potential candidate to meet this requirement. The radial reefing method involves selecting equally spaced radials of a parachute canopy and reefing these radials near the skirt; concurrently, the canopy fabric adjacent to the reefed radials is puckered. Reefing the canopy this way creates large fabric pockets near the skirt during initial canopy inflation, resulting in an accelerated and controlled parachute opening. This was confirmed by full-scale airdrop testing using single Army personnel and cargo parachutes. In addition to demonstrating promises for single-canopy low-altitude airdrop applications, the radial reefing method also shows potential to improve clustered parachute opening by minimizing canopy enfolding and slumping. Author (EI)

A95-69248

TWO-VARIABLE METHOD FOR BLOCKAGE WALL INTERFERENCE IN A CIRCULAR TUNNEL

X. QIAN Univ. of Tennessee Space Inst., Tullahoma, TN and C. F. LO Journal of Aircraft (ISSN 0021-8669) vol. 31, no. 5 September-October 1994 p. 1130-1134 refs (BTN-95-EIX95062487540) Copyright

A two-variable method for the blockage interference assessment in a circular tunnel has been developed. The Prandtl-Glauert equation is applied to describe the subsonic flowfield. Analytical solutions are obtained using Fourier transform technique, by either assuming a given body of revolution profile or representing the body of revolution by a source-sink distribution. Numerical examples computed by a small perturbation inviscid code TSFOIL and a panel

02 AERODYNAMICS

method code PMARC are utilized to validate the developed two-variable method for open jet and closed circular tunnels. Good agreement has been found on interference pressure coefficient assessment between the solutions of the two-variable method and inviscid code predictions. Results have demonstrated that the two-variable method for circular tunnel blockage wall interference is ready for experimental verification. Author (EI)

A95-69322

MEASUREMENT BY COHERENT ANTI-STOKES RAMAN SCATTERING IN THE R5CH HYPERSONIC WIND TUNNEL
M. LEFEBVRE, B. CHANETZ, T. POT, P. BOUCHARDY, and PH. VARGHESE Recherche Aerospatiale/Aerospace Research (ISSN 0034-1223) no. 4 1994 p. 295-298 refs
(BTN-95-EIX95112523811) Copyright

Rotational temperature and nitrogen number density were measured along the stagnation line in a bow shock in front of a cylinder at Mach number 10. The dual-line coherent anti-Stokes Raman scattering (DLCARS) technique was used to obtain spatially resolved measurements of the rotational distribution of N. The experiment was performed in the R5Ch hypersonic blow-down wind tunnel at ONERA. Good agreement was found between temperature and density profiles obtained by DLCARS and those predicted by a Navier-Stokes solver. Velocity measurements in the freestream flow were also performed using the single-shot time-domain CARS technique. EI

N95-19546# Aircraft Research Association Ltd., Bedford (England). **AN INVESTIGATION OF DRAG REPEATABILITY IN HALF MODEL TESTING IN THE ARA TRANSONIC WIND TUNNEL**
I. F. BURNS, J. E. GREEN, and D. R. STANNILAND Oct. 1993 28 p Presented at the 80th STA Meeting, Koeln, Germany, 17-19 Oct. 1993

(ARA-MEMO-392) Avail: CASI HC A03/MF A01

In 1990 the variability of drag measurements on a half model in the ARA Transonic Tunnel increased from the usual one drag count to between two and three drag counts. An investigation showed the primary source of the variability to be a damaged balance, with a possible air leak into the tunnel plenum chamber as an additional contributor. When these sources had been eliminated, drag repeatability was restored to approximately one count. It was found however that this was mainly a systematic, diurnal variation, caused by cyclic variation of the heat exchange between the tunnel airflow and the plenum chamber structure. A procedure was established, using measured sidewall pressures, to correct for this effect and thereby reduce drag variability within a test series to rather less than one count. As a further improvement to the tunnel for half model testing, the test section has been modified to extend the region of uniform flow and improve the aerodynamics of the diffuser. Initial results of the commissioning trials with this modification are reported. Author

N95-19772# Aircraft Research Association Ltd., Bedford (England). **MULTIPOINT PRESSURE MEASUREMENTS ON CONTINUOUSLY MOVING WIND TUNNEL MODELS**
DAVID G. COULTON Sep. 1993 10 p Presented at the ICIASF 1993, St. Louis, France, 20-23 Sep. 1993
(ARA-MEMO-391) Avail: CASI HC A02/MF A01

Tests have been performed in the large Transonic Wind Tunnel at the Aircraft Research Association Limited, Bedford, England, to investigate the possibility of improving productivity by acquiring pressure data from continuously moving models. The experimental work has been centered around the use of Electronically Scanned Pressure (ESP) Modules and has been restricted to the measurement of pressures whose absolute value has been changing relatively smoothly with model attitude. The paper shows that good agreement has been obtained between data acquired whilst the model was moving continuously and when measured in the traditional move and pause mode of operation. The recording of pressure data whilst the model incidence is continually moving permits wind tunnel testing to be performed more efficiently with a subsequent reduction in energy and overall costs. Author

N95-19863 Naval Research Lab., Washington, DC. **WIND TUNNEL TESTS OF A 42 INCH DIAMETER SELF-STARTING AUTOGYRO ROTOR Interim Report**
STEVEN K. TAYMAN 31 May 1994 19 p Limited Reproducibility: More than 20% of this document may be affected by microfiche quality (AD-A279922; NRL/MR/5710-94-7485) Avail: Issuing Activity (Defense Technical Information Center (DTIC))

The autogyro is being investigated for potential use as a small unmanned air vehicle for Navy electronic warfare missions. This paper presents wind tunnel test results for a 42 inch diameter unpowered rotor with coupling between feathering and flapping that allows for self-starting from a vertical descent. Aerodynamic performance is given for several blade pitch angles and angles of attack. DTIC

03

AIR TRANSPORTATION AND SAFETY

Includes passenger and cargo air transport operations; and aircraft accidents.

A95-68260

CORROSION PREVENTION AND CONTROL
Aerospace Engineering (Warrendale, Pennsylvania) (ISSN 0736-2536) vol. 14, no. 1 January-February 1994 p. 49-52
(BTN-95-EIX95031502753) Copyright

With the operation of transport airplanes well beyond their original economic design life suggests an increasing likelihood of significant corrosion combined with fatigue damage. This has prompted the development of corrosion prevention and control standards for all commercial transport planes. Boeing has proposed a structural audit to determine the minimum maintenance requirements for assuring continuing airworthiness. Boeing damage tolerance assessments are based on the assumption that if fatigue damage occurs, it will initiate in the structural component which is most difficult to inspect. Crack growth rates and airplane residual strength are determined on the basis of typical operating loads with stresses based on sound structure with little material loss due to corrosion. Corrosion control is one way to promote continuing airworthiness. EI

N95-19720# Federal Aviation Administration, Washington, DC. **FEDERAL AVIATION REGULATIONS, PART 91. GENERAL OPERATING AND FLIGHT RULES. CHANGE 8**
21 Jun. 1994 12 p See also PB94-194883
(PB94-217445) Avail: CASI HC A03/MF A01

This change to Part 91, General Operating and Flight Rules, incorporates two amendments: Amendment 91-241, Special Visual Flight Rules (SVFR), Denver, CO which delays the effective date of May 15, 1994 indefinitely; and Amendment 91-242, Emergency Locator Transmitters, effective June 21, 1994. This amendment affects Section 91.207. NTIS

N95-19793# National Transportation Safety Board, Washington, DC. **SPECIAL INVESTIGATION REPORT: MAINTENANCE ANOMALY RESULTING IN DRAGGED ENGINE DURING LANDING ROLLOUT. NORTHWEST AIRLINES FLIGHT 18, BOEING 747-251B, N637US, NEW TOKYO INTERNATIONAL AIRPORT, NARITA, JAPAN, 1 MAR. 1994**
20 Dec. 1994 67 p
(PB94-917006; NTSB/SIR-94/02) Avail: CASI HC A04/MF A01

This special investigation report addresses the maintenance activity at Northwest Airlines that led to the accident involving Northwest Airlines flight 18, a B-747, during the airplane's intermediate stop at Narita, Japan, while it was flying from Hong Kong to John F. Kennedy International Airport, Jamaica, New York, on March 1, 1994. Safety issues in the report focused on maintenance

operations and maintenance work environments. Safety recommendations concerning these issues were made to the Federal Aviation Administration and to Northwest Airlines. Author

N95-19805 Galaxy Scientific Corp., Pleasantville, NJ.
ROTORCRAFT DITCHINGS AND WATER-RELATED IMPACTS THAT OCCURRED FROM 1982 TO 1989, PHASE 1 Final Report

CHARLES C. CHEN, M. MULLER, and K. M. FOGARTY Oct. 1993
 116 p Limited Reproducibility: More than 20% of this document may be affected by microfiche quality
 (Contract(s)/Grant(s): DTFA03-89-C-00043)
 (AD-A279164; DOT/FAA/CT-92/13) Avail: Issuing Activity (Defense Technical Information Center (DTIC))

This report documents Phase 1 of a two-phase program that investigates ditchings and water-related impacts for rotorcraft that occurred during the years 1982-1989. The main sources of accident data were the National Transportation Safety Board and the U.S. Army Safety Center. Data from a total of 89 accidents were obtained and examined for this study. Of these, 77 cases satisfied the criteria for inclusion into the database, 67 from the NTSB and 10 from the U.S. Army. In this report the impact and post-impact conditions were categorized to assess rotorcraft behavior and occupant survivability. Three impact scenarios and two post-impact scenarios were established. Special emphasis was placed on examining rotorcraft flotation equipment performance and post-impact survivability. Six representative case studies are presented to demonstrate aspects peculiar to the rotorcraft water impact and postimpact sequence that could not be adequately covered by the statistical categorizations alone. Recommended areas requiring enhancement of occupant survivability are presented. DTIC

04

AIRCRAFT COMMUNICATIONS AND NAVIGATION

Includes digital and voice communication with aircraft; air navigation systems (satellite and ground based); and air traffic control.

A95-68185
HIGH ACCURACY NAVIGATION AND LANDING SYSTEM USING GPS/IMU SYSTEM INTEGRATION

JOCHEN MEYER-HILBERG Deutsche Aerospace AG, Ulm (Germany) and THOMAS JACOB IEEE Aerospace and Electronic Systems Magazine (ISSN 0885-8985) vol. 9, no. 7 July 1994 p. 11-17 refs
 (BTN-94-EIX94441386129) Copyright

The accuracy, integrity, and continuity of function requirements for automatic landing systems using satellite navigation systems is discussed. Such a landing system is the Integrated Navigation and Landing System (INLS) developed by Deutsche Aerospace (DASA/Ulm, Germany). The system concept of the INLS is presented. It is shown how an INLS, based on system integration of a satellite navigation system (e.g., GPS) in realtime differential mode with an inertial measurement unit (IMU) in the accuracy class of an attitude and heading reference system (AHRS), can meet the requirements: the results given are mainly devoted to the accuracy issues. Using Kalman filter techniques, an in-flight calibration of the inertial measurement unit is performed. The advantage of system integration, especially in dynamic flight conditions and during phases of flight with satellite masking, is explained. The accuracy, integrity, and continuity of function of the INLS were proven by means of flight tests in a commuter aircraft using a laser tracker as a reference. These flight tests have shown that the short-term accuracy (less than 60 seconds) of the AHRS used within the INLS has been improved from low cost sensor quality to the accuracy of a high quality laser inertial navigation system (LNIS). With the presented INLS, a landing at any airfield, not equipped with conventional instrument landing system (ILS) or microwave landing system (MLS), will be possible by using a very cost effective system. Even

curved approaches can be realized. Also holding patterns with recurring satellite masking can be flown without significant accuracy degradation. The INLS is a high accuracy navigation and landing system designed to be used instead of conventional landing systems at small airfields and to fill operational gaps of conventional navigation and landing systems in cruise and approach on large airports. Author (EI)

A95-68187
GPS/GLONASS/INS TEST PROGRAM

STEFAN VIEWEG Technical Univ Braunschweig, Braunschweig (Germany) and WOLFGANG LECHNER IEEE Aerospace and Electronic Systems Magazine (ISSN 0885-8985) vol. 9, no. 7 July 1994 p. 23-28 refs
 (BTN-94-EIX94441386131) Copyright

Under contract of different German Ministries a test program investigating the combinations of GPS, GLONASS, and inertial navigation is being carried out since 1991. Besides other goals, the aim of the project is to investigate the capabilities of GLONASS in comparison to GPS, to realize a combined GLONASS/INS solution, and to perform joint processing of GPS and GLONASS raw data. The paper describes the test procedures and presents some of the results. This includes the comparison of DGPS with stand-alone GLONASS and GLONASS/INS under different dynamic situations, e.g., driving tests, flight tests, and also the presentation of results of combined GPS/GLONASS data processing, which was successfully achieved in March '93 for the first time. The results show the potential of the non-SA-degraded GLONASS and the advantage of using both GPS and GLONASS for combined solutions. Author (EI)

A95-68188
USE OF MOBITEK WIRELESS WIDE AREA NETWORKS AS A SOLUTION TO LAND-BASED POSITIONING AND NAVIGATION

THOMAS T. YANG RAM Mobile Data, Woodbridge, NJ and YAN YIP KAI IEEE Aerospace and Electronic Systems Magazine (ISSN 0885-8985) vol. 9, no. 7 July 1994 p. 29-35
 (BTN-94-EIX94441386132) Copyright

The emergence of land-based positioning and navigation systems is the direct result of advancements in technologies relating to geographic information, wireless data communication, and navigation. The increasing demand for these systems has stimulated their rapid development. This paper identifies the wide variety of land-based positioning and navigation systems and classifies them into five groups. The basic system elements that are required in all land-based positioning and navigation systems are also discussed. A proposed system infrastructure that supports the five types of land-based positioning and navigation systems is described. The specific technologies integrated in this proposed infrastructure include the Global Positioning System (GPS), differential GPS, and the MOBITEK wireless wide area packet data networks. Real-time wireless mobile data communication is a key component of any land-based positioning and navigation system. Finally, the evaluation criteria necessary for field testing a pilot land-based positioning and navigation system are presented. This pilot system is used to determine the feasibility and effectiveness of the proposed system design. Author (EI)

A95-68278
EVALUATION OF THE RADIO FREQUENCY SUSCEPTIBILITY OF COMMERCIAL GPS RECEIVERS

JOHN K. DAHER Georgia Tech. Research Inst., Atlanta, GA, JOSEPH M. HARRIS, and MARK L. WHEELER IEEE Aerospace and Electronic Systems Magazine (ISSN 0885-8985) vol. 9, no. 10 October 1994 p. 21-25 refs
 (BTN-95-EIX95042474624) Copyright

The radio frequency (RF) susceptibility characteristics of two commercial Global Positioning System (GPS) receivers were evaluated. A first-order analysis was performed to predict the receiver susceptibility thresholds based on the receiver sensitivity and processing gain. The receiver susceptibility thresholds in the post-

04 AIRCRAFT COMMUNICATIONS AND NAVIGATION

acquisition mode were then measured for various interference signal frequencies and modulations. Both receivers exhibited very low susceptibility thresholds to in-band continuous wave (CW) signals. In addition, both receivers could be over-driven with an out-of-band signal. In this state the receivers indicated acceptable figures of merit despite loss of satellite signal lock. Author (EI)

A95-69243*

DEVELOPMENT AND FLIGHT TEST OF A DEPLOYABLE PRECISION LANDING SYSTEM

ALEX G. SIM, JAMES E. MURRAY, DAVID C. NEUFELD, and R. DALE REED Journal of Aircraft (ISSN 0021-8669) vol. 31, no. 5 September-October 1994 p. 1101-1108 refs (BTN-95-EIX95062487535) Copyright

A joint NASA Dryden Flight Research Facility and Johnson Space Center program was conducted to determine the feasibility of the autonomous recovery of a spacecraft using a ram-air parafoil system for the final stages of entry from space that included a precision landing. The feasibility of this system was studied using a flight model of a spacecraft in the generic shape of a flattened biconic that weighed approximately 150 lb and was flown under a commercially available, ram-air parachute. Key elements of the vehicle included the Global Positioning System guidance for navigation, flight control computer, ultrasonic sensing for terminal altitude, electronic compass, and onboard data recording. A flight test program was used to develop and refine the vehicle. This vehicle completed an autonomous flight from an altitude of 10,000 ft and a lateral offset of 1.7 miles that resulted in a precision flare and landing into the wind at a predetermined location. At times, the autonomous flight was conducted in the presence of winds approximately equal to vehicle airspeed. Several novel techniques for computing the winds postflight were evaluated. Future program objectives are also presented. Author (EI)

A95-69328

ON-THE-FLY CARRIER PHASE AMBIGUITY RESOLUTION FOR PRECISE AIRCRAFT LANDING

HELMUT BLOMENHOFER Univ FAF Munich, Neubiberg, Germany, GUENTER W. HEIN, and DAVID WALSH International Journal of Satellite Communications (ISSN 0737-2884) vol. 12, no. 5 September-October 1994 p. 489-497 refs (BTN-95-EIX95112522535) Copyright

Successful GPS on-the-fly (OTF) carrier phase ambiguity resolution for precise positioning at the centimeter level has already been demonstrated. This has usually been in good observation conditions, e.g. over short distances, lots of satellites, P-code pseudoranges available, and small unmodeled errors. In order for GPS to fulfill the rigorous ICAO Cat. 3 precise landing navigation requirements, centimeter-level accuracy must also be obtained in more realistic conditions, e.g. A-S on, high-unmodeled errors, and less than six satellites. Integrating GPS with other sensors, e.g. INS, is likely to aid ambiguity resolution in such conditions, but there are limitations. After discussing critically the OTF methods, approaches are examined which will provide the precise accuracy, reliability, and integrity required. Combining GPS with one or more pseudolites to provide an extra geometrical constraint to aid ambiguity resolution is described. Flight tests using different configurations of pseudolites are carried out and analyzed. Author (EI)

A95-69329

RESULTS AND PERFORMANCE OF MULTI-SITE REFERENCE STATION DIFFERENTIAL GPS

GORDON T. JOHNSTON Racal Survey Ltd, Norfolk, United Kingdom International Journal of Satellite Communications (ISSN 0737-2884) vol. 12, no. 5 September-October 1994 p. 475-488 refs (BTN-95-EIX95112522534) Copyright

The infrastructure and concept of two multisite reference station differential GPS (DGPS) options being offered to marine users by Racal Survey are described in some detail. The infrastructure of the Racal SkyFix system is briefly outlined, followed

by descriptions of Racal's internetting and network capabilities. Comparison between the two systems are made and results are presented. EI

A95-69332

INTEGRATED GPS/GLONASS NAVIGATION: ALGORITHMS AND RESULTS

PETER RABY Univ of Leeds, Leeds, United Kingdom and PETER DALY International Journal of Satellite Communications (ISSN 0737-2884) vol. 12, no. 5 September-October 1994 p. 443-451 refs (BTN-95-EIX95112522531) Copyright

The presence of selective availability (SA) on GPS has led to a variety of proposals for mitigation of its effects, for example combining GPS with other sensors or by identifying and removing the SA using redundant information in the position solution. A further method for reducing the impact of SA is the combination of GPS and GLONASS measurements. GLONASS does not have any deliberate degradation. This paper describes several algorithms for combining GPS and GLONASS measurements in real time on a single receiver. There are two least squares solutions using the code phase measurements alone: one with the measurements from both systems weighted equally, and one with the measurements weighted by the covariance of the measurements. Kalman filters with no SA model, and first- and second-order models, using both the code and carrier phase to estimate user position and velocity, are also implemented. Two different adaptive schemes are compared which attempt to identify SA model parameters in real time. The algorithms are compared in terms of their positioning accuracy, computational overhead, and robustness. A ten-channel GPS/GLONASS receiver developed at The University of Leeds is used to provide satellite data for the evaluation of the different methods. Author (EI)

A95-69333

EFFECT OF BROADCAST AND PRECISE EPHEMERIDES ON ESTIMATES OF THE FREQUENCY STABILITY OF GPS NAVSTAR CLOCKS

THOMAS B. MCCASKILL Naval Cent for Space Technology, Washington, DC, United States, WILSON G. REID, JAMES A. BUISSON, and HUGH E. WARREN International Journal of Satellite Communications (ISSN 0737-2884) vol. 12, no. 5 September-October 1994 p. 435-441 refs (BTN-95-EIX95112522530) Copyright

Frequency stability analysis of on-orbit Navstar clocks is performed by the Naval Research Laboratory using both the broadcast and the precise post-processed ephemerides. The phase offset between the Navstar clock and the reference clock is computed from pseudorange measurements obtained by dual-frequency GPS receivers at the five GPS monitor sites and at the U.S. Naval Observatory precise-time site. The broadcast ephemerides are generated at the GPS master control station by a Kalman filter using data collected from the five GPS monitor stations. The precise post-processed ephemerides are generated by the Defence Mapping Agency (DMA) using data collected from the GPS monitor sites and from five additional DMA monitor sites. The frequency stability is estimated for two Navstar cesium clocks - a Block 1 cesium clock (Navstar 9) and a Block 2 cesium clock (Navstar 23) - using both the broadcast and the precise ephemerides. A significant improvement in the estimate of the frequency stability of the Block 2 clocks has been achieved using the precise ephemeris. Author (EI)

A95-69334

SPACE FLIGHT TESTS OF ATTITUDE DETERMINATION USING GPS

CLARK E. COHEN Stanford Univ, Stanford, CA, United States, E. GLENNLIGHTSEY, BRADFORD W. PARKINSON, and WILLIAM A. FEES International Journal of Satellite Communications (ISSN 0737-2884) vol. 12, no. 5 September-October 1994 p. 427-433 refs (BTN-95-EIX95112522529) Copyright

Preliminary space flight results of attitude determination using GPS are presented from a spacecraft in low Earth orbit. Relative

position measurements accurate to the sub-centimeter level are made among multiple GPS antennas mounted on the space vehicle. A Trimble Navigation TANS Quadrex (a GPS receiver specially adapted for attitude determination by Stanford University) is used as a differential carrier phase sensor for the flight. Four GPS antennas are mounted on the zenith face of RADCAL, a polar orbiting, gravity-gradient-stabilized Air Force Space Test Program Satellite, built by Defence Systems, Inc. The four antennas are equally spaced about the perimeter of the 30 inch diameter cylindrical spacecraft bus. The Quadrex receiver measures the phase of the L-band GPS carrier (1575 MHz) at each of up to four antennas for up to six GPS satellites simultaneously. From these measurements, an initial assessment of attitude determination in space is performed in post-processing. For RADCAL, the attitude solution is greatly overdetermined. In a preliminary evaluation of system performance, the system accuracy is determined through measurement self-consistency. Analysis of the attitude motion in the context of a gravity gradient dynamic model yields further insight into the system performance. Author (EI)

N95-19810 MiTech, Inc., Pleasantville, NJ.

RESEARCH REQUIREMENTS FOR FUTURE VISUAL GUIDANCE SYSTEMS Final Report

HAROLD W. OLSON and THOMAS H. PAPROCKI Feb. 1994 101 p Limited Reproducibility: More than 20% of this document may be affected by microfiche quality (AD-A279188; DOT/FAA/CT-93/49) Avail: Issuing Activity (Defense Technical Information Center (DTIC))

Airport visual aids provide essential information to pilots to facilitate their tasks of taking off, landing, and maneuvering the aircraft on the airport surfaces. Application of state-of-the-art technology can significantly improve the design and performance of the lighting, marking, and signage visual aids that provide the pilots with essential air and ground movement guidance. This study was undertaken to identify deficiencies in existing visual guidance systems and to forecast or project needs of the future. It also describes possible applications of new technology for resolving existing deficiencies and developing state-of-the-art visual guidance systems of the future. The study report identifies a number of potential research areas and new technologies of potential benefit to visual guidance. The recommended research areas are grouped by category according to phase of operation. DTIC

05

AIRCRAFT DESIGN, TESTING AND PERFORMANCE

Includes aircraft simulation technology.

A95-66300

RECENT TRENDS IN BALLOON FLIGHTS FROM TIFR'S NATIONAL BALLOON FACILITY, HYDERABAD

S. V. DAMLE Tata Institute, Bombay, India and M. N. JOSHI Tata Institute, Bombay, India Balloon technology and observations; Symposium P3 of the COSPAR Plenary Meeting, 29th, Washington, DC, Aug. 28-Sept. 5, 1992. A95-66276 Advances in Space Research (ISSN 0273-1177) vol. 14, no. 2 February 1994 p. (2)157-(2)167 Research sponsored by the Indian Space Research Organ., the India Meteorological Dept. and the National Airport Authority Copyright

The Tata Institute of Fundamental Research (TIFR), Bombay established the TIFR National Balloon Facility (TNBF) at Hyderabad near the geomagnetic equator, in 1969. The TNBF undertakes design/fabrication of stratospheric balloons and is also responsible for balloon launch, tracking, data retrieval and recovery of scientific payload after the flight. It provides radio telemetry, telecommand, tracking and undertakes mechanical and electrical integration and test of the scientific payloads. The TNBF has also its own R&D program in balloon engineering and support instrumentation. To-

date 419 balloon flights have been carried out for space astronomy (x-ray, gamma-ray, infrared) and atmospheric sciences (ozone, aerosol, electric field and conductivity). In future several balloon flights are planned for the International Geosphere Biosphere Program (IGBP) and for the space astronomy program.

Author (Herner)

A95-66302

THE SCIENTIFIC BALLOONING IN RUSSIA

V. I. LAPSHIN Academy of Sciences of Russia, Moscow, Russia, L. L. LAZUTIN Academy of Sciences of Russia, Apatity, Russia, S. I. NIKOLSKY Academy of Sciences of Russia, Moscow, Russia, and YU. I. STOZKHOV Academy of Sciences of Russia, Moscow, Russia Balloon technology and observations; Symposium P3 of the COSPAR Plenary Meeting, 29th, Washington, DC, Aug. 28-Sept. 5, 1992. A95-66276 Advances in Space Research (ISSN 0273-1177) vol. 14, no. 2 February 1994 p. (2)173-(2)174 Copyright

Scientific research in Russia based on high altitude balloons (aerostats) began in the sixties but only after 1975 were they organized as regular research programs and a special coordinating agency - Commission on Balloon Research of the Academy of Sciences of the (former) USSR - was founded for their support. In 1974, the series of international SAMBO campaigns started during an eight year period. Five winter balloon expeditions were organized with 15-25 balloon flights from the Kiruna site (Sweden) to the Ural mountains region in Russia. There are four balloon sites for scientific ballooning in Russia. The Volsk Balloon Facility is a central one, where experiments with all types of balloons are performed. The flight altitudes are 30-35 km, the duration ranges from hours to several days; the payload weights are about 500 kg. Very brief descriptions are given of the three other sites and their flights.

Author (revised by Herner)

A95-66305

LONG DURATION BALLOONS

JAMES L. RAND Winzen International Inc., San Antonio, TX, US Balloon technology and observations; Symposium P3 of the COSPAR Plenary Meeting, 29th, Washington, DC, Aug. 28-Sept. 5, 1992. A95-66276 Advances in Space Research (ISSN 0273-1177) vol. 14, no. 2 February 1994 p. (2)183-(2)190 Copyright

Long duration flight in the middle stratosphere is a well established need of the science community. Many balloon systems have been developed to satisfy this need, with varying degrees of success. This paper will review the requirements and those systems that have been suggested to achieve various mission goals and objectives. Each system has limitations of one sort or another. It is intended to place these various limitations into perspective so that the scientist may choose an appropriate existing system or recommend the development of an advanced system that meets his mission requirements. The status of current ballasted zero pressure balloon technology will be reviewed as a baseline from which other systems may be compared. Superpressure balloon programs will be reviewed as well as the hybrid systems that combine both types of balloons. Other systems such as the Radiation Controlled Balloon and the Mongolfier Infrared system have long duration capability with some altitude excursions. Each has a place in filling the needs of science today.

Author (Herner)

A95-66500

COMPARISON OF THEORY AND EXPERIMENT FOR NON-LINEAR FLUTTER AND STALL RESPONSE OF A HELICOPTER BLADE

D. M. TANG Duke Univ., Durham, NC and E. H. DOWELL Journal of Sound and Vibration (ISSN 0022-460X) vol. 165, no. 2 August 8, 1993 p. 251-276 refs (BTN-94-EIX94351108100) Copyright

The purpose of the present paper is to study the flutter instability and forced response of a nonrotating helicopter blade model with

05 AIRCRAFT DESIGN, TESTING AND PERFORMANCE

a parabolic or cubic and freeplay torsional stiffness nonlinearity based upon the semi-empirical (linear and) nonlinear ONERA stall aerodynamic model. An experiment has also been carried out in the Duke University low speed wind tunnel. The wind tunnel test results show good agreement between theory and experiment for linear and nonlinear flutter instability; for periodic, limit cycle and chaotic flutter motion and forced response behavior; and for the effects of an initial disturbance on nonlinear flutter instability. Comparisons of the results from theory and experiment are helpful in understanding physically the nonlinear aeroelasticity phenomena and chaotic oscillations. Author (EI)

A95-68300

BILINEAR FORMULATION APPLIED TO THE RESPONSE AND STABILITY OF HELICOPTER ROTOR BLADE

GRZEGORZ KAWIECKI Univ. of Tennessee, Knoxville, TN and NITHIAM TI SIVANERI AIAA Journal (ISSN 0001-1452) vol. 32, no. 10 October 1994 p. 2036-2043 refs (BTN-95-EIX95042474400) Copyright

A time finite element method based on Hamilton's law of varying action is applied to the analysis of helicopter blade dynamics. The bilinear formulation of Hamilton's law of varying action is used to discretize the temporal dependence of the equations of motion. Variable-order shape and test functions based on Legendre polynomials are used. Two approaches for the numerical implementation of the bilinear formulation are used. One approach obtains the response of a general dynamic system using marching in time. The other approach is based on the assumption that the solution is identical at the beginning and end of one period. Therefore, this approach is suitable for periodic systems. The bilinear formulation in imposed periodicity mode is used to compute the response of a rigid blade with flap and lag degrees of freedom in forward flight. The bilinear formulation in marching mode is applied to find the Floquet transition matrix necessary to test the stability of blade motion. Author (EI)

A95-68313

POWERED LIFT FOR LAND AND SEA

VIRGINIA C. LOPEZ Aerospace Industries Associations Aerospace America (ISSN 0740-722X) vol. 32, no. 7 July 1994 p. 38-43 (BTN-95-EIX95041503010) Copyright

The USAF's hoped-for complement to the F-22 was the recently canceled multi-role fighter (MRF). The Navy is going to need a replacement for the F/A-18, AV-8B, and possibly some F-14 missions. Among the possible choices is the Common Affordable Lightweight Fighter, another attempt to build a jet that will work for both the Air Force and the Navy. This remains a daunting task since, with the exception of the FJ Fury, no U.S. land-based jet has ever been successfully adapted to shipboard duty. The difference this time is the use of powered lift technology. If it works, it will permit a land-based aircraft to operate not only from short, unprepared fields, but also from ships, with no need for the heavy reinforcement and control modifications necessary for operating afloat. The most common name for the proposed powered lift solution now being considered is Advanced Short Takeoff/Vertical Landing (ASTOVL). Originally a Navy-sponsored project, it has now come under the wing of ARPA because of its advanced technology and its multiservice application. The propulsion concept that ARPA appears to favor is the remotely powered lift fan. The lift fan as envisioned by ARPA for ASTOVL can be thought of as a lift engine with a remote gas generator. ARPA's idea is to harness the excess thrust power developed by the gas generator to drive the lift engine. EI

A95-68349

LAUNCHER WING-LEADING-EDGE DESIGN

G. REICH, U. TRABANDT, and K. KELLER Aerospace Engineering (Warrendale, Pennsylvania) (ISSN 0736-2536) vol. 14, no. 9 September 1994 p. 17-21 (BTN-95-EIX95042477110) Copyright

A C/SiC thermostructural concept was selected for the wing leading edge of a two-stage-to-orbit vehicle's first stage to help

reduce costs of space transportation. In an examination of 12 versions of the wing leading edge, researchers selected the stringer-stiffened shell version for the baseline design due to these advantages: (1) stringers increase the stiffness and lead to low deflection; (2) higher stability results to reduced wall thickness and mass; (3) moderate manufacturing complexity and cost for the ceramic matrix composites (CMC) elements; (4) possibility of on-site manufacturing of stringers; and (5) possibility of laminate optimization for the CMC prepegs. EI

A95-68356

TWO-POINT TRANSONIC AIRFOIL DESIGN USING OPTIMIZATION FOR IMPROVED OFF-DESIGN PERFORMANCE

J. O. HAGER Univ. of Illinois, Urbana, IL, S. EYI, and K. D. LEE Journal of Aircraft (ISSN 0021-8669) vol. 31, no. 5 September-October 1994 p. 1143-1147 refs (BTN-95-EIX95062487542) Copyright

A two-point, aerodynamic design method is presented that improves the aerodynamic performance of transonic airfoils over a range of the flight envelope. It couples an Euler flow solver and a numerical optimization tool. The major limitation of single-point design is the poor off-design performance. Two-point design is used to extend the optimized performance range over more of the desired flight envelope. The method is applied to several transonic flow design points, and the results are compared to single-point design results. The secondary design points are chosen by varying the Mach number and the angle of attack. The two-point designs perform better than the single-point design over the design-point range. Author (EI)

A95-68361

USING ADAPTIVE STRUCTURES TO ATTENUATE ROTARY WING AEROELASTIC RESPONSE

FRED NITZSCHE DLR Inst. of Aeroelasticity, Goettingen (Germany) and ELMAR J. BREITBACH Journal of Aircraft (ISSN 0021-8669) vol. 31, no. 5 September-October 1994 p. 1178-1188 refs (BTN-95-EIX95062487547) Copyright

This article investigates the feasibility of employing adaptive material to build both sensors and actuators to attenuate the higher harmonic loads developed at the helicopter rotor blades using the individual blade control (IBC) concept. Both the first elastic flatwise bending (second for hingeless rotors) and the first elastic torsion modes of a single blade deserve special attention in the vibration control. Theoretical investigations, supported by wind-tunnel and flight tests, confirmed that these modes are responsible for the larger amplitude loads at 3/rev in four-blade hingeless rotors. This is a situation for which IBC, based on a collocated actuator-sensor arrangement along the blade, and tailored to act specifically on the bending and the torsion modes, is expected to bring further improvements to the reduction of the overall dynamic response of rotary wings. The results indicate that there are already real situations for which the adaptive material has enough power to accomplish the task without saturation of the applied electrical field. Author (EI)

A95-68362* National Aeronautics and Space Administration. Langley Research Center, Hampton, VA.

COUPLING EQUIVALENT PLATE AND FINITE ELEMENT FORMULATIONS IN MULTIPLE-METHOD STRUCTURAL ANALYSES

GARY L. GILES National Aeronautics and Space Administration. Langley Research Center, Hampton, VA and KEITH NORWOOD Journal of Aircraft (ISSN 0021-8669) vol. 31, no. 5 September-October 1994 p. 1189-1196 refs (BTN-95-EIX95062487548) Copyright

A coupled multiple-method analysis procedure for use late in conceptual design or early in preliminary design of aircraft structures is described. Using this method, aircraft wing structures are represented with equivalent plate models, and structural details such as engine/pylon structure, landing gear, or a 'stick' model of a fuselage are represented with beam finite element models. These two analy-

sis methods are implemented in an integrated multiple-method formulation that involves the assembly and solution of a combined set of linear equations. The corresponding solution vector contains coefficients of the polynomials that describe the deflection of the wing and also the components of translations and rotations at the joints of the beam members. Two alternative approaches for coupling the methods are investigated; one using transition finite elements and the other using Lagrange multipliers. The coupled formulation is applied to the static analysis and vibration analysis of a conceptual design model of a fighter aircraft. The results from the coupled method are compared with corresponding results from an analysis in which the entire model is composed of finite elements.

Author (EI)

A95-68370

MINIMUM SINK-SPEED IN POWER-OFF GLIDE

EDMUND V. LAITONE Univ. of California, Berkeley, CA Journal of Aircraft (ISSN 0021-8669) vol. 31, no. 5 September-October 1994 p. 1223-1224 refs

(BTN-95-EIX95062487556) Copyright

Some aeronautical engineers who have participated in glider competition have insisted that the minimum sink-speed occurs at a trim velocity that is less than $V_{(sub\ mp)}$, the velocity corresponding to minimum power required for steady level flight. It is usually assumed that the trim lift coefficient $C_{(sub\ L.mp)}$ gives the minimum sink-speed for any airplane in power-off glide. The analysis presented uses the theoretical drag polar to derive a new relation that proves that the minimum sink-speed does occur with a trim lift coefficient that is slightly greater than $C_{(sub\ L.mp)}$. EI

A95-69213

NAVIER-STOKES COMPUTATION OF A VISCOUS OPTIMIZED WAVERIDER

NARUHISA TAKASHIMA Univ of Maryland, College Park, MD, United States and MARK J. LEWIS Journal of Spacecraft and Rockets (ISSN 0022-4650) vol. 31, no. 3 May-June 1994 p. 383-391 (BTN-95-EIX95041503782) Copyright

The on-design and off-design performance of a Mach 6 viscous optimized waverider was calculated by solving the three-dimensional Navier-Stokes equations. The numerical calculation was done using CFL3D, an implicit upwind-biased finite volume algorithm. The waverider geometry was generated for the design condition of Mach 6 flight at an altitude of 30 km using MAXWARP, a waverider design code. The waverider shape studied was designed from a conical flowfield and optimized for maximum lift-over-drag ratio. MAXWARP was validated by comparing the performance prediction of the design code with the results from the Navier-Stokes calculation. The effects of rounding the leading edges on the performance of the waverider was found to be negligible. The performance of the Mach 6 optimized waverider at off-design conditions of Mach 4 and 8 compared well to the performance of the viscous optimized waveriders designed for Mach 4 and Mach 8.

Author (EI)

A95-69214

HYPersonic WAVERIDER TEST VEHICLE: A LOGICAL NEXT STEP

DOUGLAS J. TINCHER Science Applications Int Corp, Huntsville, AL, United States and DAVID W. BURNETT Journal of Spacecraft and Rockets (ISSN 0022-4650) vol. 31, no. 3 May-June 1994 p. 392-399

(BTN-95-EIX95041503783) Copyright

Hypersonic waveriders have long been associated with extremely high lift-to-drag ratios (L/D) and exotic configurations with a wealth of investigation occurring from the 1950s until their fall from favor in the 1970s. Over the past few years, they have undergone a major investigative reemphasis brought about by resolution of major historical criticisms, namely poor L/D performance when viscous effects were included, and poor packagability. Although University of Maryland research resolved the viscous effects degradation issue with the viscous optimized hypersonic waverider family, this paper

discusses modified versions of the Maryland waverider family that dramatically improve packagability making them suitable for use in many of today's and tomorrow's hypersonic missions. The paper discusses their transition from idealized shapes to one vision of near-term reality, a low-cost maneuvering hypersonic test vehicle based on a focused development and validation effort. Waverider flight demonstration is crucial to enabling high-confidence technology transfer to the wealth of supersonic/hypersonic vehicle opportunities where high aerodynamic efficiency is a fundamental requirement. The paper closes by briefly discussing the suitability of these modified waveriders for application to interplanetary missions using aerogravity-assist maneuvering.

Author (EI)

A95-69242* National Aeronautics and Space Administration. Langley Research Center, Hampton, VA.

INTERPRETATION OF WAVERIDER PERFORMANCE DATA USING COMPUTATIONAL FLUID DYNAMICS

CHARLES E. COCKRELL, JR. Journal of Aircraft (ISSN 0021-8669) vol. 31, no. 5 September-October 1994 p. 1095-1100 refs

(BTN-95-EIX95062487534) Copyright

A computational study was conducted to better understand experimental results obtained from wind-tunnel tests of a Mach 4 conical-flow-derived waverider and a comparative reference configuration, which showed that the aerodynamic performance of the reference configuration was slightly better than that of the waverider. The computational results showed that the predicted surface pressure values and the integrated lift and drag coefficients were much lower for the reference model because the reference model bottom is an expansion surface. However, the lift-drag ratios for the reference model were higher due to a relatively low drag for a comparable amount of lift. The results also showed that the reference model exhibited the same shock attachment characteristics as the conical-flow-derived waverider, and is therefore also a waverider. The shock attachment characteristic gives the waverider a performance advantage over conventional hypersonic vehicles, and the results suggest that altering the bottom surface does not cause significant performance degradation. Flowfield solutions also show that the conical-flow waverider model has better propulsion/airframe integration characteristics than the reference configuration. The results also suggest that generating flowfields other than conical ones may be used to design waveriders with improved aerodynamic performance.

Author (EI)

A95-69246

SELECTING AND MANAGEMENT OF FIRE FIGHTER AIRCRAFT

L. BALIS CREMA Univ. of Roma 'La Sapienza, Rome (Italy), A. CASTELLANI, and S. GUARNIERA Journal of Aircraft (ISSN 0021-8669) vol. 31, no. 5 September-October 1994 p. 1121-1123 refs (BTN-95-EIX95062487538) Copyright

A comparison between the performance and direct operating costs of the water bombers Canadair CL215 and the CL415 Turbo-prop is presented. These aircraft are designed for fire fighting. The CL215s are currently used by the Italian Forest Service. Considering both the importance of forest-fire combating and the potential market for this type of aircraft, the Italian aerospace industry, Alenia, is designing a new aircraft designated the Advanced Amphibious Aircraft (AAA). On the basis of the design data, a comparison between the AAA and the Canadair CL215 and CL415 is shown. Based upon the Italian geographical environment, the operation of the AAA appears less expensive than that of the older aircraft.

Author (EI)

A95-69295

SERVICE LIFE EXTENSIONS FOR THE C-141

Aerospace Engineering (Warrendale, Pennsylvania) (ISSN 0736-2536) vol. 14, no. 11 November 1994 p. 11-15

(BTN-95-EIX95112530749) Copyright

Advances in fatigue knowledge have led to service life extensions for the US Air Force C-141. Fatigue design of the C-141 had been based on a reliability approach called 'safe life' to ensure that

05 AIRCRAFT DESIGN, TESTING AND PERFORMANCE

the C-141 would achieve its design service life of 30,000 flight hours. A damage tolerance assessment approach had been taken to come up with inspection and modification requirements. Recently, it was shown that extending service to 45,000 hrs can be possible with changes to the center wing box, and wing station and weep-hole cracking repairs. The fatigue test identified critical areas, but not when cracking problems will occur. Like past findings that corrosion could not be predicted, this experience reconfirmed that an aircraft reached the condition of aging when maintenance plan established it must be changed. EI

A95-69324

SIDE FORCES AT HIGH ANGLES OF ATTACK. WHY, WHEN, HOW?

P. CHAMPIGNY Office Natl d'Etudes et de Recherches Aerospatiales, Chatillon, France Recherche Aerospatiale/Aerospace Research (ISSN 0034-1223) no. 4 1994 p. 269-282 refs (BTN-95-EIX95112523809) Copyright

The demand for continually increased performance of missiles and aircraft leads to considering flights at very high angles of attack where control is very difficult. This is mainly due to the shedding of asymmetric vortices from the forebody, producing side forces even at zero sideslip. The purpose of this paper is to give an understanding of the phenomenon, based on test results obtained at ONERA or published in the literature, and answer three basic questions: Why does the flow become asymmetric? When do these phenomena occur? How can the side forces be controlled? Author (EI)

N95-19517# Wright Lab., Wright-Patterson AFB, OH.

PROCEEDINGS OF THE USAF STRUCTURAL INTEGRITY PROGRAM CONFERENCE Final Report, 30 Nov. - 2 Dec. 1993

THOMAS D. COOPER, JOHN W. LINCOLN, and JAMES L. RUDD Aug. 1994 646 p Conference held in San Antonio, TX, 30 Nov. - 2 Dec. 1993

(Contract(s)/Grant(s): AF PROJ. 2418)

(AD-A285684; WL-TR-94-4079) Avail: CASI HC A99/MF A06

The purpose of this 1993 Conference was to bring together technical personnel in DOD and the aerospace industry who are involved in the various technologies required to ensure the structural integrity of aircraft gas turbine engines, airframes and other mechanical systems. It provided a forum to exchange ideas and share new information relating to the critical aspects of durability and damage tolerance technology for aircraft systems. DTIC

N95-19693# Naval Postgraduate School, Monterey, CA.

AUTOMATION OF HARDWARE-IN-THE-LOOP TESTING OF CONTROL SYSTEMS FOR UNMANNED AIR VEHICLES M.S. Thesis

MICHAEL L. MOATS Sep. 1994 109 p (AD-A284833) Avail: CASI HC A06/MF A02

Modern computing advances allow the aerospace controls engineer the ability to design, test, and implement automatic control systems for air vehicles with breath taking speed and accuracy. This work examines the automation of the hardware-in-the-loop testing and implementation of autonomous controllers for unmanned air vehicles. Extraordinary interest is generated in this subject considering automation results in hardware-in-the-loop testing within days of completing a controller design. The entire automation process is presented, from design of the controller to implementation on a particular control platform to hardware-in-the-loop testing of the controller. This accomplishes control design and implementation in a matter of months compared to a few years or more before automation. DTIC

N95-19731 Naval Air Warfare Center, Patuxent River, MD. Aircraft Div.

AIRSHIP APPLICATIONS OF MODERN FLIGHT TEST TECHNIQUES

SEAN BRENNAN and MICHAEL MCDANIEL 1994 19 p Limited

Reproducibility: More than 20% of this document may be affected by microfiche quality

(AD-A284253) Avail: CASI HC A03

This viewgraph presentation covers the application of modern flight tests techniques to airships. Four airships were flown for a total of 19.7 flight hours. The airships ranged in size from 90 to 200 feet, and in gross weight from 1200 to 12,000 lbs. Single and twin-engine airships were flown. It was found that while the basic scientific test method works, many of the conventional test methods did not work on airships. In particular, new methods had to be developed for some dynamics and most stability characteristics. Further work is needed to refine stability and pressure system test techniques. Testing indicated that irreversible flight control systems and vectored thrust both enhance flying qualities. CASI

N95-19789# Aircraft Research Association Ltd., Bedford (England).

THE AERODYNAMIC DESIGN OF AN INTEGRATED WING LOWER SURFACE AND PYLONS FOR REDUCED DRAG

DENNIS R. STANNILAND and DIAN F. M. MACDONALD-SMITH May 1994 11 p Presented at the 19th Congress of the International Council of the Aeronautical Sciences, Anaheim, CA, Sep. 1994 Sponsored by Ministry of Defence

(ARA-MEMO-406) Avail: CASI HC A03/MF A01

The aerodynamic design of the wing for a military aircraft frequently concentrates on the clean wing performance, particularly the development of the upper surface flow at moderate and high incidence. The addition of underwing pylons and stores can cause a significant increase in drag, especially at the high subsonic Mach numbers and low incidences typical of 1-g flight at low altitude. This paper describes the design modifications to the wing lower surface and pylons of a military aircraft research model, aimed at reducing the installed drag of the pylons and stores. The redesign was carried out using the ARA Multiblock/Euler code to compute the flow around the fuselage/wing/pylon/store configuration. Geometric changes were specified using a simple relationship between the local surface curvature and the required change in surface pressure. Since the flow in the vicinity of the pylons and stores is highly viscous, the inviscid Euler code could not be relied upon to predict the drag differences between alternative designs. The success of the design modifications was therefore judged by the changes in surface pressure distributions, notably in the reduction in the shock strength on the wing lower surface. The redesigned wing/pylon combination has been tested in the ARA Transonic Wind Tunnel in conjunction with various store installations. The results demonstrate that a significant drag reduction can be achieved by redesigning the wing lower surface and pylons and a comparison with the predicted pressures shows that the CFD method has been successful in predicting the flow features accurately. Author

06

AIRCRAFT INSTRUMENTATION

Includes cockpit and cabin display devices; and flight instruments.

A95-69241* National Aeronautics and Space Administration. Ames Research Center, Moffett Field, CA.

SIMULATION AND FLIGHT TEST EVALUATION OF HEAD-UP-DISPLAY GUIDANCE FOR HARRIER APPROACH TRANSITIONS

D. W. DORR, E. MORALES, III, and V. K. MERRICK Journal of Aircraft (ISSN 0021-8669) vol. 31, no. 5 September-October 1994 p. 1089-1094 refs (BTN-95-EIX95062487533) Copyright

Position and speed guidance displays for STOVL aircraft curved, decelerating approaches to hover and vertical landing have been evaluated for their effectiveness in reducing pilot workload and

improving performance. The NASA V/STOL Systems Research Aircraft, a modified YAV-8B Harrier prototype, was used to evaluate the displays in flight, whereas the NASA Ames Vertical Motion Simulator was used to extend the flight test results to instrument meteorological conditions (IMC) and to examine performance in various conditions of wind and turbulence. The simulation data showed close correlation with the flight test data, and both demonstrated the feasibility of the displays. With the exception of the hover task in zero visibility, which was level-3, averaged Copper-Harper handling qualities ratings given during simulation were level-2 for both the approach task and the hover task in all conditions. During flight tests in calm and clear conditions, the displays also gave rise to level-2 handling qualities ratings. Pilot opinion showed that the guidance displays would be useful in visual flight, especially at night, as well as in IMC. Author (EI)

A95-69309

F/A-18 INLET CALCULATIONS AT 60-DEG ANGLE OF ATTACK AND 10-DEG SIDESLIP

S. D. PODLESKI NYMA, Inc, Brook Park, OH, United States Journal of Propulsion and Power (ISSN 0748-4658) vol. 10, no. 6 November-December 1994 p. 848-854 refs (BTN-95-EIX95112524199) Copyright

This article presents the results of numerical calculations on a 19.78% scale forebody/inlet model of the F/A-18 at a Mach number of 0.20, an angle of attack of 60 deg, and a sideslip angle of 10 deg. The main purpose of these calculations is to support an upcoming wind-tunnel test program in the prediction of engine inlet compressor face total pressure recovery and flow distortion. The CFD model includes the inlet and lip, and other aircraft components that are considered to be important to inlet performance, such as the ramp/splitter plate, the diverter and leading-edge extension (LEX) slot, and the deflected leading-edge flap. The CFD shows complex flow patterns on the fuselage surfaces below the LEX, on the ramp/splitter plate, inlet lip, and inside the inlet. The CFD tends to underpredict total pressure recovery and overpredict the flow distortion at the inlet compressor face. Author (EI)

07

AIRCRAFT PROPULSION AND POWER

Includes prime propulsion systems and systems components, e.g., gas turbine engines and compressors; and on-board auxiliary power plants for aircraft.

A95-65854

UNBALANCE RESPONSE OF A DUAL ROTOR SYSTEM: THEORY AND EXPERIMENT

K. GUPTA Indian Institute of Technology, New Delhi (India), K. D. GUPTA, and K. ATHRE Journal of Vibration and Acoustics, Transactions of the ASME (ISSN 1048-9002) vol. 115, no. 4 October 1993 p. 427-435 refs (BTN-94-EIX94351143320) Copyright

A dual rotor rig is developed and is briefly discussed. The rig is capable of simulating dynamically the two spool aeroengine, though it does not physically resemble the actual aeroengine configuration. Critical speeds, mode shape, and unbalance response are determined experimentally. An extended transfer matrix procedure in complex variables is developed for obtaining unbalance response of dual rotor system. Experimental results obtained are compared with theoretical results and are found to be in reasonable agreement. Author (EI)

A95-67298

DESIGN OPTIMIZATION OF AIRCRAFT ENGINE-MOUNT SYSTEMS.

H. ASHRAFIUON Villanova Univ., Villanova, PA. Journal of Vibration and Acoustics, Transactions of the ASME (ISSN 1048-

9002) vol. 115, no. 4 October 1993 p. 463-467 (BTN-94-EIX94351143325) Copyright

Design optimization of aircraft engine-mount systems for vibration isolation is presented. The engine is modeled as a rigid body connected to a flexible base representing the nacelle. The base (nacelle) is modeled with mass and stiffness matrices and structural damping using finite element modeling. The mounts are modeled as three-dimensional springs with hysteresis damping. The objective is to select the stiffness coefficients and orientation angles of the individual mounts in order to minimize the transmitted forces from the engine to the nacelle. Meanwhile, the mounts have to be stiff enough not to allow the engine deflection to exceed its limits under static and low frequency loadings. It is shown that with an optimal system the transmitted forces may be reduced significantly particularly when orientation angles are also treated as design variables. The optimization problems are solved using a constraint variable metric approach. The closed form derivatives of the engine vibrational amplitudes with respect to design variables are derived in order to determine the objective function gradients and consequently a more effective optimization search technique. Author (EI)

A95-68158

NEW END TUBE CLOSURE SYSTEM FOR THE RAM ACCELERATOR

DAVID W. BOGDANOFF Elore Inst., Palo Alto, CA Journal of Propulsion and Power (ISSN 0748-4658) vol. 10, no. 4 July-August 1994 p. 518-521 refs (BTN-94-EIX94441380974) Copyright

The ram accelerator is a ramjet-in-tube device which has been demonstrated at velocities up to 2.5 km/s, has potential for operation up to approximately 10 km/s, and could be used for direct space launch or large ballistic ranges. The ends of the main ram accelerator tube must have end closures which support substantial pressure differences. There are potentially serious difficulties using solid end closures such as diaphragms pierced by the projectile, explosively removed end closures, or fast acting valves. These include risks of significant damage to the projectile and launch tube and the wasting of tube length. A new end closure system which uses the momentum of an annular axial air jet to support the required pressure differences is described. This system avoids the difficulties of the solid end closure system at the cost of some increase in overall launch system complexity. A preliminary design of such an air jet end closure is presented, and it is concluded that the requirements for airflow rates and storage are reasonable and would likely add only a modest increase to the overall cost of the launch system. If the difficulties with solid end closures prove to be significant, the air jet end closure system may offer a solution. Author (EI)

A95-68161

EXPERIMENTAL AND COMPUTATIONAL RESULTS FOR THE EXTERNAL FLOWFIELD OF A SCRAMJET INLET

D. A. AULT Johns Hopkins Univ. Applied Physics Lab, Laurel, MD and D. M. VANWIE Journal of Propulsion and Power (ISSN 0748-4658) vol. 10, no. 4 July-August 1994 p. 533-539 refs (BTN-94-EIX94441380977) Copyright

A two-dimensional hypersonic scramjet inlet has been investigated in a combined experimental and analytical program aimed at addressing the fundamental issues related to the design of scramjet inlets. The experimental portion of the program was conducted in the Calspan 48-in. shock tunnel at Mach 10 and 13. The computational analysis was conducted using a two-dimensional parabolized Navier-Stokes computational fluid dynamics (CFD) code. This article addresses the issues concerned with the flow over the external forebody of the inlet which consists of a blunted wedge followed by an isentropic compression. The pressure and heat transfer distributions over the forebody are investigated for ranges of Reynolds number, Mach number, wall-to-freestream temperature ratio, and nose bluntness. Comparison of the test results and CFD predictions show that good agreement for the heat transfer distributions is

achieved. However, the predicted pressure distribution on the forward blunted wedge was consistently underpredicted by 18-33% relative to the experimental measurements. Several phenomena were investigated in an attempt to explain the discrepancy between predicted and measured pressure distributions, including classical viscous leading-edge interactions, blunt leading-edge interactions, slip flow effects, flow condensation, flow angularity, and facility Mach number uncertainty. Although the discrepancy in the forebody pressure ratios could be caused by a combination of the factors listed above, a deficiency in the modeling of the viscous interaction region by the CFD codes and facility flow angularity are shown to be the strongest contributors. Author (EI)

A95-68162

THREE-DIMENSIONAL ANALYSIS OF SCRAMJET NOZZLE FLOWS

TOMIKO ISHIGURO National Aerospace Lab., Tokyo (Japan), RYUJI TAKAKI, TOHRU MITANI, and TETSUO HIRAIWA Journal of Propulsion and Power (ISSN 0748-4658) vol. 10, no. 4 July-August 1994 p. 540-545 refs (BTN-94-EIX94441380978) Copyright

Numerical and experimental results of performance in National Aero-Space Plane-like nozzles are compared. The full Navier-Stokes equation with the Baldwin-Lomax turbulence model was adopted to solve the three-dimensional nozzle flows. A code validation study was conducted using pressure and heat-flux distributions measured. The interactions of separation shocks with the main internal flow under overexpanded conditions were investigated. The interaction yields higher performance in scramjet nozzles than that estimated assuming a two-dimensional separation. The losses in the nozzle internal flow and the overexpansion loss were evaluated. Author (EI)

A95-68182* National Aeronautics and Space Administration. Langley Research Center, Hampton, VA.

DEMONSTRATION OF AN ELASTICALLY COUPLED TWIST CONTROL CONCEPT FOR TILT ROTOR BLADE APPLICATION

R. C. LAKE, M. W. NIXON, M. L. WILBUR, J. D. SINGLETON, and P. H. MIRICK AIAA Journal (ISSN 0001-1452) vol. 32, no. 7 July 1994 p. 1549-1551 refs (BTN-94-EIX94441386633) Copyright

This study demonstrated the feasibility of passive blade twist control for composite rotor blades. Hover testing of the set of blades produced maximum twist changes of 2.54 degrees for the unballasted blade configuration and 5.24 degrees for the ballasted blade configuration. These results compared well with those obtained from a detailed finite element analysis model of the rotor blade, which yielded maximum twists of 3.02 and 5.61 degrees for the unballasted and ballasted blade configurations, respectively. EI

A95-68257

AIRCRAFT ENGINE EMISSION REDUCTION

STUART BIRCH Aerospace Engineering (Warrendale, Pennsylvania) (ISSN 0736-2536) vol. 15, no. 1 January-February 1994 p. 16-17 (BTN-95-EIX95031502750) Copyright

The paper discusses new concepts for combustion chambers to help create low pollution power plants and reduce engine emissions. Researchers see that internal combustion engines provide complete combustion when they are close to stoichiometry while gas turbines experience problems when they reach this ratio. It would be best to modify the equivalence ratio of the primary combustion zone which is responsible for the high level of NOx emissions. Reduction of pollutant emissions from aircraft engines are focused on three areas: (1) use of less polluting fuels; (2) modification of the combustion process; and (3) reduction of specific fuel consumption and consequently consumption overall. EI

A95-68311

ACTIVE CONTROL OF WAKE/BLADE-ROW INTERACTION NOISE

KENNETH A. KOUSEN United Technologies Research Cent, East Hartford, CT and JOSEPH M. VERDON AIAA Journal (ISSN 0001-1452) vol. 32, no. 10 October 1994 p. 1953-1960 refs (BTN-95-EIX95042474389) Copyright

This paper describes an analytical/computational approach for controlling the noise generated by wake/blade-row interaction through the use of antisound actuators on the blade surfaces. A representative two-dimensional section of a fan stage, composed of an upstream fan rotor and a downstream fan exit guide vane (FEGV), is examined. An existing model for the wakes generated by the rotor is analyzed to provide realistic magnitudes for the vortical excitations imposed at the inlet to the FEGV. The acoustic response of the FEGV is determined at multiples of the blade passing frequency by using the linearized unsteady flow analysis, LINFLO. An analysis then is presented to determine the complex amplitudes required for the control surface motions to best reduce the farfield noise. The effectiveness of the control is measured by the decrease in the circumferentially averaged sound pressure level, which is minimized by a standard least-squares procedure. Author (EI)

A95-69302

PLY LAYUP OPTIMIZATION AND MICROMECHANICS TAILORING OF COMPOSITE AIRCRAFT ENGINE STRUCTURES

SRINIVAS KODIYALAM General Electric Corporate R&D Cent, Schenectady, NY, United States, V. N. PARTHASARATHY, MICHAEL S. HARTLE, and RICHARD L. MCKNIGHT Journal of Propulsion and Power (ISSN 0748-4658) vol. 10, no. 6 November-December 1994 p. 897-905 refs (BTN-95-EIX95112524206) Copyright

A ply layup optimization and micromechanics tailoring capability for composites aircraft engine components is under development. The composites optimization methodology is multidisciplinary, encompassing structural, heat transfer, and aeromechanical design considerations. The methodology includes provision for handling multiple objective functions and a framework for approximation of both the response functions and its derivatives. Derivative approximations are found to be sufficiently accurate to guide the numerical search in the right direction. A micromechanics tailoring procedure to correlate the 'calculated' and 'measured' lamina properties at elevated temperatures is outlined. The micromechanics tailoring also provides the ability to back out effective (in situ) matrix properties as part of the composite. Several real life aircraft engine components are optimized for structural, thermal, and aeromechanical responses as design objectives and constraints. Author (EI)

A95-69303

ADAPTIVE MODELING OF JET ENGINE PERFORMANCE WITH APPLICATION TO CONDITION MONITORING

B. LAMBIRIS Natl Technical Univ of Athens, Athens, Greece, K. MATHIOUDAKIS, A. STAMATIS, and K. PAPALIOU Journal of Propulsion and Power (ISSN 0748-4658) vol. 10, no. 6 November-December 1994 p. 890-896 refs (BTN-95-EIX95112524205) Copyright

A method of simulation of the performance of jet engines, with the possibility of adapting to engine particularities, is presented. It employs an adaptation procedure coupled to a performance model solving the component matching problem. The proposed method can provide accurate simulation for engines of the same type, with differences that are due to manufacturing or assembly tolerances. It does not require accurate component maps, because they are derived during the adaptation procedure. It can also be used for health monitoring purposes, for component fault identification, and condition assessment. The effectiveness of the proposed method is demonstrated by application to two commercial jet engines. Author (EI)

A95-69304

DEVELOPMENT OF HYPERSONIC ENGINE SEALS: FLOW EFFECTS OF PRELOAD AND ENGINE PRESSURES

ZHONG CAI Drexel Univ, Philadelphia, PA, United States,

RAJAKKANNU MUTHARASAN, FRANK K. KO, and BRUCE M. STEINETZ *Journal of Propulsion and Power* (ISSN 0748-4658) vol. 10, no. 6 November-December 1994 p. 884-889 refs (BTN-95-EIX95112524204) Copyright

A new type of engine seal is being developed to meet the needs of advanced hypersonic engines. A seal made of emerging high-temperature ceramic fibers braided in a sheath-core construction is selected for study based on its low leakage rates. Flexible, low-leakage, high-temperature seals are required to seal the movable engine panels of advanced ramjet-scamjet engines. To predict the leakage through these flexible, porous seal structures as a function of preload and engine pressures, new analytical flow models are required. An empirical leakage resistance/preload model is proposed to characterize the observed decrease in leakage with increasing preload. Empirically determined compression modulus and preload factor are used to correlate experimental leakage data for a wide range of seal architectures. Good agreement is observed between measured and predicted values over a range of engine pressures and seal preload. Author (EI)

A95-69310* National Aeronautics and Space Administration. Langley Research Center, Hampton, VA.

NUMERICAL STUDY OF THE PERFORMANCE OF SWEEPED, CURVED COMPRESSION SURFACE SCRAMJET INLETS

JOHN J. KORTE National Aeronautics and Space Administration. Langley Research Center, Hampton, VA, D. J. SINGH, AJAY KUMAR, and AARON H. AUSLENDER *Journal of Propulsion and Power* (ISSN 0748-4658) vol. 10, no. 6 November-December 1994 p. 841-847 refs (BTN-95-EIX95112524198) Copyright

A computational performance enhancement study was performed employing systematic modifications to planar-sidewall compression scramjet inlet operating at an entrance Mach number of 4 and at a dynamic pressure of 2040 psf. The variations included modifying the planar-sidewall compression angle as a function of height, utilizing sidewall curvature, and employing, simultaneously, both forward-swept and reverse-swept compression surfaces. Turbulent flowfield solutions were generated by solving the Reynolds-averaged Navier-Stokes equations to obtain inlet performance parameters such as total-pressure recovery, mass capture, and flowfield pressure distortion (the ratio of maximum static pressure to minimum static pressure generated at the inlet exit plane). Additionally, an inviscid parametric study was performed by employing solutions to the Euler equations to optimize a cubic polynomial that defined the longitudinal sidewall geometry. A final viscous flowfield solution of the optimized inviscid inlet geometry yielded inlet performance improvements; however, inlet top-wall surface boundary-layer shock wave separation interactions persisted. Hence, this numerical study demonstrated that enhanced performance is obtainable via curved-wall geometric modifications to the standard planar-sidewall inlet design, although future work should employ constraints to mitigate detrimental flow separation effects. Author (EI)

N95-19595# Naval Postgraduate School, Monterey, CA.
AN ANALYSIS OF THE COSTS AND BENEFITS IN IMPROVING F402-RR-406A HIGH PRESSURE TURBINE, SECOND STAGE BLADES UNDER THE AIRCRAFT ENGINE COMPONENT IMPROVEMENT PROGRAM (CIP) M.S. Thesis
DONALD ALAN WALTER Sep. 1994 82 p
(AD-A285127) Avail: CASI HC A05/MF A01

This thesis is part of a continuing project at the Naval Postgraduate School attempting to validate the cost effectiveness of the Aircraft Engine Component Improvement Program. It focuses on the costs and benefits derived from Power Plant Change 159 which improved High Pressure Turbine, Second Stage blades on the Harrier (AV-8B) aircraft's Rolls-Royce Pegasus (F402-RR-F406A) engine. Because sufficient failure rate data for the improved blades was not available, the analysis considers a range of costs/benefits based on two different projected blade reliabilities. The improve-

ment to the High Pressure Turbine, Second Stage blades was found to be cost-effective from both a financial break-even point, in that the cost to produce the improvement will be recovered by the end of 1996 for the full range of projected blade reliabilities and from a Net Present Value analysis which shows that this improvement will save the Department of the Navy between \$17,192,827 and \$38,639,494 (in 1992 dollars) over the projected life cycle of the engine. DTIC

N95-19651*# NYMA, Inc., Brook Park, OH. Engineering Services Div.

PREDICTION OF WIND TUNNEL EFFECTS ON THE INSTALLED F/A-18A INLET FLOW FIELD AT HIGH ANGLES-OF-ATTACK Final Report

CRAWFORD F. SMITH Cleveland, OH NASA Jan. 1995 55 p
(Contract(s)/Grant(s): NAS3-27186; RTOP 505-68-30)
(NASA-CR-195429; E-9416; NAS 1.26:195429) Avail: CASI HC A04/MF A01

NASA Lewis is currently engaged in a research effort as a team member of the High Alpha Technology Program (HATP) within NASA. This program utilizes a specially equipped F/A-18A, the High Alpha Research Vehicle (HARV), in an ambitious effort to improve the maneuverability of high performance military aircraft at low subsonic speed, high angle of attack conditions. The overall objective of the Lewis effort is to develop inlet technology that will ensure efficient airflow delivery to the engine during these maneuvers. One part of the Lewis approach utilizes computational fluid dynamics codes to predict the installed performance of inlets for these highly maneuverable aircraft. Wind tunnel tests were a major component of the Lewis program. Since the available wind tunnel was small (9 x 15 ft) as compared to the scale of the model of the F/A-18A (19.78 percent), there were questions about the capability to obtain useful inlet performance data. The blockage effects were expected to be very large. This report represents the results of an analysis to determine how the wind tunnel walls effect inlet performance at several angles of attack. The predictions for the external particle traces along the fuselage indicate the influence of the wind tunnel side wall under the model is greater at 30 deg angle of attack than at 50 deg angle of attack on the under Leading Edge Extension (LEX) vortex trajectory. The side wall above the model appears to have negligible influence on the under LEX vortex. This may be due to the LEX acting as 'shield' to the upper wall effects. As expected, the wind tunnel has a significant influence on the external forces. The lift and drag coefficients increase significantly for the wind tunnel model as compared to free stream conditions. The wind tunnel had a small effect on the inlet recovery and on inlet total pressure distortion patterns. The predicted recoveries for the wind tunnel model are within one percentage point of the model recoveries in free stream conditions. Author

N95-19653# Advisory Group for Aerospace Research and Development, Neuilly-Sur-Seine (France). Propulsion and Energetics Panel.
EROSION, CORROSION AND FOREIGN OBJECT DAMAGE EFFECTS IN GAS TURBINES [LES CONSEQUENCES DE L'ENDOMMAGEMENT DES TURBINES A GAZ PAR EROSION, CORROSION ET OBJETS ETRANGERS]

Nov. 1994 338 p In ENGLISH and FRENCH Symposium held in Rotterdam, Netherlands, 25-28 Apr. 1994 Original contains color illustrations
(AGARD-CP-558; ISBN-92-836-0005-3) Copyright Avail: CASI HC A15/MF A03

The Conference Proceedings contains 31 papers presented at the Propulsion and Energetics Panel Symposium on Erosion, Corrosion and Foreign Object Damage Effects in Gas Turbines which was held from 25-28th April 1994, in Rotterdam, The Netherlands. The Technical Evaluation Report and the Keynote Address are included at the beginning and discussions follow most papers. The Symposium was arranged in the following Sessions: Operational Experience and Requirements (7); Deposition and Erosion (7); Foreign Object Damage (5); Coatings, Repairs and Materials As-

07 AIRCRAFT PROPULSION AND POWER

pects - 1 (4); Coatings, Repairs and Materials Aspects - 2 (7); and Testing and Certification Procedures (1). For individual titles, see N95-19654 through N95-19684.

N95-19654# Rolls-Royce Ltd., Bristol (England).
OUT OF AREA EXPERIENCES WITH THE RB199 IN TORONTO

M. G. DOWN and M. J. WILLIAMS *In* AGARD, Erosion, Corrosion and Foreign Object Damage Effects in Gas Turbines 7 p Nov. 1994
Copyright Avail: CASI HC A02/MF A03

The Turbo Union RB 199 engine was developed during the late 1960's / early 1970's to meet a specification requirement aimed at defense of the Western European NATO alliance countries against the (then) perceived threat. During the latter part of the 1980's Tornado aircraft were delivered to the Royal Saudi Air Force and, supplemented by deployed units from the Royal Air Force, were engaged in an operational role during 1990 / 1991. Aircraft operations in the Saudi Arabia climates and natural environment created problems with engine life, hitherto not encountered in the European area of operation, nor during many RAF overseas deployments, including North America. These problems, mainly concerned with turbine blade contamination from airborne sand, were alleviated by the introduction of unique engine maintenance management techniques and eliminated by design changes. Author

N95-19655# Defence Research Agency, Farnborough, Hampshire (England). Air Vehicle Performance Dept.
THE OPERATION OF GAS TURBINE ENGINES IN HOT AND SANDY CONDITIONS: ROYAL AIR FORCE EXPERIENCES IN THE GULF CONFLICT

R. C. SIRS *In* AGARD, Erosion, Corrosion and Foreign Object Damage Effects in Gas Turbines 8 p Nov. 1994
Copyright Avail: CASI HC A02/MF A03

During the initial phase of the Gulf Crisis, the principal instrument at the disposal of the British Government which could respond in time was air power. This situation continued, and throughout the period of military build up and subsequent conflict air power remained a dominant factor. During the period, many equipment modifications were incorporated to increase both performance and reliability, and the gas turbine engines which powered the RAF's aircraft were no exception. However in some cases, engines were operated at a much increased flying rate in harsh operating conditions in standard configuration. This paper reviews the operating experiences and some of the modifications incorporated, including the subsequent effect on aero-engine reliability trends. Author

N95-19656# Army Aviation Systems Command, Saint Louis, MO. Directorate for Engineering.

US ARMY ROTORCRAFT TURBOSHAFT ENGINES SAND AND DUST EROSION CONSIDERATIONS

VERNON R. EDWARDS and PETER L. ROUSE *In* AGARD, Erosion, Corrosion and Foreign Object Damage Effects in Gas Turbines 10 p Nov. 1994
Copyright Avail: CASI HC A02/MF A03

The impact of operating in a sand and dust environment on U.S. Army rotorcraft turbine engines has been a major concern since the first turbine powered UH-1 Iroquois (Huey) helicopter was fielded in the early 1960s. The implication on turbine engine performance and durability had not sufficiently been recognized, or addressed, in early engine designs. Early engine military specifications had been primarily concerned with U.S. Air Force 'jet' engines for fixed wing aircraft. Although these early specifications included sand and dust requirements relative to ingestion capability and test substantiation, actual rotorcraft field experience was not considered, nor, in fact, was actual data available. This paper provides a brief history of the impact of operation in sand and dust and operational considerations on U.S. Army rotorcraft turbine engines. The general effects of sand and dust erosion, compaction, deformation, glassing, etc., on engine turbomachinery will be discussed. Finally, the results of opera-

tion in Southeast Asia, and during Desert Shield/Desert Storm, possibly the worse case operational environment encountered to date, will be presented. Author

N95-19657# Rolls-Royce Ltd., Bristol (England).
FUTURE DIRECTIONS IN HELICOPTER PROTECTION SYSTEM CONFIGURATION

DARRELL L. MANN and GORDON D. WARNES *In* AGARD, Erosion, Corrosion and Foreign Object Damage Effects in Gas Turbines 12 p Nov. 1994
Copyright Avail: CASI HC A03/MF A03

Recent events have highlighted the fact that none of the currently available turboshaft intake protection systems, whether they be the permanent fit IPS or mission specific vortex pack types, have an adequate sand/dust separation capability. Evidence has been amply provided by low engine life, consequent support logistics problems and the necessity for development of short term emergency measures. The paper seeks to quantify the extent of the problem and define the solutions which will be required if a repeat of past experiences is to be avoided. The paper describes the directions which particles separator technology must take in order to meet future requirements. A further important aspect of future directions is the drive for an increase in an engine's ability to resist damage; the paper identifies those areas of the engine which are most prone to damage, comments on the need to strike the right balance between resistance and removal, and discusses the increasing value of sophisticated computer based design methodologies. Author

N95-19658# Naval Air Warfare Center, Trenton, NJ. Aircraft Div.
NAVY FOREIGN OBJECT DAMAGE AND ITS IMPACT ON FUTURE GAS TURBINE ENGINE LOW PRESSURE COMPRESSION SYSTEMS

PETER CHARLES DIMARCO *In* AGARD, Erosion, Corrosion and Foreign Object Damage Effects in Gas Turbines 9 p Nov. 1994
Copyright Avail: CASI HC A02/MF A03

Foreign Object Damage (FOD), Domestic Object Damage (DOD), bird ingestion, and ice ingestion are all necessary factors to be considered in the design of reliable and maintainable fan systems for future U.S. Navy aircraft applications. The high rate of fan damage reported in U.S. Navy engines and its impact on repair and maintenance requirements such as engine down time, level of repair, and number of spares have caused the Navy in recent years to scrutinize the requirements which must be met in order to design a more reliable and rugged yet highly maintainable fan system for future aircraft. This paper reports the results of an investigation into the occurrences of Foreign Object Damage in several U.S. Navy aircraft, the repair approaches presently used by the U.S. Navy, and investigates the implications which these considerations present to the design of more damage tolerant fan systems. It further investigates the trade-offs in future turbomachinery design which balance gas turbine engine performance payoff against supportability and maintainability onboard ship. Author

N95-19659# Scandinavian Airlines System, Oslo (Norway).
SCANDINAVIAN AIRLINES SYSTEMS EXPERIENCE ON EROSION, CORROSION AND FOREIGN OBJECT DAMAGE EFFECTS ON GAS TURBINES

P. STOKKE *In* AGARD, Erosion, Corrosion and Foreign Object Damage Effects in Gas Turbines 10 p Nov. 1994
Copyright Avail: CASI HC A02/MF A03

This article summarizes SAS' experience on engine FOD and compressor erosion. It will mainly focus on type of damages, debris sources, modifications developed, development of maintenance and inspection method to cope with the problem, revision of operational procedures etc. In addition the added maintenance costs implied by FOD and erosion will be discussed, as also will be the special considerations to be used for cold winter operations. Author

N95-19660# General Electric Co., Cincinnati, OH. Aircraft Engines Div.

MODERN TRANSPORT ENGINE EXPERIENCE WITH ENVIRONMENTAL INGESTION EFFECTS

T. L. ALGE and J. T. MOEHRING *In* AGARD, Erosion, Corrosion and Foreign Object Damage Effects in Gas Turbines Nov. 1994
Copyright Avail: CASI HC A02/MF A03

Modern propulsion engines have achieved a high level of reliability while manufacturers and users are always striving to further improve the safety record. The drive for safety in single-engine aircraft has resulted in safer multiple-engine applications. In modern turbofan-powered transports it is extremely unlikely that a failure intrinsic to an engine would initiate a sequence of events which could result in loss of capability for continued safe flight and landing. These rare events are limited to uncontained rotor disk fracture or uncontrolled fire. Of greater concern today are the non-intrinsic, common-cause events which involve power loss of more than one engine. These are externally-inflicted occurrences such as ingestion events or common-cause maintenance events resulting in simultaneous loss of power on more than one engine. The most frequent are those ingestion events involving products of the flying environment - flocking birds, ice, volcanic ash and extreme inclement weather. This environmental ingestion hazard viewed in overview is the primary subject of this paper. There is a body of knowledge on each of these subjects. Data from field operations and engine experience have provided guidelines for recognition of an occurrence and the proper action response. The primary precaution however remains - be aware, prevent, communicate and avoid.

Author

N95-19661# Oxford Univ., Oxford (England). Dept. of Engineering Science.

PARTICLE DEPOSITION IN GAS TURBINE BLADE FILM COOLING HOLES

V. H. M. KUK, P. T. IRELAND, T. V. JONES, and M. G. ROSE (Rolls-Royce Ltd., Derby, England.) *In* AGARD, Erosion, Corrosion and Foreign Object Damage Effects in Gas Turbines 18 p Nov. 1994
Original contains color illustrations
Copyright Avail: CASI HC A03/MF A03

The aerodynamic processes leading to film cooling hole blockage have been investigated experimentally in large scale models of idealized internal cooling passages. The experimental scaling included reproducing engine cooling passage and hole Reynolds numbers together with a new dimensionless group which was matched experimentally to ensure that the measured particle trajectories were engine representative. It has been possible to achieve correct dimensional scaling with particles one thousand times larger than engine size. Simple visualization of the particle trajectories showed concentrations of impact locations inside holes normal to and inclined to the cooling passage surface. No attempt was made to model interaction between the particles and the passage walls. A new instrument has been developed to measure the concentration of particle impacts. Use of the device provides a fast and convenient way of measuring particle impact distributions. The regions of high impact concentration are consistent with blockage structures found in engines after service. The process of internal blockage of film cooling holes has been shown to be due to inertia driven particles of the order of 1 micron in diameter. Flow conditions immune from impact concentration and hence the blockage process have been identified for the inclined film cooling hole.

Author

N95-19662# Cincinnati Univ., OH. Dept. of Aerospace Engineering and Engineering Mechanics.

EXPERIMENTAL AND NUMERICAL SIMULATIONS OF THE EFFECTS OF INGESTED PARTICLES IN GAS TURBINE ENGINES

A. HAMED and W. TABAKOFF *In* AGARD, Erosion, Corrosion and Foreign Object Damage Effects in Gas Turbines 13 p Nov. 1994
Copyright Avail: CASI HC A03/MF A03

Particles ingested in gas turbine engines follow trajectories that generally deviate from the flow streamlines and impact the compo-

nent surfaces causing erosion damage. This paper deals with the experimental and numerical simulations of particle dynamics including surface interactions and the associated blade erosion in gas turbine engines. The experimental studies of particle surface impacts include the nonintrusive measurements of particle bounce conditions and the erosion testing of blade materials and blade coatings. Data obtained in the University of Cincinnati's high temperature erosion test facility at temperatures up to 1500 F for different alloys and coatings are presented. The numerical studies to simulate the particle dynamics in the turbomachines are described. Results of combined experimental and computational modeling are presented for the particle dynamics, the associated turbomachinery blade erosion, and performance loss. The probabilistic modeling of the experimentally measured variance in the particle bounce conditions and the loss of performance associated with particle ingestion are discussed.

Author

N95-19663# Cranfield Univ., Bedford (England). School of Mechanical Engineering.

PARTICLE TRAJECTORIES IN GAS TURBINE ENGINES

S. C. TAN, R. L. ELDER, and P. K. HARRIS *In* AGARD, Erosion, Corrosion and Foreign Object Damage Effects in Gas Turbines 13 p Nov. 1994

Copyright Avail: CASI HC A03/MF A03

This paper describes the technique of particle trajectory modeling in gas turbine engines with applications in helicopter inertial particle separator, axial and centrifugal compressor. The model can be used with most CFD codes which utilize the finite volume (or element) techniques. Some qualitative validations were carried out using a laser transit anemometer in a particle separator and results show good comparison with predictions. The anemometer was also used to obtain restitution data for several target materials using quartz particle of different sizes at a range of impact velocities and angles.

Author

N95-19664# Defence Research Agency, Farnborough, Hampshire (England).

THE CALCULATION OF EROSION IN A GAS TURBINE COMPRESSOR ROTOR

G. C. HORTON, H. VIGNAU (Turbomeca S.A. - Brevets Szydlowski, Bordes, France.), and G. LEROY (Turbomeca S.A. - Brevets Szydlowski, Bordes, France.) *In* AGARD, Erosion, Corrosion and Foreign Object Damage Effects in Gas Turbines 14 p Nov. 1994
Copyright Avail: CASI HC A03/MF A03

Erosion of the turbomachinery and other components in helicopter gas turbines operating in a sandy environment is a significant problem. In order to better understand the mechanics of such erosion, and to enable the design of components better able to withstand it, a means of modelling erosion is needed. Such a method has been developed at Turbomeca. It consists of a method of predicting the trajectories of the particles within the component, on the basis of a prescribed aerodynamic field and taking into account rebounds from the walls, together with correlations for the erosion caused by impacts of the particles with the walls. The various aspects of the method have been validated by comparison with available experimental data and these comparisons are presented. Predictions of particle trajectories in two types of particle separator and in two gas turbine compressors (axial and centrifugal) are also presented, together with some comparisons with experiment.

Author

N95-19665# Motoren- und Turbinen-Union Muenchen G.m.b.H., Munich (Germany).

PERFORMANCE DETERIORATION OF AXIAL COMPRESSORS DUE TO BLADE DEFECTS

J. SCHMUECKER and A. SCHAEFFLER *In* AGARD, Erosion, Corrosion and Foreign Object Damage Effects in Gas Turbines 6 p Nov. 1994

Copyright Avail: CASI HC A02/MF A03

During flight operation the engine swallows sand or other hard particles usually from the runway. Passing through the compressors

they will damage the blades, erode the coating and deteriorate seals. The submitted paper presents some measurements, which show the effect on compressor performance due to the most important and frequent defects. The investigation - conducted at high pressure compressors - includes tests with reworked blades at leading and trailing edges, rounded rotor tips and increased tip clearances. The results are summarized in easy to handle correlations, which enables the user to estimate the deterioration and to fix repair rules within the allowed performance loss range. Author

N95-19666# National Research Council of Canada, Ottawa (Ontario). Inst. for Aerospace Research.

EROSION OF T56 5TH STAGE ROTOR BLADES DUE TO BLEED HOLE OVERTIP FLOW

B. C. BARRY and T. C. CURRIE *In* AGARD, Erosion, Corrosion and Foreign Object Damage Effects in Gas Turbines 10 p Nov. 1994 Copyright Avail: CASI HC A02/MF A03

Severe trailing edge erosion of ALLISON T56 gas turbine 5th and 10th stage compressor blades has been observed in Field Service Evaluations and sand ingestion tests. The erosion typically occurs within 3 mm of the blade tip and has been attributed to overtip flow produced by the bleed holes present over the 5th and 10th stage rotors. The overtip flow through the 5th stage bleed holes of an operating T56 has been surveyed with a laser two-focus (L2F) velocimeter in order to identify the features of the flow field responsible for the tip erosion. Two-dimensional measurements were made at 4 spanwise locations in the outer 25 percent of the span. Three-dimensional measurements were made at three spanwise stations within 7 mm of the blade tip (15 percent of span). The flow was found to be unaffected by the bleed holes beyond 3-4 mm from the blade tip. This result is consistent with erosion patterns observed on service-exposed blades and blades subjected to accelerated erosion in sand ingestion tests. Author

N95-19668# Palermo Univ. (Italy). Dipt. di Meccanica e Aeronautica. **AN AIRBORNE MONITORING SYSTEM FOR FOD AND EROSION FAULTS**

GIUSEPPE LOMBARDO and GIOVANNI TORELLA (Italian Air Force Academy, Naples, Italy.) *In* AGARD, Erosion, Corrosion and Foreign Object Damage Effects in Gas Turbine 12 p Nov. 1994 Copyright Avail: CASI HC A03/MF A03

FOD and erosion are the events causing the most part of accidental damages in gas turbine engines. When FOD is not destroying or when erosion is in progress the performance level decreases and the necessity of unscheduled maintenance actions becomes quite real. Moreover when there is a light FOD, or the erosion process is constant in time, it may be difficult to detect the exact cause of performance decrease and to plan the most effective maintenance action. This paper deals with the results of a study carried out for developing an Engine Condition Monitoring system particularly suitable for detecting the MicroFOD and erosion effects in gas turbines. The developed numerical code has been applied to a single spool turboshaft engine with free power turbine. The obtained results are presented and discussed. Author

N95-19669# Societe Nationale d'Etude et de Construction de Moteurs d'Aviation, Moissy-Cramayel (France).

DESIGN OF FAN BLADES SUBJECTED TO BIRD IMPACT [CONCEPTION DES AUBES FAN SOUMISES A L'IMPACT D'OISEAUX]

P. VIGNOLLES, P. X. BUSSONNET, and J. TALBOTEC *In* AGARD, Erosion, Corrosion and Foreign Object Damage Effects in Gas Turbines 11 p Nov. 1994 *In* FRENCH Original contains color illustrations

Copyright Avail: CASI HC A03/MF A03

The quality of fan blades in terms of behavior is one of the major parameters affecting the safety of modern aircraft driven by engines with strong by-pass ratio. The reinforcements defined as necessary in certain areas of the profiles of the fan blades must be a compromise between the objectives of mechanical resistance and aerodynamic performance. SNECMA developed a methodology to forecast

the impact behavior of the fan blades based on a mathematical model. In parallel, the progress made in aerodynamics made it possible to predict the consequences of these stresses related to ingestion on aerodynamic performance and still maintain high levels of performance. Author

N95-19670# Motoren- und Turbinen-Union Muenchen G.m.b.H., Munich (Germany).

IMPACT LOADING OF COMPRESSOR STATOR VANES BY HAILSTONE INGESTION

J. FRISCHBIER *In* AGARD, Erosion, Corrosion and Foreign Object Damage Effects in Gas Turbines 12 p Nov. 1994 Copyright Avail: CASI HC A03/MF A03

Impacts of 1 inch diameter ice bullets onto stator vanes of the first stage of an axial compressor were investigated at an impact velocity of $v = 257$ m/s. The analytical and experimental simulations of typical hailstone ingestions were performed with special emphasis on damage effects of the thin leading edges of the hidden titanium vanes. The paper includes a comprehensive overview of the ice properties used in the analytical model regarding elastic constants, strain rate dependent strength and crack propagation under compression. The influence of different impact positions and ice properties was investigated in the analytical simulations. In all cases the highest stresses occur at the leading edge of the hidden vane. When the center of impact is placed on the leading edge plastic deformations are expected and localized microcracks cannot be excluded. When the target point is positioned on the suction side of the vane (air foil flank) the energy transfer and the loading is high, but the deformations remain elastic. For verification shooting tests of ice bullets on a complete stator were performed. The ice balls were made by freezing water in liquid nitrogen and the impacts were recorded with a high speed camera. The observed leading edge deflections are in good agreement with the calculated values, but in no case plastic deformations or cracks were detected. Author

N95-19671# Oxford Univ., Oxford (England). Dept. of Engineering Science.

SOFT BODY IMPACT ON TITANIUM FAN BLADES

D. A. HUGHES, I. MARTINDALE (Rolls-Royce Ltd., Derby, England.), and C. RUIZ *In* AGARD, Erosion, Corrosion and Foreign Object Damage Effects in Gas Turbines 5 p Nov. 1994 Copyright Avail: CASI HC A01/MF A03

The strength of titanium fan blades under soft body impact has been studied by means of panel tests. The panels, representing blades with various leading edge profiles, were exposed to oblique impact in a gas gun facility by launching a block of gelatine at speeds of up to 600 m/s. High speed photography, at 100,000 f.p.s. and strain gauges provide a record of the deformation. Failure occurred either as a result of the deformation or localized tearing. Tearing was taken as determining the limiting strength of the blade, which was found to be strongly dependent on the leading edge profile. Author

N95-19672# National Aeronautics and Space Administration. Lewis Research Center, Cleveland, OH.

ICE-IMPACT ANALYSIS OF BLADES

C. C. CHAMIS, P. L. N. MURTHY, S. N. SINGHAL (NYMA, Inc., Brook Park, OH.), and E. S. REDDY (NYMA, Inc., Brook Park, OH.) *In* AGARD, Erosion, Corrosion and Foreign Object Damage Effects in Gas Turbines 12 p Nov. 1994 Copyright Avail: CASI HC A03/MF A03

A computational capability is described for evaluating the ice-impact on engine blades made from composites. The ice block is modeled as an equivalent spherical object and has the velocity opposite to that of the aircraft with direction parallel to the engine axis. A finer finite element mesh is used for a portion of the blade near the impact region compared to the course mesh for the rest of the blade. The effects of ice size and velocity on the average leading edge strain are evaluated for a simulated unswept composite propfan blade. Parametric studies are performed to assess the blade structural responses due to the ice-impact at various locations along the span. It is found that: (1) for a given engine speed, a critical

ice speed exists that corresponds to the maximum strain; and (2) the tip bending type frequencies increase after impact while the torsion frequencies decrease. Author

N95-19673# Motoren- und Turbinen-Union Muenchen G.m.b.H., Munich (Germany).

DAMAGE OF HIGH TEMPERATURE COMPONENTS BY DUST-LADEN AIR

P. KOENIG, T. MILLER, and A. ROSSMANN In AGARD, Erosion, Corrosion and Foreign Object Damage Effects in Gas Turbines 12 p Nov. 1994 Original contains color illustrations Copyright Avail: CASI HC A03/MF A03

Turbine engine operators are familiar with damage to components due to dust-laden air in the compressor, but they are less aware that such damage can also occur to high temperature components, especially turbine rotor blades. Nevertheless, the frequency of occurrence of this type of damage as well as the related costs and effects on turbine performance are also of major concern. Author

N95-19675# Liburdi Engineering Ltd., Hamilton (Ontario).

PROTECTIVE COATINGS FOR COMPRESSOR GAS PATH COMPONENTS

D. R. NAGY, V. R. PARAMESWARAN (National Research Council of Canada, Ottawa, Ontario.), J. D. MACLEOD (National Research Council of Canada, Ottawa, Ontario.), and J. P. IMMARIGÉON (National Research Council of Canada, Ottawa, Ontario.) In AGARD, Erosion, Corrosion and Foreign Object Damage Effects in Gas Turbines 10 p Nov. 1994

Copyright Avail: CASI HC A02/MF A03

The blades and vanes in gas turbine compressors operating in dusty environments are prone to degradation by solid particle erosion, which causes surface roughening and changes in airfoil geometry. This results in decreased compressor performance, and higher specific fuel consumption, leading to significantly increased operational cost. Erosion damage is more prominent in flight engines without air inlet filter protection. Application of a thin ceramic titanium nitride (TiN) coating to improve the erosion resistance of compressor airfoils was thoroughly investigated. Coatings were applied to engine hardware by a Reactive Ion Coating (RIC) process, and optimized to produce a very adherent erosion resistant coating. Computer modeling of the erosion process occurring on coated and uncoated airfoils suggested that the operational life of the compressor can be enhanced by a factor of two. A complete set of compressor blades and vanes for an Allison T56 turboprop engine was coated for engine qualification tests. Laboratory tests showed that the thin coating had no significant influence on either the resonant frequency or the fatigue resistance of the blades and the instrumented engine tests confirmed that the performance was typical of overhauled engines, with no aerothermodynamic loss. Therefore, titanium nitride coatings are suitable for service and can be used on existing engines to improve the life of the compressors. Author

N95-19676# Societe Nationale d'Etude et de Construction de Moteurs d'Aviation, Evry (France). Materials and Process Dept.

NEW TRENDS IN COATINGS DEVELOPMENTS FOR TURBINE BLADES: MATERIALS PROCESSING AND REPAIR

S. ALPERINE, R. MARTINOU, R. MEVREL (Office National d'Etudes et de Recherches Aeronautiques, Paris, France.), and J. P. HUCHIN (Sochata, Chatellerault, France.) In AGARD, Erosion, Corrosion and Foreign Object Damage Effects in Gas Turbines 10 p Nov. 1994 Copyright Avail: CASI HC A02/MF A03

Turbine engines for aeronautic applications now have to face strenuous requirements concerning not only operating performances but also reliability and repairability. This evolution of the specifications induces important consequences regarding the choice and the design of turbine blade protective coatings. This paper presents several key features concerning the deposition techniques and the real-life behavior of such coatings: (1) complex aluminides well suited to the protection against high temperature oxidation and hot corrosion of directionally solidified nickel-base superalloy turbine

blades; (2) ceramic coatings used as thermal barriers - they have to exhibit both high resistance to thermomechanical fatigue and adequate smoothness; (3) processing techniques for thermal barriers, including plasma spraying, electron beam physical vapor deposition and plasma enhanced chemical vapor deposition; and (4) blades and coatings repair techniques. Author

N95-19677# Interturbine Holding B.V., Lomm (Netherlands).

BRAZE REPAIR POSSIBILITIES FOR HOT SECTION GAS TURBINE PARTS

G. MARIJNISSEN and R. VANGESTEL (Elbar B.V., Lomm, Netherlands.) In AGARD, Erosion, Corrosion and Foreign Object Damage Effects in Gas Turbines 5 p Nov. 1994

Copyright Avail: CASI HC A01/MF A03

Overlay braze repair is a good technique for restoring aircraft vanes and industrial blades and vanes. The negative effects of the intermetallic phase, formed during the overlay braze process, can be reduced in such a way that the mechanical properties - creep rupture, strength and ductility - can be achieved close to the properties of the base materials. The elimination of the negative effects can be achieved by a combination of careful selection of the chemistries of the repair materials and the application of the correct procedures for cleaning and heat cycle. Author

N95-19678# National Aerospace Lab., Amsterdam (Netherlands). GAS TURBINE COMPRESSOR CORROSION AND EROSION IN WESTERN EUROPE

H. J. KOLKMAN In AGARD, Erosion, Corrosion and Foreign Object Damage Effects in Gas Turbines 7 p Nov. 1994

Copyright Avail: CASI HC A02/MF A03

It is shown that for gas turbines in the West European environment: (1) during operation hygroscopic salts - notably ammonium sulphate (originating from manure) and sodium and magnesium chloride (from sea salt) - are deposited on compressor components and (2) during shutdowns these wet deposits acidify owing to the absorption of the air pollutants NO₂ and SO₂. The response of the compressor metals can be broadly categorized as follows. Different steels show different degrees of corrosion. Especially pitting corrosion can lead to component rejection and compressor disintegration. This necessitates frequent washing and/or corrosion resistant coatings. Modern cleaners are environmentally friendly and contain a corrosion inhibitor. The performance of cleaners and coatings is discussed. Nickel-based superalloys and titanium alloys are not prone to corrosion in compressor applications. In order to avoid problems these materials should be used even for secondary components. This is exemplified by a crash due to stress corrosion of a component costing only a few dollars. Compressor erosion as such is not a major problem in Western Europe. However, corrosion resistant coatings usually have a poor erosion resistance. Moreover, engine manufacturers and users prefer a general compressor coating for use in both corrosive and erosive environments. Developments with respect to compressor cleaners and coatings are discussed. Author

N95-19679# Turbomeca S.A. - Brevets Szydlowski, Bordes (France). MULTILAYER ANTI-EROSION COATINGS [REKETEMENTS ANTI-EROSION MULTICOUCHE]

P. MONGE-CADET, F. PELLERIN, C. FARGES (Etablissement Technique Central de l'Armement, Arcueil, France.), D. RICKERBY (Rolls-Royce Ltd., Derby, England.), and E. QUESNEL (Nuclear Research Center of Grenoble, Grenoble, France.) In AGARD, Erosion, Corrosion and Foreign Object Damage Effects in Gas Turbines 8 p Nov. 1994 In FRENCH

Copyright Avail: CASI HC A02/MF A03

Gas turbines for helicopters are prone to high degradations by abrasive particle ingestion when taking off, landing or during low altitude flights. Multilayer coatings have been developed to protect critical compressor components. After a presentation of the relevant parameters for conception and achievement of erosion resistant coatings, the most promising systems will be described. They are based on stacking arrangement of ductile layers (tungstene) and

hard layers (solid solution of carbon or nitrogen into tungstene, titanium diboride). These multilayer coatings exhibit an erosion resistance improved by more than two orders of magnitude compared with that of uncoated Ti6Al4V alloy. Author

**N95-19680# Turbine Support Europa, Tilburg (Netherlands).
HIGH VELOCITY OXYGEN FUEL SPRAYING OF EROSION
AND WEAR RESISTANT COATINGS ON JET ENGINE
PARTS**

A. T. J. VERBEEK In AGARD, Erosion, Corrosion and Foreign Object Damage Effects in Gas Turbines 10 p Nov. 1994
Copyright Avail: CASI HC A02/MF A03

High velocity oxygen fuel (HVOF) spraying is the most recent development in the field of thermal spraying. The importance of this technique for the repair and new part manufacturing of jet engine parts is rapidly increasing. The HVOF uses a supersonic oxygen-fuel flame to heat and accelerate the powder particles that form the coating. The high particle velocity results in a high density and a low porosity, a high bond strength, and a high macro and micro hardness of the coating. The high quality of the HVOF coatings makes it possible to use these coatings on high loaded, rotating parts in jet engines. This paper will highlight the use of HVOF processes to apply erosion resistant cermet coatings to high pressure compressor blades. These blades are exposed to severe erosion. Next to the D-gun process, HVOF spraying is the only nonproprietary technique that can be used to apply these high performance coatings. Also the use of the HVOF process to apply wear resistant coatings and superalloys to jet engine parts will be discussed. The difference between HVOF coatings and plasma sprayed coatings will be highlighted. During HVOF spraying, the parts are exposed to a high heat flow. Solutions to avoid overheating, especially of titanium parts, will be presented. Author

**N95-19681# Centro Sviluppo Materiali S.p.A., Trento (Italy).
THERMAL TESTING OF HIGH PERFORMANCE THERMAL
BARRIER COATINGS FOR TURBINE BLADES**

L. BERTAMINI and A. DIGIANFRANCESCO (Centro Sviluppo Materiali S.p.A., Rome, Italy.) In AGARD, Erosion, Corrosion and Foreign Object Damage Effects in Gas Turbines 11 p Nov. 1994
Copyright Avail: CASI HC A03/MF A03

A 350 micron thick 7 wt percent Y2O3-ZrO2 (7YSZ) ceramic Thermal Barrier Coating (TBC) was manufactured in an argon atmosphere and with a strictly controlled substrate temperature on flat IN 600 samples and on IN 100 aircraft turbine blades. This new atmosphere and temperature controlled spraying (ATCS) allows the reduction of the residual stresses and an improvement in the microstructure and in the mechanical properties of the coating. The good performance of these new TBC's was assessed in thermal fatigue and in thermal shock tests carried out in air at 1100 C and at 1280 C respectively. The oxidation rate of the metal-ceramic interface was measured at 1100 C. Failure of the TBC's was induced only by the deterioration (like oxidation, cracking) of the uncoated parts of the samples, as testing temperature was too severe for the base metals. Spalling was thereafter driven by compressive stresses near the aluminum oxide layer at the metal-ceramic interface. The results of these tests underline the good quality of the ceramic coating manufactured by the new ATCS technology. Author

N95-19683# National Aeronautics and Space Administration, Lewis Research Center, Cleveland, OH.

**RESISTANCE OF SILICON NITRIDE TURBINE
COMPONENTS TO EROSION AND HOT CORROSION/
OXIDATION ATTACK**

THOMAS E. STRANGMEN (Garrett Turbine Engine Co., Phoenix, AZ.) and DENNIS S. FOX In AGARD, Erosion, Corrosion and Foreign Object Damage Effects in Gas Turbines 11 p Nov. 1994
Copyright Avail: CASI HC A03/MF A03

Silicon nitride turbine components are under intensive development by AlliedSignal to enable a new generation of higher power density auxiliary power systems. In order to be viable in the intended

applications, silicon nitride turbine airfoils must be designed for survival in aggressive oxidizing combustion gas environments. Erosive and corrosive damage to ceramic airfoils from ingested sand and sea salt must be avoided. Recent engine test experience demonstrated that NT154 silicon nitride turbine vanes have exceptional resistance to sand erosion, relative to superalloys used in production engines. Similarly, NT154 silicon nitride has excellent resistance to oxidation in the temperature range of interest - up to 1400 C. Hot corrosion attack of superalloy gas turbine components is well documented. While hot corrosion from ingested sea salt will attack silicon nitride substantially less than the superalloys being replaced in initial engine applications, this degradation has the potential to limit component lives in advanced engine applications. Hot corrosion adversely affects the strength of silicon nitride in the 850 to 1300 C range. Since unacceptable reductions in strength must be rapidly identified and avoided, AlliedSignal and the NASA Lewis Research Center have pioneered the development of an environmental life prediction model for silicon nitride turbine components. Strength retention in flexure specimens following 1 to 3300 hour exposures to high temperature oxidation and hot corrosion has been measured and used to calibrate the life prediction model. Predicted component life is dependent upon engine design (stress, temperature, pressure, fuel/air ratio, gas velocity, and inlet air filtration), mission usage (fuel sulfur content, location (salt in air), and times at duty cycle power points), and material parameters. Preliminary analyses indicate that the hot corrosion resistance of NT154 silicon nitride is adequate for AlliedSignal's initial engine applications. Protective coatings and/or inlet air filtration may be required to achieve required ceramic component lives in more aggressive environments. Author

**N95-19684# Naval Air Warfare Center, Trenton, NJ. Aircraft Div.
TESTING CONSIDERATIONS FOR MILITARY AIRCRAFT
ENGINES IN CORROSIVE ENVIRONMENTS (A NAVY
PERSPECTIVE)**

FRANK T. CARROLL and DEBORAH R. PARISH In AGARD, Erosion, Corrosion and Foreign Object Damage Effects in Gas Turbines 13 p Nov. 1994 Original contains color illustrations
Copyright Avail: CASI HC A03/MF A03

This paper describes the considerations given to the testing of aircraft engines intended for use by the United States military (primarily the Navy) in potentially corrosive environments. The origins and intent of the Navy's full-scale corrosion susceptibility test are explored, and the evolution of the test from its early form to the present 1,200-hour program is described in detail. Sample results illustrating the effectiveness of the current test procedure are presented. Also noted are the activities currently underway to improve the test's effectiveness in the face of advancing engine and test equipment technologies. Author

**N95-19769# NYMA, Inc., Cleveland, OH.
ON SUPERSONIC-INLET BOUNDARY-LAYER BLEED FLOW
Final Report**

GARY J. HARLOFF and GREGORY E. SMITH Cleveland, OH
NASA Jan. 1995 17 p
(Contract(s)/Grant(s): NAS3-27186; RTOP 505-62-20)
(NASA-CR-195426; E-9393; NAS 1.26:195426; AIAA PAPER 95-0038) Copyright Avail: CASI HC A03/MF A01

Boundary-layer bleed in supersonic inlets is typically used to avoid separation from adverse shock-wave/boundary-layer interactions and subsequent total pressure losses in the subsonic diffuser and to improve normal shock stability. Methodologies used to determine bleed requirements are reviewed. Empirical sonic flow coefficients are currently used to determine the bleed hole pattern. These coefficients depend on local Mach number, pressure ratio, hole geometry, etc. A new analytical bleed method is presented to compute sonic flow coefficients for holes and narrow slots and predictions are compared with published data to illustrate the accuracy of the model. The model can be used by inlet designers

and as a bleed boundary condition for computational fluid dynamic studies. Author

N95-19864 Purdue Univ., West Lafayette, IN. School of Mechanical Engineering.

AERO-THERMODYNAMIC DISTORTION INDUCED STRUCTURED DYNAMIC RESPONSE Final Report, 1 Jun. 1991 - 31 Dec. 1993

SANFORD FLEETER 4 May 1994 101 p Limited Reproducibility: More than 20% of this document may be affected by microfiche quality (Contract(s)/Grant(s): AF-AFOSR-0251-91) (AD-A279931; AFOSR-94-0338TR) Avail: Issuing Activity (Defense Technical Information Center (DTIC))

This final report summarizes the results obtained on Grant AFOSR-91-025. The overall objective of this basic research program was the quantitative investigation of the fundamental phenomena relevant to aero-thermodynamic distortion induced structural dynamic blade responses in multistage gas turbine engines and the study of the fundamental unsteady aerodynamics and heat transfer phenomena inherent in turbines. The technical approach involved unique benchmark experiments and also analyses. In particular, the flow physics of multistage blade row interactions were investigated, with unique unsteady aerodynamic data obtained and analyses developed to understand, quantify, and discriminate the fundamental flow phenomena as well as to direct the modeling of advanced analyses. DTIC

08

AIRCRAFT STABILITY AND CONTROL

Includes aircraft handling qualities; piloting; flight controls; and autopilots.

A95-68299
FINITE ELEMENT TIME DOMAIN - MODAL FORMULATION FOR NONLINEAR FLUTTER OF COMPOSITE PANELS

R. C. ZHOU Old Dominion Univ., Norfolk, VA, DAVID Y. XUE, and CHUHMEI AIAA Journal (ISSN 0001-1452) vol. 32, no. 10 October 1994 p. 2044-2052 refs (BTN-95-EIX95042474401) Copyright

A finite element time domain modal approach is presented for determining the nonlinear flutter characteristics of composite panels at elevated temperatures. The von Karman large-deflection strain-displacement relations, quasisteady first-order piston theory aerodynamics, and quasisteady thermal stress theory are used to formulate the nonlinear panel flutter finite element equations of motion in nodal displacements. A set of nonlinear modal equations of motion of much smaller degrees of freedom for the facilitation in time numerical integration is then obtained through a modal transformation and reduction. All five types of panel behavior - flat, buckled, limit-cycle, periodic, and chaotic motions - can be determined. Examples show the accuracy, convergence, and versatility of the present approach. Author (EI)

A95-68364
INFLUENCE OF STRUCTURAL AND AERODYNAMIC MODELING ON FLUTTER ANALYSIS

ALFRED G. STRIZ Univ. of Oklahoma, Norman, OK and VIPPERLA B. VENKAYYA Journal of Aircraft (ISSN 0021-8669) vol. 31, no. 5 September-October 1994 p. 1205-1211 refs (BTN-95-EIX95062487550) Copyright

The dynamic aeroelastic capabilities in the automated structural optimization system were used to evaluate the flutter behavior of various fully built-up finite element wing models in subsonic and supersonic flow. First, the performance of the flutter module was tested against results from other codes. Then, models of various wings with different aspect ratios were investigated for the influence on the free vibration and flutter characteristics of such modeling factors as finite element selection, structural grid refinement, num-

ber of selected modes, retention of in-plane and breathing modes, aerodynamic panel size and placement, splining of the aerodynamic grid to the structural grid, selection of extra points off the structural wing box for splining, solution procedures such as eigenvalue extraction routines, reduction schemes, etc. The results suggest that a quick initial evaluation of a preliminary wing design with a reasonably coarse grid for both the structure and the aerodynamics will result in natural frequencies and modes that are close to those from a more detailed model and in flutter speeds that tend to be conservative. Overall, such a simple model can represent a good start for a conventional redesign process as well as for optimization. Author (EI)

A95-68365
CONTINUOUS GUST RESPONSE AND SENSITIVITY DERIVATIVES USING STATE-SPACE MODELS

ARIE ZOLE Technion - Israel Inst. of Technology, Haifa (Israel) and MORDECHAY KARPEL Journal of Aircraft (ISSN 0021-8669) vol. 31, no. 5 September-October 1994 p. 1212-1214 refs (BTN-95-EIX95062487551) Copyright

An atmospheric flight vehicle is exposed to continuous gas loads which affect critical structural design conditions and even the response of the automatic flight control system. In this study, continuous gust response is analyzed by aeroservoelastic models that include unsteady aerodynamic, control, and structural dynamics effects. The gusts caused by air turbulence are defined in statistical terms by their power spectral density (PSD) functions and root-mean-square (rms) values. EI

A95-68367
OFFSET THRUST AXES AND PITCH STABILITY

U. P. SOLIES Univ. of Tennessee Space Inst., Tullahoma, TN Journal of Aircraft (ISSN 0021-8669) vol. 31, no. 5 September-October 1994 p. 1217-1219 refs (BTN-95-EIX95062487553) Copyright

This paper disproves the widespread notion that high or low thrust lines affect static longitudinal stability. Propellers and turbopans were pointed out as the ones affecting longitudinal dynamics through speed changes. Stability predictions require a dynamic analysis. A simple static margin correction based on thrust arm only is unsatisfactory and leads to wrong conclusions. EI

A95-68371
BRIEF HISTORY OF GUST MODELS FOR AIRCRAFT DESIGN
HUBERT I. FLOMENHOFT Journal of Aircraft (ISSN 0021-8669) vol. 31, no. 5 September-October 1994 p. 1225-1227 refs (BTN-95-EIX95062487557) Copyright

Increasing pressure from the International Standards Organization (ISO) to come up with standard gust and turbulence models have promoted this review of some of the history of gust models. In particular, this review aims to place in the historical record the circumstances by which the '1-minus-cosine' or 'versine' discrete gust shape was established. EI

A95-69233
FLIGHT CONTROL SYSTEM MODE TRANSITIONS INFLUENCE ON HANDLING QUALITIES AND TASK PERFORMANCE

LLOYD D. REID Univ. of Toronto, Toronto (Ontario), PAVAN RAJAGOPAL, and WOLF O. GRAFT Journal of Aircraft (ISSN 0021-8669) vol. 31, no. 5 September-October 1994 p. 1037-1042 refs (BTN-95-EIX95062487525) Copyright

The paper presents a flight research simulator modified with a digital flight control system (FCS) and a side arm controller to model a fly by wire helicopter. The simulator is used to investigate the influence of mode transition type and mode pair on pilot/helicopter response for formation flying and precision hover. A FCS mode selection algorithm was developed to carry out the commanded mode transitions. Results of the study acquired in the form of Cooper-Harper handling qualities ratings (HQR) and station keeping performance measurements showed that the mode pair affected

08 AIRCRAFT STABILITY AND CONTROL

both the HQR and performance while type of mode transition did not affect the results. EI

N95-19576* West Virginia Univ., Morgantown, VA. Dept. of Mechanical and Aerospace Engineering.

DETERMINATION OF STABILITY AND CONTROL DERIVATIVES FROM THE NASA F/A-18 HARV FROM FLIGHT DATA USING THE MAXIMUM LIKELIHOOD METHOD Progress Report

MARCELLO R. NAPOLITANO Jan. 1995 101 p

(Contract(s)/Grant(s): NCC2-759)

(NASA-CR-197320; NAS 1.26:197320) Avail: CASI HC A06/MF A02

This report is a compilation of PID (Proportional Integral Derivative) results for both longitudinal and lateral directional analysis that was completed during Fall 1994. It had earlier established that the maneuvers available for PID containing independent control surface inputs from OBES were not well suited for extracting the cross-coupling static (i.e., $C_{\text{sub N beta}}$) or dynamic (i.e., $C_{\text{sub N pf}}$) derivatives. This was due to the fact that these maneuvers were designed with the goal of minimizing any lateral directional motion during longitudinal maneuvers and vice-versa. This allows for greater simplification in the aerodynamic model as far as coupling between longitudinal and lateral directions is concerned. As a result, efforts were made to reanalyze this data and extract static and dynamic derivatives for the F/A-18 HARV (High Angle of Attack Research Vehicle) without the inclusion of the cross-coupling terms such that more accurate estimates of classical model terms could be acquired. Four longitudinal flights containing static PID maneuvers were examined. The classical state equations already available in pEst for alphadot, qdot and thetadot were used. Three lateral directional flights of PID static maneuvers were also examined. The classical state equations already available in pEst for betadot, p dot, rdot and phi dot were used. Enclosed with this document are the full set of longitudinal and lateral directional parameter estimate plots showing coefficient estimates along with Cramer-Rao bounds. In addition, a representative time history match for each type of maneuver tested at each angle of attack is also enclosed.

Derived from text

09

RESEARCH AND SUPPORT FACILITIES (AIR)

Includes airports, hangars and runways; aircraft repair and overhaul facilities; wind tunnels; shock tube facilities; and engine test blocks.

A95-69236* National Aeronautics and Space Administration. Lewis Research Center, Cleveland, OH.

REPEATABILITY OF ICE SHAPES IN THE NASA LEWIS ICING RESEARCH TUNNEL

JAIWON SHIN and THOMAS H. BOND Journal of Aircraft (ISSN 0021-8669) vol. 31, no. 5 September-October 1994 p. 1057-1063 refs

(BTN-95-EIX95062487528) Copyright

Tests were conducted in the Icing Research Tunnel (IRT) at the NASA Lewis Research Center to document the current capability of the IRT, focused mainly on the repeatability of the ice shape over a range of icing conditions. Measurements of drag increase due to the ice accretion were also made to document the repeatability of drag. The repeatability of the ice shape was very good at low temperatures, but only fair at near freezing temperatures. In general, drag data shows good repeatability. Author (EI)

N95-19848 Aeronautical Research Labs., Melbourne (Australia).

PROGRAMMABLE COCKPIT RESEARCH SIMULATOR

M. IOB, A. G. PAGE, and D. A. CRAVEN Mar. 1994 27 p Limited Reproducibility: More than 20% of this document may be affected by microfiche quality

(AD-A279219; ARL-TN-49; DODA-AR-008-375) Avail: Issuing Activity (Defense Technical Information Center (DTIC))

The 'Programmable Cockpit' is a low-cost facility to be used for study and development of the aircrew-vehicle interface for future aircraft systems. It was designed so that instrument layouts and display formats could be reconfigured rapidly and tested in a realistic aircraft representation or emulation, with the pilot under representative workload conditions. It is not intended to be used for pilot training and/or evaluation. It uses personal computers and computer graphics workstations linked together to represent the aircraft displays, and includes representative flight dynamic models for fixed-wing aircraft. Controls include a sidestick, rudder pedals, throttle, and touch sensitive screens. DTIC

10

ASTRONAUTICS

Includes astronautics (general); astrodynamics; ground support systems and facilities (space); launch vehicles and space vehicles; space transportation; spacecraft communications, command and tracking; spacecraft design, testing and performance; spacecraft instrumentation; and spacecraft propulsion and power.

A95-66301

BALLOON FLIGHTS IN FRANCE AND IN EUROPE

A. SOUBRIER Centre National d'Etudes Spatiales, Toulouse, France and M. AUDEBERT Centre National d'Etudes Spatiales, Toulouse, France Balloon technology and observations; Symposium P3 of the COSPAR Plenary Meeting, 29th, Washington, DC, Aug. 28-Sept. 5, 1992. A95-66276 Advances in Space Research (ISSN 0273-1177) vol. 14, no. 2 February 1994 p. (2)169-(2)172 Copyright

Large 'Heavy Duty' Balloons are regularly operated in Europe since 1977, where National Center for Space Studies (CNES) along with Italian and Spanish organizations, ASI and INTA, created the Transmediterranean flight facility, so-called 'ODISSEA'. More than fifty flights have since then been achieved, using large polyethylene balloons of which the volume may exceed 1 million cubic meters with payload of more than two tons. This activity has been recently extended to the Southern Hemisphere, where a first campaign took place in 1988 from a site located in Australia. A rather intense activity will be developed during 1992, as a new campaign, organized by CNES, will take place on the Australian site, followed few months later by a series of Transmediterranean flights. This paper presents the results obtained so far by the ODISSEA program, along with the results of the Australian and Transmediterranean campaigns conducted in 1992. Author (Herner)

A95-69210* National Aeronautics and Space Administration. Langley Research Center, Hampton, VA.

NAVIER-STOKES SIMULATIONS OF ORBITER

AERODYNAMIC CHARACTERISTICS INCLUDING PITCH TRIM AND BODYFLAP

K. JAMES WEILMUNSTER National Aeronautics and Space Administration. Langley Research Center, Hampton, VA, PETER A. GNOFFO, and FRANCIS A. GREENE Journal of Spacecraft and Rockets (ISSN 0022-4650) vol. 31, no. 3 May-June 1994 p. 355-366

(BTN-95-EIX95041503779) Copyright

An analysis of the longitudinal aerodynamics of the shuttle orbiter in the hypersonic flight regime is made through the use of computational fluid dynamics. Particular attention is given to establishing the cause of the 'pitching moment anomaly,' which occurred on the orbiter's first flight, and to computing the aerodynamics of a complete orbiter configuration at flight conditions. Data from ground-based facilities as well as orbiter flight data are used to validate the computed results. Analysis shows that the pitching moment anomaly is a real-gas chemistry effect that was not simulated in ground-based facilities, which used air as a test gas. Computed flight

aerodynamics for the orbiter are within 5% of the measured flight values and trim bodyflap deflections are predicted to within 10%.

Author (EI)

A95-69211* National Aeronautics and Space Administration. Langley Research Center, Hampton, VA.

MULTIBLOCK ANALYSIS FOR SHUTTLE ORBITER REENTRY HEATING FROM MACH 24 TO MACH 12

PETER A. GNOFFO National Aeronautics and Space Administration. Langley Research Center, Hampton, VA, K. JAMES WEILMUNSTER, and STEPHEN J. ALTER Journal of Spacecraft and Rockets (ISSN 0022-4650) vol. 31, no. 3 May-June 1994 p. 367-377 (BTN-95-EIX95041503780) Copyright

A multiblock, laminar heating analysis for the shuttle orbiter at three trajectory points ranging from Mach 24.3 to Mach 12.86 on reentry is described. The analysis is performed using the Langley Aerothermodynamic Upwind Relaxation Algorithm with a seven species chemical nonequilibrium model. A finite-catalytic-wall model appropriate for shuttle tiles at a radiative equilibrium wall temperature is applied. Computed heating levels are generally in good agreement with the flight data, although a few rather large discrepancies remain unexplained. The multiblock relaxation strategy partitions the flowfield into manageable blocks requiring a fraction of the computational resources (time and memory) required by a full domain approach. In fact, the computational cost for a solution at even a single trajectory point would be prohibitively expensive at the given resolution without the multiblock approach. Converged blocks are reassembled to enable a fully coupled converged solution over the entire vehicle, starting from a nearly converged initial condition.

Author (EI)

A95-69212

AERODYNAMICALLY BLUNT AND SHARP BODIES

W. H. MASON Virginia Polytechnic Inst and State Univ, Blacksburg, VA, United States and JAEWOO LEE Journal of Spacecraft and Rockets (ISSN 0022-4650) vol. 31, no. 3 May-June 1994 p. 378-382

(BTN-95-EIX95041503781) Copyright

Computational fluid dynamics studies at supersonic and hypersonic speeds have resulted in an improved understanding of the meaning of aerodynamically, as opposed to geometrically, sharp and blunt shapes. An analytic investigation using Newtonian theory was conducted to support the computational results. Based on this work, a new criterion for the definition of an aerodynamically sharp shape is proposed. Defining the power-law shape to be the relevant gauge function, one can classify bodies with n greater than $2/3$ as aerodynamically sharp, even though the initial body slope dr/dx is 90 deg. The paper describes the analysis that resulted in the new sharp and blunt shape criteria for aerodynamics.

Author (EI)

A95-69218* National Aeronautics and Space Administration. Ames Research Center, Moffett Field, CA.

TRAJECTORY-BASED HEATING ANALYSIS FOR THE EUROPEAN SPACE AGENCY/ROSETTA EARTH RETURN VEHICLE

WILLIAM D. HENLINE National Aeronautics and Space Administration. Ames Research Center, Moffett Field, CA and MICHAEL E. TAUBER Journal of Spacecraft and Rockets (ISSN 0022-4650) vol. 31, no. 3 May-June 1994 p. 421-428 (BTN-95-EIX95041503787) Copyright

A coupled, trajectory-based flowfield and material thermal-response analysis is presented for the European Space Agency proposed Rosetta comet nucleus sample return vehicle. The probe returns to earth along a hyperbolic trajectory with an entry velocity of 16.5 km/s and requires an ablative heat shield on the forebody. Combined radiative and convective ablating flowfield analyses were performed for the significant heating portion of the shallow ballistic entry trajectory. Both quasisteady ablation and fully transient analyses were performed for a heat shield composed of carbon-phenolic ablative material. Quasisteady analysis was performed using the

two-dimensional axisymmetric codes RASLE and BLIMPK. Transient computational results were obtained from the one-dimensional ablation/conduction code CMA. Results are presented for heating, temperature, and ablation rate distributions over the probe forebody for various trajectory points. Comparison of transient and quasisteady results indicates that, for the heating pulse encountered by this probe, the quasisteady approach is conservative from the standpoint of predicted surface recession.

Author (EI)

A95-69854

DESIGN DECISIONS FROM THE HISTORY OF THE EUVE SCIENCE PAYLOAD

W. MARCHANT Univ. of California, Berkeley, CA, US British Interplanetary Society, Journal (ISSN 0007-094X) vol. 46, no. 9 September 1993 p. 353-354 (HTN-95-60545) Copyright

NASA's Explorer class instruments are intended as low-cost, quick-turnaround missions. Associated with those admirable goals, however, is the necessity of accepting a higher risk of design or implementation flaws in the flight hardware and software systems. This paper will discuss some of the design issues that arose during the development of the Extreme Ultraviolet Explorer (EUVE) science payload at UC Berkeley, how they were solved, and how those decisions have worked out, based on the successful completion of the survey phase of the EUVE science mission. Author (Herner)

N95-19624*# National Aeronautics and Space Administration. Lyndon B. Johnson Space Center, Houston, TX.

DOCUMENTATION AND ARCHIVING OF THE SPACE SHUTTLE WIND TUNNEL TEST DATA BASE. VOLUME 2: USER'S GUIDE TO THE ARCHIVED DATA BASE Technical Report, 1969-1994

PAUL O. ROMERE and STEVE WESLEY BROWN Jan. 1995 186 p (NASA-TM-104806-VOL-2; S-786-VOL-2; NAS 1.15:104806-VOL-2) Avail: CASI HC A09/MF A02

Development of the Space Shuttle necessitated an extensive wind tunnel test program, with the cooperation of all the major wind tunnels in the United States. The result was approximately 100,000 hours of Space Shuttle wind tunnel testing conducted for aerodynamics, heat transfer, and structural dynamics. The test results were converted into Chrysler DATAMAN computer program format to facilitate use by analysts, a very cost effective method of collecting the wind tunnel test results from many test facilities into one centralized location. This report provides final documentation of the Space Shuttle wind tunnel program. The two-volume set covers the evolution of Space Shuttle aerodynamic configurations and gives wind tunnel test data, titles of wind tunnel data reports, sample data sets, and instructions for accessing the digital data base. Author

11

CHEMISTRY AND MATERIALS

Includes chemistry and materials (general); composite materials; inorganic and physical chemistry; metallic materials; nonmetallic materials; and propellants and fuels.

A95-68191* National Aeronautics and Space Administration. Ames Research Center, Moffett Field, CA.

REVIEW OF NUMERICAL PROCEDURES FOR COMPUTATIONAL SURFACE THERMOCHEMISTRY

FRANK S. MILOS and DANIEL J. RASKY Journal of Thermophysics and Heat Transfer (ISSN 0887-8722) vol. 8, no. 1 January-March 1994 p. 24-34 refs (BTN-94-EIX94441386682) Copyright

Models and equations for surface thermochemistry and near-

surface thermophysics of aerodynamically heated thermal protection materials are reviewed, with particular emphasis on computational boundary conditions for surface mass and energy transfer. The surface energy and mass balances, coupled with an appropriate ablation or surface catalysis model, provide complete thermochemical boundary conditions for a true multidisciplinary solution of the fully coupled fluid-dynamics/solid mechanics problem. Practical approximate solutions can be obtained by using a detailed model with full thermophysics for either the solid or fluid phase and a semianalytic method for the other half of the problem. A significant increase in the state-of-the-art in aerothermal computational fluid dynamics is possible by uniting computational fluid dynamic (CFD) methodology with surface thermochemistry boundary conditions and the heat-balance-integral method. Author (EI)

A95-69131

FATIGUE RESISTANCE OF PEENED 7050-T7451 ALUMINIUM ALLOY: REPAIR AND RE-TREATMENT OF A COMPONENT SURFACE

P. K. SHARP DSTO, Melbourne, Australia, J. Q. CLAYTON, and G. CLARK Fatigue and Fracture of Engineering Materials & Structures (ISSN 8756-758X) vol. 17, no. 3 March 1994 p. 243-252 refs (BTN-94-EIX94371347838) Copyright

Metal and glass-bead peening treatments, widely used throughout the aircraft industry to enhance the fatigue performance of many steels and titanium alloys, are now being routinely applied to high-strength aluminium-alloy components. This paper describes the effects of peening on the fatigue life of 7050 aluminium alloy material, which is representative of alloys used for many components in modern military aircraft. Using simulated service loading, two proposed peening/re-peening procedures were evaluated and compared with both the original peened surface and a simple hand-polished surface. The results show that optimisation of peening parameters to reduce surface damage can provide a substantial improvement in fatigue life over both the original peening treatment and the polished surface treatment, however, poor control of peening procedures, or unnecessary 'overpeening' can lead to a relatively poor fatigue life. For re-peened surfaces, a procedure incorporating a polishing step, designed to repair any damage from the severe peening applied initially, gave the best fatigue performance. Results are discussed in relation to the stability of the residual surface stresses under fatigue loading, the surface roughness, and the number and types of defects introduced by the peening treatments. Author (EI)

A95-69136

FATIGUE CRACK GROWTH IN NICKEL-BASED SUPERALLOYS AT 500-700 C. 1: WASPALOY

S. P. LYNCH Defence Science and Technology Organisation, Australia, T. C. RADTKE, B. J. WICKS, and R. T. BYRNES Fatigue and Fracture of Engineering Materials & Structures (ISSN 8756-758X) vol. 17, no. 3 March 1994 p. 297-311 refs (BTN-94-EIX94371347843) Copyright

The effects of cyclic frequency, hold time, and stress-intensity-factor range (ΔK) on rates of fatigue crack growth in air at 500-700 C have been studied for Waspaloy- a nickel-based superalloy used for gas-turbine engine discs. The main effects observed were: (1) higher rates of crack growth for lower cyclic frequencies at high ΔK at 600 and 700 C, and (2) lower rates of crack growth at low ΔK (and higher ΔK thresholds) for longer hold times at 700 C, compared with those at a baseline frequency of 2 Hz. Metallographic and fractographic observations suggested that the effects of cyclic frequency and hold time could be rationalised in terms of the competing effects of enhancement of cracking due to creep and inhibition of cracking caused by oxide-induced crack closure, fracture-surface-roughness induced crack closure, and crack-branching/deflection. Possible mechanisms for promoting intergranular and transgranular cracking at low cyclic frequencies or long hold times are discussed. Author (EI)

A95-69164

SURFACE MORPHOLOGY AND STRUCTURE OF CARBON-CARBON COMPOSITES IN HIGH-ENERGY SLIDING CONTACT

BING K. YEN Mitsubishi Kasei Research Cent, Yokohama, Japan and TADASHI ISHIHARA Wear (ISSN 0043-1648) vol. 174, no. 1-2 May 1994 p. 111-117 refs (BTN-94-EIX94371347996) Copyright

The surface morphology and microstructure of a carbon-carbon composite material in sliding contact have been investigated. The carbon-carbon composite sample is made from an organic binder-impregnation process. Chopped carbon fiber felt is impregnated with phenolic resin and pitch. A ring-on-ring specimen configuration with fiber randomly oriented in the plane of sliding is used to simulate aircraft brakes. The relative sliding speed between two composite rings decelerates from an initial speed of 23 m/s to a complete stop under a load of 3100 N to simulate a high energy aircraft braking process. Two types of surface morphology can be distinguished on the sample surface: a dull-looking grey surface area with a machine-finished appearance, and a lustrous black area with a mirror-like polished appearance under room light. The sliding surface on the grey area is rough. Patches of wear debris and wear tracks on top of both the fiber and the matrix are clearly visible. Large blisters formed from the compaction of wear debris are sometimes observed on this surface. The sliding surface on the lustrous area is covered with a layer of thin debris film of the order of 1 micron thick. This film is composed of aggregates of equiaxial particles and thus exhibits no preferred crystallite orientation on the surface. The existence of two types of surface morphology is due to a difference in the local contact pressure. In the grey surface area the contact pressure is higher, which leads to a rougher surface without continuous debris film coverage. In the lustrous surface area the contact pressure is lower, which allows the maintenance of a debris film. The difference in the contact pressure is due to the nonuniform frictional heat generation which causes unequal thermal expansion of the contact surface as often observed in tribological tests involving high energy dissipation rate. Author (EI)

A95-69318

MODELING OF SUPERSONIC TURBULENT COMBUSTION USING ASSUMED PROBABILITY DENSITY FUNCTIONS

R. A. BAURLE North Carolina State Univ, Raleigh, NC, United States, G. A. ALEXOPOULOS, and H. A. HASSAN Journal of Propulsion and Power (ISSN 0748-4658) vol. 10, no. 6 November-December 1994 p. 776-786 refs (BTN-95-EIX95112524190) Copyright

Recent calculations of turbulent supersonic reacting shear flows using an assumed multivariate beta probability density function (PDF) resulted in reduced production rates and a delay in the onset of combustion. This result is not consistent with available measurements. Earlier work was based on a one-equation turbulence model that required a specification of the length scale, PDFs that did not yield Favre-averaged quantities, and the gradient diffusion assumption. The present work incorporates a two-equation turbulence model based on a kappa-omega formulation, a PDF that yields Favre averages, and relaxes the gradient diffusion assumption. Results suggest that the form of the assumed multivariate PDF and the gradient diffusion assumption are the main causes of the discrepancy. Author (EI)

N95-19579# Sandia National Labs., Albuquerque, NM.

ENVIRONMENTAL EFFECTS ON COMPOSITE AIRFRAMES: A STUDY CONDUCTED FOR THE ARM UAV PROGRAM (ATMOSPHERIC RADIATION MEASUREMENT UNMANNED AEROSPACE VEHICLE)

R. A. NOGUCHI Jun. 1994 49 p (Contract(s)/Grant(s): DE-AC04-94AL-85000) (DE94-015351; SAND-94-8210) Avail: CASI HC A03/MF A01

Composite materials are affected by environments differently

than conventional airframe structural materials are. This study identifies the environmental conditions which the composite-airframe Atmospheric Radiation Measurement Unmanned Aerospace Vehicle (ARM UAV) may encounter, and discusses the potential degradation processes composite materials may undergo when subjected to those environments. This information is intended to be useful in a follow-on program to develop equipment and procedures to prevent, detect, or otherwise mitigate significant degradation with the ultimate goal of preventing catastrophic aircraft failure. DOE

12

ENGINEERING

Includes engineering (general); communications; electronics and electrical engineering; fluid mechanics and heat transfer; instrumentation and photography; lasers and masers; mechanical engineering; quality assurance and reliability; and structural mechanics.

A95-65845

DYNAMIC BEHAVIOR OF VALVES WITH PNEUMATIC CHAMBER FOR RECIPROCATING COMPRESSORS

M. KATO Kobe Steel, Ltd., Kobe (Japan), M. KUHASHI, and M. AOSHIMA Journal of Vibration and Acoustics, Transactions of the ASME (ISSN 1048-9002) vol. 115, no. 4 October 1993 p. 371-376

(BTN-94-EIX94351143311) Copyright

This paper describes the dynamic behavior of valves with pneumatic chambers for reciprocating compressors. These are known as 'damped valves' and are capable of reducing the impact on the valve seat and valve stopper. The characteristics of the dynamic behavior of the damped valves were clarified by calculating newly derived governing equations of valve dynamics. From the calculated results, it becomes apparent that the volume of the pneumatic chambers and the clearance between the pneumatic chamber and the valve have a large influence on the impact speed of the valves. Furthermore, the valves tend to close later for a higher compressor speed to oscillate at a larger amplitude for a lower density of gas such as hydrogen. These tendencies show that the selection of the specification of damped valves is very important. The stiffness of the valve spring and the lift of the valve also affect valve behavior as with valves without pneumatic chambers.

Author (EI)

A95-65897

LYAPUNOV EXPONENTS AND STOCHASTIC STABILITY OF TWO-DIMENSIONAL PARAMETRICALLY EXCITED RANDOM SYSTEMS

S. T. ARIARATNAM Univ. of Waterloo, Waterloo (Ontario) and WEI-CHAU XIE Journal of Applied Mechanics, Transactions ASME (ISSN 0021-8936) vol. 60, no. 3 September 1993 p. 677-682 (BTN-94-EIX94361122401) Copyright

The variation of the largest Lyapunov exponent for two-dimensional parametrically excited stochastic systems is studied by a method of linear transformation. The sensitivity to random disturbance of systems undergoing bifurcation is investigated. Two commonly occurring examples in structural dynamics are considered, where the random fluctuation appears in the stiffness term or the damping term. The boundaries of almost-sure stochastic stability are determined by the vanishing of the largest Lyapunov exponent of the linearized system. The validity of the approximate results is checked by numerical simulation.

Author (EI)

A95-65981

CONSTRUCTION OF NEARLY ORTHOGONAL MULTIBLOCK GRIDS FOR COMPRESSIBLE FLOW SIMULATION

M. J. MARCHANT Univ Coll of Swansea, Swansea (Wales) and

N. P. WEATHERILL Communications in Numerical Methods in Engineering (ISSN 0748-8025) vol. 9, no. 7 July 1993 p. 567-578 refs

(BTN-94-EIX94361133526) Copyright

A method is described where structured multiblock meshes can be constructed from the solution of the elliptic partial differential equations and which process the property of orthogonality close to boundaries and near orthogonality within the domain. To construct grids for various flow simulations which have appropriate point distributions close to solid boundaries these grids are used with point redistribution formulations. The result is high-quality grids for use with both inviscid and viscous flow simulation algorithms. Examples using the approach is given, and these include grids for single and multicomponent aerofoils and bluff bodies. Author (EI)

A95-67301

MODELING ROTATING SHAFTS USING AXISYMMETRIC SOLID FINITE ELEMENTS WITH MATRIX REDUCTION

R. W. STEPHENSON Kingsbury, Inc., Philadelphia, PA and K. W. ROUGH Journal of Vibration and Acoustics, Transactions of the ASME (ISSN 1048-9002) vol. 115, no. 4 October 1993 p. 484-489

(BTN-94-EIX94351143328) Copyright

An axisymmetric harmonic finite element representation is used to calculate shaft lateral critical speeds and perform stability analysis. Unlike a beam element model, an axisymmetric solid element representation allows the actual rotor geometry to be modeled. A Fourier series representation allows the three-dimensional shaft geometry to be modeled in two dimensions by only considering the radial and axial coordinates. Thus, the degrees of freedom of this element type are different from the usual two translations and two rotations at each node associated with bending of a three-dimensional beam element. A required gyroscopic matrix is also presented for completeness in analysis of rotating shafts. A matrix reduction technique is used to reduce the size of the shaft mass, gyroscopic, and stiffness matrices by condensing out slave degrees of freedom in terms of the retained master degrees of freedom. The formulation is applied to various examples for verification and to investigate the effect of selection of different master degrees of freedom for this element type on the results. Author (EI)

A95-67304

ROTOR WHIRL FORCES INDUCED BY THE TIP CLEARANCE EFFECT IN AXIAL FLOW COMPRESSORS

F. EHRICH GE Aircraft Engines, Lynn, MA Journal of Vibration and Acoustics, Transactions of the ASME (ISSN 1048-9002) vol. 115, no. 4 October 1993 p. 509-515

(BTN-94-EIX94351143331) Copyright

It is now widely recognized that destabilizing forces, tending to generate forward rotor whirl, are generated in axial flow turbines as a result of the nonuniform torque induced by the nonuniform tip-clearance in a deflected rotor-the so called Thomas/Alford force (Thomas, 1958, and Alford, 1965). It is also recognized that there will be a similar effect in axial flow compressors, but qualitative considerations cannot definitively establish the magnitude or even the direction of the induced whirling forces-that is, if they will tend to forward or backward whirl. Applying a 'parallel compressor' model to simulate the operation of a compressor rotor deflected radially in its clearance, it is possible to derive a quantitative estimate of the proportionality factor which relates the Thomas/Alford force in axial flow compressors (i.e., the tangential force generated by a radial deflection of the rotor) to the torque level in the compressor. The analysis makes use of experimental data from the GE Aircraft Engines Low Speed Research Compressor facility comparing the performance of three different axial flow compressors, each with four stages (typical of a mid-block of an aircraft gas turbine compressor) at two different clearances (expressed as a percent of blade length) - $CL/L = 1.4$ percent and $CL/L = 2.8$ percent. It is found that the value of Beta is in the range of + 0.27 to - 0.71 in the vicinity of

the stages' nominal operating line and + 0.08 to - 1.25 in the vicinity of the stages' operation at peak efficiency. The value of Beta reaches a level of between - 1.16 and - 3.36 as the compressor is operated near its stalled condition. The final result bears a very strong resemblance to the correlation obtained by improvising a normalization of the experimental data of Vance and Laudadio (1984) and a generic relationship to the analytic results of Colding-Jorgensen (1990). Author (EI)

A95-67329

SOLUTION-ADAPTIVE STRUCTURED-UNSTRUCTURED GRID METHOD FOR UNSTEADY TURBOMACHINERY ANALYSIS. PART I: METHODOLOGY

SANJAY R. MATHUR Iowa State Univ., Ames, IA, NATERI K. MADAVAN, and R. GANESH RAJAGOPALAN Journal of Propulsion and Power (ISSN 0748-4658) vol. 10, no. 4 July-August 1994 p. 576-584 refs (BTN-94-EIX94441380983) Copyright

A solution-adaptive method for the time-accurate analysis of two-dimensional flows in multistage turbomachinery is presented. The method employs a hybrid structured-unstructured zonal grid topology in conjunction with appropriate modeling equations and solution techniques in each zone, thus combining the advantages of both structured and unstructured grid methods. The viscous flow region in the immediate vicinity of the airfoils is resolved on structured O-type grids, while the rest of the domain is discretized using an unstructured mesh of triangular cells. In the inner regions, the Navier-Stokes equations are solved using an implicit, third-order accurate, upwind-biased scheme. The use of both central difference and upwind schemes is explored for the solution of the Euler equations in the outer regions. An efficient and robust grid adaptation strategy, including both grid refinement and coarsening capabilities, is developed for the unstructured grid regions. Methodologies for the accurate, conservative transfer of information at the interface between the structured and unstructured domains, as well as that between two unstructured grids in relative motion, are also developed. For generality, three-dimensional effects of stream-tube contraction are modeled. The numerical methodology is presented in detail in the present article (Part I). Results obtained using this method and comparisons of these results with experimental data and earlier structured-grid based methods are presented in a companion article (Part II). Author (EI)

A95-67342

VORTEX CUTTING BY A BLADE. PART II: COMPUTATIONS OF VORTEX RESPONSE

J. S. MARSHALL Univ. of Iowa, Iowa City, IA and R. YALAMANCHILI AIAA Journal (ISSN 0001-1452) vol. 32, no. 7 July 1994 p. 1428-1436 refs (BTN-94-EIX94441386611) Copyright

Computations of the interaction between a line vortex and blades of various thicknesses and angles of attack traveling in a direction normal to the vortex axis have been performed. A procedure to enable instantaneous cutting of the vortex is used in the case of thin blades to study vortex interaction with the blade both before and after vortex cutting has occurred. To isolate the effect of blade thickness on vortex bending, additional computations have been performed of the interaction between a line vortex and circular cylinders of various diameters. The vortex is represented by a filament model which includes axial flow within the core and nonuniform core area, and the effect of the blade or cylinder on the vortex is obtained using a vortex sheet panel method. The study particularly examines bending of the vortex and the subsequent variation in vortex core radius. It is found that the amount of vortex bending is primarily dependent on the ratio of blade thickness T (or diameter D of a circular cylinder) to ambient vortex core radius σ_0 . For blades with T/σ_0 of order unity or less, very little bending is observed for attack angles under the stall limit. For cases in which significant vortex bending is observed (T/σ_0 or D/σ_0 greater than order unity), increase in blade or cylinder

forward speed results in a decrease in vortex core radius for a given amount of bending of the vortex axis. Vortex shocks and expansion waves are also observed to propagate on the vortex after cutting by a blade, as predicted in Part 1 of the study. Author (EI)

A95-67343

ELLIPTIC TIP EFFECTS ON THE VORTEX WAKE OF AN AXISYMMETRIC BODY AT INCIDENCE

DAVID H. BRIDGES Mississippi State Univ., Mississippi State, MS and HANS G. HORNUNG AIAA Journal (ISSN 0001-1452) vol. 32, no. 7 July 1994 p. 1437-1445 refs (BTN-94-EIX94441386612) Copyright

The effectiveness of a new version of an elliptic cross-section tip in controlling the asymmetry of the vortex wake of an axisymmetric body at angle of attack has been studied. The elliptic cross sections were generated using two sixth-degree polynomials such that the tip radius, slope, and curvature would match those of a right circular cone at the point where the polynomial became tangent to a cone generator. The tip was found to be effective in varying the vortex wake geometry of a right circular cone at large angle of attack. The measured side force coefficient varied smoothly with tip roll angle for the two lowest angles of attack studied and exhibited square-wave and more undesirable variations for the larger angles of attack studied. These square-wave and peak, reduction-in-magnitude, and change-in-sign variations were caused by vortex breakaway, which allowed vortex crossover to occur. Ahead of vortex breakaway, the elliptic cross-section tip yielded smooth variations of vortex wake asymmetry with tip roll angle, indicating that the tip would possibly be a feasible control device for high-performance fighter aircraft at high angle of attack. Author (EI)

A95-68165

LAG MODEL FOR TURBULENT BOUNDARY LAYERS OVER ROUGH BLEED SURFACES

J. LEE Boeing Commercial Airplane Group, Seattle, WA, M. L. SLOAN, and G. C. PAYNTER Journal of Propulsion and Power (ISSN 0748-4658) vol. 10, no. 4 July-August 1994 p. 562-568 refs (BTN-94-EIX94441380981) Copyright

Boundary-layer mass removal (bleed) through spanwise bands of holes on a surface is used to prevent or control separation and to stabilize the normal shock in supersonic inlets. The addition of a transport equation lag relationship for eddy viscosity to the rough wall algebraic turbulence model of Cebeci and Chang was found to improve agreement between predicted and measured mean velocity distributions downstream of a bleed band. The model was demonstrated for a range of bleed configurations, bleed rates, and local freestream Mach numbers. In addition, the model was applied to the boundary-layer development over acoustic lining materials for the inlets and nozzles of commercial aircraft. The model was found to yield accurate results for integral boundary-layer properties unless there was a strong adverse pressure gradient. Author (EI)

A95-68168

STABILITY OF MAGNETIC BEARING-ROTOR SYSTEMS AND THE EFFECTS OF GRAVITY AND DAMPING

P. ZHONG Univ. of Virginia, Charlottesville, VA and M. A. TOWNSEND AIAA Journal (ISSN 0001-1452) vol. 32, no. 7 July 1994 p. 1492-1499 refs (BTN-94-EIX94441386619) Copyright

New and general stability criteria are developed for magnetic bearing-rotor systems under practical conditions of system operation and failure based on the Lyapunov second (direct) method. The unperturbed (fully nonlinear) stability of a conventional magnetic bearing-rotor configuration is analyzed for zero gravity; these results are shown to apply with gravity, based on observed similarities of the nonlinear Lagrangian equations. In addition to known results for stability and instability, the system can be stable when a magnetic bearing fails (has negative stiffness), but the net stiffness is still positive. A complete set of sufficient conditions are derived. This temporary stability depends upon inherent gyroscopic forces and is

lost when dissipative forces are introduced. However, even with damping the gyroscopic forces improve the system's relative stability. The results are applicable to other gyroscopic systems.

Author (EI)

A95-68259

HYDRAULIC SYSTEM DIAGNOSTIC SENSORS

Aerospace Engineering (Warrendale, Pennsylvania) (ISSN 0736-2536) vol. 14, no. 1 January-February 1994 p. 43-48

(BTN-95-EIX95031502752) Copyright

The use of diagnostic monitoring sensors in aircraft hydraulic systems enables the continuous evaluation of component health. Monitoring of these components results in three prime benefits: (1) early identification of component malfunction to control unscheduled repairs; (2) limiting of component malfunction to primary failure; and (3) measurement of critical component performance parameters relating to component wear rates. They are also used to monitor critical parameters like flow, temperature and differential pressure. EI

A95-68280

JOINT STARS PHASED ARRAY RADAR ANTENNA

HAROLD SHNITKIN Westinghouse Norden Systems, Inc., Norwalk, CT IEEE Aerospace and Electronic Systems Magazine (ISSN 0885-8985) vol. 9, no. 10 October 1994 p. 34-40 refs

(BTN-95-EIX95042474626) Copyright

The Joint STARS phased array radar system is capable of performing long range airborne surveillance and was used during the Persian Gulf war on two E8-A aircraft to fly many around-the-clock missions to monitor the Kuwait and Iraq battlefield from a safe distance behind the front lines. This paper is a follow-on to previous publications on the subject of the Joint STARS antenna and deals mainly with mission performance and technical aspects not previously covered. Radar data of troop movements and armament installations will be presented, a brief review of the antenna design is given, followed by technical discussions concerning the three-port interferometry, gain and sidelobe design approach, cost control, range test implementation and future improvements. Author (EI)

A95-68282

SIMPLIFIED ANALYSIS OF GENERAL INSTABILITY OF STIFFENED SHELLS WITH CUTOUTS IN PURE BENDING

DIMITRIS L. KARABALIS Gulfstream Aerospace Corp., Savannah, GA AIAA Journal (ISSN 0001-1452) vol. 32, no. 10 October 1994 p. 2128-2130 refs

(BTN-95-EIX95042474418) Copyright

A simple analytical method is presented which may be beneficial in monitoring the design of the stiffening frames of cylindrical fuselages, with or without cutouts, for failure by general instability under bending conditions. The proposed formulation follows the fundamental steps of Shanley's original study for entire circular frames and extends it to incomplete frames, with or without edge stiffeners at the perimeter of the cutout. However, whereas Shanley's criterion was the result of a straightforward correlation of test data and a simple model, the proposed criterion is only indirectly correlated to the same test data via Shanley's coefficient $c(\text{sup } f)$. EI

A95-68287

SUPPRESSION OF VORTEX ASYMMETRY AND SIDE FORCE ON A CIRCULAR CONE

A. ASGHAR King Fahd Univ. of Petroleum and Minerals, Dharan (Saudi Arabia), W. H. STAHL, and M. MAHMOOD AIAA Journal (ISSN 0001-1452) vol. 32, no. 10 October 1994 p. 2117-2120 refs

(BTN-95-EIX95042474413) Copyright

A phenomenon of an originally asymmetrical vortex pair becoming asymmetric has been noted on a circular, two-dimensional cylinder set. It was proposed that a fin between the vortices would stabilize the flow and remain symmetric. The impact of a fin on the flow past a slender cone was analyzed by using flow visualization. The fin was found to significantly suppress vortex-flow asymmetry.

Thus, a quantitative analysis of the surface pressures and forces on the cone with and without the fin was performed. Flow visualization tests revealed that a slender circular cone with and without a fin affixed to the lee side showed that the fin greatly suppressed vortex-flow asymmetry that was present on the cone without fin. The fin reduced the great side forces acting on the cone without the fin by an order of magnitude to minimal values. It appeared feasible to utilize a vertically movable fin to take advantage of the associated side force for control purposes. EI

A95-68291

ENTRAINMENT AND ACOUSTIC VARIATIONS IN A ROUND JET FROM INTRODUCED STREAMWISE VORTICITY

P. SURKS Tufts Univ., Medford, MA, C. B. ROGERS, and D. E. PAREKH AIAA Journal (ISSN 0001-1452) vol. 32, no. 10 October 1994 p. 2108-2110 refs

(BTN-95-EIX95042474409) Copyright

The effect of the half-delta wing vortex generators on the symmetry of a jet was examined by studying an asymmetric jet cross section. The symmetry of the nozzle eliminated the influence of the corners and side walls of the rectangular nozzle, isolating the asymmetry promoted by asymmetrical streamwise vorticity. Various vortex configurations were tested. The mixing validity outlined in Rogers and Parekh were incorporated as a semiquantitative mixing measurement. The mixing effectiveness measurements were carried out by efficiently measuring the concentration of smoke particles with a video camera and a light sheet. EI

A95-68302

INTERACTION OF A STREAMWISE VORTEX WITH A THIN PLATE: A SOURCE OF TURBULENT BUFFETING

ALEJANDRO MAYORI Lehigh Univ., Bethlehem, PA and DONALD ROCKWELL AIAA Journal (ISSN 0001-1452) vol. 32, no. 10 October 1994 p. 2022-2029 refs

(BTN-95-EIX95042474398) Copyright

The three-dimensional interaction of a streamwise vortex with a thin plate (simulated tail or fin) is investigated experimentally using high-image-density particle image velocimetry, which allows determination of the instantaneous streamline patterns and distributions of vorticity over entire planes of the flow. These representations of the flow reveal that the vortex-plate encounter generates a new type of vortex splitting, leading to two smaller-scale concentrations of streamwise vorticity. Their trajectories rapidly diverge from the plane of symmetry of the plate. Details of this encounter process are interpreted using instantaneous values of circulation, two-dimensional vorticity correlation functions, and length scales of the vorticity field. Author (EI)

A95-68312

COMPARISON OF NO AND OH PLANAR FLUORESCENCE TEMPERATURE MEASUREMENTS IN SCRAMJET MODEL FLOWFIELDS

B. K. MCMILLIN Natl. Inst. of Standards and Technology, Gaithersburg, MD, J. M. SEITZMAN, and R. K. HANSON AIAA Journal (ISSN 0001-1452) vol. 32, no. 10 October 1994 p. 1945-1952 refs

(BTN-95-EIX95042474388) Copyright

The use of nitric oxide (NO) and the hydroxyl radical (OH) as temperature tracers, in a two-line planar laser-induced fluorescence technique, is examined in the context of a supersonic mixing and combustion flowfield. The temperature measurements were based on the sequential excitation of two transitions, either in the A implied by X (0,0) band of NO near 226 nm or the A implied by X (1,0) band of OH near 283 nm. The measurements were obtained for each species through the use of two lasers and two cameras, with each camera integrating signal induced from only one of the lasers. Both temporally resolved and frame-averaged temperature measurements of each species are presented. Additional results include simultaneous NO and OH visualizations, in which seeded NO marks the fuel jet fluid and nascent OH marks the reaction zones and convected combustion gases. A detailed temperature comparison

shows good agreement in the common measurement regions and indicates that shot noise is the largest source of uncertainty. The comparison also illustrates the importance of a careful interpretation of the measurements, since, depending on the origin of the tracer and the degree of mixing, the measurements may be biased toward the fuel, freestream, or reaction zone temperatures. Author (EI)

A95-68393

STARTER/GENERATOR TESTING

ANON Aerospace Engineering (Warrendale, Pennsylvania) (ISSN 0736-2536) vol. 14, no. 10 October 1994 p. 7-10
(BTN-95-EIX95072498877) Copyright

Sundstrand Aerospace and GE Aircraft Engines have studied the switched reluctance machine for use as an integral starter/generator for future aircraft engines. They have conducted an initial, low-power testing of the starter/generator, which is based on power inverters using IGBT-technology semiconductors, to verify its feasibility in the externally mounted version of the integral starter/generator. This preliminary testing of the 250-kW starter/generator reveals favorable results. EI

A95-69209* National Aeronautics and Space Administration. Langley Research Center, Hampton, VA.

APPROXIMATE METHOD FOR CALCULATING HEATING RATES ON THREE-DIMENSIONAL VEHICLES

H. HARRIS HAMILTON National Aeronautics and Space Administration. Langley Research Center, Hampton, VA, FRANCIS A. GREENE, and F. R. DEJARNETTE Journal of Spacecraft and Rockets (ISSN 0022-4650) vol. 31, no. 3 May-June 1994 p. 345-354
(BTN-95-EIX95041503778) Copyright

An approximate method for calculating heating rates on three-dimensional vehicles at angle of attack is presented. The method is based on the axisymmetric analog for three-dimensional boundary layers and uses a generalized body-fitted coordinate system. Edge conditions for the boundary-layer solution are obtained from an inviscid flowfield solution, and because of the coordinate system used, the method is applicable to any blunt body geometry for which an inviscid flowfield solution can be obtained. The method is validated by comparing with experimental heating data and with thin-layer Navier-Stokes calculations on the shuttle orbiter at both wind-tunnel and flight conditions and with thin-layer Navier-Stokes calculations on the HL-20 at wind-tunnel conditions. Author (EI)

A95-69308

NONLINEAR DYNAMIC SIMULATION OF SINGLE- AND MULTISPOOL CORE ENGINES, PART 1: COMPUTATIONAL METHOD

M. T. SCHOEIRI Texas A&M Univ, College Station, TX, United States, M. ATTIA, and C. LIPPKE Journal of Propulsion and Power (ISSN 0748-4658) vol. 10, no. 6 November-December 1994 p. 855-862 refs
(BTN-95-EIX95112524200) Copyright

A new computational method for accurate simulation of the nonlinear, dynamic behavior of single- and multispool core engines, turbofan engines, and power-generation gas turbine engines is presented in part 1. In order to perform the simulation, a modularly structured computer code has been developed that includes individual mathematical modules representing various engine components. The generic structure of the code enables the simulation of arbitrary engine configurations ranging from single-spool thrust generation to multispool thrust/power generation engines under adverse dynamic operating conditions. For precise simulation of turbine and compressor components, row-by-row calculation procedures were implemented that account for the specific turbine and compressor cascade and blade geometry and characteristics. Author (EI)

N95-19567*# State Univ. of New York, Binghamton, NY. Dept. of Mechanical Engineering.

WORMGEAR GEOMETRY ADOPTED FOR IMPLEMENTING HYDROSTATIC LUBRICATION AND FORMULATION OF THE LUBRICATION PROBLEM Final Report

D. C. SUN and QIN YUAN Cleveland, OH NASA Jan. 1995 49 p

(Contract(s)/Grant(s): NAG3-1316; RTOP 505-62-OJ; DA PROJ. 1L1-61102-AH-45)

(NASA-CR-195416; E-9345; NAS 1.26:195416; ARL-CR-219) Avail: CASI HC A03/MF A01

The geometrical parameters for a wormgear intended to be used as the transmission in advanced helicopters are finalized. The resulting contact pattern of the meshing tooth surfaces is suitable for the implementation of hydrostatic lubrication. Fluid film lubrication of the contact is formulated considering external pressurization as well as hydrodynamic wedge and squeeze actions. The lubrication analysis is aimed at obtaining the oil supply pressure needed to separate the worm and gear surfaces by a prescribed minimum film thickness. The procedure of solving the mathematical problem is outlined. Author

N95-19730 Naval Postgraduate School, Monterey, CA.

INBAND RADAR CROSS SECTION OF PHASED ARRAYS WITH PARALLEL FEEDS M.S. Thesis

VASSILIOS FLOKAS Jun. 1994 66 p Limited Reproducibility: More than 20% of this document may be affected by microfiche quality (AD-A284249) Avail: CASI HC A04

Approximate formulas for the inband radar cross section of arrays with parallel feeds are presented. To obtain the formulas, multiple reflections are neglected, and devices of the same type are assumed to have identical electrical performance. The approximate results were compared to the results obtained using a scattering matrix formulation. Both methods were in agreement in predicting RCS lobe positions, levels, and behavior with scanning. The advantages of the approximate method are its computational efficiency and its flexibility in handling an arbitrary number of coupler levels. DTIC

N95-19774# Aircraft Research Association Ltd., Bedford (England).

VALIDATION AND EVALUATION OF THE ADVANCED AERONAUTICAL CFD SYSTEM SAUNA: A METHOD DEVELOPER'S VIEW

J. A. SHAW, A. J. PEACE, J. M. GEORGALA, and P. N. CHILDS Sep. 1993 44 p Presented at the Recent Developments and Applications in Aeronautical CFD, Bristol, England, 1993 Sponsored by United Kingdom Ministry of Defence
(ARA-MEMO-390) Avail: CASI HC A03/MF A01

This paper is concerned with a detailed validation and evaluation of the SAUNA CFD system for complex aircraft configurations. The methodology of the complete system is described in brief, including its unique use of differing grid generation strategies (structured, unstructured or both) depending on the geometric complexity of the configuration. A wide range of configurations and flow conditions are chosen in the validation and evaluation exercise to demonstrate the scope of SAUNA. A detailed description of the results from the method is preceded by a discussion on the philosophy behind the strategy followed in the exercise, in terms of equality assessment and the differing roles of the code developer and the code user. It is considered that SAUNA has grown into a highly usable tool for the aircraft designer, in combining flexibility and accuracy in an efficient manner. Author

N95-19775# Aircraft Research Association Ltd., Bedford (England).

APPLICATION OF THREE-DIMENSIONAL HYBRID STRUCTURED/UNSTRUCTURED GRIDS TO LAND, SEA AND AIR VEHICLES

JONATHAN A. SHAW, JEANETTE M. GEORGALA, NICHOLAS E. MAY, and MARK F. POCKOCK Apr. 1994 17 p Presented at the

4th International Conference on Numerical Grid Generation in Computational Fluid Dynamics and Related Fields, Swansea, Wales, 6-8 Apr. 1994 Sponsored by United Kingdom Ministry of Defence (ARA-MEMO-399) Avail: CASI HC A03/MF A01

The use of a numerical grid generation facility capable of forming unstructured meshes, block-structured meshes and a hybrid combination of these alternative mesh types is described. Examples of meshes created for cars, submarines, missiles and powered civil and military aircraft are given. The motives for choosing a particular type of mesh for each applied configuration are covered, with grid related data given which includes the amount of user effort required to attain the grids. Throughout the paper, algorithms are referred to which have been invoked in the creation of the meshes. These algorithms are introduced in a companion paper within the same conference proceedings. Author

N95-19776# Aircraft Research Association Ltd., Bedford (England). **VERIFICATION OF THE CFD SIMULATION SYSTEM SAUNA FOR COMPLEX AIRCRAFT CONFIGURATIONS** JONATHON A. SHAW, ANDREW J. PEACE, NICHOLAS E. MAY, and MARK F. POCKOCK Apr. 1994 19 p Presented at the 32nd Aerospace Sciences Meeting, Reno, NV, 10-13 Jan. 1994 Sponsored by United Kingdom Ministry of Defence (ARA-MEMO-401; AIAA PAPER 94-0393) Avail: CASI HC A03/MF A01

This paper is concerned with the verification for complex aircraft configurations of an advanced CFD simulation system known by the acronym SAUNA. A brief description of the complete system is given, including its unique use of differing grid generation strategies (structured, unstructured or both) depending on the geometric complexity of the addressed configuration. The majority of the paper focuses on the application of SAUNA to a variety of configurations from the military aircraft, civil aircraft and missile areas. Mesh generation issues are discussed for each geometry and experimental data are used to assess the accuracy of the inviscid (Euler) model used. It is shown that flexibility and accuracy are combined in an efficient manner, thus demonstrating the value of SAUNA in aerodynamic design. Author

N95-19777# Aircraft Research Association Ltd., Bedford (England). **INVISID AND VISCOUS FLOW MODELLING OF COMPLEX AIRCRAFT CONFIGURATIONS USING THE CFD SIMULATION SYSTEM SAUNA** ANDREW J. PEACE, NICHOLAS E. MAY, MARK F. POCKOCK, and JONATHON A. SHAW Apr. 1994 14 p Presented at the 19th Congress of the International Council of the Aeronautical Sciences, Anaheim, CA, 18-23 Sep. 1993 Sponsored by United Kingdom Ministry of Defence (ARA-MEMO-403) Avail: CASI HC A03/MF A01

This paper is concerned with the flow modelling capabilities of an advanced CFD simulation system known by the acronym SAUNA. This system is aimed primarily at complex aircraft configurations and possesses a unique grid generation strategy in its use of block-structured, unstructured or hybrid grids, depending on the geometric complexity of the addressed configuration. The main focus of the paper is in demonstrating the recently developed multi-grid, block-structured grid, viscous flow capability of SAUNA, through its evaluation on a number of configurations. Inviscid predictions are also presented, both as a means of interpreting the viscous results and with a view to showing more completely the capabilities of SAUNA. It is shown that accuracy and flexibility are combined in an efficient manner, thus demonstrating the value of SAUNA in aerodynamic design. Author

N95-19794# National Aeronautics and Space Administration. Lewis Research Center, Cleveland, OH. **IMPROVED SPEED CONTROL SYSTEM FOR THE 87,000 HP WIND TUNNEL DRIVE** EDWARD A. BECKS (NYMA, Inc., Brook Park, OH.), TIMOTHY J. BENCIC, and PHILIP Z. BLUMENTHAL (NYMA, Inc., Brook Park,

OH.) Jan. 1995 13 p Presented at the 41st International Instrumentation Symposium, Denver, CO, 7-11 May 1995; sponsored by Instrument Society of America (Contract(s)/Grant(s): NAS3-27186; RTOP 505-62-82) (NASA-TM-106840; E-9404; NAS 1.15:106840) Avail: CASI HC A03/MF A01

This paper describes the design, installation, and integrated systems tests for a new drive motor speed control system which was part of a recent rehab project for the NASA Lewis 8x6 Supersonic Wind Tunnel. The tunnel drive consists of three mechanically-coupled 29,000 HP wound rotor induction motors driving an axial flow compressor. Liquid rheostats are used to vary the impedance of the rotor circuits, thus varying the speed of the drive system. The new design utilizes a distributed digital control system with a dual touch screen CRT operator console to provide alarm monitoring, logging, and trending. The liquid rheostats are driven by brush-type servomotor systems with magnetostrictive linear displacement transducers used for position feedback. The new system achieved all goals for speed variations with load, motor load balance, and control of total power. Author

N95-19798# Michigan Univ., Ann Arbor, MI. Radiation Lab. **DESIGN CONSIDERATIONS FOR AN ARCHIMEDEAN SLOT SIGNAL ANTENNA**

MICHAEL W. NURNBERGER and JOHN L. VOLAKIS In the Simulation of Thin Slot Spirals and Dual Circular Patch Antennas Using the Finite Element Method with Mixed Elements p 21-46 Jan. 1995 Avail: CASI HC A03/MF A01

The design goal is to develop a 118-157 MHz, vertically polarized, low-profile (or conformal) antenna as a replacement for VHF AM blade antennas on aircraft. This design is to be arrived at by scaling the dimensions of an antenna designed for a center frequency of 1.1 GHz. The design prior to scaling may have the following maximum dimensions: diameter less than 3.70 in. and thickness less than 0.50 in. Although a four-arm spiral design was originally suggested, a two-arm spiral may also be used, as both mode-1 and mode-2 (sum and difference) radiation patterns aren't required. While a four-arm spiral can easily be designed should both sum and difference patterns be required, the two-arm design will provide the required sum pattern and simplify the design problem somewhat: only one feed is required, and the feed area geometry is more straightforward. Polarization requirements dictate that a slot spiral be used, as opposed to a wire spiral. Two similar radiating structures were considered. The first is the standard archimedean spiral antenna. The second is a hollow archimedean spiral antenna, essentially a standard archimedean spiral with the inner portion removed. Derived from text

N95-19809 BKM, Inc., San Diego, CA. **ADVANCED DIESEL ELECTRONIC FUEL INJECTION AND TURBOCHARGING Final Report, Jul. 1990 - Dec. 1993** N. J. BECK, R. L. BARKHIMER, D. C. STEINMEYER, and J. E. KELLY Dec. 1993 237 p Limited Reproducibility: More than 20% of this document may be affected by microfiche quality (Contract(s)/Grant(s): DAAE07-90-C-R030) (AD-A279176; F-632; TACOM-13603) Avail: Issuing Activity (Defense Technical Information Center (DTIC))

The program investigated advanced diesel air charging and fuel injection systems to improve specific power, fuel economy, noise, exhaust emissions, and cold startability. The techniques explored included variable fuel injection rate shaping, variable injection timing, full-authority electronic engine control, turbo-compound cooling, regenerative air circulation as a cold start aid, and variable geometry turbocharging. A Servojet electronic fuel injection system was designed and manufactured for the Cummins VTA-903 engine. A special Servojet twin turbocharger exhaust system was also installed. A series of high speed combustion flame photos was taken using the single cylinder optical engine at Michigan Technological University. Various fuel injection rate shapes and nozzle configurations were evaluated. Single-cylinder bench tests were

13 GEOSCIENCES

performed to evaluate regenerative inlet air heating techniques as an aid to cold starting. An exhaust-driven axial cooling air fan was manufactured and tested on the VTA-903 engine. DTIC

13

GEOSCIENCES

Includes geosciences (general); earth resources; energy production and conversion; environment pollution; geophysics; meteorology and climatology; and oceanography.

A95-66315

OBSERVATIONS OF FLUXES AND INLAND BREEZES OVER A HETEROGENEOUS SURFACE

L. MAHRT Oregon State Univ., Corvallis, OR, US, JIELUN SUN Oregon State Univ., Corvallis, OR, US, DEAN VICKERS Oregon State Univ., Corvallis, OR, US, J. I. MACPHERSON National Research Council, Ottawa, Canada, J. R. PEDERSON California Air Resources Board, Sacramento, CA, US, and R. L. DESJARDINS Centre for Land and Biological Resources Research, Ottawa, Canada *Journal of the Atmospheric Sciences* (ISSN 0022-4928) vol. 51, no. 7 September 1, 1994 p. 2484-2499 Research sponsored by the San Joaquin Valley Air Pollution Study Agency, Pacific Gas and Electric and the NRC of Canada (Contract(s)/Grant(s): DAA HO4-93-G0019; NSF ATM-89-12736) (HTN-95-80258) Copyright

Repeated aircraft runs at about 33 m over heterogeneous terrain are analyzed to study the spatial variability of the mesoscale flow and turbulent fluxes. An irrigated area, about 12 km across, generates relatively cool moist inland breeze. As this air flows out over the warmer, drier surrounding land surface, an internal boundary layer develops within the inland breeze, which then terminates at a well-defined inland breeze front located about 1 1/2 km downstream from the change of surface conditions. This front is defined by horizontal convergence, rising motion, and sharp spatial change of moisture, carbon dioxide, and ozone. Both a scale analysis and the observations suggest that the overall vertical motion associated with the inland breeze is weak. However, the observations indicate that this vertical motion and attendant vertical transport are important in the immediate vicinity of the front, and the inland breeze does lead to significant modification of the turbulent flux. In the inland breeze downstream from the surface wetness discontinuity, strong horizontal advection of moisture is associated with a rapid increase of the turbulent moisture flux with height. This large moisture flux appears to be partly due to mixing between the thin moist inland breeze and overlying drier air. As a consequence of the strong vertical divergence of the flux in the transition regions, the fluxes measured even as low as a few tens of meters are not representative of the surface fluxes. The spatial variability of the fluxes is also interpreted within the footprint format. Attempts are made to reconcile predictions by footprint and internal boundary-layer approaches.

Author (Herner)

A95-66429

NONHYDROSTATIC SIMULATION OF FRONTOGENESIS IN A MOIST ATMOSPHERE. PART 3: THERMAL WIND IMBALANCE AND RAINBANDS

J.-P. LAFORE Centre National de Recherches Meteorologiques, Toulouse, France, J.-L. REDELSPERGER Centre National de Recherches Meteorologiques, Toulouse, France, C. CAILLY Centre National de Recherches Meteorologiques, Toulouse, France, and E. ARBOGAST Centre National de Recherches Meteorologiques, Toulouse, France *Journal of the Atmospheric Sciences* (ISSN 0022-4928) vol. 51, no. 23 December 1, 1994 p. 3467-3485 Research sponsored by the Institut National des Sciences de l'Univers (HTN-95-90356) Copyright

The dynamical mechanisms contributing to the cross-front

ageostrophic circulation are identified in high-resolution (40 to 50 km) nonhydrostatic simulations of moist frontogenesis. In a first step, the importance of the alongfront ageostrophic circulation is assessed. The structure of the intense thermal wind imbalance (TWI) occurring in the vicinity of the surface cold front is diagnosed and explained using a budget of the alongfront vorticity etc. It allows one to propose a new balance in terms of the steadiness of the eta field in the system moving framework. The TWI is thus found nearly equal to the total cross-front eta transport by resolved and subgrid scales. In a second step, a general form of the Sawyer-Eliassen (SE) diagnostic equation is used, including diabatic effects as well as effects of thermal wind imbalances (or 'ageostrophic residue'). This latter effect is evaluated using the steadiness balance, which is confirmed by a budget diagnosis. The solution of this SE equation provides an accurate diagnostic of the causes of the secondary circulation, both qualitatively and quantitatively, down to small scales. Finally, the SE equation is used to explain the formation and localization of rainbands in regions of effective symmetric stability. In particular, it is shown that the 'ageostrophic residue' plays a crucial role in the behavior of the bands. It explains about 25% and 60% of the intensity of the warm sector-wide rainband and of the narrow cold-frontal rainband, respectively, for a case with intense surface friction.

Author (revised by Herner)

A95-66869

ANTARCTIC SNOW RECORD OF SOUTHERN HEMISPHERE LEAD POLLUTION

ERIC W. WOLFF Natural Environment Research Council, Cambridge, UK and EDWARD D. SUTTIE Natural Environment Research Council, Cambridge, UK *Geophysical Research Letters* (ISSN 0094-8276) vol. 21, no. 9 May 1, 1994 p. 781-784 (HTN-95-40359) Copyright

Lead concentrations from an Antarctic snow pit show the pattern of Pb reaching the Antarctic atmosphere over the last 70 years. Between 1920 and 1950, the Pb concentration shows significant variations around a mean of about 2.5 ng/kg. Between 1950 and 1980, there is a clear increase to 6 ng/kg, with an apparent reduction after that. A few high concentrations in the late 1970s are probably due to local contamination from aircraft using leaded gasoline. Excluding these anomalously high values, the chronological pattern in lead concentrations can be reconciled with estimates of emissions from vehicles and metal production processes in the southern hemisphere.

Author (Herner)

A95-66949* National Aeronautics and Space Administration. Goddard Space Flight Center, Greenbelt, MD.

USING IRI FOR THE COMPUTATION OF IONOSPHERIC CORRECTIONS FOR ALTIMETER DATA ANALYSIS

D. BILITZA Hughes STX, Greenbelt, MD, US, C. KOBLINSKY NASA, Goddard Space Flight Center, Greenbelt, MD, US, B. BECKLEY Hughes STX, Greenbelt, MD, US, S. ZIA Hughes STX, Greenbelt, MD, US, and R. WILLIAMSON Hughes STX, Greenbelt, MD, US Off median phenomena and international reference ionosphere; COSPAR International Scientific Symposium, Trieste, Italy, Oct. 19-22, 1993. A95-66933 *Advances in Space Research* (ISSN 0273-1177) vol. 15, no. 2 February 1995 p. 113-119 Copyright

Measurements by single-frequency satellite altimeter (Geosat, ERS-1) require a ionospheric correction to account for the signal time delay in the ionosphere. We propose using the International Reference Ionosphere (IRI) for the determination of this time delay. To investigate the effectiveness of an IRI correction, we have compared the IRI values with ionospheric corrections deduced from measurements by the dual-frequency Topex altimeter. By measuring at two frequencies, the Topex instrument can record (and thus eliminate) the ionospheric influence. We find that IRI agrees with the Topex data much better than the model that is currently used in Geosat data analysis. In particular the earlier model does not represent the equatorial double-peak (equator anomaly) clearly seen in the Topex data. Overall, the use of IRI results in a 30%

improvement (over the older model) in the accuracy of ionospheric corrections computed for the first year of the Topex mission.

Author (Herner)

A95-67345

PLANAR AIR DENSITY MEASUREMENTS NEAR MODEL SURFACES BY ULTRAVIOLET RAYLEIGH/RAMAN SCATTERING

G. GRUENEFELD Laser-Laboratorium Goettingen, Goettingen (Germany), V. BEUSHAUSEN, and P. ANDRESEN AIAA Journal (ISSN 0001-1452) vol. 32, no. 7 July 1994 p. 1457-1463 refs (BTN-94-EIX94441386614) Copyright

The feasibility of planar ultraviolet laser-induced Rayleigh and Raman scattering for measurements of small air density variations near model wing surfaces is tested for applications in wind tunnels. Variations in air density of less than 1% are measured quantitatively by Rayleigh scattering in a plane of 3 x 6 sq cm in about 1 s under the extreme condition in which the laser directly irradiates the metal surface of the wing. Raman scattering was tested as well because it is much less affected by surface and Mie scattering. Therefore, it can be used for density measurements much closer to the model surface and under the presence of dust and droplets with a precision of at least 2%. Further improvements of the measurement precision are possible and will be discussed.

Author (EI)

A95-67780* National Aeronautics and Space Administration. Marshall Space Flight Center, Huntsville, AL.

AIRCRAFT ELECTRIC FIELD MEASUREMENTS: CALIBRATION AND AMBIENT FIELD RETRIEVAL

WILLIAM J. KOSHAK NASA. Marshall Space Flight Center, Huntsville, AL, US, JEFF BAILEY University of Alabama, Huntsville, AL, US, HUGH J. CHRISTIAN University of Alabama, Huntsville, AL, US, and DOUGLAS M. MACH University of Alabama, Huntsville, AL, US Journal of Geophysical Research (ISSN 0148-0227) vol. 99, no. D11 November 20, 1994 p.22,781-22,792

(HTN-95-90508) Copyright

An aircraft locally distorts the ambient thundercloud electric field. In order to determine the field in the absence of the aircraft, an aircraft calibration is required. In this work a matrix inversion method is introduced for calibrating an aircraft equipped with four or more electric field sensors and a high-voltage corona point that is capable of charging the aircraft. An analytic, closed form solution for the estimate of a (3 x 3) aircraft calibration matrix is derived, and an absolute calibration experiment is used to improve the relative magnitudes of the elements of this matrix. To demonstrate the calibration procedure, we analyze actual calibration data derived from a Lear jet 28/29 that was equipped with five shutter-type field mill sensors (each with sensitivities of better than 1 V/m) located on the top, bottom, port, starboard, and aft positions. As a test of the calibration method, we analyze computer-simulated calibration data (derived from known aircraft and ambient fields) and explicitly determine the errors involved in deriving the variety of calibration matrices. We extend our formalism to arrive at an analytic solution for the ambient field, and again carry all errors explicitly.

Author (Herner)

A95-67806* National Aeronautics and Space Administration. Ames Research Center, Moffett Field, CA.

THREE-DIMENSIONAL MODEL INTERPRETATION OF NO(X) MEASUREMENTS FROM THE LOWER STRATOSPHERE

IAN FOLKINS National Center for Atmospheric Research, Boulder, CO, US, A. J. WEINHEIMER National Center for Atmospheric Research, Boulder, CO, US, GUY BRASSEUR National Center for Atmospheric Research, Boulder, CO, US, FRANCK LEFEVRE Centre National de Recherches Meteorologiques, Toulouse, France, BRIAN A. RIDLEY National Center for Atmospheric Research, Boulder, CO, US, JAMES G. WALEGA National Center for Atmospheric Research, Boulder, CO, US, JAMES E. COLLINS

Science and Technology Corporation, Hampton, VA, US, and R. F. PUESCHEL NASA. Ames Research Center, Moffett Field, CA, US Journal of Geophysical Research (ISSN 0148-0227) vol. 99, no. D11 November 20, 1994 p. 23,117-23,129 Research sponsored by NSF and the Natural Sciences and Engineering Research Council of Canada (HTN-95-90534) Copyright

A three-dimensional off-line chemistry transport model, driven by European Center for Medium-Range Forecasts winds and temperatures, is used to interpret measurements of NO and NO₂ taken from the DC-8 during the second Airborne Arctic Stratospheric Expedition. The model was run in three configurations: gas phase chemistry alone, inclusion of the N₂O₅ aerosol reaction, and inclusion of both N₂O₅ and ClONO₂ aerosol reactions. The run including the N₂O₅ aerosol reaction alone usually agreed best with measured NO(x)/NO(y) ratios in midlatitude air masses. The NO(x)/NO(y) ratios of the run with both aerosol reactions were always too low, while the gas phase ratios were usually too high, especially during March. All three simulations generated extremely low NO₂/NO(y) ratios in air parcels that had spent several days or more in the polar night. Measured NO₂/NO(y) ratios in these types of air masses were sometimes equally low but could also be considerably higher. Observed NO/NO₂ ratios differed strongly from known theory.

Author (Herner)

A95-68217

PREDICTION OF ICE ACCRETION: COMPARISON BETWEEN THE 2D AND 3D CODES

D. GUFFOND ONERA, Chatillon (France) and T. HEDDE Recherche Aerospatiale (ISSN 0034-1223) no. 2 1994 p. 103-115 refs (BTN-94-EIX94441385753) Copyright

A 2D and a 3D icing model have been developed. Both start with inviscid flow calculation followed by calculation of droplet trajectories. They derive the heat transfer coefficient from the thermal boundary layer calculation on a rough wall. In the 3D case, the runback paths are calculated from the wall streamlines. The heat and mass balance gives the accretion rate, from which we deduce the ice shape. The catch efficiency coefficient, the heat transfer coefficient, and the ice shapes are compared with experimental data. The 3D code is compared with the 2D on an infinite swept wing. We see that the corrected 2D code can predict the local catch efficiency but not the ice shape. Then the Messinger approach is discussed and the 3D 'lobster tail' effect is explained through the shadow effect and a heat transfer gradient mechanism. A qualitative ballistic model enables us to simulate this type of ice shape growth.

Author (EI)

A95-68314

OZONE, SKIN CANCER, AND THE SST

S. FRED SINGER Science & Environmental Policy Project Aerospace America (ISSN 0740-722X) vol. 32, no. 7 July 1994 p. 22-26

(BTN-95-EIX95041503011) Copyright

In 1971, the U.S. Congress cut off funding for development of supersonic transport aircraft prototypes when it was argued that the pollution created by SSTs could reduce the stratospheric ozone content and increase the incidence of skin cancer. At present, the theory of ozone depletion is in a rather uncertain state. Two examples of this are cited. First, ozone depletion may depend more on the availability of surfaces of aerosols and particles than on the content of chlorine. Second, it has been discovered that NO(x) can tie up active chlorine and thus reduce depletion from that source. We are therefore left with the paradoxical result that under certain circumstances SSTs flying in the lower stratospheric can actually counteract, at least partially, any ozone-depleting effects of CFCs. A recent study by scientists at the Brookhaven National Laboratory showed that melanoma rates would not be affected by changes in the ozone layer. If these results are confirmed, then much of the fear associated with ozone depletion disappears. It is difficult to tell how all this will affect a future supersonic transport program, since it is not clear whether a fleet of SSTs will increase or offset ozone depletion.

EI

A95-68756**AIRCRAFT ICING MEASUREMENTS IN EAST COAST WINTER STORMS**

STEWART G. COBER Cloud Physics Research Division, Downsview, Ontario, Canada, GEORGE A. ISAAC Cloud Physics Research Division, Downsview, Ontario, Canada, and J. W. STRAPP Cloud Physics Research Division, Downsview, Ontario, Canada Journal of Applied Meteorology (ISSN 0894-8763) vol. 34, no. 1 January 1995 p. 88-100 Research sponsored by the Canadian National Search and Rescue Secretariat, IAR, National Research Council of Canada, Boeing Commercial Airplane Group, and Airbus Industrie.

(HTN-95-60505) Copyright

Analysis of the aircraft icing environments of East Coast winter storms have been made from 31 flights during the second Canadian Atlantic Storms Program (CASP). Microphysical parameters have been summarized and are compared to common icing intensity envelopes and to other icing datasets. Cloud regions with supercooled liquid water had an average horizontal extent of 4.3 km, with average droplet concentrations of 130/cu cm, liquid water contents of 0.13 g/cu m, and droplet median volume diameters of 18 microns. In general, the icing intensity observed was classified as light, although moderate to severe icing was observed in several common synoptic situations and several cases are discussed. Freezing drizzle was observed on four flights, and represented the most severe icing environment encountered.

Author. (Herner)

A95-68762* National Aeronautics and Space Administration, Washington, DC.

MICROWAVE AND INFRARED SIMULATIONS OF AN INTENSE CONVECTIVE SYSTEM AND COMPARISON WITH AIRCRAFT OBSERVATIONS

N. PRASAD Science Systems and Applications, Inc., Lanham, MD, US, HWA-YOUNG M. YEH Caelum Research Center, Silver Spring, MD, US, ROBERT F. ADLER NASA, Goddard Space Flight Center, Greenbelt, MD, US, and WEI-KUO TAO NASA, Goddard Space Flight Center, Greenbelt, MD, US Journal of Applied Meteorology (ISSN 0894-8763) vol. 34, no. 1 January 1995 p. 153-174 Research sponsored by Code SE of NASA Headquarters

(HTN-95-60511) Copyright

A three-dimensional cloud model, radiative transfer model-based simulation system is tested and validated against the aircraft-based radiance observations of an intense convective system in southeastern Virginia on 29 June 1986 during the Cooperative Huntsville Meteorological Experiment. NASA's ER-2, a high-altitude research aircraft with a complement of radiometers operating at 11-micrometer infrared channel and 18-, 37-, 92-, and 183-GHz microwave channels provided data for this study. The cloud model successfully simulated the cloud system with regard to aircraft- and radar-observed cloud-top heights and diameters and with regard to radar-observed reflectivity structure. For the simulation time found to correspond best with the aircraft- and radar-observed structure, brightness temperatures $T(\text{sub } b)$ are simulated and compared with observations for all the microwave frequencies along with the 11-micrometer infrared channel. Radiance calculations at the various frequencies correspond well with the aircraft observations in the areas of deep convection. The clustering of 37-147-GHz $T(\text{sub } b)$ observations and the isolation of the 18-GHz values over the convective cores are well simulated by the model. The radiative transfer model, in general, is able to simulate the observations reasonably well from 18 GHz through 174 GHz within all convective areas of the cloud system. When the aircraft-observed 18- and 37-GHz, and 90- and 174-GHz $T(\text{sub } b)$ are plotted against each other, the relationships have a gradual difference in the slope due to the differences in the ice particle size in the convective and more stratiform areas of the cloud. The model is able to capture these differences observed by the aircraft. Brightness temperature-rain rate relationships compare reasonably well with the aircraft observations in terms of the slope of the relationship. The model calculations are also extended to select high-frequency channels at 220, 340, and 400 GHz to simulate the Millimeter-wave Imaging Radiometer aircraft instrument to be flown in

the near future. All three of these frequencies are able to discriminate the convective and anvil portions of the system, providing useful information similar to that from the frequencies below 183 GHz but with potentially enhanced spatial resolution from a satellite platform. In thin clouds, the dominant effect of water vapor is seen at 174, 340, and 400 GHz. In thick cloudy areas, the scattering effect is dominant at 90 and 220 GHz, while the overlaying water vapor can attenuate at 174, 340, and 400 GHz. All frequencies (90-400 GHz) show strong signatures in the core.

Author (Herner)

A95-68845**CONDITIONS ASSOCIATED WITH LARGE-DROP REGIONS**

BRENDA M. POBANZ Univ. of Wyoming, Laramie, WY, US, JOHN D. MARWITZ Univ. of Wyoming, Laramie, WY, US, and MARCIA K. POLITOVICH National Center for Atmospheric Research, Boulder, CO, US Journal of Applied Meteorology (ISSN 0894-8763) vol. 33, no. 11 November 1994 p. 1366-1372 Research sponsored by NCAR

(Contract(s)/Grant(s): NSF ATM-90-14763)

(HTN-95-10686) Copyright

In light of the significant icing hazard large drops pose to general aviation, two conditions have been previously associated with large-drop formation; these being a warm cloud-top temperature and a low droplet concentration. This paper identifies an additional condition associated with the development of large-drop regions. Wind shear is hypothesized as being a necessary but not sufficient condition for the formation of large drops. Wind shear at cloud top may cause turbulence, Kelvin-Helmholtz waves, and thus the inhomogeneous mixing leading to large drops. This hypothesis was tested in 29 cases where the Wyoming King Air aircraft made a climb or descent through the top of stratiform clouds. The presence of a wind shear layer was defined by the magnitude of the wind shear and the value of the bulk Richardson number across the layer. In 23 of the 29 cases, wind shear was associated with large-drop regions. A chi(squared) statistical test was applied to the data. The null hypothesis, where wind shear and large drops were considered independent of each other, was rejected to a significance level of 0.01. From this it can be inferred that large drops and wind shear are related. The depth of the shear layer was usually small, less than 150 m. The validity of the condition of low droplet concentration is questioned since several cases of large drops were found in the presence of a high droplet concentration. These cases were marked by strong wind shear.

Author (Herner)

A95-69431* Jet Propulsion Lab., California Inst. of Tech., Pasadena, CA.

POSSIBLE NEAR-IR CHANNELS FOR REMOTE SENSING PRECIPITABLE WATER VAPOR FROM GEOSTATIONARY SATELLITE PLATFORMS

B.-C. GAO Univ. of Colorado, Boulder, CO, US, A. F. H. GOETZ Univ. of Colorado, Boulder, CO, US, ED R. WESTWATER Wave Propagation Laboratory, Boulder, CO, US, J. E. CONEL Jet Propulsion Laboratory, Pasadena, CA, US, and R. O. GREEN Jet Propulsion Laboratory, Pasadena, CA, US Journal of Applied Meteorology (ISSN 0894-8763) vol. 32, no. 12 December 1993 p. 1791-1801

(Contract(s)/Grant(s): NAG5-30552)

(HTN-95-70139) Copyright

Remote sensing of tropospheric water vapor profiles from current geostationary weather satellites is made using a few broadband infrared (IR) channels in the 6-13 micron region. Uncertainties greater than 20% exist in derived water vapor values just above the surface from the IR emission measurements. In this paper, we propose three near-IR channels, one within the 0.94-micron water vapor band absorption region, and the other two in nearby atmospheric windows, for remote sensing of precipitable water vapor over land areas, excluding lakes and rivers, during daytime from future geostationary satellite platforms. The physical principles are as follows. The reflectance of most surface targets varies approximately linearly with wavelength near 1 micron. The solar radiation on the sun-surface-sensor ray path is attenuated by atmospheric water vapor. The ratio of the radiance from the absorption channel with the

radiance from the two window channels removes the surface reflectance effects and yields approximately the mean atmospheric water vapor transmittance of the absorption channel. The integrated water vapor amount from ground to space can be obtained with a precision of better than 5% from the mean transmittance. Because surface reflectances vary slowly with time, temporal variation of precipitable water vapor can be determined reliably. High spatial resolution, precipitable water vapor images are derived from spectral data collected by the Airborne Visible-Infrared Imaging Spectrometer, which measures solar radiation reflected by the surface in the 0.4-2.5 micron region in 10-nm channels and has a ground instantaneous field of view of 20 m from its platform on an ER-2 aircraft at 20 km. The proposed near-IR reflectance technique would complement the IR emission techniques for remote sensing of water vapor profiles from geostationary satellite platforms, especially in the boundary layer where most of the water vapor is located.

Author (Herner)

A95-69574

A TECHNIQUE FOR DETECTING A TROPICAL CYCLONE CENTER USING A DOPPLER RADAR

VINCENT T. WOOD NOAA, Norman, OK, US *Journal of Atmospheric and Oceanic Technology* (ISSN 0739-0572) vol. 11, no. 5 October 1994 p. 1207-1216 (HTN-95-20631) Copyright

A ground-based Doppler radar technique is developed for detecting a tropical cyclone center position. Once a network of WSR-88D Doppler radars is deployed on the United States coastlines, islands, and military bases during the 1990s, high-resolution detection and tracking of hurricanes nearing land will be possible for the first time. Simulated Doppler velocity data, which were reconstructed from wind field data collected by reconnaissance aircraft during Hurricanes Alicia (1983) and Gloria (1985), were used to test the concept of using ground-based Doppler radar data to estimate cyclone center location. The center range and azimuth estimates of a hurricane signature were calculated from the simulated coastal Doppler radar velocity data. Preliminary results indicate that the technique performed well for estimating center locations from the radar measurements compared with storm center positions determined from in situ aircraft measurements.

Author (revised by Herner)

A95-69717

WINDEX — A NEW INDEX FOR FORECASTING MICROBURST POTENTIAL

DONALD W. MCCANN National Severe Storms Forecast Center, Kansas City, MO, US *Weather and Forecasting* (ISSN 0882-8156) vol. 9, no. 4 December 1994 p. 532-541 (HTN-95-90690) Copyright

Microbursts are small-scale phenomena that have been viewed by many meteorologists as difficult to predict. However, there exists sufficient knowledge of microburst evolution by some in the research and operational communities that can be applied on the mesoscale to provide some warning to the public and aviation. This paper introduces a wind index or WINDEX that is based on this knowledge. It can be easily computed from soundings. The WINDEX is calculated from soundings known to have been taken in microburst environments and previously presented in the literature. The WINDEX can also be computed from surface observations using appropriate assumptions. This paper shows how to use the hourly surface-based WINDEX information (data) by showing its application to the infamous DFW microburst on 2 August 1985 and for three consecutive days in August 1993. The surface-based WINDEX analyses reveal a common pattern first noted by Ladd (1989); that is, microbursts primarily occur with new convection on old thunderstorm outflow boundaries. When an outflow boundary moves perpendicular to the WINDEX contours, into an area of high WINDEX values, conditions are favorable for microbursts. With this conceptual model it is possible for forecasters to give one to two hours warning that microbursts are probable for a small area.

Author (Herner)

A95-69721

FORECASTING FOR A LARGE FIELD PROGRAM: STORM-FEST

EDWARD J. SZOKE NOAA, Boulder, CO, US, JOHN M. BROWN NOAA, Boulder, CO, US, JOHN A. MCGINLEY NOAA, Boulder, CO, US, and DENNIS RODGERS NOAA, Boulder, CO, US *Weather and Forecasting* (ISSN 0882-8156) vol. 9, no. 4 December 1994 p. 593-605

(HTN-95-90694) Copyright

Stormscale Operational and Research Meteorology-Fronts Experimental Systems Test (STORM-FEST) was held from 1 February to 15 March 1992 in the central United States as a preliminary field systems test for an eventual larger-scale program. One of the systems tested was a remote operations center, located in Boulder, Colorado. In concert with the remote operations center test was a test of remote forecasting support, also centered in Boulder. The Boulder-Denver Experimental Forecast Facility (EFF) and two other newly formed EFF's, at Norman, Oklahoma, and Kansas City, Missouri, played key roles in the forecasting/nowcasting support. A description of the design and function of this remote forecasting and nowcasting support is given, followed by an assessment of its utility during STORM-FEST. Although remote forecasting support was deemed plausible based on the STORM-FEST experience, a number of suggestions are given for a more effective way to conduct forecasting experiments and provide forecasting support during a field program.

Author (revised by Herner)

A95-69766

RESEARCH AIRCRAFT OBSERVATIONS OF A POLAR LOW AT THE EAST GREENLAND ICE EDGE

MICHAEL W. DOUGLAS ERL, NOAA, Norman, OK, US, M. A. SHAPIRO ERL, NOAA, Boulder, CO, US, L. S. FEDOR ERL, NOAA, Boulder, CO, US, and LEA SAUKKONEN Finnish Meteorological Inst., Helsinki, Finland *Monthly Weather Review* (ISSN 0027-0644) vol. 123, no. 1 January 1995 p. 5-15

(HTN-95-A0175) Copyright

The structure of a subsynoptic-scale cyclone (polar low) that formed along the east Greenland ice edge during the 1989 Coordinated Eastern Arctic Research Experiment (CEAREX) is described using NOAA WP-3D research aircraft and satellite observations. Satellite imagery showed a well-defined 400-km-wide comma cloud pattern during the time of the aircraft observations. Frontal zones with marked wind shifts and thermal gradients near the surface were associated with the polar low. Although the polar low's vorticity decreased rapidly with height between 950 and 800 mb, a secondary vorticity maximum was found in the upper troposphere associated with a short-wave trough. Doppler radar and aircraft observations showed the structure of the main precipitation band to be similar to that of other polar lows observed by research aircraft. In general, the structure of the polar low resembled, except for horizontal scale, the structure of midlatitude cyclones at a similar stage of cloud field evolution.

Author (Herner)

A95-69803

MESOSCALE STRUCTURE OF PRECIPITATION BANDS IN A NORTH ATLANTIC WINTER STORM

G. B. RAGA Atmospheric Environment Service, Downsview, Ontario, Canada, R. E. STEWART Atmospheric Environment Service, Downsview, Ontario, Canada, and J. W. STRAPP Atmospheric Environment Service, Downsview, Ontario, Canada *Monthly Weather Review* (ISSN 0027-0644) vol. 122, no. 9 September 1994 p. 2039-2051 Research sponsored by the Federal Panel on Energy Research and Development

(HTN-95-40659) Copyright

The present study discusses the meso- and microscale structures of precipitation regions within a midlatitude winter storm over the North Atlantic, observed during the Experiment on Rapidly Intensifying Cyclones over the Atlantic (ERICA). Two wide regions of precipitation separated by a narrow band were observed at low levels by airborne radar. These regions were aligned parallel to the cold front and were sampled by aircraft at three different levels. The

calculated mesoscale frontogenetical forcing is dominated at low levels by confluence and at midlevels by the tilting term. The absolute magnitudes are smaller than those reported by Shapiro, and Bond and Fleagle, and are consistent with the broader and less intense front in this study. The frontogenetical forcing due to melting of ice crystals was estimated from observations of precipitation particles. The analysis indicates that the cooling due to melting of ice particles is not a dominant frontogenetical forcing at the observed stage in storm evolution. Precipitation rates larger than those observed (by a factor of 3) behind the cold front are needed before the thermal impact of melting could contribute to frontogenesis as much as confluence at the same level. The region of precipitation ahead of the cold front appears to be linked to convective instability observed in the warm sector. The observed precipitation region to the west of the cold front is consistent with the trajectories of falling particles carried by the relative wind flowing toward the back of the system. The decrease in precipitation rate observed right behind the front can be interpreted as ice particles falling through a deep region in which temperatures are close to 0 C. The presence of such a region leads to a nonuniform precipitation distribution, with areas that would appear as precipitation bands in radar images, and others in which precipitation is reduced.

Author (Herner)

A95-69833

AN AIR-DRIVEN PRESSURE BOOSTER PUMP FOR AIRCRAFT-BASED AIR SAMPLING

C. A. M. BRENNINKMEIJER National Institute of Water and Atmospheric Research, Lower Hutt, New Zealand and P. A. ROBERTS National Institute of Water and Atmospheric Research, Lower Hutt, New Zealand Journal of Atmospheric and Oceanic Technology (ISSN 0739-0572) vol. 11, no. 6 December 1994 p. 1664-1671 Research sponsored by the New Zealand Foundation for Science and Technology (HTN-95-40689) Copyright

A diaphragm pump used to boost the intake pressure of a three-stage high-pressure air compressor for collecting large air samples during aircraft flights has been developed. The pump consists of a large (17 L) spherical body divided into two chambers by means of a thin neoprene diaphragm. The pressure drop generated across an air intake and air exhaust mounted outside the aircraft drives sample air into this spherical body while the diaphragm is displaced completely to align the inside of the pump body. The air thus collected is subsequently forced into the inlet of a high-pressure compressor by letting aircraft cabin air fill the pump body from the other side of the diaphragm. The pumping cycle is controlled by the position of the diaphragm and is self-sustaining. The pressure at the intake of the high-pressure compressor is thus maintained close to that of the cabin pressure, which results in a three- to fourfold pressure boost. In this way the pumping speed of the high-pressure compressor is enhanced considerably, reducing sampling time and possible contamination of the air sampled. Details of construction, laboratory tests, and aircraft performance are given, with special attention to the problem of collecting air in the lower stratosphere for the isotopic analysis of carbon monoxide.

Author (Herner)

N95-19582# Energy and Environmental Analysis, Inc., Arlington, VA. AIR POLLUTION MITIGATION MEASURES FOR AIRPORTS AND ASSOCIATED ACTIVITY

May 1994 206 p Prepared in cooperation with K. T. Analytics, Inc., Frederick, MD

(Contract(s)/Grant(s): ARB-A132-168)

(PB94-207610; ARB-R-94/534) Avail: CASI HC A10/MF A03

This report is a reference guide to emission mitigation techniques that can be applied to aircraft and their operations, the ground support equipment that service aircraft at airports, and other airport on-road and off-road emission sources such as maintenance, passenger, and employee vehicles. Each measure is described along with guidelines for its use and constraints that may limit its effectiveness. The information can be used to quantify emission reductions that result from operational, procedural, or technological changes to these sources. Projects and plans to reduce air pollution at U.S. and

European airports are described. A detailed description of procedures used to calculate aircraft emissions is provided in an appendix.

NTIS

N95-19685# Air Force Inst. of Tech., Wright-Patterson AFB, OH. School of Engineering.

DEVELOPING AN EMISSION FACTOR FOR HAZARDOUS AIR POLLUTANTS FOR AN F-16 USING JP-8 FUEL M.S.

Thesis

DONALD J. VANSCHAACK Sep. 1994 99 p (AD-A284802; AFIT/GEE/ENS/94S-26) Avail: CASI HC A05/MF A02

The 1990 Clean Air Act amendments drastically changed the legislation of hazardous air pollutants (HAPs) or air toxics. Title 3 of the act which specifically addresses HAPs now lists 189 substances which may require regulation as air toxics. Consequently, the reporting of HAP emissions from all Air Force operations will be required in the future. However, the Department of Defense (DoD) does not have methods available to report this information. This thesis develops emission factors for selected HAPs from an F-16 C&D aircraft/F110 engine operating on JP-8 fuel. The methodology included: determining which HAPs should be selected, using past aircraft emission studies to estimate HAP concentrations for the F110 engine using JP-8 fuel, determining an emission factor formula to calculate emission factors for each HAP, and testing the developed emission factors on an airfield operation. The estimated emission factors for each HAP for the F110 engine are low for all engine modes mainly because the F110 is a newer engine with high combustion efficiency. The resultant emission inventory shows that many HAPs would be classified as major sources under current Title 3 legislation. Thus, it is important to assess airfield operations to ensure they remain in compliance with the upcoming Title 3 legislation.

DTIC

N95-19855# National Renewable Energy Lab., Golden, CO. EVIDENCE THAT AERODYNAMIC EFFECTS, INCLUDING DYNAMIC STALL, DICTATE HAWT STRUCTURAL LOADS AND POWER GENERATION IN HIGHLY TRANSIENT TIME FRAMES

D. E. SHIPLEY (Colorado Univ., Boulder, CO.), M. S. MILLER (Colorado Univ., Boulder, CO.), M. C. ROBINSON (Colorado Univ., Boulder, CO.), M. W. LUTTGES (Colorado Univ., Boulder, CO.), and D. A. SIMMS Aug. 1994 14 p Presented at the American Wind Energy Association Annual Conference and Exhibition, Minneapolis, MN, 9-13 May 1994

(Contract(s)/Grant(s): DE-AC36-83CH-10093)

(DE94-011865; NREL/TP-441-7080; CONF-940548-7) Avail: CASI HC A03/MF A01

Aerodynamic data collected from the National Renewable Energy Laboratory's Combined Experiment have shown three distinct performance regimes when the turbine is operated under relatively steady flow conditions. Operating at blade angles of attack below static stall, excellent agreement is achieved with two-dimensional wind tunnel data. Around the static stall angle, the cycle average normal force produced is greater than the static test data. Span locations near the hub produce extremely large values of normal force coefficient, well in excess of the two-dimensional data results. These performance regimes have been shown to be a function of the three-dimensional flow structure and cycle averaged dynamic stall effects. Power generation and root bending moments have also been shown to be directly dependent on the inflow wind velocity. Aerodynamic data, including episodes of dynamic stall, have been correlated on a cycle by cycle basis with the structural and power generation characteristics of a horizontal axis wind turbine. Instantaneous unsteady forces and resultant power generation indicate that peak transient levels can significantly exceed cycle averaged values. Strong coupling between transient aerodynamic and resonant response of the turbine was also observed. These results provide some initial insight into the contribution of unsteady aerodynamics on undesirable turbine structural response and fatigue life.

DOE

MATHEMATICAL AND COMPUTER SCIENCES

Includes mathematical and computer sciences (general); computer operations and hardware; computer programming and software; computer systems; cybernetics; numerical analysis; statistics and probability; systems analysis; and theoretical mathematics.

A95-68256

COMPUTERIZED MAINTENANCE AID

Aerospace Engineering (Warrendale, Pennsylvania) (ISSN 0736-2536) vol. 14, no. 1 January-February 1994 p. 7-10 (BTN-95-EIX95031502749) Copyright

The paper discussed a computerized maintenance aid developed with the U.S. Air Force for quick assessment of the damage obtained by the aircraft and determination of the mission capability impact and repair time estimation. This tool is a computer based technique developed through the Air Force's Aircraft Battle Damage Repair (ABDR) program. It allows maintenance technicians to rapidly assess technical wiring data which is currently available only in voluminous technical orders. This benefit is a significant reduction of the time required to assess damage. This tool also has significant applications for normal aircraft maintenance during peacetime.

EI

A95-68307* National Aeronautics and Space Administration. Langley Research Center, Hampton, VA.

PARALLEL IMPLICIT UNSTRUCTURED GRID EULER SOLVERS

V. VENKATAKRISHNAN AIAA Journal (ISSN 0001-1452) vol. 32, no. 10 October 1994 p. 1985-1991 refs (BTN-95-EIX95042474393) Copyright

A mesh-vertex finite volume scheme for solving the Euler equations on triangular unstructured meshes is implemented on a multiple-instruction/multiple-data stream parallel computer. An explicit four-stage Runge-Kutta scheme is used to solve two-dimensional flow problems. A family of implicit schemes is also developed to solve these problems, where the linear system that arises at each time step is solved by a preconditioned GMRES algorithm. Two partitioning strategies are employed: one that partitions triangles and the other that partitions vertices. The choice of the preconditioner in a distributed memory setting is discussed. All of the methods are compared both in terms of elapsed times and convergence rates. It is shown that the implicit schemes offer adequate parallelism at the expense of minimal sequential overhead. The use of a global coarse grid to further minimize this overhead is also investigated. The schemes are implemented on a distributed memory parallel computer, the Intel iPSC/860.

Author (EI)

N95-19688# Naval Air Warfare Center, Patuxent River, MD. Aircraft Div.

THE USE OF GENETIC ALGORITHMS FOR FLIGHT TEST AND EVALUATION OF ARTIFICIAL INTELLIGENCE AND COMPLEX SOFTWARE SYSTEMS

ELIZABETH DAVIES, JOHN MCMASTER, and MARY STARK 1994 6 p (AD-A284824) Avail: CASI HC A02/MF A01

Artificial intelligence (AI) technologies are emerging from research laboratories into industry, particularly into the field of aviation. One such application is the ARPA/USAF Pilot's Associate, a set of cooperating expert systems designed to aid the tactical pilot in a combat situation. There are currently no rigorous methods for the test and evaluation of such tactical airborne expert systems. The focus of this program, sponsored in part by the Office of Naval Technology, is the development of a test and evaluation facility for tactical airborne systems which incorporate artificial intelligence. In particular, the subject of this paper is the development of a genetic algorithm (GA) which will automatically find those test cases for which the system under test performs most poorly.

DTIC

N95-19751* Royal Military Coll. of Saint-Jean, Richelieu (Quebec). Group of Applied Research in Management Support Systems.

TRANSPORT AIRCRAFT LOADING AND BALANCING SYSTEM: USING A CLIPS EXPERT SYSTEM FOR MILITARY AIRCRAFT LOAD PLANNING

J. RICHARDSON, M. LABBE, Y. BELALA, and VINCENT LEDUC In NASA. Johnson Space Center, Third CLIPS Conference Proceedings, Volume 2 p 233-240 Nov. 1994 Avail: CASI HC A02/MF A03

The requirement for improving aircraft utilization and responsiveness in airlift operations has been recognized for quite some time by the Canadian Forces. To date, the utilization of scarce airlift resources has been planned mainly through the employment of manpower-intensive manual methods in combination with the expertise of highly qualified personnel. In this paper, we address the problem of facilitating the load planning process for military aircraft cargo planes through the development of a computer-based system. We introduce TALBAS (Transport Aircraft Loading and BALancing System), a knowledge-based system designed to assist personnel involved in preparing valid load plans for the C130 Hercules aircraft. The main features of this system which are accessible through a convivial graphical user interface, consists of the automatic generation of valid cargo arrangements given a list of items to be transported, the user-definition of load plans and the automatic validation of such load plans.

Author

N95-19759*# Yalif (Guy U.), MA.

THE COMPUTER AIDED AIRCRAFT-DESIGN PACKAGE (CAAP)

GUY U. YALIF In NASA. Johnson Space Center, Third CLIPS Conference Proceedings, Volume 2 p 303-314 Nov. 1994 Avail: CASI HC A03/MF A03

The preliminary design of an aircraft is a complex, labor-intensive, and creative process. Since the 1970's, many computer programs have been written to help automate preliminary airplane design. Time and resource analyses have identified, 'a substantial decrease in project duration with the introduction of an automated design capability'. Proof-of-concept studies have been completed which establish 'a foundation for a computer-based airframe design capability'. Unfortunately, today's design codes exist in many different languages on many, often expensive, hardware platforms. Through the use of a module-based system architecture, the Computer aided Aircraft-design Package (CAAP) will eventually bring together many of the most useful features of existing programs. Through the use of an expert system, it will add an additional feature that could be described as indispensable to entry level engineers and students: the incorporation of 'expert' knowledge into the automated design process.

Author

N95-19767*# Reticular Systems, Inc., San Diego, CA.

PALYSYS (TM): AN EXTENDED VERSION OF CLIPS FOR CONSTRUCTION AND REASONING USING BLACKBOARDS

TRAVIS BRYSON and DAN BALLARD In NASA. Johnson Space Center, Third CLIPS Conference Proceedings, Volume 2 p 377-387 Nov. 1994 Avail: CASI HC A03/MF A03

This paper describes PalymSys(TM) — an extended version of the CLIPS language that is designed to facilitate the implementation of blackboard systems. The paper first describes the general characteristics of blackboards and shows how a control blackboard architecture can be used by AI systems to examine their own behavior and adapt to real-time problem-solving situations by striking a balance between domain and control reasoning. The paper then describes the use of PalymSys in the development of a situation assessment subsystem for use aboard Army helicopters. This system performs real-time inferencing about the current battlefield situation using multiple domain blackboards as well as a control blackboard. A description of the control and domain blackboards and their implementation is presented. The paper also describes modifications made to the standard CLIPS 6.02 language in

16 PHYSICS

PalymSys(TM) 2.0. These include: (1) a dynamic Dempster-Shafer belief network whose structure is completely specifiable at run-time in the consequent of a PalymSys(TM) rule, (2) extension of the run command including a continuous run feature that enables the system to run even when the agenda is empty, and (3) a built-in communications link that uses shared memory to communicate with other independent processes. Author

16 PHYSICS

Includes physics (general); acoustics; atomic and molecular physics; nuclear and high-energy physics; optics; plasma physics; solid-state physics; and thermodynamics and statistical physics.

A95-69229* National Aeronautics and Space Administration. Langley Research Center, Hampton, VA.

RECENT STUDIES OF ROTORCRAFT BLADE-VORTEX INTERACTION NOISE

J. S. PREISSER, T. F. BROOKS, and R. M. MARTIN Journal of Aircraft (ISSN 0021-8669) vol. 31, no. 5 September-October 1994 p. 1009-1015 refs

(BTN-95-EI X95062487521) Copyright

Recent results are presented from several research efforts aimed at the understanding of rotorcraft blade-vortex interaction (BVI) in terms of the noise generation, directivity, and control. The results are based on work performed by NASA Langley Research Center researchers, both alone and in collaboration with other research organizations. Based on analysis of a simplified physical model, the critical parameters controlling BVI noise generation have been identified. The detailed mapping of the acoustic radiation field of a model rotor in a wind tunnel has revealed the extreme sensitivity of directivity to rotor advance ratio and disk attitude. The control and reduction of BVI noise through the use of higher harmonic pitch control is discussed. Author (EI)

18 SPACE SCIENCES

Includes space sciences (general); astronomy; astrophysics; lunar and planetary exploration; solar physics; and space radiation.

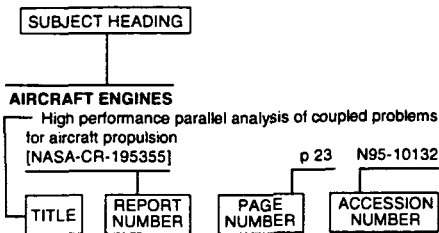
A95-69658

POWERFUL BOLIDE EXPLOSION OVER NORTH ITALY

K. KORLEVIC Visnjan Observatory, Visnjan, Croatia and G. VALDRE P. Porta San Donato, Bologna, Italy Planetary and Space Science (ISSN 0032-0633) vol. 42, no. 8 August 1994 p. 673-675 (HTN-95-80564) Copyright

In the night of 19 January 1993 at 00:33:20 +/- 15s Universal Time (UT), North Italy, Slovenia and Croatia were illuminated by powerful terminal flare during fireball disintegration. Some tens of KT were liberated as light. In the region of Emilia the low frequency, very strong roar (thunder) was also heard, shaking windows and walls, some 80-140 s after the bolide explosion. The severe fragmentation and after that a complete destruction of the fireball body took place over the Italian region of Emilia at the height of 35-40 km. Sticky film traps were used for the first time after a bright fireball event and a probable fall down of glassy spherules sizing micron was captured. This is one more case where very large meteoroids, group (type) I, II and III or small asteroids/comets (density 0.2-5 g/cu cm) were completely destroyed by aerodynamic pressure and stress in the dense part of the atmosphere, leaving no geological consequences. Author (Herner)

Typical Subject Index Listing



The subject heading is a key to the subject content of the document. The title is used to provide a description of the subject matter. When the title is insufficiently descriptive of document content, a title extension is added, separated from the title by three hyphens. The accession number and the page number are included in each entry to assist the user in locating the abstract in the abstract section. If applicable, a report number is also included as an aid in identifying the document. Under any one subject heading, the accession numbers are arranged in sequence.

A

- ABLATION**
Review of numerical procedures for computational surface thermochemistry
[BTN-94-EIX94441386682] p 205 A95-68191
- ABLATIVE MATERIALS**
Trajectory-based heating analysis for the European Space Agency/Rosetta Earth Return Vehicle
[BTN-95-EIX95041503787] p 205 A95-69218
- ABRASIVES**
Multilayer anti-erosion coatings p 201 N95-19679
- ACCIDENT PREVENTION**
Modern transport engine experience with environmental ingestion effects p 199 N95-19660
- ACOUSTICS**
Rotating Kirchhoff method for three-dimensional transonic blade-vortex interaction hover noise
[BTN-94-EIX94441386601] p 182 A95-67332
- ACTIVE CONTROL**
Active control of wake/blade-row interaction noise
[BTN-95-EIX95042474389] p 196 A95-68311
Noise and vibration control
[BTN-95-EIX95042477108] p 179 A95-68351
- ADAPTIVE CONTROL**
Using adaptive structures to attenuate rotary wing aeroelastic response
[BTN-95-EIX95062487547] p 192 A95-68361
- AERIAL RECONNAISSANCE**
Joint stars phased array radar antenna
[BTN-95-EIX95042474626] p 209 A95-68280
- AERODYNAMIC BALANCE**
Minimum sink-speed in power-off glide
[BTN-95-EIX95062487556] p 193 A95-68370
Navier-Stokes simulations of Orbiter aerodynamic characteristics including pitch trim and bodyflap
[BTN-95-EIX95041503779] p 204 A95-69210
- AERODYNAMIC CHARACTERISTICS**
Waveriders with finlets
[BTN-95-EIX95062487541] p 184 A95-68355

- Two-point transonic airfoil design using optimization for improved off-design performance
[BTN-95-EIX95062487542] p 192 A95-68356
Aerodynamic effects of delta planform tip sails on wing performance
[BTN-95-EIX95062487544] p 185 A95-68358
Hypersonic waverider test vehicle: A logical next step
[BTN-95-EIX95041503783] p 193 A95-69214
Interpretation of waverider performance data using computational fluid dynamics
[BTN-95-EIX95062487534] p 193 A95-69242
State-space representation of aerodynamic characteristics of an aircraft at high angles of attack
[BTN-95-EIX95062487536] p 187 A95-69244
Aerodynamic characteristics of strake vortex flaps on a strake-wing configuration
[BTN-95-EIX95062487537] p 187 A95-69245
Documentation and archiving of the Space Shuttle wind tunnel test data base. Volume 2: User's Guide to the Archived Data Base
[NASA-TM-104806-VOL-2] p 205 N95-19624
Evidence that aerodynamic effects, including dynamic stall, dictate HAWT structural loads and power generation in highly transient time frames
[DE94-011865] p 216 N95-19855
- AERODYNAMIC COEFFICIENTS**
Minimum sink-speed in power-off glide
[BTN-95-EIX95062487556] p 193 A95-68370
Aerodynamic sensitivity coefficients using the three-dimensional full potential equation
[BTN-95-EIX95062487530] p 186 A95-69238
Aerodynamic characteristics of strake vortex flaps on a strake-wing configuration
[BTN-95-EIX95062487537] p 187 A95-69245
- AERODYNAMIC CONFIGURATIONS**
Waveriders with finlets
[BTN-95-EIX95062487541] p 184 A95-68355
Aerodynamically blunt and sharp bodies
[BTN-95-EIX95041503781] p 205 A95-69212
Development of an efficient inverse method for supersonic and hypersonic body design
[BTN-95-EIX95041503784] p 180 A95-69215
Documentation and archiving of the Space Shuttle wind tunnel test data base. Volume 2: User's Guide to the Archived Data Base
[NASA-TM-104806-VOL-2] p 205 N95-19624
The aerodynamic design of an integrated wing lower surface and pylons for reduced drag
[ARA-MEMO-406] p 194 N95-19789
- AERODYNAMIC DRAG**
Interpretation of waverider performance data using computational fluid dynamics
[BTN-95-EIX95062487534] p 193 A95-69242
An investigation of drag repeatability in half model testing in the ARA Transonic Wind Tunnel
[ARA-MEMO-392] p 188 N95-19546
The aerodynamic design of an integrated wing lower surface and pylons for reduced drag
[ARA-MEMO-406] p 194 N95-19789
- AERODYNAMIC FORCES**
Adaptive computations of flow around a delta wing with vortex breakdown
[BTN-94-EIX94441386631] p 184 A95-68180
Comparison of electrostatic and aerodynamic forces during parachute opening
[BTN-95-EIX95062487532] p 187 A95-69240
Side forces at high angles of attack. Why, when, how?
[BTN-95-EIX95112523809] p 194 A95-69324
- AERODYNAMIC HEAT TRANSFER**
Kinetic theory in aerothermodynamics
[HTN-95-A0002] p 183 A95-67829
Prediction of ice accretion: Comparison between the 2D and 3D codes
[BTN-94-EIX94441385753] p 213 A95-68217
Approximate method for calculating heating rates on three-dimensional vehicles
[BTN-95-EIX95041503778] p 210 A95-69209
Documentation and archiving of the Space Shuttle wind tunnel test data base. Volume 2: User's Guide to the Archived Data Base
[NASA-TM-104806-VOL-2] p 205 N95-19624

- AERODYNAMIC HEATING**
Shock layers and boundary layers in hypersonic flows
[HTN-95-A0003] p 183 A95-67830
Approximate method for calculating heating rates on three-dimensional vehicles
[BTN-95-EIX95041503778] p 210 A95-69209
Multiblock analysis for Shuttle Orbiter reentry heating from Mach 24 to Mach 12
[BTN-95-EIX95041503780] p 205 A95-69211
Trajectory-based heating analysis for the European Space Agency/Rosetta Earth Return Vehicle
[BTN-95-EIX95041503787] p 205 A95-69218
- AERODYNAMIC INTERFERENCE**
Interference between tanker wing wake with roll-up and receiver aircraft
[BTN-95-EIX95062487552] p 185 A95-68366
Effect of ground and ceiling planes on shape of energized wakes
[BTN-95-EIX95062487558] p 186 A95-68372
Numerical simulation of steady and unsteady, vorticity-dominated aerodynamic interference
[BTN-95-EIX95062487524] p 186 A95-69232
Preliminary assessment of tunnel wall interference in the NDA cryogenic wind tunnel
[BTN-95-EIX95062487531] p 187 A95-69239
Two-variable method for blockage wall interference in a circular tunnel
[BTN-95-EIX95062487540] p 187 A95-69248
- AERODYNAMIC LOADS**
Continuous gust response and sensitivity derivatives using state-space models
[BTN-95-EIX95062487551] p 203 A95-68365
Brief history of gust models for aircraft design
[BTN-95-EIX95062487557] p 203 A95-68371
State-space representation of aerodynamic characteristics of an aircraft at high angles of attack
[BTN-95-EIX95062487536] p 187 A95-69244
- AERODYNAMIC NOISE**
Active control of wake/blade-row interaction noise
[BTN-95-EIX95042474389] p 196 A95-68311
- AERODYNAMIC STABILITY**
Determination of stability and control derivatives from the NASA F/A-18 HARV from flight data using the maximum likelihood method
[NASA-CR-197320] p 204 N95-19576
- AERODYNAMIC STALLING**
Comparison of theory and experiment for non-linear flutter and stall response of a helicopter blade
[BTN-94-EIX94351108100] p 191 A95-66500
Evidence that aerodynamic effects, including dynamic stall, dictate HAWT structural loads and power generation in highly transient time frames
[DE94-011865] p 216 N95-19855
- AERODYNAMICS**
Behavior of the Johnson-King turbulence model in axisymmetric supersonic flows
[BTN-94-EIX94441386606] p 183 A95-67337
Powered lift for land and sea
[BTN-95-EIX95041503010] p 192 A95-68313
Aerodynamically blunt and sharp bodies
[BTN-95-EIX95041503781] p 205 A95-69212
Numerical simulation of steady and unsteady, vorticity-dominated aerodynamic interference
[BTN-95-EIX95062487524] p 186 A95-69232
Numerical simulation of incidence and sweep effects on delta wing vortex breakdown
[BTN-95-EIX95062487526] p 186 A95-69234
Aerodynamic sensitivity coefficients using the three-dimensional full potential equation
[BTN-95-EIX95062487530] p 186 A95-69238
Comparison of electrostatic and aerodynamic forces during parachute opening
[BTN-95-EIX95062487532] p 187 A95-69240
Interpretation of waverider performance data using computational fluid dynamics
[BTN-95-EIX95062487534] p 193 A95-69242
Aerodynamic characteristics of strake vortex flaps on a strake-wing configuration
[BTN-95-EIX95062487537] p 187 A95-69245

AEROELASTICITY

- Comparison of theory and experiment for non-linear flutter and stall response of a helicopter blade
[BTN-94-EIX94351108100] p 191 A95-66500
- Aeroelastic stability of hingeless rotor blade in hover using large deflection theory
[BTN-94-EIX94441386616] p 183 A95-67347
- Using adaptive structures to attenuate rotary wing aeroelastic response
[BTN-95-EIX95062487547] p 192 A95-68361
- Influence of structural and aerodynamic modeling on flutter analysis
[BTN-95-EIX95062487550] p 203 A95-68364

AEROSERVOELASTICITY

- Continuous gust response and sensitivity derivatives using state-space models
[BTN-95-EIX95062487551] p 203 A95-68365

AEROSOLS

- Three-dimensional model interpretation of NO(x) measurements from the lower stratosphere
[HTN-95-90534] p 213 A95-67806

AEROSPACE TECHNOLOGY TRANSFER

- Reliability and maintainability
[BTN-95-EIX95042477109] p 179 A95-68350
- National AeroSpace Plane: Technology transfer
[BTN-95-EIX95072498879] p 180 A95-68395

AEROSPACE VEHICLES

- Environmental effects on composite airframes: A study conducted for the ARM UAV Program (Atmospheric Radiation Measurement Unmanned Aerospace Vehicle)
[DE94-015351] p 206 N95-19579

AEROTHERMOCHEMISTRY

- Review of numerical procedures for computational surface thermochemistry
[BTN-94-EIX94441386682] p 205 A95-68191

AEROTHERMODYNAMICS

- Multiblock analysis for Shuttle Orbiter reentry heating from Mach 24 to Mach 12
[BTN-95-EIX95041503780] p 205 A95-69211
- Aero-thermodynamic distortion induced structured dynamic response
[AD-A279931] p 203 N95-19864

AGING (MATERIALS)

- Corrosion prevention and control
[BTN-95-EIX95031502753] p 188 A95-68260
- USAF aging aircraft program
[BTN-95-EIX95072498878] p 180 A95-68394

AIR CARGO

- Transport aircraft loading and balancing system: Using a CLIPS expert system for military aircraft load planning
p 217 N95-19751

AIR CURRENTS

- Advanced diesel electronic fuel injection and turbocharging
[AD-A279176] p 211 N95-19809

AIR DROP OPERATIONS

- Radial reefing method for accelerated and controlled parachute opening
[BTN-95-EIX95062487539] p 187 A95-69247

AIR FLOW

- An investigation of drag repeatability in half model testing in the ARA Transonic Wind Tunnel
[ARA-MEMO-392] p 188 N95-19546
- Prediction of wind tunnel effects on the installed F/A-18A inlet flow field at high angles-of-attack
[NASA-CR-195429] p 197 N95-19651

AIR INTAKES

- Protective coatings for compressor gas path components
p 201 N95-19675

AIR NAVIGATION

- On-the-fly carrier phase ambiguity resolution for precise aircraft landing
[BTN-95-EIX95112522535] p 190 A95-69328

AIR POLLUTION

- Antarctic snow record of southern hemisphere lead pollution
[HTN-95-40359] p 212 A95-66869
- Aircraft engine emission reduction
[BTN-95-EIX95031502750] p 196 A95-68257
- Ozone, skin cancer, and the SST
[BTN-95-EIX95041503011] p 213 A95-68314
- Air pollution mitigation measures for airports and associated activity
[PB94-207610] p 216 N95-19582
- Damage of high temperature components by dust-laden air
p 201 N95-19673
- Gas turbine compressor corrosion and erosion in Western Europe
p 201 N95-19678
- Developing an emission factor for hazardous air pollutants for an F-16 using JP-8 fuel
[AD-A284802] p 216 N95-19685

AIR SAMPLING

- An air-driven pressure booster pump for aircraft-based air sampling
[HTN-95-40689] p 216 A95-69833

AIR TO AIR REFUELING

- Interference between tanker wing wake with roll-up and receiver aircraft
[BTN-95-EIX95062487552] p 185 A95-68366

AIRBORNE EQUIPMENT

- An airborne monitoring system for FOD and erosion faults
p 200 N95-19668

AIRCRAFT ACCIDENT INVESTIGATION

- Special investigation report: Maintenance anomaly resulting in dragged engine during landing rollout. Northwest Airlines Flight 18, Boeing 747-251B, N637US, New Tokyo International Airport, Narita, Japan, 1 Mar. 1994
[PB94-917006] p 188 N95-19793

AIRCRAFT ACCIDENTS

- Special investigation report: Maintenance anomaly resulting in dragged engine during landing rollout. Northwest Airlines Flight 18, Boeing 747-251B, N637US, New Tokyo International Airport, Narita, Japan, 1 Mar. 1994
[PB94-917006] p 188 N95-19793

AIRCRAFT ANTENNAS

- Design considerations for an archimedean slot spiral antenna
p 211 N95-19798

AIRCRAFT BRAKES

- Surface morphology and structure of carbon-carbon composites in high-energy sliding contact
[BTN-94-EIX94371347996] p 206 A95-69164

AIRCRAFT COMPARTMENTS

- Noise and vibration control
[BTN-95-EIX95042477108] p 179 A95-68351

AIRCRAFT CONFIGURATIONS

- Hypersonic waverider test vehicle: A logical next step
[BTN-95-EIX95041503783] p 193 A95-69214
- Development of an efficient inverse method for supersonic and hypersonic body design
[BTN-95-EIX95041503784] p 180 A95-69215
- Validation and evaluation of the advanced aeronautical CFD system SAUNA: A method developer's view
[ARA-MEMO-390] p 210 N95-19774
- Verification of the CFD simulation system SAUNA for complex aircraft configurations
[ARA-MEMO-401] p 211 N95-19776
- Inviscid and viscous flow modelling of complex aircraft configurations using the CFD simulation system sauna
[ARA-MEMO-403] p 211 N95-19777

AIRCRAFT CONSTRUCTION MATERIALS

- National AeroSpace Plane: Technology transfer
[BTN-95-EIX95072498879] p 180 A95-68395

AIRCRAFT CONTROL

- Side forces at high angles of attack. Why, when, how?
[BTN-95-EIX95112523809] p 194 A95-69324
- Determination of stability and control derivatives from the NASA F/A-18 HARV from flight data using the maximum likelihood method
[NASA-CR-197320] p 204 N95-19576
- The use of genetic algorithms for flight test and evaluation of artificial intelligence and complex software systems
[AD-A284824] p 217 N95-19688
- Automation of hardware-in-the-loop testing of control systems for unmanned air vehicles
[AD-A284833] p 194 N95-19693
- Airship applications of modern flight test techniques
[AD-A284253] p 194 N95-19731

AIRCRAFT DESIGN

- Maintenance requirements for a supersonic transport
[BTN-95-EIX95031502751] p 179 A95-68258
- Corrosion prevention and control
[BTN-95-EIX95031502753] p 188 A95-68260
- Two-point transonic airfoil design using optimization for improved off-design performance
[BTN-95-EIX95062487542] p 192 A95-68356
- Application of circulation control to advanced subsonic transport aircraft. Part 1: Airfoil development
[BTN-95-EIX95062487545] p 185 A95-68359
- Application of circulation control to advanced subsonic transport aircraft. Part 2: Transport application
[BTN-95-EIX95062487546] p 185 A95-68360
- Coupling equivalent plate and finite element formulations in multiple-method structural analyses
[BTN-95-EIX95062487548] p 192 A95-68362
- Brief history of gust models for aircraft design
[BTN-95-EIX95062487557] p 203 A95-68371
- Future SSTs a European approach
[BTN-95-EIX95072419883] p 180 A95-68396
- Putting the ACSYNT on aircraft design
[BTN-95-EIX95072419881] p 180 A95-68398
- Hypersonic waverider test vehicle: A logical next step
[BTN-95-EIX95041503783] p 193 A95-69214
- Development of an efficient inverse method for supersonic and hypersonic body design
[BTN-95-EIX95041503784] p 180 A95-69215
- Proceedings of the USAF Structural Integrity Program Conference
[AD-A285684] p 194 N95-19517

- The Computer Aided Aircraft-design Package (CAAP)
p 217 N95-19759

- The aerodynamic design of an integrated wing lower surface and pylons for reduced drag
[ARA-MEMO-406] p 194 N95-19789

AIRCRAFT ENGINES

- Design optimization of aircraft engine-mount systems.
[BTN-94-EIX94351143325] p 195 A95-67298
- Aircraft engine emission reduction
[BTN-95-EIX95031502750] p 196 A95-68257
- Starter/generator testing
[BTN-95-EIX95072498877] p 210 A95-68393
- Ply layout optimization and micromechanics tailoring of composite aircraft engine structures
[BTN-95-EIX95112524206] p 196 A95-69302
- Proceedings of the USAF Structural Integrity Program Conference
[AD-A285684] p 194 N95-19517
- Air pollution mitigation measures for airports and associated activity
[PB94-207610] p 216 N95-19582
- Erosion, Corrosion and Foreign Object Damage Effects in Gas Turbines
[AGARD-CP-558] p 197 N95-19653
- Out of area experiences with the RB199 in Toronto
p 198 N95-19654
- The operation of gas turbine engines in hot and sandy conditions: Royal Air Force experiences in the Gulf conflict
p 198 N95-19655
- Navy foreign object damage and its impact on future gas turbine engine low pressure compression systems
p 198 N95-19658
- Scandinavian Airlines Systems experience on erosion, corrosion and foreign object damage effects on gas turbines
p 198 N95-19659
- Modern transport engine experience with environmental ingestion effects
p 199 N95-19660
- Design of fan blades subjected to bird impact
p 200 N95-19669
- Testing considerations for military aircraft engines in corrosive environments (a Navy perspective)
p 202 N95-19684
- Developing an emission factor for hazardous air pollutants for an F-16 using JP-8 fuel
[AD-A284802] p 216 N95-19685

AIRCRAFT EQUIPMENT

- Starter/generator testing
[BTN-95-EIX95072498877] p 210 A95-68393

AIRCRAFT GUIDANCE

- Research requirements for future visual guidance systems
[AD-A279188] p 191 N95-19810

AIRCRAFT HAZARDS

- Aircraft icing measurements in East Coast winter storms
[HTN-95-60505] p 214 A95-68756

AIRCRAFT HYDRAULIC SYSTEMS

- Hydraulic system diagnostic sensors
[BTN-95-EIX95031502752] p 209 A95-68259

AIRCRAFT ICING

- Prediction of ice accretion: Comparison between the 2D and 3D codes
[BTN-94-EIX94441385753] p 213 A95-68217
- Aircraft icing measurements in East Coast winter storms
[HTN-95-60505] p 214 A95-68756
- Conditions associated with large-drop regions
[HTN-95-10686] p 214 A95-68845

AIRCRAFT INDUSTRY

- Fatigue resistance of peened 7050-T7451 aluminum alloy: Repair and re-treatment of a component surface
[BTN-94-EIX94371347838] p 206 A95-69131
- Selecting and management of fire fighter aircraft
[BTN-95-EIX95062487538] p 193 A95-69246

AIRCRAFT LANDING

- High accuracy navigation and landing system using GPS/IMU system integration
[BTN-94-EIX94441386129] p 189 A95-68185
- On-the-fly carrier phase ambiguity resolution for precise aircraft landing
[BTN-95-EIX95112522535] p 190 A95-69328

AIRCRAFT MAINTENANCE

- Computerized maintenance aid
[BTN-95-EIX95031502749] p 217 A95-68256
- Maintenance requirements for a supersonic transport
[BTN-95-EIX95031502751] p 179 A95-68258
- Hydraulic system diagnostic sensors
[BTN-95-EIX95031502752] p 209 A95-68259
- Corrosion prevention and control
[BTN-95-EIX95031502753] p 188 A95-68260
- USAF aging aircraft program
[BTN-95-EIX95072498878] p 180 A95-68394
- Service life extensions for the C-141
[BTN-95-EIX95112530749] p 193 A95-69295

- Air pollution mitigation measures for airports and associated activity
[PB94-207610] p 216 N95-19582
- Erosion, Corrosion and Foreign Object Damage Effects in Gas Turbines
[AGARD-CP-558] p 197 N95-19653
- Out of area experiences with the RB199 in Toronto
p 198 N95-19654
- The operation of gas turbine engines in hot and sandy conditions: Royal Air Force experiences in the Gulf conflict
p 198 N95-19655
- Navy foreign object damage and its impact on future gas turbine engine low pressure compression systems
p 198 N95-19658
- Scandinavian Airlines Systems experience on erosion, corrosion and foreign object damage effects on gas turbines
p 198 N95-19659
- Special investigation report: Maintenance anomaly resulting in dragged engine during landing rollout. Northwest Airlines Flight 18, Boeing 747-251B, N637US, New Tokyo International Airport, Narita, Japan, 1 Mar. 1994
[PB94-917006] p 188 N95-19793
- AIRCRAFT MODELS**
Flight experience with lightweight, low-power miniaturized instrumentation systems
[BTN-95-EIX95062487522] p 180 A95-69230
- AIRCRAFT NOISE**
Noise and vibration control
[BTN-95-EIX95042477108] p 179 A95-68351
- AIRCRAFT RELIABILITY**
Reliability and maintainability
[BTN-95-EIX95042477109] p 179 A95-68350
- USAF aging aircraft program
[BTN-95-EIX95072498878] p 180 A95-68394
- Service life extensions for the C-141
[BTN-95-EIX95112530749] p 193 A95-69295
- AIRCRAFT SAFETY**
Modern transport engine experience with environmental ingestion effects
p 199 N95-19660
- Special investigation report: Maintenance anomaly resulting in dragged engine during landing rollout. Northwest Airlines Flight 18, Boeing 747-251B, N637US, New Tokyo International Airport, Narita, Japan, 1 Mar. 1994
[PB94-917006] p 188 N95-19793
- AIRCRAFT STABILITY**
Offset thrust axes and pitch stability
[BTN-95-EIX95062487553] p 203 A95-68367
- AIRCRAFT STRUCTURES**
Launcher wing-leading-edge design
[BTN-95-EIX95042477110] p 192 A95-68349
- Coupling equivalent plate and finite element formulations in multiple-method structural analyses
[BTN-95-EIX95062487548] p 192 A95-68362
- Influence of structural and aerodynamic modeling on flutter analysis
[BTN-95-EIX95062487550] p 203 A95-68364
- Continuous gust response and sensitivity derivatives using state-space models
[BTN-95-EIX95062487551] p 203 A95-68365
- Ply layout optimization and micromechanics tailoring of composite aircraft engine structures
[BTN-95-EIX95112524206] p 196 A95-69302
- Proceedings of the USAF Structural Integrity Program Conference
[AD-A285684] p 194 N95-19517
- AIRCRAFT WAKES**
Interference between tanker wing wake with roll-up and receiver aircraft
[BTN-95-EIX95062487552] p 185 A95-68366
- AIRFOIL FENCES**
Vortical flow structure near the F/A-18 LEX at high incidence
[BTN-95-EIX95062487555] p 186 A95-68369
- AIRFOIL PROFILES**
Protective coatings for compressor gas path components
p 201 N95-19675
- AIRFOILS**
Solution-adaptive structured-unstructured grid method for unsteady turbomachinery analysis. Part I: Methodology
[BTN-94-EIX94441380983] p 208 A95-67329
- Two-point transonic airfoil design using optimization for improved off-design performance
[BTN-95-EIX95062487542] p 192 A95-68356
- Aerodynamic effects of delta platform tip sails on wing performance
[BTN-95-EIX95062487544] p 185 A95-68358
- Analysis of an oscillating Joukowski airfoil with surface suction and moving vortices
[BTN-95-EIX95062487527] p 186 A95-69235
- Aerodynamic sensitivity coefficients using the three-dimensional full potential equation
[BTN-95-EIX95062487530] p 186 A95-69238
- Preliminary assessment of tunnel wall interference in the NDA cryogenic wind tunnel
[BTN-95-EIX95062487531] p 187 A95-69239
- AIRFRAME MATERIALS**
Environmental effects on composite airframes: A study conducted for the ARM UAV Program (Atmospheric Radiation Measurement Unmanned Aerospace Vehicle) [DE94-015351] p 206 N95-19579
- AIRFRAMES**
Maintenance requirements for a supersonic transport
[BTN-95-EIX95031502751] p 179 A95-68258
- Simplified analysis of general instability of stiffened shells with cutouts in pure bending
[BTN-95-EIX95042474418] p 209 A95-68282
- Proceedings of the USAF Structural Integrity Program Conference
[AD-A285684] p 194 N95-19517
- AIRLINE OPERATIONS**
Reliability and maintainability
[BTN-95-EIX95042477109] p 179 A95-68350
- Air pollution mitigation measures for airports and associated activity
[PB94-207610] p 216 N95-19582
- AIRPORTS**
Air pollution mitigation measures for airports and associated activity
[PB94-207610] p 216 N95-19582
- Research requirements for future visual guidance systems
[AD-A279188] p 191 N95-19810
- AIRSHIPS**
The scientific ballooning in Russia
p 191 A95-66302
- A program for scientific and applied investigations using aerostat complexes
p 182 A95-66304
- Airship applications of modern flight test techniques
[AD-A284253] p 194 N95-19731
- AIRSPEED**
Minimum sink-speed in power-off glide
[BTN-95-EIX95062487556] p 193 A95-68370
- ALGORITHMS**
Parallel implicit unstructured grid Euler solvers
[BTN-95-EIX95042474393] p 217 A95-68307
- Active control of wake/blade-row interaction noise
[BTN-95-EIX95042474389] p 196 A95-68311
- Integrated GPS/Glonass navigation: Algorithms and results
[BTN-95-EIX95112522531] p 190 A95-69332
- Application of three-dimensional hybrid structured/unstructured grids to land, sea and air vehicles
[ARA-MEMO-399] p 210 N95-19775
- Verification of the CFD simulation system SAUNA for complex aircraft configurations
[ARA-MEMO-401] p 211 N95-19776
- ALUMINIDES**
New Trends in coatings developments for turbine blades: Materials processing and repair
p 201 N95-19676
- ALUMINUM ALLOYS**
Fatigue resistance of peened 7050-T7451 aluminum alloy: Repair and re-treatment of a component surface
[BTN-94-EIX94371347838] p 206 A95-69131
- AMMONIUM SULFATES**
Gas turbine compressor corrosion and erosion in Western Europe
p 201 N95-19678
- AMPHIBIOUS AIRCRAFT**
Selecting and management of fire fighter aircraft
[BTN-95-EIX95062487538] p 193 A95-69246
- ANGLE OF ATTACK**
Vortex cutting by a blade. Part II: Computations of vortex response
[BTN-94-EIX94441386611] p 208 A95-67342
- Elliptic tip effects on the vortex wake of an axisymmetric body at incidence
[BTN-94-EIX94441386612] p 208 A95-67343
- Adaptive computations of flow around a delta wing with vortex breakdown
[BTN-94-EIX94441386631] p 184 A95-68180
- Approximate method for calculating heating rates on three-dimensional vehicles
[BTN-95-EIX95041503778] p 210 A95-69209
- State-space representation of aerodynamic characteristics of an aircraft at high angles of attack
[BTN-95-EIX95062487536] p 187 A95-69244
- F/A-18 inlet calculations at 60-deg angle of attack and 10-deg sideslip
[BTN-95-EIX95112524199] p 195 A95-69309
- Side forces at high angles of attack. Why, when, how?
[BTN-95-EIX95112523809] p 194 A95-69324
- Prediction of wind tunnel effects on the installed F/A-18A inlet flow field at high angles-of-attack
[NASA-CR-195429] p 197 N95-19651
- ANNULAR FLOW**
Design and operation of a supersonic annular flow facility
[BTN-94-EIX94441386624] p 183 A95-68173
- ANTARCTIC REGIONS**
Antarctic snow record of southern hemisphere lead pollution
[HTN-95-40359] p 212 A95-66869
- ANTENNA ARRAYS**
Joint stars phased array radar antenna
[BTN-95-EIX95042474626] p 209 A95-68280
- ANTENNA DESIGN**
Joint stars phased array radar antenna
[BTN-95-EIX95042474626] p 209 A95-68280
- Design considerations for an archimedean slot spiral antenna
p 211 N95-19798
- ANTENNA FEEDS**
Inband radar cross section of phased arrays with parallel feeds
[AD-A284249] p 210 N95-19730
- Design considerations for an archimedean slot spiral antenna
p 211 N95-19798
- APPLICATIONS PROGRAMS (COMPUTERS)**
Putting the ACSYNT on aircraft design
[BTN-95-EIX95072419881] p 180 A95-68398
- Two-variable method for blockage wall interference in a circular tunnel
[BTN-95-EIX95062487540] p 187 A95-69248
- APPROACH**
Simulation and flight test evaluation of head-up-display guidance for hamier approach transitions
[BTN-95-EIX95062487533] p 194 A95-69241
- APPROXIMATION**
Approximate method for calculating heating rates on three-dimensional vehicles
[BTN-95-EIX95041503778] p 210 A95-69209
- ARCTIC REGIONS**
Research aircraft observations of a polar low at the east Greenland ice edge
[HTN-95-A0175] p 215 A95-69766
- ARTIFICIAL INTELLIGENCE**
The use of genetic algorithms for flight test and evaluation of artificial intelligence and complex software systems
[AD-A284824] p 217 N95-19688
- ASYMMETRY**
Elliptic tip effects on the vortex wake of an axisymmetric body at incidence
[BTN-94-EIX94441386612] p 208 A95-67343
- Suppression of vortex asymmetry and side force on a circular cone
[BTN-95-EIX95042474413] p 209 A95-68287
- ATLANTIC OCEAN**
Aircraft icing measurements in East Coast winter storms
[HTN-95-60505] p 214 A95-68756
- Mesoscale structure of precipitation bands in a North Atlantic winter storm
[HTN-95-40659] p 215 A95-69803
- ATMOSPHERIC CHEMISTRY**
Three-dimensional model interpretation of NO(x) measurements from the lower stratosphere
[HTN-95-90534] p 213 A95-67806
- ATMOSPHERIC CIRCULATION**
Three-dimensional model interpretation of NO(x) measurements from the lower stratosphere
[HTN-95-90534] p 213 A95-67806
- ATMOSPHERIC COMPOSITION**
Antarctic snow record of southern hemisphere lead pollution
[HTN-95-40359] p 212 A95-66869
- Three-dimensional model interpretation of NO(x) measurements from the lower stratosphere
[HTN-95-90534] p 213 A95-67806
- ATMOSPHERIC CORRECTION**
Using IRI for the computation of ionospheric corrections for altimeter data analysis
p 212 A95-66949
- ATMOSPHERIC ENTRY**
Trajectory-based heating analysis for the European Space Agency/Rosetta Earth Return Vehicle
[BTN-95-EIX95041503787] p 205 A95-69218
- Powerful bolide explosion over North Italy
[HTN-95-80564] p 218 A95-69658
- ATMOSPHERIC MODELS**
Three-dimensional model interpretation of NO(x) measurements from the lower stratosphere
[HTN-95-90534] p 213 A95-67806
- Microwave and infrared simulations of an intense convective system and comparison with aircraft observations
[HTN-95-60511] p 214 A95-68762
- Forecasting for a large field program: STORM-FEST
[HTN-95-90694] p 215 A95-69721
- ATMOSPHERIC MOISTURE**
Observations of fluxes and inland breezes over a heterogeneous surface
[HTN-95-80258] p 212 A95-66315

ATMOSPHERIC RADIATION

Possible near-IR channels for remote sensing precipitable water vapor from geostationary satellite platforms

[HTN-95-70139] p 214 A95-69431

ATMOSPHERIC TURBULENCE

Brief history of gust models for aircraft design

[BTN-95-EIX95062487557] p 203 A95-68371

ATOMIC CLOCKS

Effect of broadcast and precise ephemerides on estimates of the frequency stability of GPS Navstar clocks

[BTN-95-EIX95112522530] p 190 A95-69333

AUTOGYROS

Wind tunnel tests of a 42 inch diameter self-starting autogyro rotor

[AD-A279922] p 188 N95-19863

AUTOMOBILES

Application of three-dimensional hybrid structured/unstructured grids to land, sea and air vehicles

[ARA-MEMO-399] p 210 N95-19775

AXIAL FLOW

Rotor whirl forces induced by the tip clearance effect in axial flow compressors

[BTN-94-EIX94351143331] p 207 A95-67304

Vortex cutting by a blade. Part II: Computations of vortex response

[BTN-94-EIX94441386611] p 208 A95-67342

AXISYMMETRIC BODIES

Elliptic tip effects on the vortex wake of an axisymmetric body at incidence

[BTN-94-EIX94441386612] p 208 A95-67343

Passive porosity with free and fixed separation on a tangent-ogive forebody

[BTN-95-EIX95062487554] p 185 A95-68368

Development of an efficient inverse method for supersonic and hypersonic body design

[BTN-95-EIX95041503784] p 180 A95-69215

Minimum-drag axisymmetric bodies in the supersonic/hypersonic flow regimes

[BTN-95-EIX95041503785] p 180 A95-69216

AXISYMMETRIC FLOW

Behavior of the Johnson-King turbulence model in axisymmetric supersonic flows

[BTN-94-EIX94441386606] p 183 A95-67337

B

BALANCING

Transport aircraft loading and balancing system: Using a CLIPS expert system for military aircraft load planning

p 217 N95-19751

BALLISTIC TRAJECTORIES

Trajectory-based heating analysis for the European Space Agency/Rosetta Earth Return Vehicle

[BTN-95-EIX95041503787] p 205 A95-69218

BALLOON FLIGHT

Balloon technology and observations; Symposium P3 of the COSPAR Plenary Meeting, 29th, Washington, DC, Aug. 28-Sept. 5, 1992

[HTN-95-70250] p 181 A95-66276

French contribution to new balloon designs and materials

p 181 A95-66277

Status of the NASA balloon program

p 181 A95-66296

Overview of the NASA balloon R&D program

p 181 A95-66297

Recent trends in balloon flights from TIFR's National Balloon Facility, Hyderabad

p 191 A95-66300

Balloon flights in France and in Europe

p 204 A95-66301

The scientific ballooning in Russia

p 191 A95-66302

The joint Russian-Brazil research on balloons

p 182 A95-66303

A program for scientific and applied investigations using aerostat complexes

p 182 A95-66304

Long duration balloons

p 191 A95-66305

BALLOON SOUNDING

Balloon technology and observations; Symposium P3 of the COSPAR Plenary Meeting, 29th, Washington, DC, Aug. 28-Sept. 5, 1992

[HTN-95-70250] p 181 A95-66276

Balloon flights in France and in Europe

p 204 A95-66301

BALLOON-BORNE INSTRUMENTS

The joint Russian-Brazil research on balloons

p 182 A95-66303

BALLOONS

French contribution to new balloon designs and materials

p 181 A95-66277

A comparative study of internally and externally capped balloons using small scale test balloons

p 181 A95-66285

Status of the NASA balloon program

p 181 A95-66296

Overview of the NASA balloon R&D program

p 181 A95-66297

BASE FLOW

Numerical computations of supersonic base flow with special emphasis on turbulence modeling

[BTN-94-EIX94441386632] p 179 A95-68181

BENDING

Vortex cutting by a blade. Part II: Computations of vortex response

[BTN-94-EIX94441386611] p 208 A95-67342

Simplified analysis of general instability of stiffened shells with cutouts in pure bending

[BTN-95-EIX95042474418] p 209 A95-68282

BIRD-AIRCRAFT COLLISIONS

Design of fan blades subjected to bird impact

p 200 N95-19669

BLADE TIPS

Performance deterioration of axial compressors due to blade defects

p 199 N95-19665

Erosion of T56 5th stage rotor blades due to bleed hole overtip flow

p 200 N95-19666

BLADE-VORTEX INTERACTION

Rotating Kirchhoff method for three-dimensional transonic blade-vortex interaction hover noise

[BTN-94-EIX94441386601] p 182 A95-67332

Active control of wake/blade-row interaction noise

[BTN-95-EIX95042474389] p 196 A95-68311

Recent studies of rotorcraft blade-vortex interaction noise

[BTN-95-EIX95062487521] p 218 A95-69229

BLEEDING

On supersonic-inlet boundary-layer bleed flow

[NASA-CR-195426] p 202 N95-19769

BLOWING

Application of circulation control to advanced subsonic transport aircraft. Part 1: Airfoil development

[BTN-95-EIX95062487545] p 185 A95-68359

Application of circulation control to advanced subsonic transport aircraft. Part 2: Transport application

[BTN-95-EIX95062487546] p 185 A95-68360

BLUNT BODIES

Approximate method for calculating heating rates on three-dimensional vehicles

[BTN-95-EIX95041503778] p 210 A95-69209

Aerodynamically blunt and sharp bodies

[BTN-95-EIX95041503781] p 205 A95-69212

BODIES OF REVOLUTION

Two-variable method for blockage wall interference in a circular tunnel

[BTN-95-EIX95062487540] p 187 A95-69248

BODY-WING CONFIGURATIONS

The aerodynamic design of an integrated wing lower surface and pylons for reduced drag

[ARA-MEMO-406] p 194 N95-19789

BOEING 747 AIRCRAFT

Special investigation report: Maintenance anomaly resulting in dragged engine during landing rollout.

Northwest Airlines Flight 18, Boeing 747-251B, N637US, New Tokyo International Airport, Narita, Japan, 1 Mar. 1994

[PB94-917006] p 188 N95-19793

BOLIDES

Powerful bolide explosion over North Italy

[HTN-95-80564] p 218 A95-69658

BOUNDARIES

Aeroelastic stability of hingeless rotor blade in hover using large deflection theory

[BTN-94-EIX94441386616] p 183 A95-67347

BOUNDARY CONDITIONS

Kinetic theory in aerothermodynamics

[HTN-95-A0002] p 183 A95-67829

Shock layers and boundary layers in hypersonic flows

[HTN-95-A0003] p 183 A95-67830

On supersonic-inlet boundary-layer bleed flow

[NASA-CR-195426] p 202 N95-19769

BOUNDARY LAYER CONTROL

Lag model for turbulent boundary layers over rough bleed surfaces

[BTN-94-EIX94441380981] p 208 A95-68165

On supersonic-inlet boundary-layer bleed flow

[NASA-CR-195426] p 202 N95-19769

BOUNDARY LAYER FLOW

Supersonic and hypersonic shock/boundary-layer interaction database

[BTN-94-EIX94441386604] p 182 A95-67335

Design and operation of a supersonic annular flow facility

[BTN-94-EIX94441386624] p 183 A95-68173

On supersonic-inlet boundary-layer bleed flow

[NASA-CR-195426] p 202 N95-19769

BOUNDARY LAYER SEPARATION

Elliptic tip effects on the vortex wake of an axisymmetric body at incidence

[BTN-94-EIX94441386612] p 208 A95-67343

Experimental study of three-dimensional separation

[BTN-94-EIX94441385752] p 179 A95-68216

BOUNDARY LAYER TRANSITION

Shock layers and boundary layers in hypersonic flows

[HTN-95-A0003] p 183 A95-67830

Flight experience with lightweight, low-power miniaturized instrumentation systems

[BTN-95-EIX95062487522] p 180 A95-69230

BOUNDARY LAYERS

Observations of fluxes and inland breezes over a heterogeneous surface

[HTN-95-80258] p 212 A95-66315

Supersonic and hypersonic shock/boundary-layer interaction database

[BTN-94-EIX94441386604] p 182 A95-67335

BOW WAVES

Measurement by coherent anti-Stokes Raman scattering in the R5Ch hypersonic wind tunnel

[BTN-95-EIX95112523811] p 188 A95-69322

BOX BEAMS

Twisting smartly in the wind

[BTN-95-EIX95041503093] p 184 A95-68353

BRAZING

Braze repair possibilities for hot section gas turbine parts

p 201 N95-19677

BRISTOL-SIDDELEY BS 53 ENGINE

An analysis of the costs and benefits in improving F402-RR-406A High Pressure Turbine, second stage blades under the aircraft engine Component Improvement Program (CIP)

[AD-A285127] p 197 N95-19595

BROADCASTING

Effect of broadcast and precise ephemerides on estimates of the frequency stability of GPS Navstar clocks

[BTN-95-EIX95112522530] p 190 A95-69333

BUFFETING

Interaction of a streamwise vortex with a thin plate: A source of turbulent buffeting

[BTN-95-EIX95042474397] p 209 A95-68302

C

C-141 AIRCRAFT

Service life extensions for the C-141

[BTN-95-EIX95112530749] p 193 A95-69295

CALIBRATING

Aircraft electric field measurements: Calibration and ambient field retrieval

[HTN-95-90508] p 213 A95-67780

CAMBERED WINGS

Lift analysis of a variable camber foil using the discrete vortex-blot method

[BTN-94-EIX94441386623] p 179 A95-68172

CANADIAN AIRCRAFT

Selecting and management of fire fighter aircraft

[BTN-95-EIX95062487538] p 193 A95-69246

CANAD CONFIGURATIONS

Numerical simulation of steady and unsteady, vorticity-dominated aerodynamic interference

[BTN-95-EIX95062487524] p 186 A95-69232

CANOPIES

Radial reefing method for accelerated and controlled parachute opening

[BTN-95-EIX95062487539] p 187 A95-69247

CARBON ISOTOPES

An air-driven pressure booster pump for aircraft-based air sampling

[HTN-95-40689] p 216 A95-69833

CARBON MONOXIDE

An air-driven pressure booster pump for aircraft-based air sampling

[HTN-95-40689] p 216 A95-69833

CARBON-CARBON COMPOSITES

Surface morphology and structure of carbon-carbon composites in high-energy sliding contact

[BTN-94-EIX94371347996] p 206 A95-69164

CARBON-PHENOLIC COMPOSITES

Trajectory-based heating analysis for the European Space Agency/Rosetta Earth Return Vehicle

[BTN-95-EIX95041503787] p 205 A95-69218

CERAMIC COATINGS

Protective coatings for compressor gas path components

p 201 N95-19675

Thermal testing of high performance thermal barrier coatings for turbine blades

p 202 N95-19681

CERAMIC FIBERS

Development of hypersonic engine seals: Flow effects of preload and engine pressures

[BTN-95-EIX95112524204] p 196 A95-69304

CERAMIC MATRIX COMPOSITES

Launcher wing-leading-edge design

[BTN-95-EIX95042477110] p 192 A95-68349

SUBJECT INDEX

CERAMICS

- Resistance of silicon nitride turbine components to erosion and hot corrosion/oxidation attack
[AD-A284802] p 202 N95-19683

CERMETS

- High velocity oxygen fuel spraying of erosion and wear resistant coatings on jet engine parts
[HTN-95-A0002] p 202 N95-19680

CHANNEL FLOW

- Kinetic theory in aerothermodynamics
[HTN-95-A0002] p 183 A95-67829

CHEMICAL EQUILIBRIUM

- Linear disturbances in hypersonic, chemically reacting shock layers
[BTN-94-EIX94441386605] p 182 A95-67336

CHEMICAL REACTIONS

- Linear disturbances in hypersonic, chemically reacting shock layers
[BTN-94-EIX94441386605] p 182 A95-67336

CIRCULAR CONES

- Elliptic tip effects on the vortex wake of an axisymmetric body at incidence
[BTN-94-EIX94441386612] p 208 A95-67343

- Suppression of vortex asymmetry and side force on a circular cone
[BTN-95-EIX95042474413] p 209 A95-68287

CIRCULAR CYLINDERS

- Vortex cutting by a blade. Part II: Computations of vortex response
[BTN-94-EIX94441386611] p 208 A95-67342

CIRCULATION CONTROL AIRFOILS

- Application of circulation control to advanced subsonic transport aircraft. Part 1: Airfoil development
[BTN-95-EIX95062487545] p 185 A95-68359

- Application of circulation control to advanced subsonic transport aircraft. Part 2: Transport application
[BTN-95-EIX95062487546] p 185 A95-68360

CIVIL AVIATION

- Federal aviation regulations, part 91. General operating and flight rules. Change 8
[PB94-217445] p 188 N95-19720

- Application of three-dimensional hybrid structured/unstructured grids to land, sea and air vehicles
[ARA-MEMO-399] p 210 N95-19775

CLEARANCES

- Dynamic behavior of valves with pneumatic chamber for reciprocating compressors
[BTN-94-EIX94351143311] p 207 A95-65845

CLOSURES

- New end tube closure system for the ram accelerator
[BTN-94-EIX94441380974] p 195 A95-68158

CLOUD PHYSICS

- Aircraft icing measurements in East Coast winter storms
[HTN-95-60505] p 214 A95-68756

- Microwave and infrared simulations of an intense convective system and comparison with aircraft observations
[HTN-95-60511] p 214 A95-68762

- Conditions associated with large-drop regions
[HTN-95-10686] p 214 A95-68845

CLOUDS (METEOROLOGY)

- Microwave and infrared simulations of an intense convective system and comparison with aircraft observations
[HTN-95-60511] p 214 A95-68762

COASTS

- Aircraft icing measurements in East Coast winter storms
[HTN-95-60505] p 214 A95-68756

COATING

- High velocity oxygen fuel spraying of erosion and wear resistant coatings on jet engine parts
[AD-A279219] p 204 N95-19848

COCKPIT SIMULATORS

- Programmable cockpit research simulator
[AD-A279219] p 204 N95-19848

COCKPITS

- Programmable cockpit research simulator
[AD-A279219] p 204 N95-19848

COLD FRONTS

- Nonhydrostatic simulation of frontogenesis in a moist atmosphere. Part 3: Thermal wind imbalance and rainbands
[HTN-95-90356] p 212 A95-66429

- Mesoscale structure of precipitation bands in a North Atlantic winter storm
[HTN-95-40659] p 215 A95-69803

COMBUSTION CHAMBERS

- Aircraft engine emission reduction
[BTN-95-EIX95031502750] p 196 A95-68257

COMBUSTION PRODUCTS

- Aircraft engine emission reduction
[BTN-95-EIX95031502750] p 196 A95-68257

- Developing an emission factor for hazardous air pollutants for an F-16 using JP-8 fuel
[AD-A284802] p 216 N95-19685

COMMUNICATION NETWORKS

- Use of MOBITEK wireless wide area networks as a solution to land-based positioning and navigation
[BTN-94-EIX94441386132] p 189 A95-68188

COMPLEX VARIABLES

- Unbalance response of a dual rotor system: Theory and experiment
[BTN-94-EIX94351143320] p 195 A95-65854

COMPOSITE MATERIALS

- Environmental effects on composite airframes: A study conducted for the ARM UAV Program (Atmospheric Radiation Measurement Unmanned Aerospace Vehicle)
[DE94-015351] p 206 N95-19579

COMPOSITE STRUCTURES

- Finite element time domain - modal formulation for nonlinear flutter of composite panels
[BTN-95-EIX95042474401] p 203 A95-68299

- Twisting smartly in the wind
[BTN-95-EIX95041503093] p 184 A95-68353

COMPRESSIBLE FLOW

- Construction of nearly orthogonal multiblock grids for compressible flow simulation
[BTN-94-EIX94361133526] p 207 A95-65981

- Aspects of vortex breakdown
[HTN-95-A0001] p 183 A95-67828

- Model for compressible turbulence in hypersonic wall boundary and high-speed mixing layers
[BTN-94-EIX94441386625] p 184 A95-68174

- On supersonic-inlet boundary-layer bleed flow
[NASA-CR-195426] p 202 N95-19769

- Validation and evaluation of the advanced aeronautical CFD system SAUNA: A method developer's view
[ARA-MEMO-390] p 210 N95-19774

COMPRESSOR BLADES

- Performance deterioration of axial compressors due to blade defects
[HTN-95-A0001] p 199 N95-19665

- Erosion of T56 5th stage rotor blades due to bleed hole overtip flow
[HTN-95-A0001] p 200 N95-19666

- High velocity oxygen fuel spraying of erosion and wear resistant coatings on jet engine parts
[AD-A279219] p 202 N95-19680

COMPRESSOR EFFICIENCY

- Performance deterioration of axial compressors due to blade defects
[HTN-95-A0001] p 199 N95-19665

COMPRESSOR ROTORS

- Rotor whirl forces induced by the tip clearance effect in axial flow compressors
[BTN-94-EIX94351143331] p 207 A95-67304

- The calculation of erosion in a gas turbine compressor rotor
[HTN-95-A0001] p 199 N95-19664

COMPRESSORS

- Dynamic behavior of valves with pneumatic chamber for reciprocating compressors
[BTN-94-EIX94351143311] p 207 A95-65845

- Rotor whirl forces induced by the tip clearance effect in axial flow compressors
[BTN-94-EIX94351143331] p 207 A95-67304

- Damage of high temperature components by dust-laden air
[HTN-95-10686] p 201 N95-19673

- Protective coatings for compressor gas path components
[HTN-95-10686] p 201 N95-19675

- Gas turbine compressor corrosion and erosion in Western Europe
[HTN-95-10686] p 201 N95-19678

- Multilayer anti-erosion coatings
[HTN-95-10686] p 201 N95-19679

COMPUTATIONAL FLUID DYNAMICS

- Rotating Kirchhoff method for three-dimensional transonic blade-vortex interaction hover noise
[BTN-94-EIX94441386601] p 182 A95-67332

- Three-dimensional analysis of scramjet nozzle flows
[BTN-94-EIX94441380978] p 196 A95-68162

- Lag model for turbulent boundary layers over rough bleed surfaces
[BTN-94-EIX94441380981] p 208 A95-68165

- Lift analysis of a variable camber foil using the discrete vortex-blob method
[BTN-94-EIX94441386623] p 179 A95-68172

- Model for compressible turbulence in hypersonic wall boundary and high-speed mixing layers
[BTN-94-EIX94441386625] p 184 A95-68174

- Adaptive computations of flow around a delta wing with vortex breakdown
[BTN-94-EIX94441386631] p 184 A95-68180

- Numerical computations of supersonic base flow with special emphasis on turbulence modeling
[BTN-94-EIX94441386632] p 179 A95-68181

- Review of numerical procedures for computational surface thermochemistry
[BTN-94-EIX94441386682] p 205 A95-68191

- Prediction of ice accretion: Comparison between the 2D and 3D codes
[BTN-94-EIX94441385753] p 213 A95-68217

- Parallel implicit unstructured grid Euler solvers
[BTN-95-EIX95042474393] p 217 A95-68307

COMPUTERIZED SIMULATION

- Navier-Stokes simulations of Orbiter aerodynamic characteristics including pitch trim and bodyflap
[BTN-95-EIX95041503779] p 204 A95-69210

- Interpretation of waverider performance data using computational fluid dynamics
[BTN-95-EIX95062487534] p 193 A95-69242

- Two-variable method for blockage wall interference in a circular tunnel
[BTN-95-EIX95062487540] p 187 A95-69248

- On supersonic-inlet boundary-layer bleed flow
[NASA-CR-195426] p 202 N95-19769

- Validation and evaluation of the advanced aeronautical CFD system SAUNA: A method developer's view
[ARA-MEMO-390] p 210 N95-19774

- Application of three-dimensional hybrid structured/unstructured grids to land, sea and air vehicles
[ARA-MEMO-399] p 210 N95-19775

- Verification of the CFD simulation system SAUNA for complex aircraft configurations
[ARA-MEMO-401] p 211 N95-19776

- Inviscid and viscous flow modelling of complex aircraft configurations using the CFD simulation system sauna
[ARA-MEMO-403] p 211 N95-19777

COMPUTATIONAL GRIDS

- Solution-adaptive structured-unstructured grid method for unsteady turbomachinery analysis. Part I: Methodology
[BTN-94-EIX94441380983] p 208 A95-67329

- Parallel implicit unstructured grid Euler solvers
[BTN-95-EIX95042474393] p 217 A95-68307

- Multiblock analysis for Shuttle Orbiter reentry heating from Mach 24 to Mach 12
[BTN-95-EIX95041503780] p 205 A95-69211

- Design of fan blades subjected to bird impact
[HTN-95-60545] p 200 N95-19669

- Ice-impact analysis of blades
[HTN-95-60545] p 200 N95-19672

- Validation and evaluation of the advanced aeronautical CFD system SAUNA: A method developer's view
[ARA-MEMO-390] p 210 N95-19774

- Application of three-dimensional hybrid structured/unstructured grids to land, sea and air vehicles
[ARA-MEMO-399] p 210 N95-19775

- Verification of the CFD simulation system SAUNA for complex aircraft configurations
[ARA-MEMO-401] p 211 N95-19776

COMPUTER AIDED DESIGN

- Computerized maintenance aid
[BTN-95-EIX95031502749] p 217 A95-68256

- Two-point transonic airfoil design using optimization for improved off-design performance
[BTN-95-EIX95062487542] p 192 A95-68356

- Putting the ACSYNT on aircraft design
[BTN-95-EIX95072419881] p 180 A95-68398

- Development of an efficient inverse method for supersonic and hypersonic body design
[BTN-95-EIX95041503784] p 180 A95-69215

- Design decisions from the history of the EUVE science payload
[HTN-95-60545] p 205 A95-69854

- Design of fan blades subjected to bird impact
[HTN-95-60545] p 200 N95-19669

- Ice-impact analysis of blades
[HTN-95-60545] p 200 N95-19672

- The Computer Aided Aircraft-design Package (CAAP)
[HTN-95-60545] p 217 N95-19759

- PalymSys (TM): An extended version of CLIPS for construction and reasoning using blackboards
[HTN-95-60545] p 217 N95-19767

COMPUTER PROGRAMS

- Computerized maintenance aid
[BTN-95-EIX95031502749] p 217 A95-68256

- Flight experience with lightweight, low-power miniaturized instrumentation systems
[BTN-95-EIX95062487522] p 180 A95-69230

- Design of fan blades subjected to bird impact
[HTN-95-60545] p 200 N95-19669

COMPUTER SYSTEMS DESIGN

- Design decisions from the history of the EUVE science payload
[HTN-95-60545] p 205 A95-69854

COMPUTER TECHNIQUES

- Transport aircraft loading and balancing system: Using a CLIPS expert system for military aircraft load planning
[HTN-95-90356] p 217 N95-19751

- The Computer Aided Aircraft-design Package (CAAP)
[HTN-95-90356] p 217 N95-19759

- PalymSys (TM): An extended version of CLIPS for construction and reasoning using blackboards
[HTN-95-90356] p 217 N95-19767

COMPUTERIZED SIMULATION

- Nonhydrostatic simulation of frontogenesis in a moist atmosphere. Part 3: Thermal wind imbalance and rainbands
[HTN-95-90356] p 212 A95-66429

CONCENTRATION (COMPOSITION)

- Aircraft electric field measurements: Calibration and ambient field retrieval
[HTN-95-90508] p 213 A95-67780
- Nonlinear dynamic simulation of single- and multispool core engines, part 1: Computational method
[BTN-95-EIX95112524200] p 210 A95-69308
- Design of fan blades subjected to bird impact
p 200 N95-19669
- Ice-impact analysis of blades
p 200 N95-19672

CONCENTRATION (COMPOSITION)

- Antarctic snow record of southern hemisphere lead pollution
[HTN-95-40359] p 212 A95-66869

CONCORDE AIRCRAFT

- Maintenance requirements for a supersonic transport
[BTN-95-EIX95031502751] p 179 A95-68258

CONFERENCES

- Balloon technology and observations; Symposium P3 of the COSPAR Plenary Meeting, 29th, Washington, DC, Aug. 28-Sept. 5, 1992
[HTN-95-70250] p 181 A95-66276

- Proceedings of the USAF Structural Integrity Program Conference
[AD-A285684] p 194 N95-19517

- Erosion, Corrosion and Foreign Object Damage Effects in Gas Turbines
[AGARD-CP-558] p 197 N95-19653

CONICAL FLOW

- Interpretation of waverider performance data using computational fluid dynamics
[BTN-95-EIX95062487534] p 193 A95-69242

CONJUGATE GRADIENT METHOD

- Aerodynamic sensitivity coefficients using the three-dimensional full potential equation
[BTN-95-EIX95062487530] p 186 A95-69238

CONTAMINANTS

- Future directions in helicopter protection system configuration
p 198 N95-19657

CONTAMINATION

- Out of area experiences with the RB199 in Toronto
p 198 N95-19654

CONTROL EQUIPMENT

- Aerodynamic characteristics of strake vortex flaps on a strake-wing configuration
[BTN-95-EIX95062487537] p 187 A95-69245

CONTROL SIMULATION

- Automation of hardware-in-the-loop testing of control systems for unmanned air vehicles
[AD-A284833] p 194 N95-19693

CONTROL SYSTEMS DESIGN

- Automation of hardware-in-the-loop testing of control systems for unmanned air vehicles
[AD-A284833] p 194 N95-19693

- Improved speed control system for the 87,000 HP wind tunnel drive
[NASA-TM-106840] p 211 N95-19794

CONTROL VALVES

- Dynamic behavior of valves with pneumatic chamber for reciprocating compressors
[BTN-94-EIX94351143311] p 207 A95-65845

CONTROLLABILITY

- Side forces at high angles of attack. Why, when, how?
[BTN-95-EIX95112523809] p 194 A95-69324

CONVECTION CLOUDS

- Microwave and infrared simulations of an intense convective system and comparison with aircraft observations
[HTN-95-60511] p 214 A95-68762

CONVERGENCE

- Observations of fluxes and inland breezes over a heterogeneous surface
[HTN-95-80258] p 212 A95-66315

COORDINATES

- On wave-front curvature in linear stability theory
[BTN-94-EIX94441385756] p 184 A95-68220

CORES

- Vortex cutting by a blade. Part II: Computations of vortex response
[BTN-94-EIX94441386611] p 208 A95-67342

CORROSION

- Erosion, Corrosion and Foreign Object Damage Effects in Gas Turbines
[AGARD-CP-558] p 197 N95-19653

- Out of area experiences with the RB199 in Toronto
p 198 N95-19654

- Gas turbine compressor corrosion and erosion in Western Europe
p 201 N95-19678

- Testing considerations for military aircraft engines in corrosive environments (a Navy perspective)
p 202 N95-19684

CORROSION PREVENTION

- Corrosion prevention and control
[BTN-95-EIX95031502753] p 188 A95-68260

- Future directions in helicopter protection system configuration
p 198 N95-19657

CORROSION RESISTANCE

- Resistance of silicon nitride turbine components to erosion and hot corrosion/oxidation attack
p 202 N95-19683

CORROSION TESTS

- Testing considerations for military aircraft engines in corrosive environments (a Navy perspective)
p 202 N95-19684

COST ANALYSIS

- An analysis of the costs and benefits in improving F402-RR-406A High Pressure Turbine, second stage blades under the aircraft engine Component Improvement Program (CIP)
[AD-A285127] p 197 N95-19595

CRACK PROPAGATION

- Fatigue crack growth in nickel-based superalloys at 500-700 C. 1: Waspaloy
[BTN-94-EIX94371347843] p 206 A95-69136

- Impact loading of compressor stator vanes by hailstone ingestion
p 200 N95-19670

CRITICAL FLOW

- Hydraulic system diagnostic sensors
[BTN-95-EIX95031502752] p 209 A95-68259

CRITICAL VELOCITY

- Unbalance response of a dual rotor system: Theory and experiment
[BTN-94-EIX94351143320] p 195 A95-65854

CROSS FLOW

- Phenomenological description and simplified modelling of the vortex wake issuing from a jet in a crossflow
[BTN-94-EIX94441385754] p 184 A95-68218

CRYOGENIC WIND TUNNELS

- Preliminary assessment of tunnel wall interference in the NDA cryogenic wind tunnel
[BTN-95-EIX95062487531] p 187 A95-69239

CUMULATIVE DAMAGE

- Computerized maintenance aid
[BTN-95-EIX95031502749] p 217 A95-68256

CURVATURE

- Elliptic tip effects on the vortex wake of an axisymmetric body at incidence
[BTN-94-EIX94441386612] p 208 A95-67343

- On wave-front curvature in linear stability theory
[BTN-94-EIX94441385756] p 184 A95-68220

CUTTING

- Vortex cutting by a blade. Part II: Computations of vortex response
[BTN-94-EIX94441386611] p 208 A95-67342

CYCLIC LOADS

- Damage of high temperature components by dust-laden air
p 201 N95-19673

CYCLOGENESIS

- Research aircraft observations of a polar low at the east Greenland ice edge
[HTN-95-A0175] p 215 A95-69766

- Mesoscale structure of precipitation bands in a North Atlantic winter storm
[HTN-95-40659] p 215 A95-69803

CYCLONES

- Research aircraft observations of a polar low at the east Greenland ice edge
[HTN-95-A0175] p 215 A95-69766

- Mesoscale structure of precipitation bands in a North Atlantic winter storm
[HTN-95-40659] p 215 A95-69803

CYLINDRICAL BODIES

- Numerical computations of supersonic base flow with special emphasis on turbulence modeling
[BTN-94-EIX94441386632] p 179 A95-68181

CYLINDRICAL SHELLS

- Simplified analysis of general instability of stiffened shells with cutouts in pure bending
[BTN-95-EIX95042474418] p 209 A95-68282

D

DAMAGE

- Navy foreign object damage and its impact on future gas turbine engine low pressure compression systems
p 198 N95-19658

- Scandinavian Airlines Systems experience on erosion, corrosion and foreign object damage effects on gas turbines
p 198 N95-19659

- Experimental and numerical simulations of the effects of ingested particles in gas turbine engines
p 199 N95-19662

- Damage of high temperature components by dust-laden air
p 201 N95-19673

DAMAGE ASSESSMENT

- Computerized maintenance aid
[BTN-95-EIX95031502749] p 217 A95-68256

- Corrosion prevention and control
[BTN-95-EIX95031502753] p 188 A95-68260

DAMPING

- Lyapunov exponents and stochastic stability of two-dimensional parametrically excited random systems
[BTN-94-EIX94361122401] p 207 A95-65897

- Stability of magnetic bearing-rotor systems and the effects of gravity and damping
[BTN-94-EIX94441386619] p 208 A95-68168

DATA ACQUISITION

- Forecasting for a large field program: STORM-FEST
[HTN-95-90694] p 215 A95-69721

- Multipoint pressure measurements on continuously moving wind tunnel models
[ARA-MEMO-391] p 188 N95-19772

DATA BASE MANAGEMENT SYSTEMS

- Supersonic and hypersonic shock/boundary-layer interaction database
[BTN-94-EIX94441386604] p 182 A95-67335

DATA BASES

- Supersonic and hypersonic shock/boundary-layer interaction database
[BTN-94-EIX94441386604] p 182 A95-67335

- Computerized maintenance aid
[BTN-95-EIX95031502749] p 217 A95-68256

- Documentation and archiving of the Space Shuttle wind tunnel test data base. Volume 2: User's Guide to the Archived Data Base
[NASA-TM-104806-VOL-2] p 205 N95-19624

DEBRIS

- Scandinavian Airlines Systems experience on erosion, corrosion and foreign object damage effects on gas turbines
p 198 N95-19659

DEFECTS

- Performance deterioration of axial compressors due to blade defects
p 199 N95-19665

DEFLECTION

- Aeroelastic stability of hingeless rotor blade in hover using large deflection theory
[BTN-94-EIX94441386616] p 183 A95-67347

DEGRADATION

- Environmental effects on composite airframes: A study conducted for the ARM UAV Program (Atmospheric Radiation Measurement Unmanned Aerospace Vehicle)
[DE94-015351] p 206 N95-19579

- Protective coatings for compressor gas path components
p 201 N95-19675

- Multilayer anti-erosion coatings
p 201 N95-19679

DELTA WINGS

- Aspects of vortex breakdown
[HTN-95-A0001] p 183 A95-67828

- Adaptive computations of flow around a delta wing with vortex breakdown
[BTN-94-EIX94441386631] p 184 A95-68180

- Experimental investigations on limit cycle wing rock of slender wings
[BTN-95-EIX95062487543] p 185 A95-68357

- Numerical simulation of incidence and sweep effects on delta wing vortex breakdown
[BTN-95-EIX95062487526] p 186 A95-69234

DENSITY MEASUREMENT

- Planar air density measurements near model surfaces by ultraviolet Rayleigh/Raman scattering
[BTN-94-EIX94441386614] p 213 A95-67345

- Measurement by coherent anti-Stokes Raman scattering in the RSCh hypersonic wind tunnel
[BTN-95-EIX95112523811] p 188 A95-69322

DEPOSITION

- Erosion, Corrosion and Foreign Object Damage Effects in Gas Turbines
[AGARD-CP-558] p 197 N95-19653

- Particle deposition in gas turbine blade film cooling holes
p 199 N95-19661

DEPOSITS

- Gas turbine compressor corrosion and erosion in Western Europe
p 201 N95-19678

DESCENT

- Wind tunnel tests of a 42 inch diameter self-starting autogyro rotor
[AD-A279922] p 188 N95-19863

DESIGN ANALYSIS

- Proceedings of the USAF Structural Integrity Program Conference
[AD-A285684] p 194 N95-19517

DIAMETERS

- Vortex cutting by a blade. Part II: Computations of vortex response
[BTN-94-EIX94441386611] p 208 A95-67342

DIESEL FUELS

- Advanced diesel electronic fuel injection and turbocharging
[AD-A279176] p 211 N95-19809

DIFFERENTIAL EQUATIONS

- Solution-adaptive structured-unstructured grid method for unsteady turbomachinery analysis. Part I: Methodology
[BTN-94-EIX94441380983] p 208 A95-67329

DIFFERENTIAL PRESSURE

Hydraulic system diagnostic sensors
[BTN-95-EIX95031502752] p 209 A95-68259

DIGITAL SYSTEMS

Flight control system mode transitions influence on handling qualities and task performance
[BTN-95-EIX95062487525] p 203 A95-69233

DISPLACEMENT

Aeroelastic stability of hingeless rotor blade in hover using large deflection theory
[BTN-94-EIX94441386616] p 183 A95-67347

DISPLAY DEVICES

Simulation and flight test evaluation of head-up-display guidance for hamier approach transitions
[BTN-95-EIX95062487533] p 194 A95-69241

DISTORTION

Aero-thermodynamic distortion induced structured dynamic response
[AD-A279931] p 203 N95-19864

DOPPLER RADAR

A technique for detecting a tropical cyclone center using a Doppler radar
[HTN-95-20631] p 215 A95-69574

DOWNTIME

Navy foreign object damage and its impact on future gas turbine engine low pressure compression systems
p 198 N95-19658

DRAG

Repeatability of ice shapes in the NASA Lewis icing research tunnel
[BTN-95-EIX95062487528] p 204 A95-69236

DRAG MEASUREMENT

Repeatability of ice shapes in the NASA Lewis icing research tunnel
[BTN-95-EIX95062487528] p 204 A95-69236
An investigation of drag repeatability in half model testing in the ARA Transonic Wind Tunnel
[ARA-MEMO-392] p 188 N95-19546

DRAG REDUCTION

The aerodynamic design of an integrated wing lower surface and pylons for reduced drag
[ARA-MEMO-406] p 194 N95-19789

DROP SIZE

Conditions associated with large-drop regions
[HTN-95-10686] p 214 A95-68845

DUCTED FLOW

Design and operation of a supersonic annular flow facility
[BTN-94-EIX94441386624] p 183 A95-68173

DUCTILITY

Multilayer anti-erosion coatings p 201 N95-19679

DURABILITY

Proceedings of the USAF Structural Integrity Program Conference
[AD-A258684] p 194 N95-19517

DUST

Out of area experiences with the RB199 in Toronto
p 198 N95-19654
The operation of gas turbine engines in hot and sandy conditions: Royal Air Force experiences in the Gulf conflict
p 198 N95-19655
US Army rotorcraft turboshaft engines sand and dust erosion considerations
p 198 N95-19656
Future directions in helicopter protection system configuration
p 198 N95-19657
Damage of high temperature components by dust-laden air
p 201 N95-19673

DUST COLLECTORS

Particle trajectories in gas turbine engines
p 199 N95-19663

DYNAMIC CHARACTERISTICS

Dynamic behavior of valves with pneumatic chamber for reciprocating compressors
[BTN-94-EIX94351143311] p 207 A95-65845

DYNAMIC CONTROL

Demonstration of an elastically coupled twist control concept for tilt rotor blade application
[BTN-94-EIX94441386633] p 196 A95-68182
Using adaptive structures to attenuate rotary wing aeroelastic response
[BTN-95-EIX95062487547] p 192 A95-68361

DYNAMIC LOADS

Evidence that aerodynamic effects, including dynamic stall, dictate HAWT structural loads and power generation in highly transient time frames
[DE94-011865] p 216 N95-19855

DYNAMIC RESPONSE

Unbalance response of a dual rotor system: Theory and experiment
[BTN-94-EIX94351143320] p 195 A95-65854
Using adaptive structures to attenuate rotary wing aeroelastic response
[BTN-95-EIX95062487547] p 192 A95-68361
Continuous gust response and sensitivity derivatives using state-space models
[BTN-95-EIX95062487551] p 203 A95-68365

Nonlinear dynamic simulation of single- and multispool core engines, part 1: Computational method
[BTN-95-EIX95112524200] p 210 A95-69308
Documentation and archiving of the Space Shuttle wind tunnel test data base. Volume 2: User's Guide to the Archived Data Base
[NASA-TM-104806-VOL-2] p 205 N95-19624
Aero-thermodynamic distortion induced structured dynamic response
[AD-A279931] p 203 N95-19864

DYNAMIC STRUCTURAL ANALYSIS

Lyapunov exponents and stochastic stability of two-dimensional parametrically excited random systems
[BTN-94-EIX94361122401] p 207 A95-65897
Coupling equivalent plate and finite element formulations in multiple-method structural analyses
[BTN-95-EIX95062487548] p 192 A95-68362
Continuous gust response and sensitivity derivatives using state-space models
[BTN-95-EIX95062487551] p 203 A95-68365
Documentation and archiving of the Space Shuttle wind tunnel test data base. Volume 2: User's Guide to the Archived Data Base
[NASA-TM-104806-VOL-2] p 205 N95-19624

DYNAMICS

Modeling rotating shafts using axisymmetric solid finite elements with matrix reduction
[BTN-94-EIX94351143328] p 207 A95-67301

E

EARTH ATMOSPHERE

Powerful bolide explosion over North Italy
[HTN-95-80564] p 218 A95-69658

EARTH IONOSPHERE

Using IRI for the computation of ionospheric corrections for altimeter data analysis
p 212 A95-66949

EDDY VISCOSITY

Lag model for turbulent boundary layers over rough bleed surfaces
[BTN-94-EIX94441380981] p 208 A95-68165

ELASTIC DEFORMATION

Impact loading of compressor stator vanes by hailstone ingestion
p 200 N95-19670

ELASTIC PROPERTIES

Lyapunov exponents and stochastic stability of two-dimensional parametrically excited random systems
[BTN-94-EIX94361122401] p 207 A95-65897

ELECTRIC CORONA

Aircraft electric field measurements: Calibration and ambient field retrieval
[HTN-95-90508] p 213 A95-67780

ELECTRIC EQUIPMENT TESTS

Starter/generator testing
[BTN-95-EIX95072498877] p 210 A95-68393

ELECTRIC FIELDS

Aircraft electric field measurements: Calibration and ambient field retrieval
[HTN-95-90508] p 213 A95-67780

ELECTRIC GENERATORS

Starter/generator testing
[BTN-95-EIX95072498877] p 210 A95-68393

ELECTRIC WIRE

Computerized maintenance aid
[BTN-95-EIX95031502749] p 217 A95-68256

ELECTROMAGNETIC SCATTERING

Inband radar cross section of phased arrays with parallel feeds
[AD-A284249] p 210 N95-19730

ELECTRONIC CONTROL

Advanced diesel electronic fuel injection and turbocharging
[AD-A279176] p 211 N95-19809

ELECTRONIC WARFARE

Wind tunnel tests of a 42 inch diameter self-starting autogyro rotor
[AD-A279922] p 188 N95-19863

ELECTROSTATICS

Comparison of electrostatic and aerodynamic forces during parachute opening
[BTN-95-EIX95062487532] p 187 A95-69240

EMERGENCY LOCATOR TRANSMITTERS

Federal aviation regulations, part 91. General operating and flight rules. Change 8
[PB94-217445] p 188 N95-19720

ENERGY TRANSFER

Impact loading of compressor stator vanes by hailstone ingestion
p 200 N95-19670

ENGINE CONTROL

Advanced diesel electronic fuel injection and turbocharging
[AD-A279176] p 211 N95-19809

ENGINE DESIGN

Aircraft engine emission reduction
[BTN-95-EIX95031502750] p 196 A95-68257

Ply layout optimization and micromechanics tailoring of composite aircraft engine structures
[BTN-95-EIX95112524206] p 196 A95-69302
Future directions in helicopter protection system configuration
p 198 N95-19657
Navy foreign object damage and its impact on future gas turbine engine low pressure compression systems
p 198 N95-19658
Design of fan blades subjected to bird impact
p 200 N95-19669

ENGINE FAILURE

Modern transport engine experience with environmental ingestion effects
p 199 N95-19660

ENGINE INLETS

F/A-18 inlet calculations at 60-deg angle of attack and 10-deg sideslip
[BTN-95-EIX95112524199] p 195 A95-69309
Numerical study of the performance of swept, curved compression surface scramjet inlets
[BTN-95-EIX95112524198] p 197 A95-69310
Prediction of wind tunnel effects on the installed F/A-18A inlet flow field at high angles-of-attack
[NASA-CR-195429] p 197 N95-19651

ENGINE MONITORING INSTRUMENTS

An airborne monitoring system for FOD and erosion faults
p 200 N95-19668

ENGINE PARTS

Ply layout optimization and micromechanics tailoring of composite aircraft engine structures
[BTN-95-EIX95112524206] p 196 A95-69302
Development of hypersonic engine seals: Flow effects of preload and engine pressures
[BTN-95-EIX95112524204] p 196 A95-69304
Nonlinear dynamic simulation of single- and multispool core engines, part 1: Computational method
[BTN-95-EIX95112524200] p 210 A95-69308

ENGINE STARTERS

Starter/generator testing
[BTN-95-EIX95072498877] p 210 A95-68393

ENGINE TESTS

Damage of high temperature components by dust-laden air
p 201 N95-19673
Testing considerations for military aircraft engines in corrosive environments (a Navy perspective)
p 202 N95-19684

ENTHALPY

Shock layers and boundary layers in hypersonic flows
[HTN-95-A0003] p 183 A95-67830

ENTRAINMENT

Entrainment and acoustic variations in a round jet from introduced streamwise vorticity
[BTN-95-EIX95042474409] p 209 A95-68291

ENVIRONMENT EFFECTS

Ozone, skin cancer, and the SST
[BTN-95-EIX95041503011] p 213 A95-68314
Modern transport engine experience with environmental ingestion effects
p 199 N95-19660

EPHEMERIDES

Effect of broadcast and precise ephemerides on estimates of the frequency stability of GPS Navstar clocks
[BTN-95-EIX9511252530] p 190 A95-69333

EQUATIONS OF MOTION

Solution-adaptive structured-unstructured grid method for unsteady turbomachinery analysis. Part I: Methodology
[BTN-94-EIX94441380983] p 208 A95-67329
Aeroelastic stability of hingeless rotor blade in hover using large deflection theory
[BTN-94-EIX94441386616] p 183 A95-67347
Particle trajectories in gas turbine engines
p 199 N95-19663

EQUATIONS OF STATE

Shock layers and boundary layers in hypersonic flows
[HTN-95-A0003] p 183 A95-67830
Determination of stability and control derivatives from the NASA F/A-18 HARV from flight data using the maximum likelihood method
[NASA-CR-197320] p 204 N95-19576

EQUIPMENT SPECIFICATIONS

An air-driven pressure booster pump for aircraft-based air sampling
[HTN-95-40689] p 216 A95-69833

EROSION

Erosion, Corrosion and Foreign Object Damage Effects in Gas Turbines
[AGARD-CP-558] p 197 N95-19653
The operation of gas turbine engines in hot and sandy conditions: Royal Air Force experiences in the Gulf conflict
p 198 N95-19655
US Army rotorcraft turboshaft engines sand and dust erosion considerations
p 198 N95-19656
Experimental and numerical simulations of the effects of ingested particles in gas turbine engines
p 199 N95-19662

Particle trajectories in gas turbine engines p 199 N95-19663
The calculation of erosion in a gas turbine compressor rotor p 199 N95-19664
Erosion of T56 5th stage rotor blades due to bleed hole overlap flow p 200 N95-19666
An airborne monitoring system for FOD and erosion faults p 200 N95-19668
Gas turbine compressor corrosion and erosion in Western Europe p 201 N95-19678
High velocity oxygen fuel spraying of erosion and wear resistant coatings on jet engine parts p 202 N95-19680
Resistance of silicon nitride turbine components to erosion and hot corrosion/oxidation attack p 202 N95-19683

ERROR ANALYSIS

Possible near-IR channels for remote sensing precipitable water vapor from geostationary satellite platforms [HTN-95-70139] p 214 A95-69431

ERROR CORRECTING DEVICES

Hydraulic system diagnostic sensors [BTN-95-EIX95031502752] p 209 A95-68259

EULER EQUATIONS OF MOTION

Parallel implicit unstructured grid Euler solvers [BTN-95-EIX95042474393] p 217 A95-68307
Validation and evaluation of the advanced aeronautical CFD system SAUNA: A method developer's view [ARA-MEMO-390] p 210 N95-19774
Verification of the CFD simulation system SAUNA for complex aircraft configurations [ARA-MEMO-401] p 211 N95-19776

EXCITATION

Comparison of NO and OH planar fluorescence temperature measurements in scramjet model flowfields [BTN-95-EIX95042474388] p 209 A95-68312

EXHAUST EMISSION

Antarctic snow record of southern hemisphere lead pollution [HTN-95-40359] p 212 A95-66869
Aircraft engine emission reduction [BTN-95-EIX95031502750] p 196 A95-68257
Air pollution mitigation measures for airports and associated activity [PB94-207610] p 216 N95-19582
Developing an emission factor for hazardous air pollutants for an F-16 using JP-8 fuel [AD-A284802] p 216 N95-19685
Advanced diesel electronic fuel injection and turbocharging [AD-A279176] p 211 N95-19809

EXHAUST GASES

Aircraft engine emission reduction [BTN-95-EIX95031502750] p 196 A95-68257
Developing an emission factor for hazardous air pollutants for an F-16 using JP-8 fuel [AD-A284802] p 216 N95-19685

EXHAUST SYSTEMS

Advanced diesel electronic fuel injection and turbocharging [AD-A279176] p 211 N95-19809

EXPERT SYSTEMS

The use of genetic algorithms for flight test and evaluation of artificial intelligence and complex software systems [AD-A284824] p 217 N95-19688
Transport aircraft loading and balancing system: Using a CLIPS expert system for military aircraft load planning p 217 N95-19751
The Computer Aided Aircraft-design Package (CAAP) p 217 N95-19759
PalymSys (TM): An extended version of CLIPS for construction and reasoning using blackboards p 217 N95-19767

EXTREME ULTRAVIOLET EXPLORER SATELLITE

Design decisions from the history of the EUVE science payload [HTN-95-60545] p 205 A95-69854

F

F-16 AIRCRAFT

Developing an emission factor for hazardous air pollutants for an F-16 using JP-8 fuel [AD-A284802] p 216 N95-19685

F-18 AIRCRAFT

Vortical flow structure near the F/A-18 LEX at high incidence [BTN-95-EIX95062487555] p 186 A95-68369
F/A-18 inlet calculations at 60-deg angle of attack and 10-deg sideslip [BTN-95-EIX95112524199] p 195 A95-69309

Prediction of wind tunnel effects on the installed F/A-18A inlet flow field at high angles-of-attack [NASA-CR-195429] p 197 N95-19651

FAILURE MODES

Soft body impact on titanium fan blades p 200 N95-19671
Damage of high temperature components by dust-laden air p 201 N95-19673

FAN BLADES

Design of fan blades subjected to bird impact p 200 N95-19669
Soft body impact on titanium fan blades p 200 N95-19671

FATIGUE (MATERIALS)

Corrosion prevention and control [BTN-95-EIX95031502753] p 188 A95-68260
Fatigue resistance of peened 7050-T7451 aluminium alloy: Repair and re-treatment of a component surface [BTN-94-EIX94371347838] p 206 A95-69131
Fatigue crack growth in nickel-based superalloys at 500-700 C. 1: Waspaloy [BTN-94-EIX94371347843] p 206 A95-69136
Service life extensions for the C-141 [BTN-95-EIX95112530749] p 193 A95-69295

FAULT DETECTION

An airborne monitoring system for FOD and erosion faults p 200 N95-19668

FEATHERING

Wind tunnel tests of a 42 inch diameter self-starting autogyro rotor [AD-A279922] p 188 N95-19863

FIBER COMPOSITES

Twisting smartly in the wind [BTN-95-EIX95041503093] p 184 A95-68353

FIBER ORIENTATION

Theoretical and actual performance of a long duration superpressure balloon made from a biaxially oriented nylon-6 film p 181 A95-66282

FIGHTER AIRCRAFT

Powered lift for land and sea [BTN-95-EIX95041503010] p 192 A95-68313
Proceedings of the USAF Structural Integrity Program Conference [AD-A285684] p 194 N95-19517

FILM COOLING

Influence of injectant Mach number and temperature on supersonic film cooling [BTN-94-EIX94441386686] p 184 A95-68195
Particle deposition in gas turbine blade film cooling holes p 199 N95-19661

FILM THICKNESS

A comparative study of internally and externally capped balloons using small scale test balloons p 181 A95-66285

FINITE ELEMENT METHOD

Design optimization of aircraft engine-mount systems. [BTN-94-EIX94351143325] p 195 A95-67298
Modeling rotating shafts using axisymmetric solid finite elements with matrix reduction [BTN-94-EIX94351143328] p 207 A95-67301
Aeroelastic stability of hingeless rotor blade in hover using large deflection theory [BTN-94-EIX94441386616] p 183 A95-67347
Finite element time domain - modal formulation for nonlinear flutter of composite panels [BTN-95-EIX95042474401] p 203 A95-68299
Bilinear formulation applied to the response and stability of helicopter rotor blade [BTN-95-EIX95042474400] p 192 A95-68300
Coupling equivalent plate and finite element formulations in multiple-method structural analyses [BTN-95-EIX95062487548] p 192 A95-68362
Influence of structural and aerodynamic modeling on flutter analysis [BTN-95-EIX95062487550] p 203 A95-68364
Soft body impact on titanium fan blades p 200 N95-19671
Ice-impact analysis of blades p 200 N95-19672

FINS

Suppression of vortex asymmetry and side force on a circular cone [BTN-95-EIX95042474413] p 209 A95-68287
Waveriders with finlets [BTN-95-EIX95062487541] p 184 A95-68355

FIRE FIGHTING

Selecting and management of fire fighter aircraft [BTN-95-EIX95062487538] p 193 A95-69246

FLAPPING

Wind tunnel tests of a 42 inch diameter self-starting autogyro rotor [AD-A279922] p 188 N95-19863

FLAPS (CONTROL SURFACES)

Navier-Stokes simulations of Orbiter aerodynamic characteristics including pitch trim and bodyflap [BTN-95-EIX95041503779] p 204 A95-69210

FLIGHT CHARACTERISTICS

State-space representation of aerodynamic characteristics of an aircraft at high angles of attack [BTN-95-EIX95062487536] p 187 A95-69244
Airship applications of modern flight test techniques [AD-A284253] p 194 N95-19731

FLIGHT CONTROL

Flight control system mode transitions influence on handling qualities and task performance [BTN-95-EIX95062487525] p 203 A95-69233
Development and flight test of a deployable precision landing system [BTN-95-EIX95062487535] p 190 A95-69243
The use of genetic algorithms for flight test and evaluation of artificial intelligence and complex software systems [AD-A284824] p 217 N95-19688
Automation of hardware-in-the-loop testing of control systems for unmanned air vehicles [AD-A284833] p 194 N95-19693

FLIGHT HAZARDS

WINDEX -- A new index for forecasting microburst potential [HTN-95-90690] p 215 A95-69717

FLIGHT INSTRUMENTS

Flight experience with lightweight, low-power miniaturized instrumentation systems [BTN-95-EIX95062487522] p 180 A95-69230

FLIGHT SAFETY

Federal aviation regulations, part 91. General operating and flight rules. Change 8 [PB94-217445] p 188 N95-19720

FLIGHT SIMULATION

Simulation and flight test evaluation of head-up-display guidance for harrier approach transitions [BTN-95-EIX95062487533] p 194 A95-69241

FLIGHT SIMULATORS

Flight experience with lightweight, low-power miniaturized instrumentation systems [BTN-95-EIX95062487522] p 180 A95-69230
Flight control system mode transitions influence on handling qualities and task performance [BTN-95-EIX95062487525] p 203 A95-69233

FLIGHT TEST VEHICLES

Hypersonic waverider test vehicle: A logical next step [BTN-95-EIX95041503783] p 193 A95-69214

FLIGHT TESTS

Overview of the NASA balloon R&D program p 181 A95-66297
High accuracy navigation and landing system using GPS/IMU system integration [BTN-94-EIX94441386129] p 189 A95-68185
Simulation and flight test evaluation of head-up-display guidance for harrier approach transitions [BTN-95-EIX95062487533] p 194 A95-69241
Development and flight test of a deployable precision landing system [BTN-95-EIX95062487535] p 190 A95-69243
Space flight tests of attitude determination using GPS [BTN-95-EIX95112522529] p 190 A95-69334
The use of genetic algorithms for flight test and evaluation of artificial intelligence and complex software systems [AD-A284824] p 217 N95-19688
Airship applications of modern flight test techniques [AD-A284253] p 194 N95-19731

FLOW CHARACTERISTICS

Passive porosity with free and fixed separation on a tangent-ogive forebody [BTN-95-EIX95062487554] p 185 A95-68368
Vortical flow structure near the F/A-18 LEX at high incidence [BTN-95-EIX95062487555] p 186 A95-68369

FLOW DISTORTION

F/A-18 inlet calculations at 60-deg angle of attack and 10-deg sideslip [BTN-95-EIX95112524199] p 195 A95-69309
Numerical study of the performance of swept, curved compression surface scramjet inlets [BTN-95-EIX95112524198] p 197 A95-69310

FLOW DISTRIBUTION

Experimental and computational results for the external flowfield of a scramjet inlet [BTN-94-EIX94441380977] p 195 A95-68161
Experimental investigations on limit cycle wing rock of slender wings [BTN-95-EIX95062487543] p 185 A95-68357
Prediction of wind tunnel effects on the installed F/A-18A inlet flow field at high angles-of-attack [NASA-CR-195429] p 197 N95-19651

FLOW MEASUREMENT

Measurement by coherent anti-Stokes Raman scattering in the R5Ch hypersonic wind tunnel [BTN-95-EIX95112523811] p 188 A95-69322

FLOW STABILITY

- Aspects of vortex breakdown
[HTN-95-A0001] p 183 A95-67828
- Tip vortex on a swept wing. Mean flow and unsteady phenomena
[BTN-94-EIX94441385755] p 184 A95-68219
- Numerical simulation of steady and unsteady, vorticity-dominated aerodynamic interference
[BTN-95-EIX95062487524] p 186 A95-69232

FLOW VISUALIZATION

- Suppression of vortex asymmetry and side force on a circular cone
[BTN-95-EIX95042474413] p 209 A95-68287

FLUID DYNAMICS

- Solution-adaptive structured-unstructured grid method for unsteady turbomachinery analysis. Part I: Methodology
[BTN-94-EIX94441380983] p 208 A95-67329
- Rotating Kirchhoff method for three-dimensional transonic blade-vortex interaction hover noise
[BTN-94-EIX94441386601] p 182 A95-67332
- Supersonic and hypersonic shock/boundary-layer interaction database
[BTN-94-EIX94441386604] p 182 A95-67335

FLUID FILMS

- Wormgear geometry adopted for implementing hydrostatic lubrication and formulation of the lubrication problem
[NASA-CR-195416] p 210 N95-19567

FLUID FILTERS

- Hydraulic system diagnostic sensors
[BTN-95-EIX95031502752] p 209 A95-68259

FLUID PRESSURE

- Hydraulic system diagnostic sensors
[BTN-95-EIX95031502752] p 209 A95-68259

FLUID-SOLID INTERACTIONS

- Review of numerical procedures for computational surface thermochemistry
[BTN-94-EIX94441386682] p 205 A95-68191
- Interaction of a streamwise vortex with a thin plate: A source of turbulent buffeting
[BTN-95-EIX95042474398] p 209 A95-68302

FLUTTER

- Comparison of theory and experiment for non-linear flutter and stall response of a helicopter blade
[BTN-94-EIX94351108100] p 191 A95-66500
- Influence of structural and aerodynamic modeling on flutter analysis
[BTN-95-EIX95062487550] p 203 A95-68364

FLUTTER ANALYSIS

- Finite element time domain - modal formulation for nonlinear flutter of composite panels
[BTN-95-EIX95042474401] p 203 A95-68299
- Influence of structural and aerodynamic modeling on flutter analysis
[BTN-95-EIX95062487550] p 203 A95-68364

FLY BY WIRE CONTROL

- Flight control system mode transitions influence on handling qualities and task performance
[BTN-95-EIX95062487525] p 203 A95-69233

FOREBODIES

- Experimental and computational results for the external flowfield of a scramjet inlet
[BTN-94-EIX94441380977] p 195 A95-68161
- Passive porosity with free and fixed separation on a tangent-ogive forebody
[BTN-95-EIX95062487554] p 185 A95-68368
- Aerodynamically blunt and sharp bodies
[BTN-95-EIX95041503781] p 205 A95-69212

FOREIGN BODIES

- Erosion, Corrosion and Foreign Object Damage Effects in Gas Turbines
[AGARD-CP-558] p 197 N95-19653

FORMAT

- Programmable cockpit research simulator
[AD-A279219] p 204 N95-19848

FOURIER TRANSFORMATION

- Two-variable method for blockage wall interference in a circular tunnel
[BTN-95-EIX95062487540] p 187 A95-69248

FRACTURE STRENGTH

- Fatigue resistance of peened 7050-T7451 aluminium alloy: Repair and re-treatment of a component surface
[BTN-94-EIX94371347838] p 206 A95-69131

FREE VIBRATION

- Influence of structural and aerodynamic modeling on flutter analysis
[BTN-95-EIX95062487550] p 203 A95-68364

FREQUENCIES

- Fatigue crack growth in nickel-based superalloys at 500-700 C. 1: Waspaloy
[BTN-94-EIX94371347843] p 206 A95-69136

FREQUENCY STABILITY

- Effect of broadcast and precise ephemerides on estimates of the frequency stability of GPS Navstar clocks
[BTN-95-EIX95112522530] p 190 A95-69333

FRONTS (METEOROLOGY)

- Observations of fluxes and inland breezes over a heterogeneous surface
[HTN-95-80258] p 212 A95-66315
- Mesoscale structure of precipitation bands in a North Atlantic winter storm
[HTN-95-40659] p 215 A95-69803

FUEL COMBUSTION

- Aircraft engine emission reduction
[BTN-95-EIX95031502750] p 196 A95-68257

FUEL CONSUMPTION

- Aircraft engine emission reduction
[BTN-95-EIX95031502750] p 196 A95-68257
- Protective coatings for compressor gas path components
p 201 N95-19675

FUEL INJECTION

- Advanced diesel electronic fuel injection and turbocharging
[AD-A279176] p 211 N95-19809

FULL SCALE TESTS

- Testing considerations for military aircraft engines in corrosive environments (a Navy perspective)
p 202 N95-19684

FUSELAGES

- Simplified analysis of general instability of stiffened shells with cutouts in pure bending
[BTN-95-EIX95042474418] p 209 A95-68282

G

GAS DYNAMICS

- Kinetic theory in aerothermodynamics
[HTN-95-A0002] p 183 A95-67829

GAS INJECTION

- Influence of injectant Mach number and temperature on supersonic film cooling
[BTN-94-EIX94441386686] p 184 A95-68195

GAS TURBINE ENGINES

- Fatigue crack growth in nickel-based superalloys at 500-700 C. 1: Waspaloy
[BTN-94-EIX94371347843] p 206 A95-69136
- Nonlinear dynamic simulation of single- and multispool core engines, part 1: Computational method
[BTN-95-EIX95112524200] p 210 A95-69308
- Proceedings of the USAF Structural Integrity Program Conference
[AD-A285684] p 194 N95-19517
- Erosion, Corrosion and Foreign Object Damage Effects in Gas Turbines
[AGARD-CP-558] p 197 N95-19653
- Out of area experiences with the RB199 in Toronto
p 198 N95-19654
- The operation of gas turbine engines in hot and sandy conditions: Royal Air Force experiences in the Gulf conflict
p 198 N95-19655
- US Army rotorcraft turboshaft engines sand and dust erosion considerations
p 198 N95-19656
- Navy foreign object damage and its impact on future gas turbine engine low pressure compression systems
p 198 N95-19658
- Experimental and numerical simulations of the effects of ingested particles in gas turbine engines
p 199 N95-19662
- Particle trajectories in gas turbine engines
p 199 N95-19663
- An airborne monitoring system for FOD and erosion faults
p 200 N95-19668
- Aero-thermodynamic distortion induced structured dynamic response
[AD-A279931] p 203 N95-19864

GAS TURBINES

- Rotor whirl forces induced by the tip clearance effect in axial flow compressors
[BTN-94-EIX94351143331] p 207 A95-67304
- Aircraft engine emission reduction
[BTN-95-EIX95031502750] p 196 A95-68257
- Scandinavian Airlines Systems experience on erosion, corrosion and foreign object damage effects on gas turbines
p 198 N95-19659
- Particle deposition in gas turbine blade film cooling holes
p 199 N95-19661
- The calculation of erosion in a gas turbine compressor rotor
p 199 N95-19664
- Erosion of T56 5th stage rotor blades due to bleed hole overtip flow
p 200 N95-19666
- Protective coatings for compressor gas path components
p 201 N95-19675
- Braze repair possibilities for hot section gas turbine parts
p 201 N95-19677

- Gas turbine compressor corrosion and erosion in Western Europe
p 201 N95-19678
- Multilayer anti-erosion coatings
p 201 N95-19679

GEAR TEETH

- Wormgear geometry adopted for implementing hydrostatic lubrication and formulation of the lubrication problem
[NASA-CR-195416] p 210 N95-19567

GEARS

- Wormgear geometry adopted for implementing hydrostatic lubrication and formulation of the lubrication problem
[NASA-CR-195416] p 210 N95-19567

GENETIC ALGORITHMS

- The use of genetic algorithms for flight test and evaluation of artificial intelligence and complex software systems
[AD-A284824] p 217 N95-19688

GLIDERS

- Flight experience with lightweight, low-power miniaturized instrumentation systems
[BTN-95-EIX95062487522] p 180 A95-69230

GLIDING

- Minimum sink-speed in power-off glide
[BTN-95-EIX95062487556] p 193 A95-68370

GLOBAL POSITIONING SYSTEM

- High accuracy navigation and landing system using GPS/IMU system integration
[BTN-94-EIX94441386129] p 189 A95-68185
- GPS/GLONASS/INS test program
[BTN-94-EIX94441386131] p 189 A95-68187
- Use of MOBITEK wireless wide area networks as a solution to land-based positioning and navigation
[BTN-94-EIX94441386132] p 189 A95-68188
- Evaluation of the radio frequency susceptibility of commercial GPS receivers
[BTN-95-EIX95042474624] p 189 A95-68278
- On-the-fly carrier phase ambiguity resolution for precise aircraft landing
[BTN-95-EIX95112522535] p 190 A95-69328
- Results and performance of multi-site reference station differential GPS
[BTN-95-EIX95112522534] p 190 A95-69329
- Integrated GPS/Glonass navigation: Algorithms and results
[BTN-95-EIX95112522531] p 190 A95-69332
- Effect of broadcast and precise ephemerides on estimates of the frequency stability of GPS Navstar clocks
[BTN-95-EIX95112522530] p 190 A95-69333
- Space flight tests of attitude determination using GPS
[BTN-95-EIX95112522529] p 190 A95-69334

GLONASS

- GPS/GLONASS/INS test program
[BTN-94-EIX94441386131] p 189 A95-68187
- Integrated GPS/Glonass navigation: Algorithms and results
[BTN-95-EIX95112522531] p 190 A95-69332

GRAUPEL

- Microwave and infrared simulations of an intense convective system and comparison with aircraft observations
[HTN-95-60511] p 214 A95-68762

GRAVITATIONAL EFFECTS

- Stability of magnetic bearing-rotor systems and the effects of gravity and damping
[BTN-94-EIX94441386619] p 208 A95-68168

GRID GENERATION (MATHEMATICS)

- Adaptive computations of flow around a delta wing with vortex breakdown
[BTN-94-EIX94441386631] p 184 A95-68180
- Validation and evaluation of the advanced aeronautical CFD system SAUNA: A method developer's view
[ARA-MEMO-390] p 210 N95-19774
- Application of three-dimensional hybrid structured/unstructured grids to land, sea and air vehicles
[ARA-MEMO-399] p 210 N95-19775
- Verification of the CFD simulation system SAUNA for complex aircraft configurations
[ARA-MEMO-401] p 211 N95-19776
- Inviscid and viscous flow modelling of complex aircraft configurations using the CFD simulation system sauna
[ARA-MEMO-403] p 211 N95-19777

GROUND EFFECT (AERODYNAMICS)

- Effect of ground and ceiling planes on shape of energized wakes
[BTN-95-EIX95062487558] p 186 A95-68372

GROUND STATIONS

- Results and performance of multi-site reference station differential GPS
[BTN-95-EIX95112522534] p 190 A95-69329

GROUND WIND

- Observations of fluxes and inland breezes over a heterogeneous surface
[HTN-95-80258] p 212 A95-66315

GUSTS

- Continuous gust response and sensitivity derivatives using state-space models
[BTN-95-EIX95062487551] p 203 A95-68365
- Brief history of gust models for aircraft design
[BTN-95-EIX95062487557] p 203 A95-68371
- GYROSCOPIC STABILITY**
Stability of magnetic bearing-rotor systems and the effects of gravity and damping
[BTN-94-EIX94441386619] p 208 A95-68168

H

H-INFINITY CONTROL

- Automation of hardware-in-the-loop testing of control systems for unmanned air vehicles
[AD-A284833] p 194 N95-19693

HAIL

- Impact loading of compressor stator vanes by hailstone ingestion
p 200 N95-19670

HARMONIC CONTROL

- Recent studies of rotorcraft blade-vortex interaction noise
[BTN-95-EIX95062487521] p 218 A95-69229

HARRIER AIRCRAFT

- Simulation and flight test evaluation of head-up-display guidance for harrier approach transitions
[BTN-95-EIX95062487533] p 194 A95-69241
- An analysis of the costs and benefits in improving F402-RR-406A High Pressure Turbine, second stage blades under the aircraft engine Component Improvement Program (CIP)
[AD-A285127] p 197 N95-19595

HAZARDS

- Radial reefing method for accelerated and controlled parachute opening
[BTN-95-EIX95062487539] p 187 A95-69247

HEAT FLUX

- Kinetic theory in aerothermodynamics
[HTN-95-A0002] p 183 A95-67829

HEAT RESISTANT ALLOYS

- National AeroSpace Plane: Technology transfer
[BTN-95-EIX95072498879] p 180 A95-68395
- Fatigue crack growth in nickel-based superalloys at 500-700 C. 1: Waspaloy
[BTN-94-EIX94371347843] p 206 A95-69136
- New Trends in coatings developments for turbine blades: Materials processing and repair
p 201 N95-19676

HEAT TRANSFER

- Nonhydrostatic simulation of frontogenesis in a moist atmosphere. Part 3: Thermal wind imbalance and rainbands
[HTN-95-90356] p 212 A95-66429
- Experimental and computational results for the external flowfield of a scramjet inlet
[BTN-94-EIX94441380977] p 195 A95-68161
- An investigation of drag repeatability in half model testing in the ARA Transonic Wind Tunnel
[ARA-MEMO-392] p 188 N95-19546

HELICOPTER ENGINES

- US Army rotorcraft turboshaft engines sand and dust erosion considerations
p 198 N95-19656
- Future directions in helicopter protection system configuration
p 198 N95-19657

HELICOPTERS

- Bilinear formulation applied to the response and stability of helicopter rotor blade
[BTN-95-EIX95042474400] p 192 A95-68300
- Flight control system mode transitions influence on handling qualities and task performance
[BTN-95-EIX95062487525] p 203 A95-69233
- Particle trajectories in gas turbine engines
p 199 N95-19663
- The calculation of erosion in a gas turbine compressor rotor
p 199 N95-19664
- Multilayer anti-erosion coatings
p 201 N95-19679

HIGH ALTITUDE BALLOONS

- Balloon technology and observations; Symposium P3 of the COSPAR Plenary Meeting, 29th, Washington, DC, Aug. 28-Sept. 5, 1992
[HTN-95-70250] p 181 A95-66276
- Balloon flights in France and in Europe
p 204 A95-66301
- The scientific ballooning in Russia
p 191 A95-66302
- A program for scientific and applied investigations using aerostat complexes
p 182 A95-66304
- HIGH ALTITUDE ENVIRONMENTS**
An air-driven pressure booster pump for aircraft-based air sampling
[HTN-95-40689] p 216 A95-69833

HIGH PRESSURE

- An analysis of the costs and benefits in improving F402-RR-406A High Pressure Turbine, second stage blades under the aircraft engine Component Improvement Program (CIP)
[AD-A285127] p 197 N95-19595

HIGH SPEED

- Advanced diesel electronic fuel injection and turbocharging
[AD-A279176] p 211 N95-19809

HIGH TEMPERATURE

- Damage of high temperature components by dust-laden air
p 201 N95-19673
- New Trends in coatings developments for turbine blades: Materials processing and repair
p 201 N95-19676

HISTORIES

- Design decisions from the history of the EUVE science payload
[HTN-95-60545] p 205 A95-69854

HOLES

- Erosion of T56 5th stage rotor blades due to bleed hole overtip flow
p 200 N95-19666

HOLES (MECHANICS)

- Particle deposition in gas turbine blade film cooling holes
p 199 N95-19661

HOT CORROSION

- New Trends in coatings developments for turbine blades: Materials processing and repair
p 201 N95-19676
- Resistance of silicon nitride turbine components to erosion and hot corrosion/oxidation attack
p 202 N95-19683

HOVERING

- Rotating Kirchhoff method for three-dimensional transonic blade-vortex interaction hover noise
[BTN-94-EIX94441386601] p 182 A95-67332
- Aeroelastic stability of hingeless rotor blade in hover using large deflection theory
[BTN-94-EIX94441386616] p 183 A95-67347
- Simulation and flight test evaluation of head-up-display guidance for harrier approach transitions
[BTN-95-EIX95062487533] p 194 A95-69241

HUMAN PERFORMANCE

- Flight control system mode transitions influence on handling qualities and task performance
[BTN-95-EIX95062487525] p 203 A95-69233

HURRICANES

- A technique for detecting a tropical cyclone center using a Doppler radar
[HTN-95-20631] p 215 A95-69574

HYBRID NAVIGATION SYSTEMS

- Integrated GPS/Glonass navigation: Algorithms and results
[BTN-95-EIX95112522531] p 190 A95-69332

HYDRAULIC FLUIDS

- Hydraulic system diagnostic sensors
[BTN-95-EIX95031502752] p 209 A95-68259

HYDROSTATICS

- Wormgear geometry adopted for implementing hydrostatic lubrication and formulation of the lubrication problem
[NASA-CR-195416] p 210 N95-19567

HYDROXYL RADICALS

- Comparison of NO and OH planar fluorescence temperature measurements in scramjet model flowfields
[BTN-95-EIX95042474388] p 209 A95-68312

HYGROSCOPICITY

- Gas turbine compressor corrosion and erosion in Western Europe
p 201 N95-19678

HYPERSONIC AIRCRAFT

- Hyperersonic waverider test vehicle: A logical next step
[BTN-95-EIX95041503783] p 193 A95-69214
- Development of an efficient inverse method for supersonic and hypersonic body design
[BTN-95-EIX95041503784] p 180 A95-69215

HYPERSONIC BOUNDARY LAYER

- Shock layers and boundary layers in hypersonic flows
[HTN-95-A0003] p 183 A95-67830
- Model for compressible turbulence in hypersonic wall boundary and high-speed mixing layers
[BTN-94-EIX94441386625] p 184 A95-68174

HYPERSONIC FLIGHT

- Navier-Stokes simulations of Orbiter aerodynamic characteristics including pitch trim and bodyflap
[BTN-95-EIX95041503779] p 204 A95-69210
- Multiblock analysis for Shuttle Orbiter reentry heating from Mach 24 to Mach 12
[BTN-95-EIX95041503780] p 205 A95-69211

HYPERSONIC FLOW

- Shock layers and boundary layers in hypersonic flows
[HTN-95-A0003] p 183 A95-67830
- Experimental and computational results for the external flowfield of a scramjet inlet
[BTN-94-EIX94441380977] p 195 A95-68161
- Measurement by coherent anti-Stokes Raman scattering in the R5Ch hypersonic wind tunnel
[BTN-95-EIX95112523811] p 188 A95-69322

HYPERSONIC INLETS

- Experimental and computational results for the external flowfield of a scramjet inlet
[BTN-94-EIX94441380977] p 195 A95-68161

HYPERSONIC REENTRY

- Shock layers and boundary layers in hypersonic flows
[HTN-95-A0003] p 183 A95-67830

HYPERSONIC SHOCK

- Linear disturbances in hypersonic, chemically reacting shock layers
[BTN-94-EIX94441386605] p 182 A95-67336

HYPERSONIC SPEED

- Aerodynamically blunt and sharp bodies
[BTN-95-EIX95041503781] p 205 A95-69212
- Navier-Stokes computation of a viscous optimized waverider
[BTN-95-EIX95041503782] p 193 A95-69213
- Minimum-drag axisymmetric bodies in the supersonic/hypersonic flow regimes
[BTN-95-EIX95041503785] p 180 A95-69216

HYPERSONIC VEHICLES

- Navier-Stokes computation of a viscous optimized waverider
[BTN-95-EIX95041503782] p 193 A95-69213
- Interpretation of waverider performance data using computational fluid dynamics
[BTN-95-EIX95062487534] p 193 A95-69242

HYPERSONICS

- Supersonic and hypersonic shock/boundary-layer interaction database
[BTN-94-EIX94441386604] p 182 A95-67335
- Waveriders with finlets
[BTN-95-EIX95062487541] p 184 A95-68355

HYPERVELOCITY LAUNCHERS

- New end tube closure system for the ram accelerator
[BTN-94-EIX94441380974] p 195 A95-68158

ICE

- Repeatability of ice shapes in the NASA Lewis icing research tunnel
[BTN-95-EIX95062487528] p 204 A95-69236
- Ice-impact analysis of blades
p 200 N95-19672

ICE CLOUDS

- Microwave and infrared simulations of an intense convective system and comparison with aircraft observations
[HTN-95-60511] p 214 A95-68762

ICE FORMATION

- Aircraft icing measurements in East Coast winter storms
[HTN-95-60505] p 214 A95-68756
- Conditions associated with large-drop regions
[HTN-95-10686] p 214 A95-68845
- Repeatability of ice shapes in the NASA Lewis icing research tunnel
[BTN-95-EIX95062487528] p 204 A95-69236

IDEAL GAS

- Linear disturbances in hypersonic, chemically reacting shock layers
[BTN-94-EIX94441386605] p 182 A95-67336

ILLUMINATION

- Powerful bolide explosion over North Italy
[HTN-95-80564] p 218 A95-69658

IMPACT

- Particle deposition in gas turbine blade film cooling holes
p 199 N95-19661

IMPACT DAMAGE

- An airborne monitoring system for FOD and erosion faults
p 200 N95-19668
- Design of fan blades subjected to bird impact
p 200 N95-19669
- Impact loading of compressor stator vanes by hailstone ingestion
p 200 N95-19670
- Soft body impact on titanium fan blades
p 200 N95-19671

Ice-impact analysis of blades

- p 200 N95-19672

IMPACT LOADS

- Impact loading of compressor stator vanes by hailstone ingestion
p 200 N95-19670

IMPACT TESTS

- Soft body impact on titanium fan blades
p 200 N95-19671

INCOMPRESSIBLE FLOW

- Aspects of vortex breakdown
[HTN-95-A0001] p 183 A95-67828

INDUCTION MOTORS

- Improved speed control system for the 87,000 HP wind tunnel drive
[NASA-TM-106840] p 211 N95-19794

INERTIAL NAVIGATION

- High accuracy navigation and landing system using GPS/IMU system integration
[BTN-94-EIX94441386129] p 189 A95-68185

SUBJECT INDEX

- GPS/GLONASS/INS test program**
[BTN-94-EIX94441386131] p 189 A95-68187
- INFRARED RADIOMETERS**
Microwave and infrared simulations of an intense convective system and comparison with aircraft observations
[HTN-95-60511] p 214 A95-68762
- INFRARED SPECTROMETERS**
Possible near-IR channels for remote sensing precipitable water vapor from geostationary satellite platforms
[HTN-95-70139] p 214 A95-69431
- INGESTION (ENGINES)**
Modern transport engine experience with environmental ingestion effects p 199 N95-19660
Experimental and numerical simulations of the effects of ingested particles in gas turbine engines p 199 N95-19662
- INLET FLOW**
Experimental and computational results for the external flowfield of a scramjet inlet
[BTN-94-EIX94441380977] p 195 A95-68161
Lag model for turbulent boundary layers over rough bleed surfaces
[BTN-94-EIX94441380981] p 208 A95-68165
Numerical study of the performance of swept, curved compression surface scramjet inlets
[BTN-95-EIX95112524198] p 197 A95-69310
Prediction of wind tunnel effects on the installed F/A-18A inlet flow field at high angles-of-attack
[NASA-CR-195429] p 197 N95-19651
- INLET PRESSURE**
F/A-18 inlet calculations at 60-deg angle of attack and 10-deg sideslip
[BTN-95-EIX95112524199] p 195 A95-69309
- INTAKE SYSTEMS**
Prediction of wind tunnel effects on the installed F/A-18A inlet flow field at high angles-of-attack
[NASA-CR-195429] p 197 N95-19651
- INTERACTION AERODYNAMICS**
Interference between tanker wing wake with roll-up and receiver aircraft
[BTN-95-EIX95062487552] p 185 A95-68366
- INTERFEROMETRY**
Joint stars phased array radar antenna
[BTN-95-EIX95042474626] p 209 A95-68280
- INTERMETALLICS**
Braze repair possibilities for hot section gas turbine parts p 201 N95-19677
- INTERNAL COMBUSTION ENGINES**
Aircraft engine emission reduction
[BTN-95-EIX95031502750] p 196 A95-68257
- INTERNAL FLOW**
State-space representation of aerodynamic characteristics of an aircraft at high angles of attack
[BTN-95-EIX95062487536] p 187 A95-69244
- INTERPROCESSOR COMMUNICATION**
PalymSys (TM): An extended version of CLIPS for construction and reasoning using blackboards p 217 N95-19767
- INVISCID FLOW**
Construction of nearly orthogonal multiblock grids for compressible flow simulation
[BTN-94-EIX94361133526] p 207 A95-65981
Two-variable method for blockage wall interference in a circular tunnel
[BTN-95-EIX95062487540] p 187 A95-69248
Validation and evaluation of the advanced aeronautical CFD system SAUNA: A method developer's view
[ARA-MEMO-390] p 210 N95-19774
Verification of the CFD simulation system SAUNA for complex aircraft configurations
[ARA-MEMO-401] p 211 N95-19776
Inviscid and viscous flow modelling of complex aircraft configurations using the CFD simulation system sauna
[ARA-MEMO-403] p 211 N95-19777
- IONIZING RADIATION**
The joint Russian-Brazil research on balloons p 182 A95-66303
- IONOSPHERIC PROPAGATION**
Using IRI for the computation of ionospheric corrections for altimeter data analysis p 212 A95-66949
- J**
- JET ENGINES**
Design optimization of aircraft engine-mount systems.
[BTN-94-EIX94351143325] p 195 A95-67298
Adaptive modeling of jet engine performance with application to condition monitoring
[BTN-95-EIX95112524205] p 196 A95-69303
Developing an emission factor for hazardous air pollutants for an F-16 using JP-8 fuel
[AD-A284802] p 216 N95-19685

- JET FLOW**
Phenomenological description and simplified modelling of the vortex wake issuing from a jet in a crossflow
[BTN-94-EIX94441385754] p 184 A95-68218
- JET NOZZLES**
Entrainment and acoustic variations in a round jet from introduced streamwise vorticity
[BTN-95-EIX95042474409] p 209 A95-68291
- JP-8 JET FUEL**
Developing an emission factor for hazardous air pollutants for an F-16 using JP-8 fuel
[AD-A284802] p 216 N95-19685

K

- KELVIN-HELMHOLTZ INSTABILITY**
Conditions associated with large-drop regions
[HTN-95-10686] p 214 A95-68845
- KINETIC THEORY**
Kinetic theory in aerothermodynamics
[HTN-95-A0002] p 183 A95-67829
- KNUDSEN FLOW**
Kinetic theory in aerothermodynamics
[HTN-95-A0002] p 183 A95-67829

L

- LAGRANGE MULTIPLIERS**
Coupling equivalent plate and finite element formulations in multiple-method structural analyses
[BTN-95-EIX95062487548] p 192 A95-68362
- LAMINAR BOUNDARY LAYER**
Fight experience with lightweight, low-power miniaturized instrumentation systems
[BTN-95-EIX95062487522] p 180 A95-69230
- LAMINAR HEAT TRANSFER**
Multiblock analysis for Shuttle Orbiter reentry heating from Mach 24 to Mach 12
[BTN-95-EIX95041503780] p 205 A95-69211
- LAMINATES**
Launcher wing-leading-edge design
[BTN-95-EIX95042477110] p 192 A95-68349
Ply layout optimization and micromechanics tailoring of composite aircraft engine structures
[BTN-95-EIX95112524206] p 196 A95-69302
- LANDING AIDS**
High accuracy navigation and landing system using GPS/IMU system integration
[BTN-94-EIX94441386129] p 189 A95-68185
Development and flight test of a deployable precision landing system
[BTN-95-EIX95062487535] p 190 A95-69243
On-the-fly carrier phase ambiguity resolution for precise aircraft landing
[BTN-95-EIX95112522535] p 190 A95-69328
- LASER INDUCED FLUORESCENCE**
Comparison of NO and OH planar fluorescence temperature measurements in scramjet model flowfields
[BTN-95-EIX95042474388] p 209 A95-68312
- LASERS**
Planar air density measurements near model surfaces by ultraviolet Rayleigh/Raman scattering
[BTN-94-EIX94441386614] p 213 A95-67345
- LATERAL CONTROL**
Determination of stability and control derivatives from the NASA F/A-18 HARV from flight data using the maximum likelihood method
[NASA-CR-197320] p 204 N95-19576
- LATERAL STABILITY**
Aerodynamic characteristics of strake vortex flaps on a strake-wing configuration
[BTN-95-EIX95062487537] p 187 A95-69245
- LAUNCH VEHICLES**
Launcher wing-leading-edge design
[BTN-95-EIX95042477110] p 192 A95-68349
- LAY-UP**
Ply layout optimization and micromechanics tailoring of composite aircraft engine structures
[BTN-95-EIX95112524206] p 196 A95-69302
- LAYOUTS**
Programmable cockpit research simulator
[AD-A279219] p 204 N95-19848
- LEAD (METAL)**
Antarctic snow record of southern hemisphere lead pollution
[HTN-95-40359] p 212 A95-66869
- LEADING EDGE SWEEP**
Aerodynamic effects of delta planform tip sails on wing performance
[BTN-95-EIX95062487544] p 185 A95-68358
- LEADING EDGES**
Launcher wing-leading-edge design
[BTN-95-EIX95042477110] p 192 A95-68349

LUBRICATION

- Vortical flow structure near the F/A-18 LEX at high incidence
[BTN-95-EIX95062487555] p 186 A95-68369
- Numerical simulation of incidence and sweep effects on delta wing vortex breakdown
[BTN-95-EIX95062487526] p 186 A95-69234
- Impact loading of compressor stator vanes by hailstone ingestion p 200 N95-19670
- Soft body impact on titanium fan blades p 200 N95-19671
- Ice-impact analysis of blades p 200 N95-19672
- LEAKAGE**
Development of hypersonic engine seals: Flow effects of preload and engine pressures
[BTN-95-EIX95112524204] p 196 A95-69304
- LEGENDRE FUNCTIONS**
Bilinear functional applied to the response and stability of helicopter rotor blade
[BTN-95-EIX95042474400] p 192 A95-68300
- LIFT**
Nonhydrostatic simulation of frontogenesis in a moist atmosphere. Part 3: Thermal wind imbalance and rainbands
[HTN-95-90356] p 212 A95-66429
Lift analysis of a variable camber foil using the discrete vortex-blob method
[BTN-94-EIX94441386623] p 179 A95-68172
Application of circulation control to advanced subsonic transport aircraft. Part 2: Transport application
[BTN-95-EIX95062487546] p 185 A95-68360
Minimum sink-speed in power-off glide
[BTN-95-EIX95062487556] p 193 A95-68370
Numerical simulation of incidence and sweep effects on delta wing vortex breakdown
[BTN-95-EIX95062487526] p 186 A95-69234
Analysis of an oscillating Joukowski airfoil with surface suction and moving vortices
[BTN-95-EIX95062487527] p 186 A95-69235
Interpretation of waverider performance data using computational fluid dynamics
[BTN-95-EIX95062487534] p 193 A95-69242
- LIFT DRAG RATIO**
Navier-Stokes computation of a viscous optimized waverider
[BTN-95-EIX95041503782] p 193 A95-69213
- LIGHTNING**
Aircraft electric field measurements: Calibration and ambient field retrieval
[HTN-95-90508] p 213 A95-67780
- LINEAR ARRAYS**
Inband radar cross section of phased arrays with parallel feeds
[AD-A284249] p 210 N95-19730
- LINEAR TRANSFORMATIONS**
Lyapunov exponents and stochastic stability of two-dimensional parametrically excited random systems
[BTN-94-EIX94361122401] p 207 A95-65897
- LOAD DISTRIBUTION (FORCES)**
Transport aircraft loading and balancing system: Using a CLIPS expert system for military aircraft load planning p 217 N95-19751
- LOADING OPERATIONS**
Transport aircraft loading and balancing system: Using a CLIPS expert system for military aircraft load planning p 217 N95-19751
- LONGITUDINAL CONTROL**
Determination of stability and control derivatives from the NASA F/A-18 HARV from flight data using the maximum likelihood method
[NASA-CR-197320] p 204 N95-19576
- LONGITUDINAL STABILITY**
Offset thrust axes and pitch stability
[BTN-95-EIX95062487553] p 203 A95-68367
Navier-Stokes simulations of Orbiter aerodynamic characteristics including pitch trim and bodyflap
[BTN-95-EIX95041503779] p 204 A95-69210
- LOW ALTITUDE**
Multilayer anti-erosion coatings p 201 N95-19679
- LOW COST**
Programmable cockpit research simulator
[AD-A279219] p 204 N95-19848
- LOW PRESSURE**
Research aircraft observations of a polar low at the east Greenland ice edge
[HTN-95-A0175] p 215 A95-69766
- LUBRICATION**
Wormgear geometry adopted for implementing hydrostatic lubrication and formulation of the lubrication problem
[NASA-CR-195416] p 210 N95-19567

M

MACH NUMBER

- Supersonic and hypersonic shock/boundary-layer interaction database
[BTN-94-EIX94441386604] p 182 A95-67335
- Linear disturbances in hypersonic, chemically reacting shock layers
[BTN-94-EIX94441386605] p 182 A95-67336
- Behavior of the Johnson-King turbulence model in axisymmetric supersonic flows
[BTN-94-EIX94441386606] p 183 A95-67337
- Influence of injectant Mach number and temperature on supersonic film cooling
[BTN-94-EIX94441386686] p 184 A95-68195
- Multiblock analysis for Shuttle Orbiter reentry heating from Mach 24 to Mach 12
[BTN-95-EIX95041503780] p 205 A95-69211
- Navier-Stokes computation of a viscous optimized waverider
[BTN-95-EIX95041503782] p 193 A95-69213
- Minimum-drag axisymmetric bodies in the supersonic/hypersonic flow regimes
[BTN-95-EIX95041503785] p 180 A95-69216
- MAGNESIUM CHLORIDES**
Gas turbine compressor corrosion and erosion in Western Europe p 201 N95-19678
- MAGNETIC ANOMALIES**
The joint Russian-Brazil research on balloons p 182 A95-66303
- MAGNETIC BEARINGS**
Stability of magnetic bearing-rotor systems and the effects of gravity and damping
[BTN-94-EIX94441386619] p 208 A95-68168
- MAGNETIC FIELDS**
Powerful bolide explosion over North Italy
[HTN-95-80564] p 218 A95-69658
- MAINTAINABILITY**
Maintenance requirements for a supersonic transport
[BTN-95-EIX95031502751] p 179 A95-68258
- Reliability and maintainability
[BTN-95-EIX95042477109] p 179 A95-68350
- Navy foreign object damage and its impact on future gas turbine engine low pressure compression systems p 198 N95-19658
- New Trends in coatings developments for turbine blades: Materials processing and repair p 201 N95-19676
- MAINTENANCE**
Fatigue resistance of peened 7050-T7451 aluminum alloy: Repair and re-treatment of a component surface
[BTN-94-EIX94371347838] p 206 A95-69131
- Performance deterioration of axial compressors due to blade defects p 199 N95-19665
- An airborne monitoring system for FOD and erosion faults p 200 N95-19668
- Braze repair possibilities for hot section gas turbine parts p 201 N95-19677
- MANEUVERABILITY**
Side forces at high angles of attack. Why, when, how?
[BTN-95-EIX95112523809] p 194 A95-69324
- MARINE ENVIRONMENTS**
Aircraft icing measurements in East Coast winter storms
[HTN-95-60505] p 214 A95-68756
- MARINE METEOROLOGY**
Research aircraft observations of a polar low at the east Greenland ice edge
[HTN-95-A0175] p 215 A95-69766
- MARINE TRANSPORTATION**
Results and performance of multi-site reference station differential GPS
[BTN-95-EIX9511252534] p 190 A95-69329
- MASS TRANSFER**
Passive porosity with free and fixed separation on a tangent-ogive forebody
[BTN-95-EIX95062487554] p 185 A95-68368
- MATHEMATICAL MODELS**
Phenomenological description and simplified modelling of the vortex wake issuing from a jet in a crossflow
[BTN-94-EIX94441385754] p 184 A95-68218
- Brief history of gust models for aircraft design
[BTN-95-EIX95062487557] p 203 A95-68371
- Numerical simulation of steady and unsteady, vorticity-dominated aerodynamic interference
[BTN-95-EIX95062487524] p 186 A95-69232
- State-space representation of aerodynamic characteristics of an aircraft at high angles of attack
[BTN-95-EIX95062487536] p 187 A95-69244
- Adaptive modeling of jet engine performance with application to condition monitoring
[BTN-95-EIX95112524205] p 196 A95-69303
- Particle trajectories in gas turbine engines p 199 N95-19663
- The calculation of erosion in a gas turbine compressor rotor p 199 N95-19664

- Design of fan blades subjected to bird impact p 200 N95-19669
- Soft body impact on titanium fan blades p 200 N95-19671
- Ice-impact analysis of blades p 200 N95-19672
- Damage of high temperature components by dust-laden air p 201 N95-19673
- On supersonic-inlet boundary-layer bleed flow
[NASA-CR-195426] p 202 N95-19769
- MATRICES (MATHEMATICS)**
Unbalance response of a dual rotor system: Theory and experiment
[BTN-94-EIX94351143320] p 195 A95-65854
- MAXIMUM LIKELIHOOD ESTIMATES**
Determination of stability and control derivatives from the NASA F/A-18 HARV from flight data using the maximum likelihood method
[NASA-CR-197320] p 204 N95-19576
- MECHANICAL MEASUREMENT**
Design optimization of aircraft engine-mount systems.
[BTN-94-EIX94351143325] p 195 A95-67298
- MECHANICAL PROPERTIES**
Environmental effects on composite airframes: A study conducted for the ARM UAV Program (Atmospheric Radiation Measurement Unmanned Aerospace Vehicle)
[OE94-015351] p 206 N95-19579
- MEMORY (COMPUTERS)**
Parallel implicit unstructured grid Euler solvers
[BTN-95-EIX95042474393] p 217 A95-68307
- MESOMETEOROLOGY**
Forecasting for a large field program: STORM-FEST
[HTN-95-90694] p 215 A95-69721
- MESOSCALE PHENOMENA**
Observations of fluxes and inland breezes over a heterogeneous surface
[HTN-95-80258] p 212 A95-66315
- Research aircraft observations of a polar low at the east Greenland ice edge
[HTN-95-A0175] p 215 A95-69766
- METAL FATIGUE**
Fatigue resistance of peened 7050-T7451 aluminum alloy: Repair and re-treatment of a component surface
[BTN-94-EIX94371347838] p 206 A95-69131
- METAL SURFACES**
Planar air density measurements near model surfaces by ultraviolet Rayleigh-Raman scattering
[BTN-94-EIX94441386614] p 213 A95-67345
- METALLOGRAPHY**
Fatigue crack growth in nickel-based superalloys at 500-700 C. 1: Waspaloy
[BTN-94-EIX94371347843] p 206 A95-69136
- METEOROLOGICAL RESEARCH AIRCRAFT**
An air-driven pressure booster pump for aircraft-based air sampling
[HTN-95-40689] p 216 A95-69833
- METEOROLOGY**
Powerful bolide explosion over North Italy
[HTN-95-80564] p 218 A95-69658
- MICROBURSTS (METEOROLOGY)**
WINDEX - A new index for forecasting microburst potential
[HTN-95-90690] p 215 A95-69717
- MICROCRACKS**
Impact loading of compressor stator vanes by hailstone ingestion p 200 N95-19670
- MICROMECHANICS**
Ply layout optimization and micromechanics tailoring of composite aircraft engine structures
[BTN-95-EIX95112524206] p 196 A95-69302
- MICROSTRUCTURE**
Surface morphology and structure of carbon-carbon composites in high-energy sliding contact
[BTN-94-EIX94371347996] p 206 A95-69164
- MICROWAVE RADIOMETERS**
Microwave and infrared simulations of an intense convective system and comparison with aircraft observations
[HTN-95-60511] p 214 A95-68762
- MIDLATITUDE ATMOSPHERE**
Mesoscale structure of precipitation bands in a North Atlantic winter storm
[HTN-95-40659] p 215 A95-69803
- MILITARY AIRCRAFT**
USAF aging aircraft program
[BTN-95-EIX95072498878] p 180 A95-68394
- Application of three-dimensional hybrid structured/unstructured grids to land, sea and air vehicles
[ARA-MEMO-399] p 210 N95-19775
- MILITARY HELICOPTERS**
US Army rotorcraft turboshaft engines sand and dust erosion considerations p 198 N95-19656
- MILITARY OPERATIONS**
Joint stars phased array radar antenna
[BTN-95-EIX95042474626] p 209 A95-68280

MILITARY TECHNOLOGY

- Reliability and maintainability
[BTN-95-EIX95042477109] p 179 A95-68350
- MINIMUM DRAG**
Minimum-drag axisymmetric bodies in the supersonic/hypersonic flow regimes
[BTN-95-EIX95041503785] p 180 A95-69216
- MISSILE CONFIGURATIONS**
Application of three-dimensional hybrid structured/unstructured grids to land, sea and air vehicles
[ARA-MEMO-399] p 210 N95-19775
- MISSILE CONTROL**
Side forces at high angles of attack. Why, when, how?
[BTN-95-EIX95112523809] p 194 A95-69324
- MISSION PLANNING**
Design decisions from the history of the EUVE science payload
[HTN-95-60545] p 205 A95-69854
- MIXING**
Comparison of NO and OH planar fluorescence temperature measurements in scramjet model flowfields
[BTN-95-EIX95042474388] p 209 A95-68312
- MIXING LAYERS (FLUIDS)**
Model for compressible turbulence in hypersonic wall boundary and high-speed mixing layers
[BTN-94-EIX94441386625] p 184 A95-68174
- MIXING LENGTH FLOW THEORY**
Model for compressible turbulence in hypersonic wall boundary and high-speed mixing layers
[BTN-94-EIX94441386625] p 184 A95-68174
- MOBILE COMMUNICATION SYSTEMS**
Use of MOBITEK wireless wide area networks as a solution to land-based positioning and navigation
[BTN-94-EIX94441386132] p 189 A95-68188
- MOLECULAR FLOW**
Kinetic theory in aerothermodynamics
[HTN-95-A0002] p 183 A95-67829
- MOLECULAR ROTATION**
Measurement by coherent anti-Stokes Raman scattering in the R5Ch hypersonic wind tunnel
[BTN-95-EIX95112523811] p 188 A95-69322
- MONITORS**
Hydraulic system diagnostic sensors
[BTN-95-EIX95031502752] p 209 A95-68259
- MOTION**
Multiport pressure measurements on continuously moving wind tunnel models
[ARA-MEMO-391] p 188 N95-19772
- MRC AIRCRAFT**
Out of area experiences with the RB199 in Toronto p 198 N95-19654
- MULTIDISCIPLINARY DESIGN OPTIMIZATION**
Ply layout optimization and micromechanics tailoring of composite aircraft engine structures
[BTN-95-EIX95112524206] p 196 A95-69302
- MULTIGRID METHODS**
Linear disturbances in hypersonic, chemically reacting shock layers
[BTN-94-EIX94441386605] p 182 A95-67336
- Shock layers and boundary layers in hypersonic flows
[HTN-95-A0003] p 183 A95-67830
- Three-dimensional analysis of scramjet nozzle flows
[BTN-94-EIX94441380978] p 196 A95-68162
- Navier-Stokes computation of a viscous optimized waverider
[BTN-95-EIX95041503782] p 193 A95-69213
- Numerical simulation of incidence and sweep effects on delta wing vortex breakdown
[BTN-95-EIX95062487526] p 186 A95-69234
- Inviscid and viscous flow modelling of complex aircraft configurations using the CFD simulation system sauna
[ARA-MEMO-403] p 211 N95-19777

N

NASA PROGRAMS

- Status of the NASA balloon program p 181 A95-66296
- Overview of the NASA balloon R&D program p 181 A95-66297

NATIONAL AEROSPACE PLANE PROGRAM

- National AeroSpace Plane: Technology transfer
[BTN-95-EIX95072498879] p 180 A95-68395

NAVIER-STOKES EQUATION

- Solution-adaptive structured-unstructured grid method for unsteady turbomachinery analysis. Part I: Methodology
[BTN-94-EIX94441380983] p 208 A95-67329
- Linear disturbances in hypersonic, chemically reacting shock layers
[BTN-94-EIX94441386605] p 182 A95-67336
- Shock layers and boundary layers in hypersonic flows
[HTN-95-A0003] p 183 A95-67830
- Three-dimensional analysis of scramjet nozzle flows
[BTN-94-EIX94441380978] p 196 A95-68162
- Navier-Stokes computation of a viscous optimized waverider
[BTN-95-EIX95041503782] p 193 A95-69213
- Numerical simulation of incidence and sweep effects on delta wing vortex breakdown
[BTN-95-EIX95062487526] p 186 A95-69234
- Inviscid and viscous flow modelling of complex aircraft configurations using the CFD simulation system sauna
[ARA-MEMO-403] p 211 N95-19777

NAVIGATION

- Development and flight test of a deployable precision landing system
[BTN-95-EIX95062487535] p 190 A95-69243

NAVIGATION AIDS

- On-the-fly carrier phase ambiguity resolution for precise aircraft landing
[BTN-95-EIX95112522535] p 190 A95-69328

NAVSTAR SATELLITES

- Effect of broadcast and precise ephemerides on estimates of the frequency stability of GPS Navstar clocks
[BTN-95-EIX95112522530] p 190 A95-69333

NEAR FIELDS

- Rotating Kirchhoff method for three-dimensional transonic blade-vortex interaction hover noise
[BTN-94-EIX94441386601] p 182 A95-67332

NEAR INFRARED RADIATION

- Possible near-IR channels for remote sensing precipitable water vapor from geostationary satellite platforms
[HTN-95-70139] p 214 A95-69431

NEWFOUNDLAND

- Aircraft icing measurements in East Coast winter storms
[HTN-95-60505] p 214 A95-68756

NICKEL ALLOYS

- Fatigue crack growth in nickel-based superalloys at 500-700 C. 1: Waspaloy
[BTN-94-EIX94371347843] p 206 A95-69136

NITRIC OXIDE

- Comparison of NO and OH planar fluorescence temperature measurements in scramjet model flowfields
[BTN-95-EIX95042474388] p 209 A95-68312

NITROGEN

- Measurement by coherent anti-Stokes Raman scattering in the R5Ch hypersonic wind tunnel
[BTN-95-EIX95112523811] p 188 A95-69322

NITROGEN DIOXIDE

- Three-dimensional model interpretation of NO(x) measurements from the lower stratosphere
[HTN-95-90534] p 213 A95-67806

NITROGEN OXIDES

- Three-dimensional model interpretation of NO(x) measurements from the lower stratosphere
[HTN-95-90534] p 213 A95-67806

NOISE GENERATORS

- Recent studies of rotorcraft blade-vortex interaction noise
[BTN-95-EIX95062487521] p 218 A95-69229

NOISE PREDICTION

- Rotating Kirchhoff method for three-dimensional transonic blade-vortex interaction hover noise
[BTN-94-EIX94441386601] p 182 A95-67332

NOISE REDUCTION

- Active control of wake/blade-row interaction noise
[BTN-95-EIX95042474389] p 196 A95-68311
- Noise and vibration control
[BTN-95-EIX95042477108] p 179 A95-68351

NONLINEAR EQUATIONS

- Finite element time domain - modal formulation for nonlinear flutter of composite panels
[BTN-95-EIX95042474401] p 203 A95-68299

NONLINEARITY

- Aeroelastic stability of hingeless rotor blade in hover using large deflection theory
[BTN-94-EIX94441386616] p 183 A95-67347

NOWCASTING

- Forecasting for a large field program: STORM-FEST
[HTN-95-90694] p 215 A95-69721

NOZZLE FLOW

- Three-dimensional analysis of scramjet nozzle flows
[BTN-94-EIX94441380978] p 196 A95-68162
- Lag model for turbulent boundary layers over rough bleed surfaces
[BTN-94-EIX94441380981] p 208 A95-68165
- Entrainment and acoustic variations in a round jet from introduced streamwise vorticity
[BTN-95-EIX95042474409] p 209 A95-68291

NUMERICAL ANALYSIS

- Construction of nearly orthogonal multiblock grids for compressible flow simulation
[BTN-94-EIX94361133526] p 207 A95-65981
- Solution-adaptive structured-unstructured grid method for unsteady turbomachinery analysis. Part I: Methodology
[BTN-94-EIX94441380983] p 208 A95-67329

NUMERICAL CONTROL

- Improved speed control system for the 87,000 HP wind tunnel drive
[NASA-TM-106840] p 211 N95-19794

NUMERICAL WEATHER FORECASTING

- WINDEX -- A new index for forecasting microburst potential
[HTN-95-90690] p 215 A95-69717

NYLON (TRADEMARK)

- Theoretical and actual performance of a long duration superpressure balloon made from a biaxially oriented nylon-6 film
p 181 A95-66282

O

OGIVES

- Passive porosity with free and fixed separation on a tangent-ogive forebody
[BTN-95-EIX95062487554] p 185 A95-68368

OPERATING COSTS

- Selecting and management of fire fighter aircraft
[BTN-95-EIX95062487538] p 193 A95-69246
- Protective coatings for compressor gas path components
p 201 N95-19675

OPERATIONAL HAZARDS

- Erosion, Corrosion and Foreign Object Damage Effects in Gas Turbines
[AGARD-CP-558] p 197 N95-19653
- The operation of gas turbine engines in hot and sandy conditions: Royal Air Force experiences in the Gulf conflict
p 198 N95-19655

OPTIMIZATION

- Two-point transonic airfoil design using optimization for improved off-design performance
[BTN-95-EIX95062487542] p 192 A95-68356
- Navier-Stokes computation of a viscous optimized waverider
[BTN-95-EIX95041503782] p 193 A95-69213

ORTHOGONALITY

- Construction of nearly orthogonal multiblock grids for compressible flow simulation
[BTN-94-EIX94361133526] p 207 A95-65981

OSCILLATIONS

- Linear disturbances in hypersonic, chemically reacting shock layers
[BTN-94-EIX94441386605] p 182 A95-67336
- Analysis of an oscillating Joukowski airfoil with surface suction and moving vortices
[BTN-95-EIX95062487527] p 186 A95-69235

OXIDATION

- Resistance of silicon nitride turbine components to erosion and hot corrosion/oxidation attack
p 202 N95-19683

OZONE DEPLETION

- Ozone, skin cancer, and the SST
[BTN-95-EIX95041503011] p 213 A95-68314

OZONOSPHERE

- Ozone, skin cancer, and the SST
[BTN-95-EIX95041503011] p 213 A95-68314

P

PANEL FLUTTER

- Finite element time domain - modal formulation for nonlinear flutter of composite panels
[BTN-95-EIX95042474401] p 203 A95-68299

PANEL METHOD (FLUID DYNAMICS)

- Vortex cutting by a blade. Part II: Computations of vortex response
[BTN-94-EIX94441386611] p 208 A95-67342

PANELS

- Soft body impact on titanium fan blades
p 200 N95-19671

PARACHUTE DESCENT

- Radial reefing method for accelerated and controlled parachute opening
[BTN-95-EIX95062487539] p 187 A95-69247

PARACHUTES

- Comparison of electrostatic and aerodynamic forces during parachute opening
[BTN-95-EIX95062487532] p 187 A95-69240
- Radial reefing method for accelerated and controlled parachute opening
[BTN-95-EIX95062487539] p 187 A95-69247

PARAFOILS

- Development and flight test of a deployable precision landing system
[BTN-95-EIX95062487535] p 190 A95-69243

PARALLEL COMPUTERS

- Parallel implicit unstructured grid Euler solvers
[BTN-95-EIX95042474393] p 217 A95-68307

PARALLEL PROCESSING (COMPUTERS)

- Parallel implicit unstructured grid Euler solvers
[BTN-95-EIX95042474393] p 217 A95-68307

PARTICLE SIZE DISTRIBUTION

- The calculation of erosion in a gas turbine compressor rotor
p 199 N95-19664

PARTICLE TRAJECTORIES

- Particle deposition in gas turbine blade film cooling holes
p 199 N95-19661

- Experimental and numerical simulations of the effects of ingested particles in gas turbine engines
p 199 N95-19662

- Particle trajectories in gas turbine engines
p 199 N95-19663

- The calculation of erosion in a gas turbine compressor rotor
p 199 N95-19664

PASSENGER AIRCRAFT

- Maintenance requirements for a supersonic transport
[BTN-95-EIX95031502751] p 179 A95-68258

PAYLOADS

- Recent trends in balloon flights from TIFR's National Balloon Facility, Hyderabad
p 191 A95-66300
- Design decisions from the history of the EUVE science payload
[HTN-95-60545] p 205 A95-69854

PEENING

- Fatigue resistance of peened 7050-T7451 aluminum alloy: Repair and re-treatment of a component surface
[BTN-94-EIX94371347838] p 206 A95-69131

PERFORMANCE PREDICTION

- Adaptive modeling of jet engine performance with application to condition monitoring
[BTN-95-EIX95112524205] p 196 A95-69303
- Nonlinear dynamic simulation of single- and multispool core engines, part 1: Computational method
[BTN-95-EIX95112524200] p 210 A95-69308

PERFORMANCE TESTS

- GPS/GLONASS/INS test program
[BTN-94-EIX94441386131] p 189 A95-68187
- Space flight tests of attitude determination using GPS
[BTN-95-EIX95112522529] p 190 A95-69334

PERTURBATION

- Aeroelastic stability of hingeless rotor blade in hover using large deflection theory
[BTN-94-EIX94441386616] p 183 A95-67347

PHASE SHIFT KEYING

- Evaluation of the radio frequency susceptibility of commercial GPS receivers
[BTN-95-EIX95042474624] p 189 A95-68278

PHASED ARRAYS

- Joint stars phased array radar antenna
[BTN-95-EIX95042474626] p 209 A95-68280
- Inband radar cross section of phased arrays with parallel feeds
[AD-A284249] p 210 N95-19730

PILOT PERFORMANCE

- Simulation and flight test evaluation of head-up-display guidance for harrier approach transitions
[BTN-95-EIX95062487533] p 194 A95-69241

PILOT TRAINING

- Programmable cockpit research simulator
[AD-A279219] p 204 N95-19848

PILOTLESS AIRCRAFT

- Environmental effects on composite airframes: A study conducted for the ARM UAV Program (Atmospheric Radiation Measurement Unmanned Aerospace Vehicle)
[DE94-015351] p 206 N95-19579

- Automation of hardware-in-the-loop testing of control systems for unmanned air vehicles
[AD-A284833] p 194 N95-19693

PISTON THEORY

- Finite element time domain - modal formulation for nonlinear flutter of composite panels
[BTN-95-EIX95042474401] p 203 A95-68299

PITCH (INCLINATION)

- Offset thrust axes and pitch stability
[BTN-95-EIX95062487553] p 203 A95-68367

PITCHING MOMENTS

- Navier-Stokes simulations of Orbiter aerodynamic characteristics including pitch trim and bodyflap
[BTN-95-EIX95041503779] p 204 A95-69210

PLANFORMS

- Aerodynamic effects of delta planform tip sails on wing performance
[BTN-95-EIX95062487544] p 185 A95-68358

PLASTIC DEFORMATION

- Impact loading of compressor stator vanes by hailstone ingestion
p 200 N95-19670
- Soft body impact on titanium fan blades
p 200 N95-19671

PLATE THEORY

- Coupling equivalent plate and finite element formulations in multiple-method structural analyses
[BTN-95-EIX95062487548] p 192 A95-68362

PNEUMATICS

- Dynamic behavior of valves with pneumatic chamber for reciprocating compressors
[BTN-94-EIX94351143311] p 207 A95-65845

POLAR METEOROLOGY

- Research aircraft observations of a polar low at the east Greenland ice edge
[HTN-95-A0175] p 215 A95-69766

POLISHING

- Fatigue resistance of peened 7050-T7451 aluminium alloy: Repair and re-treatment of a component surface [BTN-94-EIX94371347838] p 206 A95-69131

POLLUTION CONTROL

- Air pollution mitigation measures for airports and associated activity [PB94-207610] p 216 N95-19582

POLYETHYLENES

- French contribution to new balloon designs and materials p 181 A95-66277
Balloon flights in France and in Europe p 204 A95-66301

POLYMERIC FILMS

- Theoretical and actual performance of a long duration superpressure balloon made from a biaxially oriented nylon-6 film p 181 A95-66282
Recent trends in balloon flights from TIFR's National Balloon Facility, Hyderabad p 191 A95-66300

POLYNOMIALS

- Elliptic tip effects on the vortex wake of an axisymmetric body at incidence [BTN-94-EIX94441386612] p 208 A95-67343

POROSITY

- Passive porosity with free and fixed separation on a tangent-ogive forebody [BTN-95-EIX95062487554] p 185 A95-68368

POWERED LIFT AIRCRAFT

- Powered lift for land and sea [BTN-95-EIX95041503010] p 192 A95-68313

PRECIPITATION (METEOROLOGY)

- Aircraft icing measurements in East Coast winter storms [HTN-95-60505] p 214 A95-68756
WINDEX -- A new index for forecasting microburst potential [HTN-95-90690] p 215 A95-69717
Mesoscale structure of precipitation bands in a North Atlantic winter storm [HTN-95-40659] p 215 A95-69803

PRESSURE DISTRIBUTION

- Experimental and computational results for the external flowfield of a scramjet inlet [BTN-94-EIX94441380977] p 195 A95-68161
Suppression of vortex asymmetry and side force on a circular cone [BTN-95-EIX95042474413] p 209 A95-68287

PRESSURE EFFECTS

- Development of hypersonic engine seals: Flow effects of preload and engine pressures [BTN-95-EIX95112524204] p 196 A95-69304

PRESSURE GRADIENTS

- Behavior of the Johnson-King turbulence model in axisymmetric supersonic flows [BTN-94-EIX94441386606] p 183 A95-67337

PRESSURE MEASUREMENT

- Multiport pressure measurements on continuously moving wind tunnel models [ARA-MEMO-391] p 188 N95-19772

PRESSURE RECOVERY

- F/A-18 inlet calculations at 60-deg angle of attack and 10-deg sideslip [BTN-95-EIX95112524199] p 195 A95-69309
Numerical study of the performance of swept, curved compression surface scramjet inlets [BTN-95-EIX95112524198] p 197 A95-69310

PRESSURE REDUCTION

- Erosion of T56 5th stage rotor blades due to bleed hole overtip flow p 200 N95-19666

PRESSURE SENSORS

- Multiport pressure measurements on continuously moving wind tunnel models [ARA-MEMO-391] p 188 N95-19772

PRESTRESSING

- Development of hypersonic engine seals: Flow effects of preload and engine pressures [BTN-95-EIX95112524204] p 196 A95-69304

PROBABILITY DENSITY FUNCTIONS

- Modeling of supersonic turbulent combustion using assumed probability density functions [BTN-95-EIX95112524190] p 206 A95-69318

PROBLEM SOLVING

- PalymSys (TM): An extended version of CLIPS for construction and reasoning using blackboards p 217 N95-19767

PROPELLER BLADES

- Ice-impact analysis of blades p 200 N95-19672

PROPELLER FANS

- Ice-impact analysis of blades p 200 N95-19672

PROPULSION

- Powered lift for land and sea [BTN-95-EIX95041503010] p 192 A95-68313

PROPULSION SYSTEM PERFORMANCE

- Adaptive modeling of jet engine performance with application to condition monitoring [BTN-95-EIX95112524205] p 196 A95-69303

- Nonlinear dynamic simulation of single- and multispool core engines, part 1: Computational method [BTN-95-EIX95112524200] p 210 A95-69308

PROTECTIVE COATINGS

- Erosion, Corrosion and Foreign Object Damage Effects in Gas Turbines [AGARD-CP-558] p 197 N95-19653
Protective coatings for compressor gas path components p 201 N95-19675
New Trends in coatings developments for turbine blades: Materials processing and repair p 201 N95-19676
High velocity oxygen fuel spraying of erosion and wear resistant coatings on jet engine parts p 202 N95-19680

PUMPS

- An air-driven pressure booster pump for aircraft-based air sampling [HTN-95-40689] p 216 A95-69833

PYLONS

- The aerodynamic design of an integrated wing lower surface and pylons for reduced drag [ARA-MEMO-406] p 194 N95-19789

R

RADAR ANTENNAS

- Joint stars phased array radar antenna [BTN-95-EIX95042474626] p 209 A95-68280

RADAR CROSS SECTIONS

- Inband radar cross section of phased arrays with parallel feeds [AD-A284249] p 210 N95-19730

RADAR SCATTERING

- Inband radar cross section of phased arrays with parallel feeds [AD-A284249] p 210 N95-19730

RADAR TRACKING

- Joint stars phased array radar antenna [BTN-95-EIX95042474626] p 209 A95-68280

RADIATIVE TRANSFER

- Microwave and infrared simulations of an intense convective system and comparison with aircraft observations [HTN-95-60511] p 214 A95-68762

RADIO ANTENNAS

- Space flight tests of attitude determination using GPS [BTN-95-EIX95112522529] p 190 A95-69334
Design considerations for an archimedean slot spiral antenna p 211 N95-19798

RADIO FREQUENCY INTERFERENCE

- Evaluation of the radio frequency susceptibility of commercial GPS receivers [BTN-95-EIX95042474624] p 189 A95-68278

RADIO NAVIGATION

- GPS/GLONASS/INS test program [BTN-94-EIX94441386131] p 189 A95-68187
Integrated GPS/Glonass navigation: Algorithms and results [BTN-95-EIX95112522531] p 190 A95-69332

RADIO RECEIVERS

- Evaluation of the radio frequency susceptibility of commercial GPS receivers [BTN-95-EIX95042474624] p 189 A95-68278
Space flight tests of attitude determination using GPS [BTN-95-EIX95112522529] p 190 A95-69334

RAIN

- Nonhydrostatic simulation of frontogenesis in a moist atmosphere. Part 3: Thermal wind imbalance and rainbands [HTN-95-90356] p 212 A95-66429
Microwave and infrared simulations of an intense convective system and comparison with aircraft observations [HTN-95-60511] p 214 A95-68762

RAM ACCELERATORS

- New end tube closure system for the ram accelerator [BTN-94-EIX94441380974] p 195 A95-68158

RAMAN SPECTRA

- Planar air density measurements near model surfaces by ultraviolet Rayleigh/Raman scattering [BTN-94-EIX94441386614] p 213 A95-67345
Measurement by coherent anti-Stokes Raman scattering in the R5Ch hypersonic wind tunnel [BTN-95-EIX95112523811] p 188 A95-69322

RAMJET ENGINES

- Development of hypersonic engine seals: Flow effects of preload and engine pressures [BTN-95-EIX95112524204] p 196 A95-69304

RAYLEIGH SCATTERING

- Planar air density measurements near model surfaces by ultraviolet Rayleigh/Raman scattering [BTN-94-EIX94441386614] p 213 A95-67345

REACTING FLOW

- Modeling of supersonic turbulent combustion using assumed probability density functions [BTN-95-EIX95112524190] p 206 A95-69318

REACTION KINETICS

- Aircraft engine emission reduction [BTN-95-EIX95031502750] p 196 A95-68257

REAL TIME OPERATION

- PalymSys (TM): An extended version of CLIPS for construction and reasoning using blackboards p 217 N95-19767

RECIPROCATION

- Dynamic behavior of valves with pneumatic chamber for reciprocating compressors [BTN-94-EIX94351143311] p 207 A95-65845

RECTANGULAR WINGS

- Aerodynamic effects of delta planform tip sails on wing performance [BTN-95-EIX95062487544] p 185 A95-68358

REENTRY SHIELDING

- Trajectory-based heating analysis for the European Space Agency/Rosetta Earth Return Vehicle [BTN-95-EIX95041503787] p 205 A95-69218

REENTRY TRAJECTORIES

- Multiblock analysis for Shuttle Orbiter reentry heating from Mach 24 to Mach 12 [BTN-95-EIX95041503780] p 205 A95-69211

REENTRY VEHICLES

- Trajectory-based heating analysis for the European Space Agency/Rosetta Earth Return Vehicle [BTN-95-EIX95041503787] p 205 A95-69218

REFERENCE ATMOSPHERES

- Using IRI for the computation of ionospheric corrections for altimeter data analysis p 212 A95-66949

REFLECTANCE

- Possible near-IR channels for remote sensing precipitable water vapor from geostationary satellite platforms [HTN-95-70139] p 214 A95-69431

REGULATIONS

- Federal aviation regulations, part 91. General operating and flight rules. Change 8 [PB94-217445] p 188 N95-19720

REINFORCED SHELLS

- Launcher wing-leading-edge design [BTN-95-EIX95042477110] p 192 A95-68349

RELIABILITY ANALYSIS

- USAF aging aircraft program [BTN-95-EIX95072498878] p 180 A95-68394

REMOTE SENSING

- Possible near-IR channels for remote sensing precipitable water vapor from geostationary satellite platforms [HTN-95-70139] p 214 A95-69431

RESEARCH

- Aero-thermodynamic distortion induced structured dynamic response [AD-A279931] p 203 N95-19864

RESEARCH AIRCRAFT

- Microwave and infrared simulations of an intense convective system and comparison with aircraft observations [HTN-95-60511] p 214 A95-68762

RESEARCH AND DEVELOPMENT

- Balloon technology and observations; Symposium P3 of the COSPAR Plenary Meeting, 29th, Washington, DC, Aug. 28-Sept. 5, 1992 [HTN-95-70250] p 181 A95-66276

RESEARCH PROJECTS

- Future SSTs a European approach [BTN-95-EIX95072419883] p 180 A95-68396

RESEARCH VEHICLES

- Determination of stability and control derivatives from the NASA F/A-18 HARV from flight data using the maximum likelihood method [NASA-CR-197320] p 204 N95-19576

RESOLUTION

- Research requirements for future visual guidance systems [AD-A279188] p 191 N95-19810

RIGID ROTORS

- Aeroelastic stability of hingeless rotor blade in hover using large deflection theory [BTN-94-EIX94441386616] p 183 A95-67347

ROLLING MOMENTS

- Interference between tanker wing wake with roll-up and receiver aircraft [BTN-95-EIX95062487552] p 185 A95-68366

ROTARY WING AIRCRAFT

- Recent studies of rotorcraft blade-vortex interaction noise [BTN-95-EIX95062487521] p 218 A95-69229
Rotorcraft ditchings and water-related impacts that occurred from 1982 to 1989, phase 1 [AD-A279164] p 189 N95-19805

ROTARY WINGS

- Comparison of theory and experiment for non-linear flutter and stall response of a helicopter blade
[BTN-94-EIX94351108100] p 191 A95-66500
- Rotating Kirchhoff method for three-dimensional transonic blade-vortex interaction hover noise
[BTN-94-EIX94441386601] p 182 A95-67332
- Bilinear formulation applied to the response and stability of helicopter rotor blade
[BTN-95-EIX95042474400] p 192 A95-68300
- Using adaptive structures to attenuate rotary wing aeroelastic response
[BTN-95-EIX95062487547] p 192 A95-68361

ROTATING SHAFTS

- Modeling rotating shafts using axisymmetric solid finite elements with matrix reduction
[BTN-94-EIX94351143328] p 207 A95-67301

ROTATION

- Rotating Kirchhoff method for three-dimensional transonic blade-vortex interaction hover noise
[BTN-94-EIX94441386601] p 182 A95-67332
- Aeroelastic stability of hingeless rotor blade in hover using large deflection theory
[BTN-94-EIX94441386616] p 183 A95-67347

ROTOR BLADES (TURBOMACHINERY)

- Demonstration of an elastically coupled twist control concept for tilt rotor blade application
[BTN-94-EIX94441386633] p 196 A95-68182

ROTOR DYNAMICS

- Stability of magnetic bearing-rotor systems and the effects of gravity and damping
[BTN-94-EIX94441386619] p 208 A95-68168
- Demonstration of an elastically coupled twist control concept for tilt rotor blade application
[BTN-94-EIX94441386633] p 196 A95-68182
- Using adaptive structures to attenuate rotary wing aeroelastic response
[BTN-95-EIX95062487547] p 192 A95-68361

ROTORS

- Unbalance response of a dual rotor system: Theory and experiment
[BTN-94-EIX94351143320] p 195 A95-65854
- Modeling rotating shafts using axisymmetric solid finite elements with matrix reduction
[BTN-94-EIX94351143328] p 207 A95-67301
- Stability of magnetic bearing-rotor systems and the effects of gravity and damping
[BTN-94-EIX94441386619] p 208 A95-68168
- Recent studies of rotorcraft blade-vortex interaction noise
[BTN-95-EIX95062487521] p 218 A95-69229
- Wind tunnel tests of a 42 inch diameter self-starting autogyro rotor
[AD-A279922] p 188 N95-19863

RUNGE-KUTTA METHOD

- Parallel implicit unstructured grid Euler solvers
[BTN-95-EIX95042474393] p 217 A95-68307

S

SAFETY MANAGEMENT

- Rotorcraft ditchings and water-related impacts that occurred from 1982 to 1989, phase 1
[AD-A279164] p 189 N95-19805

SANDS

- The operation of gas turbine engines in hot and sandy conditions: Royal Air Force experiences in the Gulf conflict
p 198 N95-19655
- US Army rotorcraft turboshaft engines sand and dust erosion considerations
p 198 N95-19656
- Future directions in helicopter protection system configuration
p 198 N95-19657
- Erosion of T56 5th stage rotor blades due to bleed hole overtip flow
p 200 N95-19666

SATELLITE ALTIMETRY

- Using IRI for the computation of ionospheric corrections for altimeter data analysis
p 212 A95-66949

SATELLITE ATTITUDE CONTROL

- Space flight tests of attitude determination using GPS
[BTN-95-EIX9511252529] p 190 A95-69334

SATELLITE NAVIGATION SYSTEMS

- High accuracy navigation and landing system using GPS/IMU system integration
[BTN-94-EIX94441386129] p 189 A95-68185
- Results and performance of multi-site reference station differential GPS
[BTN-95-EIX9511252534] p 190 A95-69329

SATELLITE OBSERVATION

- Possible near-IR channels for remote sensing precipitable water vapor from geostationary satellite platforms
[HTN-95-70139] p 214 A95-69431

SCALE MODELS

- Particle deposition in gas turbine blade film cooling holes
p 199 N95-19661

SCATTERING

- Planar air density measurements near model surfaces by ultraviolet Rayleigh/Raman scattering
[BTN-94-EIX94441386614] p 213 A95-67345

SEALS (STOPPERS)

- Development of hypersonic engine seals: Flow effects of preload and engine pressures
[BTN-95-EIX95112524204] p 196 A95-69304

SEATS

- Dynamic behavior of valves with pneumatic chamber for reciprocating compressors
[BTN-94-EIX94351143311] p 207 A95-65845

SEPARATED FLOW

- State-space representation of aerodynamic characteristics of an aircraft at high angles of attack
[BTN-95-EIX95062487536] p 187 A95-69244

SEPARATORS

- Future directions in helicopter protection system configuration
p 198 N95-19657

SERVICE LIFE

- USAF aging aircraft program
[BTN-95-EIX95072498878] p 180 A95-68394
- Service life extensions for the C-141
[BTN-95-EIX95112530749] p 193 A95-69295

SHAPE FUNCTIONS

- Bilinear formulation applied to the response and stability of helicopter rotor blade
[BTN-95-EIX95042474400] p 192 A95-68300

SHAPES

- Repeatability of ice shapes in the NASA Lewis icing research tunnel
[BTN-95-EIX95062487528] p 204 A95-69236

SHOCK LAYERS

- Linear disturbances in hypersonic, chemically reacting shock layers
[BTN-94-EIX94441386605] p 182 A95-67336

SHOCK WAVE INTERACTION

- Aspects of vortex breakdown
[HTN-95-A0001] p 183 A95-67828

SHOCK WAVES

- Supersonic and hypersonic shock/boundary-layer interaction database
[BTN-94-EIX94441386604] p 182 A95-67335
- Shock layers and boundary layers in hypersonic flows
[HTN-95-A0003] p 183 A95-67830
- Measurement by coherent anti-Stokes Raman scattering in the R5Ch hypersonic wind tunnel
[BTN-95-EIX95112523811] p 188 A95-69322

SIDESLIP

- F/A-18 inlet calculations at 60-deg angle of attack and 10-deg sideslip
[BTN-95-EIX95112524199] p 195 A95-69309

SIGNAL PROCESSING

- Using IRI for the computation of ionospheric corrections for altimeter data analysis
p 212 A95-66949
- Evaluation of the radio frequency susceptibility of commercial GPS receivers
[BTN-95-EIX95042474624] p 189 A95-68278

SILICON CARBIDES

- Launcher wing-leading-edge design
[BTN-95-EIX95042477110] p 192 A95-68349

SILICON NITRIDES

- Resistance of silicon nitride turbine components to erosion and hot corrosion/oxidation attack
p 202 N95-19683

SIMULATION

- Unbalance response of a dual rotor system: Theory and experiment
[BTN-94-EIX94351143320] p 195 A95-65854
- Construction of nearly orthogonal multiblock grids for compressible flow simulation
[BTN-94-EIX94361133526] p 207 A95-65981

SKIN FRICTION

- Behavior of the Johnson-King turbulence model in axisymmetric supersonic flows
[BTN-94-EIX94441386606] p 183 A95-67337
- Vortical flow structure near the F/A-18 LEX at high incidence
[BTN-95-EIX95062487555] p 186 A95-68369

SLENDER BODIES

- Passive porosity with free and fixed separation on a tangent-ogive forebody
[BTN-95-EIX95062487554] p 185 A95-68368
- Aerodynamically blunt and sharp bodies
[BTN-95-EIX95041503781] p 205 A95-69212

SLENDER CONES

- Linear disturbances in hypersonic, chemically reacting shock layers
[BTN-94-EIX94441386605] p 182 A95-67336

SLENDER WINGS

- Experimental investigations on limit cycle wing rock of slender wings
[BTN-95-EIX95062487543] p 185 A95-68357

SLIDING FRICTION

- Surface morphology and structure of carbon-carbon composites in high-energy sliding contact
[BTN-94-EIX94371347996] p 206 A95-69164

SLOPES

- Elliptic tip effects on the vortex wake of an axisymmetric body at incidence
[BTN-94-EIX94441386612] p 208 A95-67343

SLOT ANTENNAS

- Design considerations for an archimedean slot spiral antenna
p 211 N95-19798

SMART STRUCTURES

- Twisting smartly in the wind
[BTN-95-EIX95041503093] p 184 A95-68353

SNOW

- Antarctic snow record of southern hemisphere lead pollution
[HTN-95-40359] p 212 A95-66869

SODIUM CHLORIDES

- Gas turbine compressor corrosion and erosion in Western Europe
p 201 N95-19678

SOFTWARE TOOLS

- The Computer Aided Aircraft-design Package (CAAP)
p 217 N95-19759

SOLID SOLUTIONS

- Multilayer anti-erosion coatings
p 201 N95-19679

SOUND FIELDS

- Rotating Kirchhoff method for three-dimensional transonic blade-vortex interaction hover noise
[BTN-94-EIX94441386601] p 182 A95-67332

SOUTHERN HEMISPHERE

- Antarctic snow record of southern hemisphere lead pollution
[HTN-95-40359] p 212 A95-66869

SPACE SHUTTLE ORBITERS

- Navier-Stokes simulations of Orbiter aerodynamic characteristics including pitch trim and bodyflap
[BTN-95-EIX95041503779] p 204 A95-69210
- Multiblock analysis for Shuttle Orbiter reentry heating from Mach 24 to Mach 12
[BTN-95-EIX95041503780] p 205 A95-69211

SPACE SHUTTLES

- Documentation and archiving of the Space Shuttle wind tunnel test data base. Volume 2: User's Guide to the Archived Data Base
[NASA-TM-104806-VOL-2] p 205 N95-19624

SPACECRAFT ANTENNAS

- Space flight tests of attitude determination using GPS
[BTN-95-EIX9511252529] p 190 A95-69334

SPACECRAFT RECOVERY

- Development and flight test of a deployable precision landing system
[BTN-95-EIX95062487535] p 190 A95-69243

SPACECRAFT REENTRY

- Multiblock analysis for Shuttle Orbiter reentry heating from Mach 24 to Mach 12
[BTN-95-EIX95041503780] p 205 A95-69211

SPACECRAFT SHIELDING

- Trajectory-based heating analysis for the European Space Agency/Rosetta Earth Return Vehicle
[BTN-95-EIX95041503787] p 205 A95-69218

SPEED CONTROL

- Improved speed control system for the 87,000 HP wind tunnel drive
[NASA-TM-106840] p 211 N95-19794

SPIRAL ANTENNAS

- Design considerations for an archimedean slot spiral antenna
p 211 N95-19798

SPRAYED COATINGS

- High velocity oxygen fuel spraying of erosion and wear resistant coatings on jet engine parts
p 202 N95-19680

SPRAYING

- High velocity oxygen fuel spraying of erosion and wear resistant coatings on jet engine parts
p 202 N95-19680

- Thermal testing of high performance thermal barrier coatings for turbine blades
p 202 N95-19681

STABILITY

- Lyapunov exponents and stochastic stability of two-dimensional parametrically excited random systems
[BTN-94-EIX94361122401] p 207 A95-65897
- Modeling rotating shafts using axisymmetric solid finite elements with matrix reduction
[BTN-94-EIX94351143328] p 207 A95-67301
- Linear disturbances in hypersonic, chemically reacting shock layers
[BTN-94-EIX94441386605] p 182 A95-67336
- Aeroelastic stability of hingeless rotor blade in hover using large deflection theory
[BTN-94-EIX94441386616] p 183 A95-67347
- Bilinear formulation applied to the response and stability of helicopter rotor blade
[BTN-95-EIX95042474400] p 192 A95-68300

- Fatigue resistance of peened 7050-T7451 aluminum alloy: Repair and re-treatment of a component surface [BTN-94-EIX94371347838] p 206 A95-69131
- STABILITY DERIVATIVES**
- State-space representation of aerodynamic characteristics of an aircraft at high angles of attack [BTN-95-EIX95062487536] p 187 A95-69244
- Aerodynamic characteristics of strake vortex flaps on a strake-wing configuration [BTN-95-EIX95062487537] p 187 A95-69245
- STABILITY TESTS**
- Linear disturbances in hypersonic, chemically reacting shock layers [BTN-94-EIX94441386605] p 182 A95-67336
- State-space representation of aerodynamic characteristics of an aircraft at high angles of attack [BTN-95-EIX95062487536] p 187 A95-69244
- STAGNATION FLOW**
- Measurement by coherent anti-Stokes Raman scattering in the R5Ch hypersonic wind tunnel [BTN-95-EIX95112523811] p 188 A95-69322
- STANDARDS**
- Corrosion prevention and control [BTN-95-EIX95031502753] p 188 A95-68260
- STATIC STABILITY**
- Offset thrust axes and pitch stability [BTN-95-EIX95062487533] p 203 A95-68367
- STATORS**
- Impact loading of compressor stator vanes by hailstone ingestion p 200 N95-19670
- STIFFNESS**
- Lyapunov exponents and stochastic stability of two-dimensional parametrically excited random systems [BTN-94-EIX94361122401] p 207 A95-65897
- STOCHASTIC PROCESSES**
- Lyapunov exponents and stochastic stability of two-dimensional parametrically excited random systems [BTN-94-EIX94361122401] p 207 A95-65897
- STORMS (METEOROLOGICAL)**
- Aircraft icing measurements in East Coast winter storms [HTN-95-60505] p 214 A95-68756
- Mesoscale structure of precipitation bands in a North Atlantic winter storm [HTN-95-40659] p 215 A95-69803
- STOVL AIRCRAFT**
- Powered lift for land and sea [BTN-95-EIX95041503010] p 192 A95-68313
- Simulation and flight test evaluation of head-up-display guidance for harrier approach transitions [BTN-95-EIX95062487533] p 194 A95-69241
- STRAKES**
- Aerodynamic characteristics of strake vortex flaps on a strake-wing configuration [BTN-95-EIX95062487537] p 187 A95-69245
- STRATOSPHERE**
- Recent trends in balloon flights from TIFR's National Balloon Facility, Hyderabad p 191 A95-66300
- Long duration balloons p 191 A95-66305
- Three-dimensional model interpretation of NO(x) measurements from the lower stratosphere [HTN-95-90534] p 213 A95-67806
- Ozone, skin cancer, and the SST [BTN-95-EIX95041503011] p 213 A95-68314
- An air-driven pressure booster pump for aircraft-based air sampling [HTN-95-40689] p 216 A95-69833
- STRESS ANALYSIS**
- A comparative study of internally and externally capped balloons using small scale test balloons p 181 A95-66285
- STRESS FUNCTIONS**
- Theoretical and actual performance of a long duration superpressure balloon made from a biaxially oriented nylon-6 film p 181 A95-66282
- STRESS INTENSITY FACTORS**
- Fatigue crack growth in nickel-based superalloys at 500-700 C. 1: Waspaloy [BTN-94-EIX94371347843] p 206 A95-69136
- STRUCTURAL ANALYSIS**
- A comparative study of internally and externally capped balloons using small scale test balloons p 181 A95-66285
- Overview of the NASA balloon R&D program p 181 A95-66297
- Computerized maintenance aid [BTN-95-EIX95031502749] p 217 A95-68256
- Simplified analysis of general instability of stiffened shells with cutouts in pure bending [BTN-95-EIX95042474418] p 209 A95-68282
- Biinert formulation applied to the response and stability of helicopter rotor blade [BTN-95-EIX95042474400] p 192 A95-68300
- Proceedings of the USAF Structural Integrity Program Conference [AD-A285684] p 194 N95-19517

STRUCTURAL DESIGN

- Coupling equivalent plate and finite element formulations in multiple-method structural analyses [BTN-95-EIX95062487548] p 192 A95-68362
- Ply layout optimization and micromechanics tailoring of composite aircraft engine structures [BTN-95-EIX95112524206] p 196 A95-69302
- STRUCTURAL FAILURE**
- Simplified analysis of general instability of stiffened shells with cutouts in pure bending [BTN-95-EIX95042474418] p 209 A95-68282
- Proceedings of the USAF Structural Integrity Program Conference [AD-A285684] p 194 N95-19517
- STRUCTURAL MEMBERS**
- Lyapunov exponents and stochastic stability of two-dimensional parametrically excited random systems [BTN-94-EIX94361122401] p 207 A95-65897
- STRUCTURAL RELIABILITY**
- USAF aging aircraft program [BTN-95-EIX95072498878] p 180 A95-68394
- STRUCTURAL VIBRATION**
- Noise and vibration control [BTN-95-EIX95042477108] p 179 A95-68351
- SUBMARINES**
- Application of three-dimensional hybrid structured/unstructured grids to land, sea and air vehicles [ARA-MEMO-399] p 210 N95-19775
- SUBSONIC FLOW**
- F/A-18 inlet calculations at 60-deg angle of attack and 10-deg sideslip [BTN-95-EIX95112524199] p 195 A95-69309
- SUBSONIC SPEED**
- Preliminary assessment of tunnel wall interference in the NDA cryogenic wind tunnel [BTN-95-EIX95062487531] p 187 A95-69239
- SUCTION**
- Analysis of an oscillating Joukowski airfoil with surface suction and moving vortices [BTN-95-EIX95062487527] p 186 A95-69235
- SULFUR DIOXIDES**
- Gas turbine compressor corrosion and erosion in Western Europe p 201 N95-19678
- SUPERCARGERS**
- Advanced diesel electronic fuel injection and turbocharging [AD-A279176] p 211 N95-19809
- SUPERPRESSURE BALLOONS**
- Theoretical and actual performance of a long duration superpressure balloon made from a biaxially oriented nylon-6 film p 181 A95-66282
- Long duration balloons p 191 A95-66305
- SUPERSONIC AIRCRAFT**
- Ozone, skin cancer, and the SST [BTN-95-EIX95041503011] p 213 A95-68314
- Development of an efficient inverse method for supersonic and hypersonic body design [BTN-95-EIX95041503784] p 180 A95-69215
- SUPERSONIC COMBUSTION**
- Comparison of NO and OH planar fluorescence temperature measurements in scramjet model flowfields [BTN-95-EIX95042474388] p 209 A95-68312
- Modeling of supersonic turbulent combustion using assumed probability density functions [BTN-95-EIX95112524190] p 206 A95-69318
- SUPERSONIC COMBUSTION RAMJET ENGINES**
- Experimental and computational results for the external flowfield of a scramjet inlet [BTN-94-EIX94441380977] p 195 A95-68161
- Three-dimensional analysis of scramjet nozzle flows [BTN-94-EIX94441380978] p 196 A95-68162
- Comparison of NO and OH planar fluorescence temperature measurements in scramjet model flowfields [BTN-95-EIX95042474388] p 209 A95-68312
- Numerical study of the performance of swept, curved compression surface scramjet inlets [BTN-95-EIX95112524198] p 197 A95-69310
- SUPERSONIC CRUISE AIRCRAFT RESEARCH**
- Future SSTs a European approach [BTN-95-EIX95072419883] p 180 A95-68396
- SUPERSONIC FLOW**
- Behavior of the Johnson-King turbulence model in axisymmetric supersonic flows [BTN-94-EIX94441386606] p 183 A95-67337
- Design and operation of a supersonic annular flow facility [BTN-94-EIX94441386624] p 183 A95-68173
- Numerical computations of supersonic base flow with special emphasis on turbulence modeling [BTN-94-EIX94441386632] p 179 A95-68181
- Influence of injectant Mach number and temperature on supersonic film cooling [BTN-94-EIX94441386686] p 184 A95-68195

- Numerical study of the performance of swept, curved compression surface scramjet inlets [BTN-95-EIX95112524198] p 197 A95-69310
- SUPERSONIC INLETS**
- Lag model for turbulent boundary layers over rough bleed surfaces [BTN-94-EIX94441380981] p 208 A95-68165
- Numerical study of the performance of swept, curved compression surface scramjet inlets [BTN-95-EIX95112524198] p 197 A95-69310
- On supersonic-inlet boundary-layer bleed flow [NASA-CR-195426] p 202 N95-19769
- SUPERSONIC NOZZLES**
- Three-dimensional analysis of scramjet nozzle flows [BTN-94-EIX94441380978] p 196 A95-68162
- SUPERSONIC SPEED**
- Aerodynamically blunt and sharp bodies [BTN-95-EIX95041503781] p 205 A95-69212
- Minimum-drag axisymmetric bodies in the supersonic/hypersonic flow regimes [BTN-95-EIX95041503785] p 180 A95-69216
- Interpretation of waverider performance data using computational fluid dynamics [BTN-95-EIX95062487534] p 193 A95-69242
- SUPERSONIC TRANSPORTS**
- Future SSTs a European approach [BTN-95-EIX95072419883] p 180 A95-68396
- SUPERSONIC WIND TUNNELS**
- Design and operation of a supersonic annular flow facility [BTN-94-EIX94441386624] p 183 A95-68173
- Improved speed control system for the 87,000 HP wind tunnel drive [NASA-TM-106840] p 211 N95-19794
- SURFACE NAVIGATION**
- Use of MOBITEK wireless wide area networks as a solution to land-based positioning and navigation [BTN-94-EIX94441386132] p 189 A95-68188
- Results and performance of multi-site reference station differential GPS [BTN-95-EIX95112522534] p 190 A95-69329
- SURFACE PROPERTIES**
- Observations of fluxes and inland breezes over a heterogeneous surface [HTN-95-80258] p 212 A95-66315
- Surface morphology and structure of carbon-carbon composites in high-energy sliding contact [BTN-94-EIX94371347996] p 206 A95-69164
- Possible near-IR channels for remote sensing precipitable water vapor from geostationary satellite platforms [HTN-95-70139] p 214 A95-69431
- Experimental and numerical simulations of the effects of ingested particles in gas turbine engines p 199 N95-19662
- SURFACE REACTIONS**
- Review of numerical procedures for computational surface thermochemistry [BTN-94-EIX94441386682] p 205 A95-68191
- Powerful bolide explosion over North Italy [HTN-95-80564] p 218 A95-69658
- Experimental and numerical simulations of the effects of ingested particles in gas turbine engines p 199 N95-19662
- SURFACE TREATMENT**
- Fatigue resistance of peened 7050-T7451 aluminum alloy: Repair and re-treatment of a component surface [BTN-94-EIX94371347838] p 206 A95-69131
- SWEEP ANGLE**
- Aerodynamic effects of delta planform tip sails on wing performance [BTN-95-EIX95062487544] p 185 A95-68358
- SWEEP EFFECT**
- Numerical simulation of incidence and sweep effects on delta wing vortex breakdown [BTN-95-EIX95062487526] p 186 A95-69234
- SWEEP WINGS**
- Tip vortex on a swept wing. Mean flow and unsteady phenomena [BTN-94-EIX94441385755] p 184 A95-68219
- SYNCHRONOUS MOTORS**
- Starter/generator testing [BTN-95-EIX95072498877] p 210 A95-68393
- SYNCHRONOUS SATELLITES**
- Possible near-IR channels for remote sensing precipitable water vapor from geostationary satellite platforms [HTN-95-70139] p 214 A95-69431
- SYNOPTIC METEOROLOGICAL**
- Research aircraft observations of a polar low at the east Greenland ice edge [HTN-95-A0175] p 215 A95-69766
- Mesoscale structure of precipitation bands in a North Atlantic winter storm [HTN-95-40659] p 215 A95-69803

SYSTEMS ANALYSIS

- GPS/GLONASS/INS test program
[BTN-94-EIX94441386131] p 189 A95-68187

T

TEMPERATURE EFFECTS

- Theoretical and actual performance of a long duration superpressure balloon made from a biaxially oriented nylon-6 film p 181 A95-66282
Influence of injectant Mach number and temperature on supersonic film cooling [BTN-94-EIX94441386686] p 184 A95-68195
An investigation of drag repeatability in half model testing in the ARA Transonic Wind Tunnel [ARA-MEMO-392] p 188 N95-19546

TEMPERATURE MEASUREMENT

- Comparison of NO and OH planar fluorescence temperature measurements in scramjet model flowfields [BTN-95-EIX95042474388] p 209 A95-68312
Measurement by coherent anti-Stokes Raman scattering in the R5Ch hypersonic wind tunnel [BTN-95-EIX95112523811] p 188 A95-69322

TENSILE TESTS

- Soft body impact on titanium fan blades p 200 N95-19671

THERMAL ANALYSIS

- Multiblock analysis for Shuttle Orbiter reentry heating from Mach 24 to Mach 12 [BTN-95-EIX95041503780] p 205 A95-69211
Trajectory-based heating analysis for the European Space Agency/Rosetta Earth Return Vehicle [BTN-95-EIX95041503787] p 205 A95-69218

THERMAL BOUNDARY LAYER

- Prediction of ice accretion: Comparison between the 2D and 3D codes [BTN-94-EIX94441385753] p 213 A95-68217

THERMAL CONTROL COATINGS

- Thermal testing of high performance thermal barrier coatings for turbine blades p 202 N95-19681

THERMAL FATIGUE

- Thermal testing of high performance thermal barrier coatings for turbine blades p 202 N95-19681

THERMAL INSULATION

- Review of numerical procedures for computational surface thermochemistry [BTN-94-EIX94441386682] p 205 A95-68191

THERMAL SHOCK

- Thermal testing of high performance thermal barrier coatings for turbine blades p 202 N95-19681

THERMAL STABILITY

- Nonhydrostatic simulation of frontogenesis in a moist atmosphere. Part 3: Thermal wind imbalance and rainbands [HTN-95-90356] p 212 A95-66429

THERMAL STRESSES

- Finite element time domain - modal formulation for nonlinear flutter of composite panels [BTN-95-EIX95042474401] p 203 A95-68299

THIN PLATES

- Interaction of a streamwise vortex with a thin plate: A source of turbulent buffeting [BTN-95-EIX95042474398] p 209 A95-68302

THREE DIMENSIONAL BOUNDARY LAYER

- Experimental study of three-dimensional separation [BTN-94-EIX94441385752] p 179 A95-68216
Approximate method for calculating heating rates on three-dimensional vehicles [BTN-95-EIX95041503778] p 210 A95-69209

THREE DIMENSIONAL FLOW

- Three-dimensional analysis of scramjet nozzle flows [BTN-94-EIX94441380978] p 196 A95-68162
Prediction of ice accretion: Comparison between the 2D and 3D codes [BTN-94-EIX94441385753] p 213 A95-68217
Interaction of a streamwise vortex with a thin plate: A source of turbulent buffeting [BTN-95-EIX95042474398] p 209 A95-68302
Validation and evaluation of the advanced aeronautical CFD system SAUNA: A method developer's view [ARA-MEMO-390] p 210 N95-19774

THREE DIMENSIONAL MODELS

- Microwave and infrared simulations of an intense convective system and comparison with aircraft observations [HTN-95-60511] p 214 A95-68762
Numerical simulation of incidence and sweep effects on delta wing vortex breakdown [BTN-95-EIX95062487526] p 186 A95-69234
Application of three-dimensional hybrid structured/unstructured grids to land, sea and air vehicles [ARA-MEMO-399] p 210 N95-19775

THREE DIMENSIONAL MOTION

- Aerodynamic sensitivity coefficients using the three-dimensional full potential equation [BTN-95-EIX95062487530] p 186 A95-69238

THRUST

- Offset thrust axes and pitch stability [BTN-95-EIX95062487553] p 203 A95-68367

THUNDERSTORMS

- WINDEX -- A new index for forecasting microburst potential [HTN-95-90690] p 215 A95-69717

TILTING ROTORS

- Demonstration of an elastically coupled twist control concept for tilt rotor blade application [BTN-94-EIX94441386633] p 196 A95-68182

TIME LAG

- Using IRI for the computation of ionospheric corrections for altimeter data analysis p 212 A95-66949

TITANIUM

- Soft body impact on titanium fan blades p 200 N95-19671

TITANIUM ALLOYS

- National AeroSpace Plane: Technology transfer [BTN-95-EIX95072498879] p 180 A95-68395
Fatigue resistance of peened 7050-T7451 aluminium alloy: Repair and re-treatment of a component surface [BTN-94-EIX94371347838] p 206 A95-69131

TITANIUM NITRIDES

- Protective coatings for compressor gas path components p 201 N95-19675

TOLERANCES (MECHANICS)

- Corrosion prevention and control [BTN-95-EIX95031502753] p 188 A95-68260
Proceedings of the USAF Structural Integrity Program Conference [AD-A285684] p 194 N95-19517

TOXIC HAZARDS

- Developing an emission factor for hazardous air pollutants for an F-16 using JP-8 fuel [AD-A284802] p 216 N95-19685

TRACKING (POSITION)

- A technique for detecting a tropical cyclone center using a Doppler radar [HTN-95-20631] p 215 A95-69574

TRAILING EDGES

- Erosion of T56 5th stage rotor blades due to bleed hole overtip flow p 200 N95-19666

TRAINING EVALUATION

- Programmable cockpit research simulator [AD-A279219] p 204 N95-19848

TRANSONIC FLIGHT

- Aerodynamic sensitivity coefficients using the three-dimensional full potential equation [BTN-95-EIX95062487530] p 186 A95-69238

TRANSONIC FLOW

- Rotating Kirchhoff method for three-dimensional transonic blade-vortex interaction hover noise [BTN-94-EIX94441386601] p 182 A95-67332
Validation and evaluation of the advanced aeronautical CFD system SAUNA: A method developer's view [ARA-MEMO-390] p 210 N95-19774

TRANSONIC SPEED

- Two-point transonic airfoil design using optimization for improved off-design performance [BTN-95-EIX95062487542] p 192 A95-68356

TRANSONIC WIND TUNNELS

- An investigation of drag repeatability in half model testing in the ARA Transonic Wind Tunnel [ARA-MEMO-392] p 188 N95-19546
Multiport pressure measurements on continuously moving wind tunnel models [ARA-MEMO-391] p 188 N95-19772

TRANSPORT AIRCRAFT

- Corrosion prevention and control [BTN-95-EIX95031502753] p 188 A95-68260
Ozone, skin cancer, and the SST [BTN-95-EIX95041503011] p 213 A95-68314
Application of circulation control to advanced subsonic transport aircraft. Part 1: Airfoil development [BTN-95-EIX95062487545] p 185 A95-68359
Application of circulation control to advanced subsonic transport aircraft. Part 2: Transport application [BTN-95-EIX95062487546] p 185 A95-68360
Proceedings of the USAF Structural Integrity Program Conference [AD-A285684] p 194 N95-19517
Transport aircraft loading and balancing system: Using a CLIPS expert system for military aircraft load planning [AD-A279164] p 217 N95-19751

TRANSPORT PROPERTIES

- Kinetic theory in aerothermodynamics [HTN-95-A0002] p 183 A95-67829

TRANSPORTATION

- Rotorcraft ditchings and water-related impacts that occurred from 1982 to 1989, phase 1 [AD-A279164] p 189 N95-19805

TRAPPED VORTICES

- Analysis of an oscillating Joukowski airfoil with surface suction and moving vortices [BTN-95-EIX95062487527] p 186 A95-69235

TRENDS

- New Trends in coatings developments for turbine blades: Materials processing and repair p 201 N95-19676

TRIBOLOGY

- Surface morphology and structure of carbon-carbon composites in high-energy sliding contact [BTN-94-EIX94371347996] p 206 A95-69164

TROPOSPHERE

- Possible near-IR channels for remote sensing precipitable water vapor from geostationary satellite platforms [HTN-95-70139] p 214 A95-69431

TURBINE BLADES

- An analysis of the costs and benefits in improving F402-RR-406A High Pressure Turbine, second stage blades under the aircraft engine Component Improvement Program (CIP) [AD-A285127] p 197 N95-19595
Out of area experiences with the RB199 in Toronto p 198 N95-19654
Particle deposition in gas turbine blade film cooling holes p 199 N95-19661
Experimental and numerical simulations of the effects of ingested particles in gas turbine engines p 199 N95-19662
Damage of high temperature components by dust-laden air p 201 N95-19673
New Trends in coatings developments for turbine blades: Materials processing and repair p 201 N95-19676
Thermal testing of high performance thermal barrier coatings for turbine blades p 202 N95-19681
Resistance of silicon nitride turbine components to erosion and hot corrosion/oxidation attack p 202 N95-19683
Evidence that aerodynamic effects, including dynamic stall, dictate HAWT structural loads and power generation in highly transient time frames [DE94-011865] p 216 N95-19855

TURBINE ENGINES

- Modern transport engine experience with environmental ingestion effects p 199 N95-19660
Damage of high temperature components by dust-laden air p 201 N95-19673
New Trends in coatings developments for turbine blades: Materials processing and repair p 201 N95-19676

TURBOCOMPRESSORS

- Performance deterioration of axial compressors due to blade defects p 199 N95-19665
Impact loading of compressor stator vanes by dust-laden ingestion p 200 N95-19670
Advanced diesel electronic fuel injection and turbocharging [AD-A279176] p 211 N95-19809

TURBOJET ENGINES

- Unbalance response of a dual rotor system: Theory and experiment [BTN-94-EIX94351143320] p 195 A95-65854

TURBOMACHINERY

- Rotor whirl forces induced by the tip clearance effect in axial flow compressors [BTN-94-EIX94351143331] p 207 A95-67304
Solution-adaptive structured-unstructured grid method for unsteady turbomachinery analysis. Part I: Methodology [BTN-94-EIX94441380983] p 208 A95-67329

TURBOSHAPTS

- US Army rotorcraft turboshaft engines sand and dust erosion considerations p 198 N95-19656
Future directions in helicopter protection system configuration p 198 N95-19657

TURBULENCE

- Model for compressible turbulence in hypersonic wall boundary and high-speed mixing layers [BTN-94-EIX94441386625] p 184 A95-68174
Tip vortex on a swept wing. Mean flow and unsteady phenomena [BTN-94-EIX94441385755] p 184 A95-68219

TURBULENCE MODELS

- Supersonic and hypersonic shock/boundary-layer interaction database [BTN-94-EIX94441386604] p 182 A95-67335
Behavior of the Johnson-King turbulence model in axisymmetric supersonic flows [BTN-94-EIX94441386606] p 183 A95-67337
Shock layers and boundary layers in hypersonic flows [HTN-95-A0003] p 183 A95-67830
Lag model for turbulent boundary layers over rough bleed surfaces [BTN-94-EIX94441380981] p 208 A95-68165
Model for compressible turbulence in hypersonic wall boundary and high-speed mixing layers [BTN-94-EIX94441386625] p 184 A95-68174

Numerical computations of supersonic base flow with special emphasis on turbulence modeling
[BTN-94-EIX94441386632] p 179 A95-68181
Numerical simulation of incidence and sweep effects on delta wing vortex breakdown
[BTN-95-EIX95062487526] p 186 A95-69234
Modeling of supersonic turbulent combustion using assumed probability density functions
[BTN-95-EIX95112524190] p 206 A95-69318
Inviscid and viscous flow modelling of complex aircraft configurations using the CFD simulation system sauna [ARA-MEMO-403] p 211 N95-19777

TURBULENT BOUNDARY LAYER

Lag model for turbulent boundary layers over rough bleed surfaces
[BTN-94-EIX94441380981] p 208 A95-68165
Design and operation of a supersonic annular flow facility
[BTN-94-EIX94441386624] p 183 A95-68173
Experimental study of three-dimensional separation
[BTN-94-EIX94441385752] p 179 A95-68216

TURBULENT COMBUSTION

Modeling of supersonic turbulent combustion using assumed probability density functions
[BTN-95-EIX95112524190] p 206 A95-69318

TURBULENT FLOW

Observations of fluxes and inland breezes over a heterogeneous surface
[HTN-95-80258] p 212 A95-66315
Aspects of vortex breakdown
[HTN-95-A0001] p 183 A95-67828
Design and operation of a supersonic annular flow facility
[BTN-94-EIX94441386624] p 183 A95-68173
Numerical computations of supersonic base flow with special emphasis on turbulence modeling
[BTN-94-EIX94441386632] p 179 A95-68181
Interaction of a streamwise vortex with a thin plate: A source of turbulent buffeting
[BTN-95-EIX95042474398] p 209 A95-68302
Numerical study of the performance of swept, curved compression surface scramjet inlets
[BTN-95-EIX95112524198] p 197 A95-69310

TURBULENT WAKES

Phenomenological description and simplified modelling of the vortex wake issuing from a jet in a crossflow
[BTN-94-EIX94441385754] p 184 A95-68218

TWISTED WINGS

Demonstration of an elastically coupled twist control concept for tilt rotor blade application
[BTN-94-EIX94441386633] p 196 A95-68182

TWISTING

Twisting smartly in the wind
[BTN-95-EIX95041503093] p 184 A95-68353

TWO DIMENSIONAL FLOW

Prediction of ice accretion: Comparison between the 2D and 3D codes
[BTN-94-EIX94441385753] p 213 A95-68217
Parallel implicit unstructured grid Euler solvers
[BTN-95-EIX95042474393] p 217 A95-68307

TWO DIMENSIONAL MODELS

Nonhydrostatic simulation of frontogenesis in a moist atmosphere. Part 3: Thermal wind imbalance and rainbands
[HTN-95-90356] p 212 A95-66429

U

UNSTEADY AERODYNAMICS

Continuous gust response and sensitivity derivatives using state-space models
[BTN-95-EIX95062487551] p 203 A95-68365
State-space representation of aerodynamic characteristics of an aircraft at high angles of attack
[BTN-95-EIX95062487536] p 187 A95-69244
Evidence that aerodynamic effects, including dynamic stall, dictate HAWT structural loads and power generation in highly transient time frames
[DE94-011865] p 216 N95-19855

UNSTEADY FLOW

Solution-adaptive structured-unstructured grid method for unsteady turbomachinery analysis. Part I: Methodology
[BTN-94-EIX94441380983] p 208 A95-67329
Rotating Kirchhoff method for three-dimensional transonic blade-vortex interaction hover noise
[BTN-94-EIX94441386601] p 182 A95-67332
Lift analysis of a variable camber foil using the discrete vortex-blob method
[BTN-94-EIX94441386623] p 179 A95-68172
Tip vortex on a swept wing. Mean flow and unsteady phenomena
[BTN-94-EIX94441385755] p 184 A95-68219
Active control of wake/blade-row interaction noise
[BTN-95-EIX95042474389] p 196 A95-68311

URBAN TRANSPORTATION

Air pollution mitigation measures for airports and associated activity
[PB94-207610] p 216 N95-19582

V

VANES

Impact loading of compressor stator vanes by hailstone ingestion
p 200 N95-19670
Protective coatings for compressor gas path components
p 201 N95-19675
Braze repair possibilities for hot section gas turbine parts
p 201 N95-19677

VELOCITY DISTRIBUTION

Aspects of vortex breakdown
[HTN-95-A0001] p 183 A95-67828

VERTICAL DISTRIBUTION

Nonhydrostatic simulation of frontogenesis in a moist atmosphere. Part 3: Thermal wind imbalance and rainbands
[HTN-95-90356] p 212 A95-66429
Possible near-IR channels for remote sensing precipitable water vapor from geostationary satellite platforms
[HTN-95-70139] p 214 A95-69431

VERTICAL LANDING

Simulation and flight test evaluation of head-up-display guidance for carrier approach transitions
[BTN-95-EIX95062487533] p 194 A95-69241

VERTICAL MOTION

Observations of fluxes and inland breezes over a heterogeneous surface
[HTN-95-80258] p 212 A95-66315

VIBRATION DAMPING

Design optimization of aircraft engine-mount systems.
[BTN-94-EIX94351143325] p 195 A95-67298
Noise and vibration control
[BTN-95-EIX95042477108] p 179 A95-68351
Using adaptive structures to attenuate rotary wing aeroelastic response
[BTN-95-EIX95062487547] p 192 A95-68361

VIBRATION MODE

Unbalance response of a dual rotor system: Theory and experiment
[BTN-94-EIX94351143320] p 195 A95-65854

VISCOUS FLOW

Construction of nearly orthogonal multiblock grids for compressible flow simulation
[BTN-94-EIX94361133526] p 207 A95-65981
Solution-adaptive structured-unstructured grid method for unsteady turbomachinery analysis. Part I: Methodology
[BTN-94-EIX94441380983] p 208 A95-67329
Inviscid and viscous flow modelling of complex aircraft configurations using the CFD simulation system sauna [ARA-MEMO-403] p 211 N95-19777

VISUAL AIDS

Research requirements for future visual guidance systems
[AD-A279188] p 191 N95-19810

VISUAL FLIGHT RULES

Federal aviation regulations, part 91. General operating and flight rules. Change 8
[PB94-217445] p 188 N95-19720

VORTEX ADVISORY SYSTEM

A technique for detecting a tropical cyclone center using a Doppler radar
[HTN-95-20631] p 215 A95-69574

VORTEX BREAKDOWN

Aspects of vortex breakdown
[HTN-95-A0001] p 183 A95-67828
Adaptive computations of flow around a delta wing with vortex breakdown
[BTN-94-EIX94441386631] p 184 A95-68180
Numerical simulation of incidence and sweep effects on delta wing vortex breakdown
[BTN-95-EIX95062487526] p 186 A95-69234

VORTEX FLAPS

Aerodynamic characteristics of strake vortex flaps on a strake-wing configuration
[BTN-95-EIX95062487537] p 187 A95-69245

VORTEX GENERATORS

Experimental study of three-dimensional separation
[BTN-94-EIX94441385752] p 179 A95-68216
Entrainment and acoustic variations in a round jet from introduced streamwise vorticity
[BTN-95-EIX95042474409] p 209 A95-68291

VORTEX LATTICE METHOD

Numerical simulation of steady and unsteady, vorticity-dominated aerodynamic interference
[BTN-95-EIX95062487524] p 186 A95-69232

VORTEX SHEETS

Vortex cutting by a blade. Part II: Computations of vortex response
[BTN-94-EIX94441386611] p 208 A95-67342
Tip vortex on a swept wing. Mean flow and unsteady phenomena
[BTN-94-EIX94441385755] p 184 A95-68219

VORTICES

Vortex cutting by a blade. Part II: Computations of vortex response
[BTN-94-EIX94441386611] p 208 A95-67342
Elliptic tip effects on the vortex wake of an axisymmetric body at incidence
[BTN-94-EIX94441386612] p 208 A95-67343
Aspects of vortex breakdown
[HTN-95-A0001] p 183 A95-67828
Lift analysis of a variable camber foil using the discrete vortex-blob method
[BTN-94-EIX94441386623] p 179 A95-68172
Adaptive computations of flow around a delta wing with vortex breakdown
[BTN-94-EIX94441386631] p 184 A95-68180
Experimental study of three-dimensional separation
[BTN-94-EIX94441385752] p 179 A95-68216
Phenomenological description and simplified modelling of the vortex wake issuing from a jet in a crossflow
[BTN-94-EIX94441385754] p 184 A95-68218
Suppression of vortex asymmetry and side force on a circular cone
[BTN-95-EIX95042474413] p 209 A95-68287
Entrainment and acoustic variations in a round jet from introduced streamwise vorticity
[BTN-95-EIX95042474409] p 209 A95-68291
Vortical flow structure near the F/A-18 LEX at high incidence
[BTN-95-EIX95062487555] p 186 A95-68369
Research aircraft observations of a polar low at the east Greenland ice edge
[HTN-95-A0175] p 215 A95-69766

VORTICITY

Nonhydrostatic simulation of frontogenesis in a moist atmosphere. Part 3: Thermal wind imbalance and rainbands
[HTN-95-90356] p 212 A95-66429
Entrainment and acoustic variations in a round jet from introduced streamwise vorticity
[BTN-95-EIX95042474409] p 209 A95-68291
Interaction of a streamwise vortex with a thin plate: A source of turbulent buffeting
[BTN-95-EIX95042474398] p 209 A95-68302
Numerical simulation of steady and unsteady, vorticity-dominated aerodynamic interference
[BTN-95-EIX95062487524] p 186 A95-69232

W

WAKES

Elliptic tip effects on the vortex wake of an axisymmetric body at incidence
[BTN-94-EIX94441386612] p 208 A95-67343
Active control of wake/blade-row interaction noise
[BTN-95-EIX95042474389] p 196 A95-68311
Effect of ground and ceiling planes on shape of energized wakes
[BTN-95-EIX95062487558] p 186 A95-68372

WALL FLOW

Design and operation of a supersonic annular flow facility
[BTN-94-EIX94441386624] p 183 A95-68173
Model for compressible turbulence in hypersonic wall boundary and high-speed mixing layers
[BTN-94-EIX94441386625] p 184 A95-68174
Preliminary assessment of tunnel wall interference in the NDA cryogenic wind tunnel
[BTN-95-EIX95062487531] p 187 A95-69239
Two-variable method for blockage wall interference in a circular tunnel
[BTN-95-EIX95062487540] p 187 A95-69248

WASPALOY

Fatigue crack growth in nickel-based superalloys at 500-700 C. 1: Waspaloy
[BTN-94-EIX94371347843] p 206 A95-69136

WATER VAPOR

Possible near-IR channels for remote sensing precipitable water vapor from geostationary satellite platforms
[HTN-95-70139] p 214 A95-69431

WAVE FRONTS

On wave-front curvature in linear stability theory
[BTN-94-EIX94441385756] p 184 A95-68220

WAVERIDERS

Waveriders with finlets
[BTN-95-EIX95062487541] p 184 A95-68355

SUBJECT INDEX

Navier-Stokes computation of a viscous optimized waverider
[BTN-95-EIX95041503782] p 193 A95-69213

Hypersonic waverider test vehicle: A logical next step
[BTN-95-EIX95041503783] p 193 A95-69214

Interpretation of waverider performance data using computational fluid dynamics
[BTN-95-EIX95062487534] p 193 A95-69242

WEAR
Surface morphology and structure of carbon-carbon composites in high-energy sliding contact
[BTN-94-EIX94371347996] p 206 A95-69164

WEAR RESISTANCE
Corrosion prevention and control
[BTN-95-EIX95031502753] p 188 A95-68260

High velocity oxygen fuel spraying of erosion and wear resistant coatings on jet engine parts
p 202 N95-19680

WEATHER FORECASTING
A technique for detecting a tropical cyclone center using a Doppler radar
[HTN-95-20631] p 215 A95-69574

WIND SHEAR
Conditions associated with large-drop regions
[HTN-95-10686] p 214 A95-68845

WIND TUNNEL DRIVES
Improved speed control system for the 87,000 HP wind tunnel drive
[NASA-TM-106840] p 211 N95-19794

WIND TUNNEL MODELS
Preliminary assessment of tunnel wall interference in the NDA cryogenic wind tunnel
[BTN-95-EIX95062487531] p 187 A95-69239

Multipoint pressure measurements on continuously moving wind tunnel models
[ARA-MEMO-391] p 188 N95-19772

WIND TUNNEL TESTS
Comparison of theory and experiment for non-linear flutter and stall response of a helicopter blade
[BTN-94-EIX94351108100] p 191 A95-66500

Experimental study of three-dimensional separation
[BTN-94-EIX94441385752] p 179 A95-68216

Tip vortex on a swept wing. Mean flow and unsteady phenomena
[BTN-94-EIX94441385755] p 184 A95-68219

Suppression of vortex asymmetry and side force on a circular cone
[BTN-95-EIX95042474413] p 209 A95-68287

Vortical flow structure near the F/A-18A LEX at high incidence
[BTN-95-EIX95062487555] p 186 A95-68369

Effect of ground and ceiling planes on shape of energized wakes
[BTN-95-EIX95062487558] p 186 A95-68372

Recent studies of rotorcraft blade-vortex interaction noise
[BTN-95-EIX95062487521] p 218 A95-69229

Repeatability of ice shapes in the NASA Lewis icing research tunnel
[BTN-95-EIX95062487528] p 204 A95-69236

Preliminary assessment of tunnel wall interference in the NDA cryogenic wind tunnel
[BTN-95-EIX95062487531] p 187 A95-69239

Comparison of electrostatic and aerodynamic forces during parachute opening
[BTN-95-EIX95062487532] p 187 A95-69240

An investigation of drag repeatability in half model testing in the ARA Transonic Wind Tunnel
[ARA-MEMO-392] p 188 N95-19546

Documentation and archiving of the Space Shuttle wind tunnel test data base: Volume 2: User's Guide to the Archived Data Base
[NASA-TM-104806-VOL-2] p 205 N95-19624

Prediction of wind tunnel effects on the installed F/A-18A inlet flow field at high angles-of-attack
[NASA-CR-195429] p 197 N95-19651

Multipoint pressure measurements on continuously moving wind tunnel models
[ARA-MEMO-391] p 188 N95-19772

Wind tunnel tests of a 42 inch diameter self-starting autogyro rotor
[AD-A279922] p 188 N95-19863

WIND TUNNEL WALLS
Preliminary assessment of tunnel wall interference in the NDA cryogenic wind tunnel
[BTN-95-EIX95062487531] p 187 A95-69239

Two-variable method for blockage wall interference in a circular tunnel
[BTN-95-EIX95062487540] p 187 A95-69248

Prediction of wind tunnel effects on the installed F/A-18A inlet flow field at high angles-of-attack
[NASA-CR-195429] p 197 N95-19651

WIND TUNNELS
Planar air density measurements near model surfaces by ultraviolet Rayleigh/Raman scattering
[BTN-94-EIX94441386614] p 213 A95-67345

Prediction of wind tunnel effects on the installed F/A-18A inlet flow field at high angles-of-attack
[NASA-CR-195429] p 197 N95-19651

WIND TURBINES
Evidence that aerodynamic effects, including dynamic stall, dictate HAWT structural loads and power generation in highly transient time frames
[DE94-011865] p 216 N95-19855

WIND VELOCITY
A technique for detecting a tropical cyclone center using a Doppler radar
[HTN-95-20631] p 215 A95-69574

WING CAMBER
Lift analysis of a variable camber foil using the discrete vortex-blob method
[BTN-94-EIX94441386623] p 179 A95-68172

WING LOADING
Experimental investigations on limit cycle wing rock of slender wings
[BTN-95-EIX95062487543] p 185 A95-68357

WING OSCILLATIONS
Experimental investigations on limit cycle wing rock of slender wings
[BTN-95-EIX95062487543] p 185 A95-68357

WING TIP VORTICES
Tip vortex on a swept wing. Mean flow and unsteady phenomena
[BTN-94-EIX94441385755] p 184 A95-68219

WING-FUSELAGE STORES
The aerodynamic design of an integrated wing lower surface and pylons for reduced drag
[ARA-MEMO-406] p 194 N95-19789

WINGLETS
Aerodynamic effects of delta planform tip sails on wing performance
[BTN-95-EIX95062487544] p 185 A95-68358

WINGS
Planar air density measurements near model surfaces by ultraviolet Rayleigh/Raman scattering
[BTN-94-EIX94441386614] p 213 A95-67345

Launcher wing-leading-edge design
[BTN-95-EIX95042477110] p 192 A95-68349

Twisting smartly in the wind
[BTN-95-EIX95041503093] p 184 A95-68353

Application of circulation control to advanced subsonic transport aircraft. Part 1: Airfoil development
[BTN-95-EIX95062487545] p 185 A95-68359

Application of circulation control to advanced subsonic transport aircraft. Part 2: Transport application
[BTN-95-EIX95062487546] p 185 A95-68360

Influence of structural and aerodynamic modeling on flutter analysis
[BTN-95-EIX95062487550] p 203 A95-68364

Interference between tanker wing wake with roll-up and receiver aircraft
[BTN-95-EIX95062487552] p 185 A95-68366

Numerical simulation of steady and unsteady, vorticity-dominated aerodynamic interference
[BTN-95-EIX95062487524] p 186 A95-69232

Analysis of an oscillating Joukowski airfoil with surface suction and moving vortices
[BTN-95-EIX95062487527] p 186 A95-69235

Aerodynamic sensitivity coefficients using the three-dimensional full potential equation
[BTN-95-EIX95062487530] p 186 A95-69238

Aerodynamic characteristics of strake vortex flaps on a strake-wing configuration
[BTN-95-EIX95062487537] p 187 A95-69245

WINTER
Aircraft icing measurements in East Coast winter storms
[HTN-95-60505] p 214 A95-68756

Mesoscale structure of precipitation bands in a North Atlantic winter storm
[HTN-95-40659] p 215 A95-69803

WIRELESS COMMUNICATION
Use of MOBITEK wireless wide area networks as a solution to land-based positioning and navigation
[BTN-94-EIX94441386132] p 189 A95-68188

WORKLOADS (PSYCHOPHYSIOLOGY)
Programmable cockpit research simulator
[AD-A279219] p 204 N95-19848

X

X-29 AIRCRAFT
Numerical simulation of steady and unsteady, vorticity-dominated aerodynamic interference
[BTN-95-EIX95062487524] p 186 A95-69232

ZIRCONIUM OXIDES

Y

YTTRIUM OXIDES

Thermal testing of high performance thermal barrier coatings for turbine blades p 202 N95-19681

Z

ZIRCONIUM OXIDES

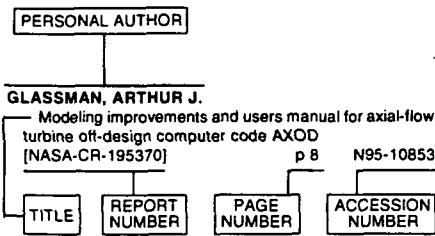
Thermal testing of high performance thermal barrier coatings for turbine blades p 202 N95-19681

PERSONAL AUTHOR INDEX

AERONAUTICAL ENGINEERING / A Continuing Bibliography (Supplement 317)

May 1995

Typical Personal Author Index Listing



Listings in this index are arranged alphabetically by personal author. The title of the document is used to provide a brief description of the subject matter. The report number helps to indicate the type of document (e.g., NASA report, translation, NASA contractor report). The page and accession numbers are located beneath and to the right of the title. Under any one author's name the accession numbers are arranged in sequence.

A

- ADLER, ROBERT F.**
Microwave and infrared simulations of an intense convective system and comparison with aircraft observations
[HTN-95-60511] p 214 A95-68762
- ALEXOPOULOS, G. A.**
Modeling of supersonic turbulent combustion using assumed probability density functions
[BTN-95-EIX95112524190] p 206 A95-69318
- ALGE, T. L.**
Modern transport engine experience with environmental ingestion effects
p 199 N95-19660
- ALPERINE, S.**
New Trends in coatings developments for turbine blades: Materials processing and repair
p 201 N95-19676
- ALTER, STEPHEN J.**
Multiblock analysis for Shuttle Orbiter reentry heating from Mach 24 to Mach 12
[BTN-95-EIX95041503780] p 205 A95-69211
- ANDRESEN, P.**
Planar air density measurements near model surfaces by ultraviolet Rayleigh/Raman scattering
[BTN-94-EIX94441386614] p 213 A95-67345
- ANON**
Starter/generator testing
[BTN-95-EIX95072498877] p 210 A95-68393
National AeroSpace Plane: Technology transfer
[BTN-95-EIX95072498879] p 180 A95-68395
- AOSHIMA, M.**
Dynamic behavior of valves with pneumatic chamber for reciprocating compressors
[BTN-94-EIX94351143311] p 207 A95-65845
- ARBOGAST, E.**
Nonhydrostatic simulation of frontogenesis in a moist atmosphere. Part 3: Thermal wind imbalance and rainbands
[HTN-95-90356] p 212 A95-66429
- ARENA, ANDREW S., JR.**
Experimental investigations on limit cycle wing rock of slender wings
[BTN-95-EIX95062487543] p 185 A95-68357

- ARIARATNAM, S. T.**
Lyapunov exponents and stochastic stability of two-dimensional parametrically excited random systems
[BTN-94-EIX94361122401] p 207 A95-65897
- ARNAL, D.**
Shock layers and boundary layers in hypersonic flows
[HTN-95-A0003] p 183 A95-67830
- ASGHAR, A.**
Suppression of vortex asymmetry and side force on a circular cone
[BTN-95-EIX95042474413] p 209 A95-68287
- ASHRAFIUON, H.**
Design optimization of aircraft engine-mount systems.
[BTN-94-EIX94351143325] p 195 A95-67298
- ATHRE, K.**
Unbalance response of a dual rotor system: Theory and experiment
[BTN-94-EIX94351143320] p 195 A95-65854
- ATTIA, M.**
Nonlinear dynamic simulation of single- and multispool core engines, part 1: Computational method
[BTN-95-EIX95112524200] p 210 A95-69308
- AUDEBERT, M.**
Balloon flights in France and in Europe
p 204 A95-66301
- AULT, D. A.**
Experimental and computational results for the external flowfield of a scramjet inlet
[BTN-94-EIX94441380977] p 195 A95-68161
- AUPOIX, B.**
Shock layers and boundary layers in hypersonic flows
[HTN-95-A0003] p 183 A95-67830
- AUSLENDER, AARON H.**
Numerical study of the performance of swept, curved compression surface scramjet inlets
[BTN-95-EIX95112524198] p 197 A95-69310

B

- BAILEY, JEFF**
Aircraft electric field measurements: Calibration and ambient field retrieval
[HTN-95-90508] p 213 A95-67780
- BALLARD, DAN**
PalymSys (TM): An extended version of CLIPS for construction and reasoning using blackboards
p 217 N95-19767
- BANKS, DANIEL W.**
Passive porosity with free and fixed separation on a tangent-ogive forebody
[BTN-95-EIX95062487554] p 185 A95-68368
- BARBERIS, D.**
Experimental study of three-dimensional separation
[BTN-94-EIX94441385752] p 179 A95-68216
- BARKHIMER, R. L.**
Advanced diesel electronic fuel injection and turbocharging
[AD-A279176] p 211 N95-19809
- BARRY, B. C.**
Erosion of T56 5th stage rotor blades due to bleed hole overtup flow
p 200 N95-19666
- BAUER, STEVEN X. S.**
Passive porosity with free and fixed separation on a tangent-ogive forebody
[BTN-95-EIX95062487554] p 185 A95-68368
- BAURLE, R. A.**
Modeling of supersonic turbulent combustion using assumed probability density functions
[BTN-95-EIX95112524190] p 206 A95-69318
- BECK, N. J.**
Advanced diesel electronic fuel injection and turbocharging
[AD-A279176] p 211 N95-19809
- BECKLEY, B.**
Using IRI for the computation of ionospheric corrections for altimeter data analysis
p 212 A95-66949
- BECKS, EDWARD A.**
Improved speed control system for the 87,000 HP wind tunnel drive
[NASA-TM-106840] p 211 N95-19794
- BELALA, Y.**
Transport aircraft loading and balancing system: Using a CLIPS expert system for military aircraft load planning
p 217 N95-19751
- BELL, DOUGLAS P.**
A comparative study of internally and externally capped balloons using small scale test balloons
p 181 A95-66285
- BENCIC, TIMOTHY J.**
Improved speed control system for the 87,000 HP wind tunnel drive
[NASA-TM-106840] p 211 N95-19794
- BERTAMINI, L.**
Thermal testing of high performance thermal barrier coatings for turbine blades
p 202 N95-19681
- BEUSHAUSEN, V.**
Planar air density measurements near model surfaces by ultraviolet Rayleigh/Raman scattering
[BTN-94-EIX94441386614] p 213 A95-67345
- BILITZA, D.**
Using IRI for the computation of ionospheric corrections for altimeter data analysis
p 212 A95-66949
- BIRCH, STUART**
Aircraft engine emission reduction
[BTN-95-EIX95031502750] p 196 A95-68257
Maintenance requirements for a supersonic transport
[BTN-95-EIX95031502751] p 179 A95-68258
- BLOMENHOFER, HELMUT**
On-the-fly carrier phase ambiguity resolution for precise aircraft landing
[BTN-95-EIX95112522535] p 190 A95-69328
- BLOY, A. W.**
Interference between tanker wing wake with roll-up and receiver aircraft
[BTN-95-EIX95062487552] p 185 A95-68366
- BLUMENTHAL, PHILIP Z.**
Improved speed control system for the 87,000 HP wind tunnel drive
[NASA-TM-106840] p 211 N95-19794
- BOGDANOFF, DAVID W.**
New end tube closure system for the ram accelerator
[BTN-94-EIX94441380974] p 195 A95-68158
- BOND, THOMAS H.**
Repeatability of ice shapes in the NASA Lewis icing research tunnel
[BTN-95-EIX95062487528] p 204 A95-69236
- BONEY, B.**
A program for scientific and applied investigations using aerostat complexes
p 182 A95-66304
- BOUCHARDY, P.**
Measurement by coherent anti-Stokes Raman scattering in the R5Ch hypersonic wind tunnel
[BTN-95-EIX95112523811] p 188 A95-69322
- BOWERSOX, RODNEY D. W.**
Model for compressible turbulence in hypersonic wall boundary and high-speed mixing layers
[BTN-94-EIX94441386625] p 184 A95-68174
- BRASSEUR, GUY**
Three-dimensional model interpretation of NO(x) measurements from the lower stratosphere
[HTN-95-90534] p 213 A95-67806
- BRAZIER, J. PH.**
Shock layers and boundary layers in hypersonic flows
[HTN-95-A0003] p 183 A95-67830
- BREITBACH, ELMAR J.**
Using adaptive structures to attenuate rotary wing aeroelastic response
[BTN-95-EIX95062487547] p 192 A95-68361
- BRENNAN, SEAN**
Airship applications of modern flight test techniques
[AD-A284253] p 194 N95-19731
- BRENNINKMEIJER, C. A. M.**
An air-driven pressure booster pump for aircraft-based air sampling
[HTN-95-40689] p 216 A95-69833
- BRIDGES, DAVID H.**
Elliptic tip effects on the vortex wake of an axisymmetric body at incidence
[BTN-94-EIX94441386612] p 208 A95-67343

AUTHOR

BROOKS, T. F.

- BROOKS, T. F.**
Recent studies of rotorcraft blade-vortex interaction noise
[BTN-95-EIX95062487521] p 218 A95-69229
- BROWN, JOHN M.**
Forecasting for a large field program: STORM-FEST
[HTN-95-90694] p 215 A95-69721
- BROWN, STEVE WESLEY**
Documentation and archiving of the Space Shuttle wind tunnel test data base. Volume 2: User's Guide to the Archived Data Base
[NASA-TM-104806-VOL-2] p 205 N95-19624
- BRYSON, TRAVIS**
PalymSys (TM): An extended version of CLIPS for construction and reasoning using blackboards
p 217 N95-19767
- BUISSON, JAMES A.**
Effect of broadcast and precise ephemerides on estimates of the frequency stability of GPS Navstar clocks
[BTN-95-EIX95112522530] p 190 A95-69333
- BUIVUN, N. A.**
The joint Russian-Brazil research on balloons
p 182 A95-66303
- BURNETT, DAVID W.**
Hypersonic waverider test vehicle: A logical next step
[BTN-95-EIX95041503783] p 193 A95-69214
- BURNS, I. F.**
An investigation of drag repeatability in half model testing in the ARA Transonic Wind Tunnel
[ARA-MEMO-392] p 188 N95-19546
- BUSONNET, P. X.**
Design of fan blades subjected to bird impact
p 200 N95-19669
- BYRNES, R. T.**
Fatigue crack growth in nickel-based superalloys at 500-700 C. 1: Waspaloy
[BTN-94-EIX94371347843] p 206 A95-69136

C

- CAI, ZHONG**
Development of hypersonic engine seals: Flow effects of preload and engine pressures
[BTN-95-EIX95112524204] p 196 A95-69304
- CAILLY, C.**
Nonhydrostatic simulation of frontogenesis in a moist atmosphere. Part 3: Thermal wind imbalance and rainbands
[HTN-95-90356] p 212 A95-66429
- CARLSON, LELAND A.**
Aerodynamic sensitivity coefficients using the three-dimensional full potential equation
[BTN-95-EIX95062487530] p 186 A95-69238
- CARROLL, FRANK T.**
Testing considerations for military aircraft engines in corrosive environments (a Navy perspective)
p 202 N95-19684
- CASTELLANI, A.**
Selecting and management of fire fighter aircraft
[BTN-95-EIX95062487538] p 193 A95-69246
- CHAMIS, C. C.**
Ice-impact analysis of blades
p 200 N95-19672
- CHAMPIGNY, P.**
Side forces at high angles of attack. Why, when, how?
[BTN-95-EIX95112523809] p 194 A95-69324
- CHANETZ, B.**
Measurement by coherent anti-Stokes Raman scattering in the R5Ch hypersonic wind tunnel
[BTN-95-EIX95112523811] p 188 A95-69322
- CHEN, CHARLES C.**
Rotorcraft ditchings and water-related impacts that occurred from 1982 to 1989, phase 1
[AD-A279164] p 189 N95-19805
- CHILDS, P. N.**
Validation and evaluation of the advanced aeronautical CFD system SAUNA: A method developer's view
[ARA-MEMO-390] p 210 N95-19774
- CHIU, CHYN-SHAN**
Analysis of an oscillating Joukowski airfoil with surface suction and moving vortices
[BTN-95-EIX95062487527] p 186 A95-69235
- CHO, MAENG HYO**
Aeroelastic stability of hingeless rotor blade in hover using large deflection theory
[BTN-94-EIX94441386616] p 183 A95-67347
- CHRISTIAN, HUGH J.**
Aircraft electric field measurements: Calibration and ambient field retrieval
[HTN-95-90508] p 213 A95-67780
- CLARK, G.**
Fatigue resistance of peened 7050-T7451 aluminum alloy: Repair and re-treatment of a component surface
[BTN-94-EIX94371347838] p 206 A95-69131

B-2

- CLAYTON, J. Q.**
Fatigue resistance of peened 7050-T7451 aluminum alloy: Repair and re-treatment of a component surface
[BTN-94-EIX94371347838] p 206 A95-69131
- COBER, STEWART G.**
Aircraft icing measurements in East Coast winter storms
[HTN-95-60505] p 214 A95-68756
- COCKRELL, CHARLES E., JR.**
Interpretation of waverider performance data using computational fluid dynamics
[BTN-95-EIX95062487534] p 193 A95-69242
- COHEN, CLARK E.**
Space flight tests of attitude determination using GPS
[BTN-95-EIX95112522529] p 190 A95-69334
- COLLINS, JAMES E.**
Three-dimensional model interpretation of NO(x) measurements from the lower stratosphere
[HTN-95-90534] p 213 A95-67806
- CONEL, J. E.**
Possible near-IR channels for remote sensing precipitable water vapor from geostationary satellite platforms
[HTN-95-70139] p 214 A95-69431
- COOPER, THOMAS D.**
Proceedings of the USAF Structural Integrity Program Conference
[AD-A285684] p 194 N95-19517
- COULTON, DAVID G.**
Multiport pressure measurements on continuously moving wind tunnel models
[ARA-MEMO-391] p 188 N95-19772
- COUSTEIX, J.**
Shock layers and boundary layers in hypersonic flows
[HTN-95-A0003] p 183 A95-67830
- COX, R. A.**
Wavenders with finlets
[BTN-95-EIX95062487541] p 184 A95-68355
- CRAVEN, D. A.**
Programmable cockpit research simulator
[AD-A279219] p 204 N95-19848
- CREMA, L. BALIS**
Selecting and management of fire fighter aircraft
[BTN-95-EIX95062487538] p 193 A95-69246
- CURRIE, T. C.**
Erosion of T56 5th stage rotor blades due to bleed hole overtup flow
p 200 N95-19666
- DAHER, JOHN K.**
Evaluation of the radio frequency susceptibility of commercial GPS receivers
[BTN-95-EIX95042474624] p 189 A95-68278
- DALY, PETER**
Integrated GPS/Glonass navigation: Algorithms and results
[BTN-95-EIX95112522531] p 190 A95-69332
- DAMLE, S. V.**
Recent trends in balloon flights from TIFR's National Balloon Facility, Hyderabad
p 191 A95-66300
- DAVIES, ELIZABETH**
The use of genetic algorithms for flight test and evaluation of artificial intelligence and complex software systems
[AD-A284824] p 217 N95-19688
- DECKER, R. A.**
Lift analysis of a variable camber foil using the discrete vortex-blob method
[BTN-94-EIX94441386623] p 179 A95-68172
- DEJARNETTE, F. R.**
Approximate method for calculating heating rates on three-dimensional vehicles
[BTN-95-EIX95041503778] p 210 A95-69209
- DELERY, JEAN M.**
Aspects of vortex breakdown
[HTN-95-A0001] p 183 A95-67828
- DESJARDINS, R. L.**
Observations of fluxes and inland breezes over a heterogeneous surface
[HTN-95-80258] p 212 A95-66315
- DIGIANFRANCESCO, A.**
Thermal testing of high performance thermal barrier coatings for turbine blades
p 202 N95-19681
- DIMARCO, PETER CHARLES**
Navy foreign object damage and its impact on future gas turbine engine low pressure compression systems
p 198 N95-19658
- DJEPA-PETROVA, V. S.**
A program for scientific and applied investigations using aerostat complexes
p 182 A95-66304
- DODSON, LORI J.**
Supersonic and hypersonic shock/boundary-layer interaction database
[BTN-94-EIX94441386604] p 182 A95-67335

PERSONAL AUTHOR INDEX

- DORR, D. W.**
Simulation and flight test evaluation of head-up-display guidance for harrier approach transitions
[BTN-95-EIX95062487533] p 194 A95-69241
- DOUGLAS, MICHAEL W.**
Research aircraft observations of a polar low at the east Greenland ice edge
[HTN-95-A0175] p 215 A95-69766
- DOWELL, E. H.**
Comparison of theory and experiment for non-linear flutter and stall response of a helicopter blade
[BTN-94-EIX94351108100] p 191 A95-66500
- DOWN, M. G.**
Out of area experiences with the RB199 in Toronto
p 198 N95-19654

E

- EDWARDS, VERNON R.**
US Army rotorcraft turboshaft engines sand and dust erosion considerations
p 198 N95-19656
- EHRICH, F.**
Rotor whirl forces induced by the tip clearance effect in axial flow compressors
[BTN-94-EIX94351143331] p 207 A95-67304
- EKATERINARIS, J. A.**
Numerical simulation of incidence and sweep effects on delta wing vortex breakdown
[BTN-95-EIX95062487526] p 186 A95-69234
- EL-BANNA, HESHAM M.**
Aerodynamic sensitivity coefficients using the three-dimensional full potential equation
[BTN-95-EIX95062487530] p 186 A95-69238
- ELDER, R. L.**
Particle trajectories in gas turbine engines
p 199 N95-19663
- ELLIOTT, WILLIAM R.**
USAF aging aircraft program
[BTN-95-EIX95072498878] p 180 A95-68394
- ELZEDDA, JAMAL M.**
Numerical simulation of steady and unsteady, vorticity-dominated aerodynamic interference
[BTN-95-EIX95062487524] p 186 A95-69232
- ENGLAR, ROBERT J.**
Application of circulation control to advanced subsonic transport aircraft. Part 1: Airfoil development
[BTN-95-EIX95062487545] p 185 A95-68359
- ENGLAR, ROBERT J.**
Application of circulation control to advanced subsonic transport aircraft. Part 2: Transport application
[BTN-95-EIX95062487546] p 185 A95-68360
- EYL, S.**
Two-point transonic airfoil design using optimization for improved off-design performance
[BTN-95-EIX95062487542] p 192 A95-68356

F

- FARGES, C.**
Multilayer anti-erosion coatings
p 201 N95-19679
- FEDOR, L. S.**
Research aircraft observations of a polar low at the east Greenland ice edge
[HTN-95-A0175] p 215 A95-69766
- FEES, WILLIAM A.**
Space flight tests of attitude determination using GPS
[BTN-95-EIX95112522529] p 190 A95-69334
- FLEETER, SANFORD**
Aero-thermodynamic distortion induced structured dynamic response
[AD-A279931] p 203 N95-19864
- FLOKAS, VASSILIOS**
Inband radar cross section of phased arrays with parallel feeds
[AD-A284249] p 210 N95-19730
- FROMENHOFF, HUBERT I.**
Brief history of gust models for aircraft design
[BTN-95-EIX95062487557] p 203 A95-68371
- FOGARTY, K. M.**
Rotorcraft ditchings and water-related impacts that occurred from 1982 to 1989, phase 1
[AD-A279164] p 189 N95-19805
- FOLKINS, IAN**
Three-dimensional model interpretation of NO(x) measurements from the lower stratosphere
[HTN-95-90534] p 213 A95-67806
- FOX, DENNIS S.**
Resistance of silicon nitride turbine components to erosion and hot corrosion/oxidation attack
p 202 N95-19683
- FRADKIN, M. I.**
The joint Russian-Brazil research on balloons
p 182 A95-66303

FRISCHBIER, J.

Impact loading of compressor stator vanes by hailstone ingestion p 200 N95-19670

G

GAO, B.-C.

Possible near-IR channels for remote sensing precipitable water vapor from geostationary satellite platforms [HTN-95-70139] p 214 A95-69431

GARFINKLE, MOISHE

Twisting smartly in the wind [BTN-95-EIX95041503093] p 184 A95-68353

GEHAUSEN, PAUL

Putting the ACSYNT on aircraft design [BTN-95-EIX95072419881] p 180 A95-68398

GEORGALA, J. M.

Validation and evaluation of the advanced aeronautical CFD system SAUNA: A method developer's view [ARA-MEMO-390] p 210 N95-19774

GEORGALA, JEANETTE M.

Application of three-dimensional hybrid structured/unstructured grids to land, sea and air vehicles [ARA-MEMO-399] p 210 N95-19775

GESSNER, F. B.

Design and operation of a supersonic annular flow facility [BTN-94-EIX94441386624] p 183 A95-68173

GILES, GARY L.

Coupling equivalent plate and finite element formulations in multiple-method structural analyses [BTN-95-EIX95062487548] p 192 A95-68362

GLENNLIGHTSEY, E.

Space flight tests of attitude determination using GPS [BTN-95-EIX95112522529] p 190 A95-69334

GNOFFO, PETER A.

Navier-Stokes simulations of Orbiter aerodynamic characteristics including pitch trim and bodyflap [BTN-95-EIX95041503779] p 204 A95-69210
Multiblock analysis for Shuttle Orbiter reentry heating from Mach 24 to Mach 12 [BTN-95-EIX95041503780] p 205 A95-69211

GOETZ, A. F. H.

Possible near-IR channels for remote sensing precipitable water vapor from geostationary satellite platforms [HTN-95-70139] p 214 A95-69431

GOMAN, M.

State-space representation of aerodynamic characteristics of an aircraft at high angles of attack [BTN-95-EIX95062487536] p 187 A95-69244

GRAFT, WOLF O.

Flight control system mode transitions influence on handling qualities and task performance [BTN-95-EIX95062487525] p 203 A95-69233

GREEN, J. E.

An investigation of drag repeatability in half model testing in the ARA Transonic Wind Tunnel [ARA-MEMO-392] p 188 N95-19546

GREEN, R. O.

Possible near-IR channels for remote sensing precipitable water vapor from geostationary satellite platforms [HTN-95-70139] p 214 A95-69431

GREENE, FRANCIS A.

Approximate method for calculating heating rates on three-dimensional vehicles [BTN-95-EIX95041503778] p 210 A95-69209

Navier-Stokes simulations of Orbiter aerodynamic characteristics including pitch trim and bodyflap [BTN-95-EIX95041503779] p 204 A95-69210

GRUENEFELD, G.

Planar air density measurements near model surfaces by ultraviolet Rayleigh/Raman scattering [BTN-94-EIX94441386614] p 213 A95-67345

GUARNIERA, S.

Selecting and management of fire fighter aircraft [BTN-95-EIX95062487538] p 193 A95-69246

GUFFOND, D.

Prediction of ice accretion: Comparison between the 2D and 3D codes [BTN-94-EIX94441385753] p 213 A95-68217

GUPTA, K.

Unbalance response of a dual rotor system: Theory and experiment [BTN-94-EIX94351143320] p 195 A95-65854

GUPTA, K. D.

Unbalance response of a dual rotor system: Theory and experiment [BTN-94-EIX94351143320] p 195 A95-65854

H

HAGER, J. O.

Two-point transonic airfoil design using optimization for improved off-design performance [BTN-95-EIX95062487542] p 192 A95-68356

HAMED, A.

Experimental and numerical simulations of the effects of ingested particles in gas turbine engines p 199 N95-19662

HAMILTON, H. HARRIS

Approximate method for calculating heating rates on three-dimensional vehicles [BTN-95-EIX95041503778] p 210 A95-69209

HAMORY, PHILIP J.

Flight experience with lightweight, low-power miniaturized instrumentation systems [BTN-95-EIX95062487522] p 180 A95-69230

HANSON, R. K.

Comparison of NO and OH planar fluorescence temperature measurements in scramjet model flowfields [BTN-95-EIX95042474388] p 209 A95-68312

HARLOFF, G. J.

Design and operation of a supersonic annular flow facility [BTN-94-EIX94441386624] p 183 A95-68173

HARLOFF, GARY J.

On supersonic-inlet boundary-layer bleed flow [NASA-CR-195426] p 202 N95-19769

HARRIS, JOSEPH M.

Evaluation of the radio frequency susceptibility of commercial GPS receivers [BTN-95-EIX95042474624] p 189 A95-68278

HARRIS, P. K.

Particle trajectories in gas turbine engines p 199 N95-19663

HARTLE, MICHAEL S.

Ply layout optimization and micromechanics tailoring of composite aircraft engine structures [BTN-95-EIX95112524206] p 196 A95-69302

HASSAN, H. A.

Modeling of supersonic turbulent combustion using assumed probability density functions [BTN-95-EIX95112524190] p 206 A95-69318

HE, X.

Waveriders with finlets [BTN-95-EIX95062487541] p 184 A95-68355

HEDDE, T.

Prediction of ice accretion: Comparison between the 2D and 3D codes [BTN-94-EIX94441385753] p 213 A95-68217

HEIN, GUENTER W.

On-the-fly carrier phase ambiguity resolution for precise aircraft landing [BTN-95-EIX95112522535] p 190 A95-69328

HENLINE, WILLIAM D.

Trajectory-based heating analysis for the European Space Agency/Rosetta Earth Return Vehicle [BTN-95-EIX95041503787] p 205 A95-69218

HIRAIWA, TETSUO

Three-dimensional analysis of scramjet nozzle flows [BTN-94-EIX94441380978] p 196 A95-68162

HORENSTEIN, M.

Comparison of electrostatic and aerodynamic forces during parachute opening [BTN-95-EIX95062487532] p 187 A95-69240

HORNUNG, HANS G.

Elliptic tip effects on the vortex wake of an axisymmetric body at incidence [BTN-94-EIX94441386612] p 208 A95-67343

HORTON, G. C.

The calculation of erosion in a gas turbine compressor rotor p 199 N95-19664

HOTIMSKII, S.

A program for scientific and applied investigations using aerostat complexes p 182 A95-66304

HOWARD, THOMAS J.

Reliability and maintainability [BTN-95-EIX95042477109] p 179 A95-68350

HUCHIN, J. P.

New Trends in coatings developments for turbine blades: Materials processing and repair p 201 N95-19676

HUGHES, D. A.

Soft body impact on titanium fan blades p 200 N95-19671

HUNT, M. L.

Influence of injectant Mach number and temperature on supersonic film cooling [BTN-94-EIX94441386686] p 184 A95-68195

I

IMMARIGEON, J. P.

Protective coatings for compressor gas path components p 201 N95-19675

IOB, M.

Programmable cockpit research simulator [AD-A279219] p 204 N95-19848

IRELAND, P. T.

Particle deposition in gas turbine blade film cooling holes p 199 N95-19661

ISAAC, GEORGE A.

Aircraft icing measurements in East Coast winter storms [HTN-95-60505] p 214 A95-68756

ISHIGURO, TOMIKO

Three-dimensional analysis of scramjet nozzle flows [BTN-94-EIX94441380978] p 196 A95-68162

ISHIHARA, TADASHI

Surface morphology and structure of carbon-carbon composites in high-energy sliding contact [BTN-94-EIX94371347996] p 206 A95-69164

J

JACOB, THOMAS

High accuracy navigation and landing system using GPS/IMU system integration [BTN-94-EIX94441386129] p 189 A95-68185

JACQUIN, L.

Phenomenological description and simplified modelling of the vortex wake issuing from a jet in a crossflow [BTN-94-EIX94441386754] p 184 A95-68218

JOHNSTON, GORDON T.

Results and performance of multi-site reference station differential GPS [BTN-95-EIX95112522534] p 190 A95-69329

JONES, T. V.

Particle deposition in gas turbine blade film cooling holes p 199 N95-19661

JOSHI, M. N.

Recent trends in balloon flights from TIFR's National Balloon Facility, Hyderabad p 191 A95-66300

JUHANDY, K. A.

Influence of injectant Mach number and temperature on supersonic film cooling [BTN-94-EIX94441386686] p 184 A95-68195

K

KAI, YAN YIP

Use of MOBITEK wireless wide area networks as a solution to land-based positioning and navigation [BTN-94-EIX94441386132] p 189 A95-68188

KARABALIS, DIMITRIS L.

Simplified analysis of general instability of stiffened shells with cutouts in pure bending [BTN-95-EIX95042474418] p 209 A95-68282

KARPEL, MORDECHAY

Continuous gust response and sensitivity derivatives using state-space models [BTN-95-EIX95062487551] p 203 A95-68365

KATO, M.

Dynamic behavior of valves with pneumatic chamber for reciprocating compressors [BTN-94-EIX94351143311] p 207 A95-65845

KAWIECKI, GRZEGORZ

Bilinear formulation applied to the response and stability of helicopter rotor blade [BTN-95-EIX95042474400] p 192 A95-68300

KELLER, K.

Launcher wing-leading-edge design [BTN-95-EIX95042477110] p 192 A95-68349

KELLEY, SEAN M.

Application of circulation control to advanced subsonic transport aircraft. Part 1: Airfoil development [BTN-95-EIX95062487545] p 185 A95-68359

Application of circulation control to advanced subsonic transport aircraft. Part 2: Transport application [BTN-95-EIX95062487546] p 185 A95-68360

KELLY, J. E.

Advanced diesel electronic fuel injection and turbocharging [AD-A279176] p 211 N95-19809

KHRABROV, A.

State-space representation of aerodynamic characteristics of an aircraft at high angles of attack [BTN-95-EIX95062487536] p 187 A95-69244

KO, FRANK K.

Development of hypersonic engine seals: Flow effects of preload and engine pressures [BTN-95-EIX95112524204] p 196 A95-69304

KOBILINSKY, C.

Using IRI for the computation of ionospheric corrections for altimeter data analysis p 212 A95-66949

KODIYALAM, SRINIVAS

Ply layout optimization and micromechanics tailoring of composite aircraft engine structures [BTN-95-EIX95112524206] p 196 A95-69302

- KOENIG, P.**
Damage of high temperature components by dust-laden air p 201 N95-19673
- KOGAN, M. N.**
Kinetic theory in aerothermodynamics [HTN-95-A0002] p 183 A95-67829
- KOLKMAN, H. J.**
Gas turbine compressor corrosion and erosion in Western Europe p 201 N95-19678
- KORLEVIC, K.**
Powerful bolide explosion over North Italy [HTN-95-80564] p 218 A95-69658
- KORTE, JOHN J.**
Numerical study of the performance of swept, curved compression surface scramjet inlets [BTN-95-EIX95112524198] p 197 A95-69310
- KOSHAK, WILLIAM J.**
Aircraft electric field measurements: Calibration and ambient field retrieval [HTN-95-90508] p 213 A95-67780
- KOUSEN, KENNETH A.**
Active control of wake/blade-row interaction noise [BTN-95-EIX95042474389] p 196 A95-68311
- KUK, V. H. M.**
Particle deposition in gas turbine blade film cooling holes p 199 N95-19661
- KUMAR, AJAY**
Numerical study of the performance of swept, curved compression surface scramjet inlets [BTN-95-EIX95112524198] p 197 A95-69310
- KUROHASHI, M.**
Dynamic behavior of valves with pneumatic chamber for reciprocating compressors [BTN-94-EIX94351143311] p 207 A95-65845
- L**
- LABBE, M.**
Transport aircraft loading and balancing system: Using a CLIPS expert system for military aircraft load planning p 217 N95-19751
- LAFON, A.**
Shock layers and boundary layers in hypersonic flows [HTN-95-A0003] p 183 A95-67830
- LAFORE, J.-P.**
Nonhydrostatic simulation of frontogenesis in a moist atmosphere. Part 3: Thermal wind imbalance and rainbands [HTN-95-90356] p 212 A95-66429
- LAITONE, EDMUND V.**
Minimum sink-speed in power-off glide [BTN-95-EIX95062487556] p 193 A95-68370
- LAKE, R. C.**
Demonstration of an elastically coupled twist control concept for tilt rotor blade application [BTN-94-EIX94441386633] p 196 A95-68182
- LAMBIRIS, B.**
Adaptive modeling of jet engine performance with application to condition monitoring [BTN-95-EIX95112524205] p 196 A95-69303
- LAPSHIN, V.**
A program for scientific and applied investigations using aerostat complexes p 182 A95-66304
- LAPSHIN, V. I.**
The scientific ballooning in Russia p 191 A95-66302
- The joint Russian-Brasil research on balloons p 182 A95-66303
- LAVERDURE, JOHN P.**
Reliability and maintainability [BTN-95-EIX95042477109] p 179 A95-68350
- LAZUTIN, L. L.**
The scientific ballooning in Russia p 191 A95-66302
- The joint Russian-Brasil research on balloons p 182 A95-66303
- LECHNER, WOLFGANG**
GPS/GLONASS/INS test program [BTN-94-EIX94441386131] p 189 A95-68187
- LEDUC, VINCENT**
Transport aircraft loading and balancing system: Using a CLIPS expert system for military aircraft load planning p 217 N95-19751
- LEE, B. H. K.**
Vortical flow structure near the F/A-18 LEX at high incidence [BTN-95-EIX95062487555] p 186 A95-68369
- LEE, CALVIN K.**
Radial reefing method for accelerated and controlled parachute opening [BTN-95-EIX95062487539] p 187 A95-69247
- LEE, IN**
Aeroelastic stability of hingeless rotor blade in hover using large deflection theory [BTN-94-EIX94441386616] p 183 A95-67347

- LEE, J.**
Lag model for turbulent boundary layers over rough bleed surfaces [BTN-94-EIX94441380981] p 208 A95-68165
- LEE, JAEWOO**
Aerodynamically blunt and sharp bodies [BTN-95-EIX95041503781] p 205 A95-69212
- Development of an efficient inverse method for supersonic and hypersonic body design [BTN-95-EIX95041503784] p 180 A95-69215
- Minimum-drag axisymmetric bodies in the supersonic/hypersonic flow regimes [BTN-95-EIX95041503785] p 180 A95-69216
- LEE, K. D.**
Two-point transonic airfoil design using optimization for improved off-design performance [BTN-95-EIX95062487542] p 192 A95-68356
- LEFEBVRE, M.**
Measurement by coherent anti-Stokes Raman scattering in the R5Ch hypersonic wind tunnel [BTN-95-EIX95112523811] p 188 A95-69322
- LEFEVRE, FRANCK**
Three-dimensional model interpretation of NO(x) measurements from the lower stratosphere [HTN-95-90534] p 213 A95-67806
- LERDY, G.**
The calculation of erosion in a gas turbine compressor rotor p 199 N95-19664
- LEVSHUK, B.**
A program for scientific and applied investigations using aerostat complexes p 182 A95-66304
- LEW, T.**
Theoretical and actual performance of a long duration superpressure balloon made from a biaxially oriented nylon-6 film p 181 A95-66282
- LEWIS, MARK J.**
Navier-Stokes computation of a viscous optimized waverider [BTN-95-EIX95041503782] p 193 A95-69213
- LINCOLN, JOHN W.**
USAF aging aircraft program [BTN-95-EIX95072498878] p 180 A95-68394
- Proceedings of the USAF Structural Integrity Program Conference [AD-A285684] p 194 N95-19517
- LIPPKE, C.**
Nonlinear dynamic simulation of single- and multispool core engines, part 1: Computational method [BTN-95-EIX95112524200] p 210 A95-69308
- LO, C. F.**
Two-variable method for blockage wall interference in a circular tunnel [BTN-95-EIX95062487540] p 187 A95-69248
- LOMBARDO, GIUSEPPE**
An airborne monitoring system for FOD and erosion faults p 200 N95-19668
- LOPEZ, VIRGINIA C.**
Powered lift for land and sea [BTN-95-EIX95041503010] p 192 A95-68313
- LUTTGES, M. W.**
Evidence that aerodynamic effects, including dynamic stall, dictate HAWT structural loads and power generation in highly transient time frames [DE94-011865] p 216 N95-19855
- LYNCH, S. P.**
Fatigue crack growth in nickel-based superalloys at 500-700 C. 1: Waspaloy [BTN-94-EIX94371347843] p 206 A95-69136
- LYRINTZIS, A. S.**
Rotating Kirchhoff method for three-dimensional transonic blade-vortex interaction hover noise [BTN-94-EIX94441386601] p 182 A95-67332

M

- MACDONALD-SMITH, DIAN F. M.**
The aerodynamic design of an integrated wing lower surface and pylons for reduced drag [ARA-MEMO-406] p 194 N95-19789
- MACH, DOUGLAS M.**
Aircraft electric field measurements: Calibration and ambient field retrieval [HTN-95-90508] p 213 A95-67780
- MACLEAN, B. J.**
Lift analysis of a variable camber foil using the discrete vortex-blob method [BTN-94-EIX94441386623] p 179 A95-68172
- MACLEOD, J. D.**
Protective coatings for compressor gas path components p 201 N95-19675
- MACPHERSON, J. I.**
Observations of fluxes and inland breezes over a heterogeneous surface [HTN-95-80258] p 212 A95-66315

- MADAVAN, NATERI K.**
Solution-adaptive structured-unstructured grid method for unsteady turbomachinery analysis. Part I: Methodology [BTN-94-EIX94441380983] p 208 A95-67329
- MAHMOOD, M.**
Suppression of vortex asymmetry and side force on a circular cone [BTN-95-EIX95042474413] p 209 A95-68287
- MAHRT, L. U**
Observations of fluxes and inland breezes over a heterogeneous surface [HTN-95-80258] p 212 A95-66315
- MANN, DARRELL L.**
Future directions in helicopter protection system configuration p 198 N95-19657
- MARCHANT, M. J.**
Construction of nearly orthogonal multiblock grids for compressible flow simulation [BTN-94-EIX94361133526] p 207 A95-65981
- MARCHANT, W.**
Design decisions from the history of the EUVE science payload [HTN-95-60545] p 205 A95-69854
- MARIJNISSEN, G.**
Braze repair possibilities for hot section gas turbine parts p 201 N95-19677
- MARSHALL, J. S.**
Vortex cutting by a blade. Part II: Computations of vortex response [BTN-94-EIX94441386611] p 208 A95-67342
- MARTIN, I. M.**
The joint Russian-Brasil research on balloons p 182 A95-66303
- MARTIN, R. M.**
Recent studies of rotorcraft blade-vortex interaction noise [BTN-95-EIX95062487521] p 218 A95-69229
- MARTINDALE, I.**
Soft body impact on titanium fan blades p 200 N95-19671
- MARTINOU, R.**
New Trends in coatings developments for turbine blades: Materials processing and repair p 201 N95-19676
- MARWITZ, JOHN D.**
Conditions associated with large-drop regions [HTN-95-10686] p 214 A95-68845
- MASON, W. H.**
Aerodynamically blunt and sharp bodies [BTN-95-EIX95041503781] p 205 A95-69212
- Development of an efficient inverse method for supersonic and hypersonic body design [BTN-95-EIX95041503784] p 180 A95-69215
- Minimum-drag axisymmetric bodies in the supersonic/hypersonic flow regimes [BTN-95-EIX95041503785] p 180 A95-69216
- MATHIOUDAKIS, K.**
Adaptive modeling of jet engine performance with application to condition monitoring [BTN-95-EIX95112524205] p 196 A95-69303
- MATHUR, SANJAY R.**
Solution-adaptive structured-unstructured grid method for unsteady turbomachinery analysis. Part I: Methodology [BTN-94-EIX94441380983] p 208 A95-67329
- MAY, NICHOLAS E.**
Application of three-dimensional hybrid structured/unstructured grids to land, sea and air vehicles [ARA-MEMO-399] p 210 N95-19775
- Verification of the CFD simulation system SAUNA for complex aircraft configurations [ARA-MEMO-401] p 211 N95-19776
- Inviscid and viscous flow modelling of complex aircraft configurations using the CFD simulation system sauna [ARA-MEMO-403] p 211 N95-19777
- MAYORI, ALEJANDRO**
Interaction of a streamwise vortex with a thin plate: A source of turbulent buffeting [BTN-95-EIX95042474398] p 209 A95-68302
- MCCANN, DONALD W.**
WINDEX - A new index for forecasting microburst potential [HTN-95-90690] p 215 A95-69717
- MCCASKILL, THOMAS B.**
Effect of broadcast and precise ephemerides on estimates of the frequency stability of GPS Navstar clocks [BTN-95-EIX95112522530] p 190 A95-69333
- MCDANIEL, MICHAEL**
Airsip applications of modern flight test techniques [AD-A284253] p 194 N95-19731
- MCGINLEY, JOHN A.**
Forecasting for a large field program: STORM-FEST [HTN-95-90694] p 215 A95-69721

MCKNIGHT, RICHARD L.

Ply layout optimization and micromechanics tailoring of composite aircraft engine structures
[BTN-95-EIX95112524206] p 196 A95-69302

MCMMASTER, JOHN

The use of genetic algorithms for flight test and evaluation of artificial intelligence and complex software systems
[AD-A284824] p 217 N95-19688

MCMILLIN, B. K.

Comparison of NO and OH planar fluorescence temperature measurements in scramjet model flowfields
[BTN-95-EIX95042474388] p 209 A95-68312

MEI, CHUH

Finite element time domain - modal formulation for nonlinear flutter of composite panels
[BTN-95-EIX95042474401] p 203 A95-68299

MERRICK, V. K.

Simulation and flight test evaluation of head-up-display guidance for harrier approach transitions
[BTN-95-EIX95062487533] p 194 A95-69241

MEVREL, R.

New Trends in coatings developments for turbine blades: Materials processing and repair p 201 N95-19676

MEYER-HILBERG, JOCHEN

High accuracy navigation and landing system using GPS/IMU system integration
[BTN-94-EIX94441386129] p 189 A95-68185

MILLER, M. S.

Evidence that aerodynamic effects, including dynamic stall, dictate HAWT structural loads and power generation in highly transient time frames
[DE94-011865] p 216 N95-19855

MILLER, T.

Damage of high temperature components by dust-laden air p 201 N95-19673

MILOS, FRANK S.

Review of numerical procedures for computational surface thermochemistry
[BTN-94-EIX94441386682] p 205 A95-68191

MIRICK, P. H.

Demonstration of an elastically coupled twist control concept for tilt rotor blade application
[BTN-94-EIX94441386633] p 196 A95-68182

MITANI, TOHRU

Three-dimensional analysis of scramjet nozzle flows
[BTN-94-EIX94441380978] p 196 A95-68162

MOATS, MICHAEL L.

Automation of hardware-in-the-loop testing of control systems for unmanned air vehicles
[AD-A284833] p 194 N95-19693

MODIANO, DAVID L.

Adaptive computations of flow around a delta wing with vortex breakdown
[BTN-94-EIX94441386631] p 184 A95-68180

MOEHRING, J. T.

Modern transport engine experience with environmental ingestion effects p 199 N95-19660

MONGE-CADET, P.

Multilayer anti-erosion coatings p 201 N95-19679

MOOK, DEAN T.

Numerical simulation of steady and unsteady, vorticity-dominated aerodynamic interference
[BTN-95-EIX95062487524] p 186 A95-69232

MORALEZ, E., III

Simulation and flight test evaluation of head-up-display guidance for harrier approach transitions
[BTN-95-EIX95062487533] p 194 A95-69241

MULLER, M.

Rotorcraft ditchings and water-related impacts that occurred from 1982 to 1989, phase 1
[AD-A279164] p 189 N95-19805

MURMAN, EARLL M.

Adaptive computations of flow around a delta wing with vortex breakdown
[BTN-94-EIX94441386631] p 184 A95-68180

MURRAY, JAMES E.

Flight experience with lightweight, low-power miniaturized instrumentation systems
[BTN-95-EIX95062487522] p 180 A95-69230

Development and flight test of a deployable precision landing system
[BTN-95-EIX95062487535] p 190 A95-69243

MURTHY, P. L. N.

Ice-impact analysis of blades p 200 N95-19672

MUTHARASAN, RAJAKKANNU

Development of hypersonic engine seals: Flow effects of preload and engine pressures
[BTN-95-EIX95112524204] p 196 A95-69304

MYKLEBUST, ARVID

Putting the ACSYNT on aircraft design
[BTN-95-EIX95072419881] p 180 A95-68398

N**NAGY, D. R.**

Protective coatings for compressor gas path components p 201 N95-19675

NAPOLITANO, MARCELLO R.

Determination of stability and control derivatives from the NASA F/A-18 HARV from flight data using the maximum likelihood method
[NASA-CR-197320] p 204 N95-19576

NAYFEH, ALI H.

Numerical simulation of steady and unsteady, vorticity-dominated aerodynamic interference
[BTN-95-EIX95062487524] p 186 A95-69232

NEEDLEMAN, H. C.

Status of the NASA balloon program p 181 A95-66296

NELSON, ROBERT C.

Experimental investigations on limit cycle wing rock of slender wings
[BTN-95-EIX95062487543] p 185 A95-68357

NEUFELD, DAVID C.

Development and flight test of a deployable precision landing system
[BTN-95-EIX95062487535] p 190 A95-69243

NIKOLOV, N.

A program for scientific and applied investigations using aerostat complexes p 182 A95-66304

NIKOLSKY, S. I.

The scientific ballooning in Russia p 191 A95-66302
The joint Russian-Brasil research on balloons p 182 A95-66303

NITZSCHE, FRED

Using adaptive structures to attenuate rotary wing aeroelastic response
[BTN-95-EIX95062487547] p 192 A95-68361

NIXON, M. W.

Demonstration of an elastically coupled twist control concept for tilt rotor blade application
[BTN-94-EIX94441386633] p 196 A95-68182

NOGUCHI, R. A.

Environmental effects on composite airframes: A study conducted for the ARM UAV Program (Atmospheric Radiation Measurement Unmanned Aerospace Vehicle)
[DE94-015351] p 206 N95-19579

NOGUCHI, YASUO

Behavior of the Johnson-King turbulence model in axisymmetric supersonic flows
[BTN-94-EIX94441386606] p 183 A95-67337

NORWOOD, KEITH

Coupling equivalent plate and finite element formulations in multiple-method structural analyses
[BTN-95-EIX95062487548] p 192 A95-68362

NURNBERGER, MICHAEL W.

Design considerations for an archimedean slot spiral antenna p 211 N95-19798

O**OLSON, HAROLD W.**

Research requirements for future visual guidance systems
[AD-A279188] p 191 N95-19810

P**PAGE, A. G.**

Programmable cockpit research simulator
[AD-A279219] p 204 N95-19848

PAPAILIOU, K.

Adaptive modeling of jet engine performance with application to condition monitoring
[BTN-95-EIX95112524205] p 196 A95-69303

PAPROCKI, THOMAS H.

Research requirements for future visual guidance systems
[AD-A279188] p 191 N95-19810

PARAMESWARAN, V. R.

Protective coatings for compressor gas path components p 201 N95-19675

PAREKH, D. E.

Entrainment and acoustic variations in a round jet from introduced streamwise vorticity
[BTN-95-EIX95042474409] p 209 A95-68291

PARISH, DEBORAH R.

Testing considerations for military aircraft engines in corrosive environments (a Navy perspective) p 202 N95-19684

PARKINSON, BRADFORD W.

Space flight tests of attitude determination using GPS
[BTN-95-EIX95112522529] p 190 A95-69334

PARTHASARATHY, V. N.

Ply layout optimization and micromechanics tailoring of composite aircraft engine structures
[BTN-95-EIX95112524206] p 196 A95-69302

PAYNTER, G. C.

Lag model for turbulent boundary layers over rough bleed surfaces
[BTN-94-EIX94441380981] p 208 A95-68165

PEACE, A. J.

Validation and evaluation of the advanced aeronautical CFD system SAUNA: A method developer's view
[ARA-MEMO-390] p 210 N95-19774

PEACE, ANDREW J.

Verification of the CFD simulation system SAUNA for complex aircraft configurations
[ARA-MEMO-401] p 211 N95-19776

Inviscid and viscous flow modelling of complex aircraft configurations using the CFD simulation system sauna
[ARA-MEMO-403] p 211 N95-19777

PEDERSON, J. R.

Observations of fluxes and inland breezes over a heterogeneous surface
[HTN-95-80258] p 212 A95-66315

PELLERIN, F.

Multilayer anti-erosion coatings p 201 N95-19679

PETROV, P.

A program for scientific and applied investigations using aerostat complexes p 182 A95-66304

POBANZ, BRENDA M.

Conditions associated with large-drop regions
[HTN-95-10686] p 214 A95-68845

POCOCK, MARK F.

Application of three-dimensional hybrid structured/unstructured grids to land, sea and air vehicles
[ARA-MEMO-399] p 210 N95-19775

Verification of the CFD simulation system SAUNA for complex aircraft configurations
[ARA-MEMO-401] p 211 N95-19776

Inviscid and viscous flow modelling of complex aircraft configurations using the CFD simulation system sauna
[ARA-MEMO-403] p 211 N95-19777

PODLESKI, S. D.

F/A-18 inlet calculations at 60-deg angle of attack and 10-deg sideslip
[BTN-95-EIX95112524199] p 195 A95-69309

POISSON-QUINTON, PHILIPPE

Future SSTs a European approach
[BTN-95-EIX95072419883] p 180 A95-68396

POLITOVICH, MARCIA K.

Conditions associated with large-drop regions
[HTN-95-10686] p 214 A95-68845

POT, T.

Measurement by coherent anti-Stokes Raman scattering in the R5Ch hypersonic wind tunnel
[BTN-95-EIX95112523811] p 188 A95-69322

PRASAD, N.

Microwave and infrared simulations of an intense convective system and comparison with aircraft observations
[HTN-95-60511] p 214 A95-68762

PREISSER, J. S.

Recent studies of rotorcraft blade-vortex interaction noise
[BTN-95-EIX95062487521] p 218 A95-69229

PUESCHEL, R. F.

Three-dimensional model interpretation of NO(x) measurements from the lower stratosphere
[HTN-95-90534] p 213 A95-67806

Q**QIAN, X.**

Two-variable method for blockage wall interference in a circular tunnel
[BTN-95-EIX95062487540] p 187 A95-69248

QUESNEL, E.

Multilayer anti-erosion coatings p 201 N95-19679

R**RABY, PETER**

Integrated GPS/Glonass navigation: Algorithms and results
[BTN-95-EIX9511252531] p 190 A95-69332

RADTKE, T. C.

Fatigue crack growth in nickel-based superalloys at 500-700 C. 1: Waspaloy
[BTN-94-EIX94371347843] p 206 A95-69136

RAGA, G. B.

Mesoscale structure of precipitation bands in a North Atlantic winter storm
[HTN-95-40659] p 215 A95-69803

RAI, R.

Theoretical and actual performance of a long duration superpressure balloon made from a biaxially oriented nylon-6 film p 181 A95-66282

RAJAGOPAL, PAVAN

Flight control system mode transitions influence on handling qualities and task performance [BTN-95-EIX95062487525] p 203 A95-69233

RAJAGOPALAN, R. GANESH

Solution-adaptive structured-unstructured grid method for unsteady turbomachinery analysis. Part I: Methodology [BTN-94-EIX94441380983] p 208 A95-67329

RAND, JAMES L.

Long duration balloons p 191 A95-66305

RASKY, DANIEL J.

Review of numerical procedures for computational surface thermochemistry [BTN-94-EIX94441386682] p 205 A95-68191

RASMUSSEN, M. L.

Waveriders with finlets [BTN-95-EIX95062487541] p 184 A95-68355

REDDY, E. S.

Ice-impact analysis of blades p 200 A95-19672

REDELSPERGER, J.-L.

Nonhydrostatic simulation of frontogenesis in a moist atmosphere. Part 3: Thermal wind imbalance and rainbands [HTN-95-90356] p 212 A95-66429

REED, HELEN L.

Linear disturbances in hypersonic, chemically reacting shock layers [BTN-94-EIX94441386605] p 182 A95-67336

REED, R. DALE

Development and flight test of a deployable precision landing system [BTN-95-EIX95062487535] p 190 A95-69243

REICH, G.

Launcher wing-leading-edge design [BTN-95-EIX95042477110] p 192 A95-68349

REID, LLOYD D.

Flight control system mode transitions influence on handling qualities and task performance [BTN-95-EIX95062487525] p 203 A95-69233

REID, WILSON G.

Effect of broadcast and precise ephemerides on estimates of the frequency stability of GPS Navstar clocks [BTN-95-EIX95112522530] p 190 A95-69333

RICHARDSON, J.

Transport aircraft loading and balancing system: Using a CLIPS expert system for military aircraft load planning p 217 A95-19751

RICKERBY, D.

Multilayer anti-erosion coatings p 201 A95-19679

RIDLEY, BRIAN A.

Three-dimensional model interpretation of NO(x) measurements from the lower stratosphere [HTN-95-90534] p 213 A95-67806

RIEDLER, W.

Balloon technology and observations: Symposium P3 of the COSPAR Plenary Meeting, 29th, Washington, DC, Aug. 28-Sept. 5, 1992 [HTN-95-70250] p 181 A95-66276

ROBERTS, N.

Comparison of electrostatic and aerodynamic forces during parachute opening [BTN-95-EIX95062487532] p 187 A95-69240

ROBERTS, P. A.

An air-driven pressure booster pump for aircraft-based air sampling [HTN-95-40689] p 216 A95-69833

ROBINSON, M. C.

Evidence that aerodynamic effects, including dynamic stall, dictate HAWT structural loads and power generation in highly transient time frames [DE94-011865] p 216 A95-19855

ROCKWELL, DONALD

Interaction of a streamwise vortex with a thin plate: A source of turbulent buffeting [BTN-95-EIX95042474398] p 209 A95-68302

RODGERS, DENNIS

Forecasting for a large field program: STORM-FEST [HTN-95-90694] p 215 A95-69721

ROGERS, C. B.

Entrainment and acoustic variations in a round jet from introduced streamwise vorticity [BTN-95-EIX95042474409] p 209 A95-68291

ROMERE, PAUL O.

Documentation and archiving of the Space Shuttle wind tunnel test data base. Volume 2: User's Guide to the Archived Data Base [NASA-TM-104806-VOL-2] p 205 A95-19624

ROSE, M. G.

Particle deposition in gas turbine blade film cooling holes p 199 A95-19661

ROSSMANN, A.

Damage of high temperature components by dust-laden air p 201 A95-19673

ROSSOW, VERNON J.

Effect of ground and ceiling planes on shape of energized wakes [BTN-95-EIX95062487558] p 186 A95-68372

ROUCH, K. W.

Modeling rotating shafts using axisymmetric solid finite elements with matrix reduction [BTN-94-EIX94351143328] p 207 A95-67301

ROUSE, PETER L.

US Army rotorcraft turboshaft engines sand and dust erosion considerations p 198 A95-19656

ROVER, RICHARD C., III

Application of circulation control to advanced subsonic transport aircraft. Part 1: Airfoil development [BTN-95-EIX95062487545] p 185 A95-68359

Application of circulation control to advanced subsonic transport aircraft. Part 2: Transport application [BTN-95-EIX95062487546] p 185 A95-68360

RUDD, JAMES L.

Proceedings of the USAF Structural Integrity Program Conference [AD-A285684] p 194 A95-19517

RUIZ, C.

Soft body impact on titanium fan blades p 200 A95-19671

S

SAHU, JUBARAJ

Numerical computations of supersonic base flow with special emphasis on turbulence modeling [BTN-94-EIX94441386632] p 179 A95-68181

SAITO, TERUO

Preliminary assessment of tunnel wall interference in the NDA cryogenic wind tunnel [BTN-95-EIX95062487531] p 187 A95-69239

SAKAUE, TADASHI

Preliminary assessment of tunnel wall interference in the NDA cryogenic wind tunnel [BTN-95-EIX95062487531] p 187 A95-69239

SAUKKONEN, LEA

Research aircraft observations of a polar low at the east Greenland ice edge [HTN-95-A0175] p 215 A95-69766

SCHAEFFLER, A.

Performance deterioration of axial compressors due to blade defects p 199 A95-19665

SCHETZ, JOSEPH A.

Model for compressible turbulence in hypersonic wall boundary and high-speed mixing layers [BTN-94-EIX94441386625] p 184 A95-68174

SCHIFF, LEWIS B.

Numerical simulation of incidence and sweep effects on delta wing vortex breakdown [BTN-95-EIX95062487526] p 186 A95-69234

SCHMUECKER, J.

Performance deterioration of axial compressors due to blade defects p 199 A95-19665

SCHOBELER, M. T.

Nonlinear dynamic simulation of single- and multispool core engines, part 1: Computational method [BTN-95-EIX95112524200] p 210 A95-69308

SCHRAUF, G.

On wave-front curvature in linear stability theory [BTN-94-EIX94441385756] p 184 A95-68220

SEELY, L.

Theoretical and actual performance of a long duration superpressure balloon made from a biaxially oriented nylon-6 film p 181 A95-66282

SEITZMAN, J. M.

Comparison of NO and OH planar fluorescence temperature measurements in scramjet model flowfields [BTN-95-EIX95042474388] p 209 A95-68312

SETTLES, GARY S.

Supersonic and hypersonic shock/boundary-layer interaction database [BTN-94-EIX94441386604] p 182 A95-67335

SHAPIRO, M. A.

Research aircraft observations of a polar low at the east Greenland ice edge [HTN-95-A0175] p 215 A95-69766

SHARP, P. K.

Fatigue resistance of peened 7050-T7451 aluminium alloy: Repair and re-treatment of a component surface [BTN-94-EIX94371347838] p 206 A95-69131

SHAW, J. A.

Validation and evaluation of the advanced aeronautical CFD system SAUNA: A method developer's view [ARA-MEMO-390] p 210 A95-19774

SHAW, JONATHAN A.

Application of three-dimensional hybrid structured/unstructured grids to land, sea and air vehicles [ARA-MEMO-399] p 210 A95-19775

Verification of the CFD simulation system SAUNA for complex aircraft configurations [ARA-MEMO-401] p 211 A95-19776

Inviscid and viscous flow modelling of complex aircraft configurations using the CFD simulation system sauna [ARA-MEMO-403] p 211 A95-19777

SHIN, JAIWON

Repeatability of ice shapes in the NASA Lewis icing research tunnel [BTN-95-EIX95062487528] p 204 A95-69236

SHIPLEY, D. E.

Evidence that aerodynamic effects, including dynamic stall, dictate HAWT structural loads and power generation in highly transient time frames [DE94-011865] p 216 A95-19855

SHIRATORI, TOSHIMASA

Behavior of the Johnson-King turbulence model in axisymmetric supersonic flows [BTN-94-EIX94441386606] p 183 A95-67337

SHNITKIN, HAROLD

Joint stars phased array radar antenna [BTN-95-EIX95042474626] p 209 A95-68280

SIM, ALEX G.

Development and flight test of a deployable precision landing system [BTN-95-EIX95062487535] p 190 A95-69243

SIMMS, D. A.

Evidence that aerodynamic effects, including dynamic stall, dictate HAWT structural loads and power generation in highly transient time frames [DE94-011865] p 216 A95-19855

SINGER, S. FRED

Ozone, skin cancer, and the SST [BTN-95-EIX95041503011] p 213 A95-68314

SINGH, D. J.

Numerical study of the performance of swept, curved compression surface scramjet inlets [BTN-95-EIX95112524198] p 197 A95-69310

SINGHAL, S. N.

Ice-impact analysis of blades p 200 A95-19672

SINGLETON, J. D.

Demonstration of an elastically coupled twist control concept for tilt rotor blade application [BTN-94-EIX94441386633] p 196 A95-68182

SIRS, R. C.

The operation of gas turbine engines in hot and sandy conditions: Royal Air Force experiences in the Gulf conflict p 198 A95-19655

SIVANERI, NITHIAM TI

Bi-linear formulation applied to the response and stability of helicopter rotor blade [BTN-95-EIX95042474400] p 192 A95-68300

SIVO, J. M.

Influence of injectant Mach number and temperature on supersonic film cooling [BTN-94-EIX94441386686] p 184 A95-68195

SLOAN, M. L.

Lag model for turbulent boundary layers over rough bleed surfaces [BTN-94-EIX94441380981] p 208 A95-68165

SMITH, CRAWFORD F.

Prediction of wind tunnel effects on the installed F/A-18A inlet flow field at high angles-of-attack [NASA-CR-195429] p 197 A95-19651

SMITH, GREGORY E.

On supersonic-inlet boundary-layer bleed flow [NASA-CR-195426] p 202 A95-19769

SMITH, I. STEVE, JR.

Overview of the NASA balloon R&D program p 181 A95-66297

SMITH, MARILYN J.

Application of circulation control to advanced subsonic transport aircraft. Part 1: Airfoil development [BTN-95-EIX95062487545] p 185 A95-68359

Application of circulation control to advanced subsonic transport aircraft. Part 2: Transport application [BTN-95-EIX95062487546] p 185 A95-68360

SOLIES, U. P.

Offset thrust axes and pitch stability [BTN-95-EIX95062487553] p 203 A95-68367

SOUBRIER, A.

French contribution to new balloon designs and materials p 181 A95-66277

Balloon flights in France and in Europe p 204 A95-66301

STAHL, W. H.

Suppression of vortex asymmetry and side force on a circular cone [BTN-95-EIX95042474413] p 209 A95-68287

- STAMATIS, A.**
Adaptive modeling of jet engine performance with application to condition monitoring
[BTN-95-EIX95112524205] p 196 A95-69303
- STANNILAND, D. R.**
An investigation of drag repeatability in half model testing in the ARA Transonic Wind Tunnel
[ARA-MEMO-392] p 188 N95-19546
- STANNILAND, DENNIS R.**
The aerodynamic design of an integrated wing lower surface and pylons for reduced drag
[ARA-MEMO-406] p 194 N95-19789
- STARK, MARY**
The use of genetic algorithms for flight test and evaluation of artificial intelligence and complex software systems
[AD-A284824] p 217 N95-19688
- STEINETZ, BRUCE M.**
Development of hypersonic engine seals: Flow effects of preload and engine pressures
[BTN-95-EIX95112524204] p 196 A95-69304
- STEINMEYER, D. C.**
Advanced diesel electronic fuel injection and turbocharging
[AD-A279176] p 211 N95-19809
- STEPHENSON, R. W.**
Modeling rotating shafts using axisymmetric solid finite elements with matrix reduction
[BTN-94-EIX94351143328] p 207 A95-67301
- STEWART, R. E.**
Mesoscale structure of precipitation bands in a North Atlantic winter storm
[HTN-95-40659] p 215 A95-69803
- STOKKE, P.**
Scandinavian Airlines Systems experience on erosion, corrosion and foreign object damage effects on gas turbines
p 198 N95-19659
- STOZKHOV, YU. I.**
The scientific ballooning in Russia
p 191 A95-66302
- The joint Russian-Brazil research on balloons
p 182 A95-66303
- STRANGMEN, THOMAS E.**
Resistance of silicon nitride turbine components to erosion and hot corrosion/oxidation attack
p 202 N95-19683
- STRAPP, J. W.**
Aircraft icing measurements in East Coast winter storms
[HTN-95-60505] p 214 A95-68756
- Mesoscale structure of precipitation bands in a North Atlantic winter storm
[HTN-95-40659] p 215 A95-69803
- STRIZ, ALFRED G.**
Influence of structural and aerodynamic modeling on flutter analysis
[BTN-95-EIX95062487550] p 203 A95-68364
- STUCKERT, GREG**
Linear disturbances in hypersonic, chemically reacting shock layers
[BTN-94-EIX94441386605] p 182 A95-67336
- SUN, D. C.**
Wormgear geometry adopted for implementing hydrostatic lubrication and formulation of the lubrication problem
[NASA-CR-195416] p 210 N95-19567
- SUN, JIELUN**
Observations of fluxes and inland breezes over a heterogeneous surface
[HTN-95-80258] p 212 A95-66315
- SURKS, P.**
Entrainment and acoustic variations in a round jet from introduced streamwise vorticity
[BTN-95-EIX95042474409] p 209 A95-68291
- SUTTIE, EDWARD D.**
Antarctic snow record of southern hemisphere lead pollution
[HTN-95-40359] p 212 A95-66869
- SZOKE, EDWARD J.**
Forecasting for a large field program: STORM-FEST
[HTN-95-90694] p 215 A95-69721

T

- TALBOTEC, J.**
Design of fan blades subjected to bird impact
p 200 N95-19669
- TAN, S. C.**
Particle trajectories in gas turbine engines
p 199 N95-19663
- TANG, D. M.**
Comparison of theory and experiment for non-linear flutter and stall response of a helicopter blade
[BTN-94-EIX94351108100] p 191 A95-66500
- TAO, WEI-KUO**
Microwave and infrared simulations of an intense convective system and comparison with aircraft observations
[HTN-95-60511] p 214 A95-68762
- TAUBER, MICHAEL E.**
Trajectory-based heating analysis for the European Space Agency/Rosetta Earth Return Vehicle
[BTN-95-EIX95041503787] p 205 A95-69218
- TAYMAN, STEVEN K.**
Wind tunnel tests of a 42 inch diameter self-starting autogyro rotor
[AD-A279922] p 188 N95-19863
- TENSI, J.**
Tip vortex on a swept wing. Mean flow and unsteady phenomena
[BTN-94-EIX94441385755] p 184 A95-68219
- TINCHER, DOUGLAS J.**
Hypersonic waverider test vehicle: A logical next step
[BTN-95-EIX95041503783] p 193 A95-69214
- TORELLA, GIOVANNI**
An airborne monitoring system for FOD and erosion faults
p 200 N95-19668
- TORKAR, K. M.**
Balloon technology and observations; Symposium P3 of the COSPAR Plenary Meeting, 29th, Washington, DC, Aug. 28-Sept. 5, 1992
[HTN-95-70250] p 181 A95-66276
- TOWNSEND, M. A.**
Stability of magnetic bearing-rotor systems and the effects of gravity and damping
[BTN-94-EIX94441386619] p 208 A95-68168
- TRABANDT, U.**
Launcher wing-leading-edge design
[BTN-95-EIX9504277110] p 192 A95-68349
- TRAUB, LANCE W.**
Aerodynamic effects of delta platform tip sails on wing performance
[BTN-95-EIX95062487544] p 185 A95-68358
- Aerodynamic characteristics of strake vortex flaps on a strake-wing configuration
[BTN-95-EIX95062487537] p 187 A95-69245
- TREGO, LINDA F.**
Noise and vibration control
[BTN-95-EIX95042477108] p 179 A95-68351
- TURTELLY, A. JR.**
The joint Russian-Brazil research on balloons
p 182 A95-66303

V

- VALDRE, G.**
Powerful bolide explosion over North Italy
[HTN-95-80564] p 218 A95-69658
- VALERIO, N. R.**
Vertical flow structure near the F/A-18 LEX at high incidence
[BTN-95-EIX95062487555] p 186 A95-68369
- VANDERMERWE, JUAN**
Aerodynamic characteristics of strake vortex flaps on a strake-wing configuration
[BTN-95-EIX95062487537] p 187 A95-69245
- VANGESTEL, R.**
Brazing repair possibilities for hot section gas turbine parts
p 201 N95-19677
- VANSCHAACK, DONALD J.**
Developing an emission factor for hazardous air pollutants for an F-16 using JP-8 fuel
[AD-A284802] p 216 N95-19685
- VANWIE, D. M.**
Experimental and computational results for the external flowfield of a scramjet inlet
[BTN-94-EIX94441380977] p 195 A95-68161
- VARGHESE, PH.**
Measurement by coherent anti-Stokes Raman scattering in the R5Ch hypersonic wind tunnel
[BTN-95-EIX95112523811] p 188 A95-69322
- VENKATKRISHNAN, V.**
Parallel implicit unstructured grid Euler solvers
[BTN-95-EIX95042474393] p 217 A95-68307
- VENKAYYA, VIPPERLA B.**
Influence of structural and aerodynamic modeling on flutter analysis
[BTN-95-EIX95062487550] p 203 A95-68364
- VERBEEK, A. T. J.**
High velocity oxygen fuel spraying of erosion and wear resistant coatings on jet engine parts
p 202 N95-19680
- VERDON, JOSEPH M.**
Active control of wake/blade-row interaction noise
[BTN-95-EIX95042474389] p 196 A95-68311
- VICKERS, DEAN**
Observations of fluxes and inland breezes over a heterogeneous surface
[HTN-95-80258] p 212 A95-66315
- VIEWEG, STEFAN**
GPS/GLONASS/INS test program
[BTN-94-EIX94441386131] p 189 A95-68187
- VIGNAU, H.**
The calculation of erosion in a gas turbine compressor rotor
p 199 N95-19664
- VIGNOLLES, P.**
Design of fan blades subjected to bird impact
p 200 N95-19669
- VOLAKIS, JOHN L.**
Design considerations for an archimedean slot spiral antenna
p 211 N95-19798

W

- WALEGA, JAMES G.**
Three-dimensional model interpretation of NO(x) measurements from the lower stratosphere
[HTN-95-90534] p 213 A95-67806
- WALSH, DAVID**
On-the-fly carrier phase ambiguity resolution for precise aircraft landing
[BTN-95-EIX95112522535] p 190 A95-69328
- WALTER, DONALD ALAN**
An analysis of the costs and benefits in improving F402-RR-406A High Pressure Turbine, second stage blades under the aircraft engine Component Improvement Program (CIP)
[AD-A285127] p 197 N95-19595
- WARNES, GORDON D.**
Future directions in helicopter protection system configuration
p 198 N95-19657
- WARREN, HUGH E.**
Effect of broadcast and precise ephemerides on estimates of the frequency stability of GPS Navstar clocks
[BTN-95-EIX95112522530] p 190 A95-69333
- WEATHERILL, N. P.**
Construction of nearly orthogonal multiblock grids for compressible flow simulation
[BTN-94-EIX94361133526] p 207 A95-65981
- WEILMUNSTER, K. JAMES**
Navier-Stokes simulations of Orbiter aerodynamic characteristics including pitch trim and bodyflap
[BTN-95-EIX95041503779] p 204 A95-69210
- Multiblock analysis for Shuttle Orbiter reentry heating from Mach 24 to Mach 12
[BTN-95-EIX95041503780] p 205 A95-69211
- WEINHEIMER, A. J.**
Three-dimensional model interpretation of NO(x) measurements from the lower stratosphere
[HTN-95-90534] p 213 A95-67806
- WEST, M. G.**
Interference between tanker wing wake with roll-up and receiver aircraft
[BTN-95-EIX95062487552] p 185 A95-68366
- WESTWATER, ED R.**
Possible near-IR channels for remote sensing precipitable water vapor from geostationary satellite platforms
[HTN-95-70139] p 214 A95-69431
- WHEELER, MARK L.**
Evaluation of the radio frequency susceptibility of commercial GPS receivers
[BTN-95-EIX95042474624] p 189 A95-68278
- WICKS, B. J.**
Fatigue crack growth in nickel-based superalloys at 500-700 C. 1: Waspaloy
[BTN-94-EIX94371347843] p 206 A95-69136
- WILBUR, M. L.**
Demonstration of an elastically coupled twist control concept for tilt rotor blade application
[BTN-94-EIX94441386633] p 196 A95-68182
- WILLIAMS, K. E.**
Design and operation of a supersonic annular flow facility
[BTN-94-EIX94441386624] p 183 A95-68173
- WILLIAMS, M. J.**
Out of area experiences with the RB199 in Toronto
p 198 N95-19654
- WILLIAMSON, R.**
Using IRI for the computation of ionospheric corrections for altimeter data analysis
p 212 A95-66949

WOLFF, ERIC W.

Antarctic snow record of southern hemisphere lead
pollution
[HTN-95-40359] p 212 A95-66869

WOOD, RICHARD M.

Passive porosity with free and fixed separation on a
tangent-ogive forebody
[BTN-95-EIX95062487554] p 185 A95-68368

WOOD, VINCENT T.

A technique for detecting a tropical cyclone center using
a Doppler radar
[HTN-95-20631] p 215 A95-69574

X

XIE, WEI-CHAU

Lyapunov exponents and stochastic stability of
two-dimensional parametrically excited random systems
[BTN-94-EIX94361122401] p 207 A95-65897

XUE, DAVID Y.

Finite element time domain - modal formulation for
nonlinear flutter of composite panels
[BTN-95-EIX95042474401] p 203 A95-68299

XUE, YU

Rotating Kirchhoff method for three-dimensional
transonic blade-vortex interaction hover noise
[BTN-94-EIX94441386601] p 182 A95-67332

Y

YALAMANCHILI, R.

Vortex cutting by a blade. Part II: Computations of vortex
response
[BTN-94-EIX94441386611] p 208 A95-67342

YALIF, GUY U.

The Computer Aided Aircraft-design Package (CAAP)
p 217 N95-19759

YAMAGUCHI, YUTAKA

Preliminary assessment of tunnel wall interference in
the NDA cryogenic wind tunnel
[BTN-95-EIX95062487531] p 187 A95-69239

YANG, THOMAS T.

Use of MOBITEK wireless wide area networks as a
solution to land-based positioning and navigation
[BTN-94-EIX94441386132] p 189 A95-68188

YEH, HWA-YOUNG M.

Microwave and infrared simulations of an intense
convective system and comparison with aircraft
observations
[HTN-95-60511] p 214 A95-68762

YEN, BING K.

Surface morphology and structure of carbon-carbon
composites in high-energy sliding contact
[BTN-94-EIX94371347996] p 206 A95-69164

YOROZU, MASAHIRO

Preliminary assessment of tunnel wall interference in
the NDA cryogenic wind tunnel
[BTN-95-EIX95062487531] p 187 A95-69239

YUAN, QIN

Wormgear geometry adopted for implementing
hydrostatic lubrication and formulation of the lubrication
problem
[NASA-CR-195416] p 210 N95-19567

Z

ZHONG, P.

Stability of magnetic bearing-rotor systems and the
effects of gravity and damping
[BTN-94-EIX94441386619] p 208 A95-68168

ZHOU, R. C.

Finite element time domain - modal formulation for
nonlinear flutter of composite panels
[BTN-95-EIX95042474401] p 203 A95-68299

ZIA, S.

Using IRI for the computation of ionospheric corrections
for altimeter data analysis p 212 A95-66949

ZOLE, ARIE

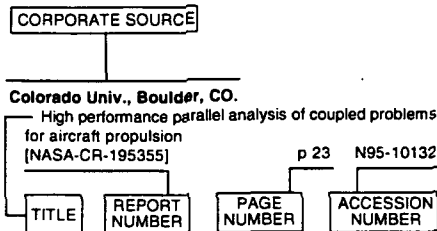
Continuous gust response and sensitivity derivatives
using state-space models
[BTN-95-EIX95062487551] p 203 A95-68365

CORPORATE SOURCE INDEX

AERONAUTICAL ENGINEERING / A Continuing Bibliography (Supplement 317)

May 1995

Typical Corporate Source Index Listing



Listings in this index are arranged alphabetically by corporate source. The title of the document is used to provide a brief description of the subject matter. The page number and the accession number are included in each entry to assist the user in locating the abstract in the abstract section. If applicable, a report number is also included as an aid in identifying the document.

A

- Advisory Group for Aerospace Research and Development, Neuilly-Sur-Seine (France).**
Erosion, Corrosion and Foreign Object Damage Effects in Gas Turbines
[AGARD-CP-558] p 197 N95-19653
- Aeronautical Research Labs., Melbourne (Australia).**
Programmable cockpit research simulator
[AD-A279219] p 204 N95-19848
- Air Force Inst. of Tech., Wright-Patterson AFB, OH.**
Developing an emission factor for hazardous air pollutants for an F-16 using JP-8 fuel
[AD-A284802] p 216 N95-19685
- Aircraft Research Association Ltd., Bedford (England).**
An investigation of drag repeatability in half model testing in the ARA Transonic Wind Tunnel
[ARA-MEMO-392] p 188 N95-19546
- Multipoint pressure measurements on continuously moving wind tunnel models
[ARA-MEMO-391] p 188 N95-19772
- Validation and evaluation of the advanced aeronautical CFD system SAUNA: A method developer's view
[ARA-MEMO-390] p 210 N95-19774
- Application of three-dimensional hybrid structured/unstructured grids to land, sea and air vehicles
[ARA-MEMO-399] p 210 N95-19775
- Verification of the CFD simulation system SAUNA for complex aircraft configurations
[ARA-MEMO-401] p 211 N95-19776
- Inviscid and viscous flow modelling of complex aircraft configurations using the CFD simulation system sauna
[ARA-MEMO-403] p 211 N95-19777
- The aerodynamic design of an integrated wing lower surface and pylons for reduced drag
[ARA-MEMO-406] p 194 N95-19789
- Army Aviation Systems Command, Saint Louis, MO.**
US Army rotorcraft turboshaft engines sand and dust erosion considerations p 198 N95-19656

B

- BKM, Inc., San Diego, CA.**
Advanced diesel electronic fuel injection and turbocharging
[AD-A279176] p 211 N95-19809

C

- Centro Sviluppo Materiali S.p.A., Trento (Italy).**
Thermal testing of high performance thermal barrier coatings for turbine blades p 202 N95-19681
- Cincinnati Univ., OH.**
Experimental and numerical simulations of the effects of ingested particles in gas turbine engines p 199 N95-19662
- Cranfield Univ., Bedford (England).**
Particle trajectories in gas turbine engines p 199 N95-19663

D

- Defence Research Agency, Farnborough, Hampshire (England).**
The operation of gas turbine engines in hot and sandy conditions: Royal Air Force experiences in the Gulf conflict p 198 N95-19655
- The calculation of erosion in a gas turbine compressor rotor p 199 N95-19664

E

- Energy and Environmental Analysis, Inc., Arlington, VA.**
Air pollution mitigation measures for airports and associated activity
[PB94-207610] p 216 N95-19582

F

- Federal Aviation Administration, Washington, DC.**
Federal aviation regulations, part 91. General operating and flight rules. Change 8
[PB94-217445] p 188 N95-19720

G

- Galaxy Scientific Corp., Pleasantville, NJ.**
Rotorcraft ditchings and water-related impacts that occurred from 1982 to 1989, phase 1
[AD-A279164] p 189 N95-19805
- General Electric Co., Cincinnati, OH.**
Modern transport engine experience with environmental ingestion effects p 199 N95-19660

I

- Interturbine Holding B.V., Lomm (Netherlands).**
Braze repair possibilities for hot section gas turbine parts p 201 N95-19677

J

- Jet Propulsion Lab., California Inst. of Tech., Pasadena, CA.**
Possible near-IR channels for remote sensing precipitable water vapor from geostationary satellite platforms
[HTN-95-70139] p 214 A95-69431

K

- K. T. Analytics, Inc. Frederick, MD.**
Air pollution mitigation measures for airports and associated activity
[PB94-207610] p 216 N95-19582

L

- Liburdi Engineering Ltd., Hamilton (Ontario).**
Protective coatings for compressor gas path components p 201 N95-19675

M

- Michigan Univ., Ann Arbor, MI.**
Design considerations for an archimedean slot spiral antenna p 211 N95-19798
- MITech, Inc., Pleasantville, NJ.**
Research requirements for future visual guidance systems
[AD-A279188] p 191 N95-19810
- Motoren- und Turbinen-Union Muenchen G.m.b.H., Munich (Germany).**
Performance deterioration of axial compressors due to blade defects p 199 N95-19665
- Impact loading of compressor stator vanes by hailstone ingestion p 200 N95-19670
- Damage of high temperature components by dust-laden air p 201 N95-19673

N

- National Aeronautics and Space Administration, Washington, DC.**
Microwave and infrared simulations of an intense convective system and comparison with aircraft observations
[HTN-95-60511] p 214 A95-68762
- National Aeronautics and Space Administration, Ames Research Center, Moffett Field, CA.**
Three-dimensional model interpretation of NO(x) measurements from the lower stratosphere
[HTN-95-90534] p 213 A95-67806
- Review of numerical procedures for computational surface thermochemistry
[BTN-94-EIX94441386682] p 205 A95-68191
- Effect of ground and ceiling planes on shape of energized wakes
[BTN-95-EIX95062487558] p 186 A95-68372
- Trajectory-based heating analysis for the European Space Agency/Rosetta Earth Return Vehicle
[BTN-95-EIX95041503787] p 205 A95-69218
- Numerical simulation of incidence and sweep effects on delta wing vortex breakdown
[BTN-95-EIX95062487526] p 186 A95-69234
- Simulation and flight test evaluation of head-up-display guidance for hammer approach transitions
[BTN-95-EIX95062487533] p 194 A95-69241
- National Aeronautics and Space Administration, Goddard Space Flight Center, Greenbelt, MD.**
Using IRI for the computation of ionospheric corrections for altimeter data analysis p 212 A95-66949
- Microwave and infrared simulations of an intense convective system and comparison with aircraft observations
[HTN-95-60511] p 214 A95-68762
- Possible near-IR channels for remote sensing precipitable water vapor from geostationary satellite platforms
[HTN-95-70139] p 214 A95-69431
- National Aeronautics and Space Administration, Hugh L. Dryden Flight Research Facility, Edwards, CA.**
Flight experience with lightweight, low-power miniaturized instrumentation systems
[BTN-95-EIX95062487522] p 180 A95-69230
- National Aeronautics and Space Administration, Lyndon B. Johnson Space Center, Houston, TX.**
Documentation and archiving of the Space Shuttle wind tunnel test data base. Volume 2: User's Guide to the Archived Data Base
[NASA-TM-104806-VOL-2] p 205 N95-19624
- National Aeronautics and Space Administration, Langley Research Center, Hampton, VA.**
Demonstration of an elastically coupled twist control concept for tilt rotor blade application
[BTN-94-EIX94441386633] p 196 A95-68182

Parallel implicit unstructured grid Euler solvers
[BTN-95-EIX95042474393] p 217 A95-68307

Coupling equivalent plate and finite element formulations in multiple-method structural analyses
[BTN-95-EIX95062487548] p 192 A95-68362

Passive porosity with free and fixed separation on a tangent-ogive forebody
[BTN-95-EIX95062487554] p 185 A95-68368

Approximate method for calculating heating rates on three-dimensional vehicles
[BTN-95-EIX95041503778] p 210 A95-69209

Navier-Stokes simulations of Orbiter aerodynamic characteristics including pitch trim and bodyflap
[BTN-95-EIX95041503779] p 204 A95-69210

Multiblock analysis for Shuttle Orbiter reentry heating from Mach 24 to Mach 12
[BTN-95-EIX95041503780] p 205 A95-69211

Recent studies of rotorcraft blade-vortex interaction noise
[BTN-95-EIX95062487521] p 218 A95-69229

Interpretation of waverider performance data using computational fluid dynamics
[BTN-95-EIX95062487534] p 193 A95-69242

Numerical study of the performance of swept, curved compression surface scramjet inlets
[BTN-95-EIX95112524198] p 197 A95-69310

National Aeronautics and Space Administration. Lewis Research Center, Cleveland, OH.

Repeatability of ice shapes in the NASA Lewis icing research tunnel
[BTN-95-EIX95062487528] p 204 A95-69236

Ice-impact analysis of blades p 200 N95-19672

Resistance of silicon nitride turbine components to erosion and hot corrosion/oxidation attack p 202 N95-19683

Improved speed control system for the 87,000 HP wind tunnel drive
[NASA-TM-106840] p 211 N95-19794

National Aeronautics and Space Administration. Marshall Space Flight Center, Huntsville, AL.

Aircraft electric field measurements: Calibration and ambient field retrieval
[HTN-95-90508] p 213 A95-67780

National Aeronautics and Space Administration. Wallops Flight Center, Wallops Island, VA.

A comparative study of internally and externally capped balloons using small scale test balloons p 181 A95-66285

Status of the NASA balloon program p 181 A95-66296

Overview of the NASA balloon R&D program p 181 A95-66297

National Aerospace Lab., Amsterdam (Netherlands).

Gas turbine compressor corrosion and erosion in Western Europe p 201 N95-19678

National Renewable Energy Lab., Golden, CO.

Evidence that aerodynamic effects, including dynamic stall, dictate HAWT structural loads and power generation in highly transient time frames
[DE94-011865] p 216 N95-19855

National Research Council of Canada, Ottawa (Ontario).

Erosion of T56 5th stage rotor blades due to bleed hole overtip flow p 200 N95-19666

National Transportation Safety Board, Washington, DC.

Special investigation report: Maintenance anomaly resulting in dragged engine during landing rollout. Northwest Airlines Flight 18, Boeing 747-251B, N637US, New Tokyo International Airport, Narita, Japan, 1 Mar. 1994
[PB94-917006] p 188 N95-19793

Naval Air Warfare Center, Patuxent River, MD.

The use of genetic algorithms for flight test and evaluation of artificial intelligence and complex software systems
[AD-A284824] p 217 N95-19688

Airship applications of modern flight test techniques
[AD-A284253] p 194 N95-19731

Naval Air Warfare Center, Trenton, NJ.

Navy foreign object damage and its impact on future gas turbine engine low pressure compression systems p 198 N95-19658

Testing considerations for military aircraft engines in corrosive environments (a Navy perspective) p 202 N95-19684

Naval Postgraduate School, Monterey, CA.

An analysis of the costs and benefits in improving F402-RR-406A High Pressure Turbine, second stage blades under the aircraft engine Component Improvement Program (CIP)
[AD-A285127] p 197 N95-19595

Automation of hardware-in-the-loop testing of control systems for unmanned air vehicles
[AD-A284833] p 194 N95-19693

Inband radar cross section of phased arrays with parallel feeds
[AD-A284249] p 210 N95-19730

Naval Research Lab., Washington, DC.

Wind tunnel tests of a 42 inch diameter self-starting autogyro rotor
[AD-A279922] p 188 N95-19863

NYMA, Inc., Brook Park, OH.

Prediction of wind tunnel effects on the installed F/A-18A inlet flow field at high angles-of-attack
[NASA-CR-195429] p 197 N95-19651

NYMA, Inc., Cleveland, OH.

On supersonic-inlet boundary-layer bleed flow
[NASA-CR-195426] p 202 N95-19769

O

Oxford Univ., Oxford (England).

Particle deposition in gas turbine blade film cooling holes p 199 N95-19661

Soft body impact on titanium fan blades p 200 N95-19671

P

Palermo Univ. (Italy).

An airborne monitoring system for FOD and erosion faults p 200 N95-19668

Purdue Univ., West Lafayette, IN.

Aero-thermodynamic distortion induced structured dynamic response
[AD-A279931] p 203 N95-19864

R

Reticular Systems, Inc., San Diego, CA.

PalymSys (TM): An extended version of CLIPS for construction and reasoning using blackboards p 217 N95-19767

Rolls-Royce Ltd., Bristol (England).

Out of area experiences with the RB199 in Toronto p 198 N95-19654

Future directions in helicopter protection system configuration p 198 N95-19657

Royal Military Coll. of Saint-Jean, Richelieu (Quebec).

Transport aircraft loading and balancing system: Using a CLIPS expert system for military aircraft load planning p 217 N95-19751

S

Sendia National Labs., Albuquerque, NM.

Environmental effects on composite airframes: A study conducted for the ARM UAV Program (Atmospheric Radiation Measurement Unmanned Aerospace Vehicle)
[DE94-015351] p 206 N95-19579

Scandinavian Airlines System, Oslo (Norway).

Scandinavian Airlines Systems experience on erosion, corrosion and foreign object damage effects on gas turbines p 198 N95-19659

Societe Nationale d'Etude et de Construction de Moteurs d'Aviation, Evry (France).

New Trends in coatings developments for turbine blades: Materials processing and repair p 201 N95-19676

Societe Nationale d'Etude et de Construction de Moteurs d'Aviation, Moissy-Cramayel (France).

Design of fan blades subjected to bird impact p 200 N95-19669

State Univ. of New York, Binghamton, NY.

Wormgear geometry adopted for implementing hydrostatic lubrication and formulation of the lubrication problem
[NASA-CR-195416] p 210 N95-19567

T

Turbine Support Europa, Tilburg (Netherlands).

High velocity oxygen fuel spraying of erosion and wear resistant coatings on jet engine parts p 202 N95-19680

Turbomeca S.A. - Brevets Szydlowski, Bordes (France).

Multilayer anti-erosion coatings p 201 N95-19679

W

West Virginia Univ., Morgantown, VA.

Determination of stability and control derivatives from the NASA F/A-18 HARV from flight data using the maximum likelihood method
[NASA-CR-197320] p 204 N95-19576

Wright Lab., Wright-Patterson AFB, OH.

Proceedings of the USAF Structural Integrity Program Conference
[AD-A285684] p 194 N95-19517

Y

Yalif (Guy U.), MA.

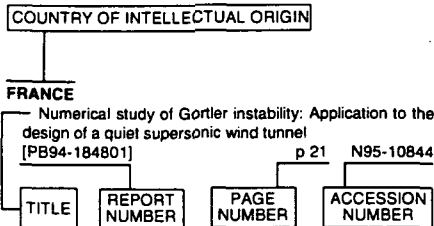
The Computer Aided Aircraft-design Package (CAAP)
p 217 N95-19759

FOREIGN TECHNOLOGY INDEX

AERONAUTICAL ENGINEERING / A Continuing Bibliography (Supplement 317)

May 1995

Typical Foreign Technology Index Listing



Listings in this index are arranged alphabetically by country of intellectual origin. The title of the document is used to provide a brief description of the subject matter. The page number and accession number are included in each entry to assist the user in locating the abstract in the abstract section. If applicable, a report number is also included as an aid in identifying the document.

A

AUSTRALIA

- Fatigue resistance of peened 7050-T7451 aluminium alloy: Repair and re-treatment of a component surface [BTN-94-EIX94371347838] p 206 A95-69131
- Fatigue crack growth in nickel-based superalloys at 500-700 C. 1: Waspaloy [BTN-94-EIX94371347843] p 206 A95-69136
- Programmable cockpit research simulator [AD-A279219] p 204 N95-19848

AUSTRIA

- Balloon technology and observations; Symposium P3 of the COSPAR Plenary Meeting, 29th, Washington, DC, Aug. 28-Sept. 5, 1992 [HTN-95-70250] p 181 A95-66276

B

BRAZIL

- The joint Russian-Brazil research on balloons p 182 A95-66303

BULGARIA

- A program for scientific and applied investigations using aerostat complexes p 182 A95-66304

C

CANADA

- Lyapunov exponents and stochastic stability of two-dimensional parametrically excited random systems [BTN-94-EIX94361122401] p 207 A95-65897
- Vortical flow structure near the F/A-18 LEX at high incidence [BTN-95-EIX95062487555] p 186 A95-68369
- Aircraft icing measurements in East Coast winter storms [HTN-95-60505] p 214 A95-68756

- Flight control system mode transitions influence on handling qualities and task performance [BTN-95-EIX95062487525] p 203 A95-69233
- Mesoscale structure of precipitation bands in a North Atlantic winter storm [HTN-95-40659] p 215 A95-69803
- Erosion of T56 5th stage rotor blades due to bleed hole overtip flow p 200 N95-19666
- Protective coatings for compressor gas path components p 201 N95-19675
- Transport aircraft loading and balancing system: Using a CLIPS expert system for military aircraft load planning p 217 N95-19751

CROATIA

- Powerful bolide explosion over North Italy [HTN-95-80564] p 218 A95-69658

F

FRANCE

- French contribution to new balloon designs and materials p 181 A95-66277
- Balloon flights in France and in Europe p 204 A95-66301
- Nonhydrostatic simulation of frontogenesis in a moist atmosphere. Part 3: Thermal wind imbalance and rainbands [HTN-95-90356] p 212 A95-66429
- Aspects of vortex breakdown [HTN-95-A0001] p 183 A95-67828
- Shock layers and boundary layers in hypersonic flows [HTN-95-A0003] p 183 A95-67830
- Experimental study of three-dimensional separation [BTN-94-EIX94441385752] p 179 A95-68216
- Prediction of ice accretion: Comparison between the 2D and 3D codes [BTN-94-EIX94441385753] p 213 A95-68217
- Phenomenological description and simplified modelling of the vortex wake issuing from a jet in a crossflow [BTN-94-EIX94441385754] p 184 A95-68218
- Tip vortex on a swept wing. Mean flow and unsteady phenomena [BTN-94-EIX94441385755] p 184 A95-68219
- Future SSTs a European approach [BTN-95-EIX95072419883] p 180 A95-68396
- Measurement by coherent anti-Stokes Raman scattering in the R5Ch hypersonic wind tunnel [BTN-95-EIX95112523811] p 188 A95-69322
- Side forces at high angles of attack. Why, when, how? [BTN-95-EIX95112523809] p 194 A95-69324
- Erosion, Corrosion and Foreign Object Damage Effects in Gas Turbines [AGARD-CP-558] p 197 N95-19653
- Design of fan blades subjected to bird impact p 200 N95-19669
- New Trends in coatings developments for turbine blades: Materials processing and repair p 201 N95-19676
- Multilayer anti-erosion coatings p 201 N95-19679

G

GERMANY

- Planar air density measurements near model surfaces by ultraviolet Rayleigh/Raman scattering [BTN-94-EIX94441386614] p 213 A95-67345
- High accuracy navigation and landing system using GPS/IMU system integration [BTN-94-EIX94441386129] p 189 A95-68185
- GPS/GLONASS/INS test program [BTN-94-EIX94441386131] p 189 A95-68187
- On wave-front curvature in linear stability theory [BTN-94-EIX94441385756] p 184 A95-68220
- Using adaptive structures to attenuate rotary wing aeroelastic response [BTN-95-EIX95062487547] p 192 A95-68361
- On-the-fly carrier phase ambiguity resolution for precise aircraft landing [BTN-95-EIX95112522535] p 190 A95-69328
- Performance deterioration of axial compressors due to blade defects p 199 N95-19665

- Impact loading of compressor stator vanes by hailstone ingestion p 200 N95-19670
- Damage of high temperature components by dust-laden air p 201 N95-19673

GREECE

- Adaptive modeling of jet engine performance with application to condition monitoring [BTN-95-EIX95112524205] p 196 A95-69303

INDIA

- Unbalance response of a dual rotor system: Theory and experiment [BTN-94-EIX94351143320] p 195 A95-65854
- Recent trends in balloon flights from TIFR's National Balloon Facility, Hyderabad p 191 A95-66300

ISRAEL

- Continuous gust response and sensitivity derivatives using state-space models [BTN-95-EIX95062487551] p 203 A95-68365

ITALY

- Selecting and management of fire fighter aircraft [BTN-95-EIX95062487538] p 193 A95-69246
- An airborne monitoring system for FOD and erosion faults p 200 N95-19668
- Thermal testing of high performance thermal barrier coatings for turbine blades p 202 N95-19681

J

JAPAN

- Dynamic behavior of valves with pneumatic chamber for reciprocating compressors [BTN-94-EIX94351143311] p 207 A95-65845
- Three-dimensional analysis of scramjet nozzle flows [BTN-94-EIX94441380978] p 196 A95-68162
- Surface morphology and structure of carbon-carbon composites in high-energy sliding contact [BTN-94-EIX94371347996] p 206 A95-69164
- Preliminary assessment of tunnel wall interference in the NDA cryogenic wind tunnel [BTN-95-EIX95062487531] p 187 A95-69239

K

KOREA, REPUBLIC OF

- Aeroelastic stability of hingeless rotor blade in hover using large deflection theory [BTN-94-EIX94441386616] p 183 A95-67347

N

NETHERLANDS

- Braze repair possibilities for hot section gas turbine parts p 201 N95-19677
- Gas turbine compressor corrosion and erosion in Western Europe p 201 N95-19678
- High velocity oxygen fuel spraying of erosion and wear resistant coatings on jet engine parts p 202 N95-19680

NEW ZEALAND

- An air-driven pressure booster pump for aircraft-based air sampling [HTN-95-40689] p 216 A95-69833

NORWAY

- Scandinavian Airlines Systems experience on erosion, corrosion and foreign object damage effects on gas turbines p 198 N95-19659

R

RUSSIA

- The scientific ballooning in Russia p 191 A95-66302
- Kinetic theory in aerothermodynamics [HTN-95-A0002] p 183 A95-67829

SAUDI ARABIA

State-space representation of aerodynamic characteristics of an aircraft at high angles of attack
[BTN-95-EIX95062487536] p 187 A95-69244

S

SAUDI ARABIA

Suppression of vortex asymmetry and side force on a circular cone
[BTN-95-EIX95042474413] p 209 A95-68287

SOUTH AFRICA

Aerodynamic effects of delta planform tip sails on wing performance
[BTN-95-EIX95062487544] p 185 A95-68358
Aerodynamic characteristics of strake vortex flaps on a strake-wing configuration
[BTN-95-EIX95062487537] p 187 A95-69245

T

TAIWAN, PROVINCE OF CHINA

Analysis of an oscillating Joukowski airfoil with surface suction and moving vortices
[BTN-95-EIX95062487527] p 186 A95-69235

U

UNITED KINGDOM

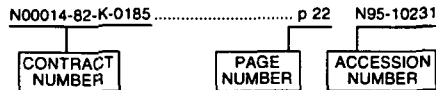
Construction of nearly orthogonal multiblock grids for compressible flow simulation
[BTN-94-EIX94361133526] p 207 A95-65981
Antarctic snow record of southern hemisphere lead pollution
[HTN-95-40359] p 212 A95-66869
Behavior of the Johnson-King turbulence model in axisymmetric supersonic flows
[BTN-94-EIX94441386606] p 183 A95-67337
Interference between tanker wing wake with roll-up and receiver aircraft
[BTN-95-EIX95062487552] p 185 A95-68366
Results and performance of multi-site reference station differential GPS
[BTN-95-EIX95112522534] p 190 A95-69329
Integrated GPS/Glonass navigation: Algorithms and results
[BTN-95-EIX95112522531] p 190 A95-69332
An investigation of drag repeatability in half model testing in the ARA Transonic Wind Tunnel
[ARA-MEMO-392] p 188 N95-19546
Out of area experiences with the RB199 in Toronto
p 198 N95-19654
The operation of gas turbine engines in hot and sandy conditions: Royal Air Force experiences in the Gulf conflict
p 198 N95-19655
Future directions in helicopter protection system configuration
p 198 N95-19657
Particle deposition in gas turbine blade film cooling holes
p 199 N95-19661
Particle trajectories in gas turbine engines
p 199 N95-19663
The calculation of erosion in a gas turbine compressor rotor
p 199 N95-19664
Soft body impact on titanium fan blades
p 200 N95-19671
Multiport pressure measurements on continuously moving wind tunnel models
[ARA-MEMO-391] p 188 N95-19772
Validation and evaluation of the advanced aeronautical CFD system SAUNA: A method developer's view
[ARA-MEMO-390] p 210 N95-19774
Application of three-dimensional hybrid structured/unstructured grids to land, sea and air vehicles
[ARA-MEMO-399] p 210 N95-19775
Verification of the CFD simulation system SAUNA for complex aircraft configurations
[ARA-MEMO-401] p 211 N95-19776
Inviscid and viscous flow modelling of complex aircraft configurations using the CFD simulation system sauna
[ARA-MEMO-403] p 211 N95-19777
The aerodynamic design of an integrated wing lower surface and pylons for reduced drag
[ARA-MEMO-406] p 194 N95-19789

CONTRACT NUMBER INDEX

AERONAUTICAL ENGINEERING / A Continuing Bibliography (Supplement 317)

May 1995

Typical Contract Number Index Listing



Listings in this index are arranged alphanumerically by contract number. Under each contract number the accession numbers denoting documents that have been produced as a result of research done under the contract are shown. The accession number denotes the number by which the citation is identified in the abstract section. Preceding the accession number is the page number on which the citation may be found.

AF PROJ. 2418	p 194	N95-19517
AF-AFOSR-0251-91	p 203	N95-19864
ARB-A132-168	p 216	N95-19582
DA PROJ. 1L1-61102-AH-45	p 210	N95-19567
DAA HO4-93-G0019	p 212	A95-66315
DAAE07-90-C-R030	p 211	N95-19809
DE-AC04-94AL-85000	p 206	N95-19579
DE-AC36-83CH-10093	p 216	N95-19855
DTFA03-89-C-00043	p 189	N95-19805
NAG3-1316	p 210	N95-19567
NAG5-30552	p 214	A95-69431
NAS3-27186	p 197	N95-19651
	p 202	N95-19769
	p 211	N95-19794
NCC2-759	p 204	N95-19576
NSF ATM-89-12736	p 212	A95-66315
NSF ATM-90-14763	p 214	A95-68845
RTOP 505-62-OJ	p 210	N95-19567
RTOP 505-62-20	p 202	N95-19769
RTOP 505-62-82	p 211	N95-19794
RTOP 505-68-30	p 197	N95-19651

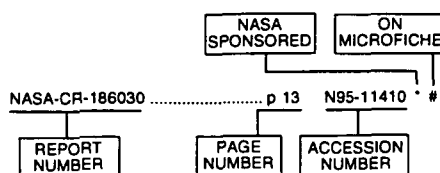
CONTRACT

REPORT NUMBER INDEX

AERONAUTICAL ENGINEERING / A Continuing Bibliography (Supplement 317)

May 1995

Typical Report Number Index Listing



Listings in this index are arranged alphanumerically by report number. The page number indicates the page on which the citation is located. The accession number denotes the number by which the citation is identified. An asterisk (*) indicates that the item is a NASA report. A pound sign (#) indicates that the item is available on microfiche.

AD-A279164	p 189	N95-19805
AD-A279176	p 211	N95-19809
AD-A279188	p 191	N95-19810
AD-A279219	p 204	N95-19848
AD-A279922	p 188	N95-19863
AD-A279931	p 203	N95-19864
AD-A284249	p 210	N95-19730
AD-A284253	p 194	N95-19731
AD-A284802	p 216	N95-19685 #
AD-A284824	p 217	N95-19688 #
AD-A284833	p 194	N95-19693 #
AD-A285127	p 197	N95-19595 #
AD-A285684	p 194	N95-19517 #
AFIT/GEE/ENS/94S-26	p 216	N95-19685 #
AFOSR-94-0338TR	p 203	N95-19864
AGARD-CP-558	p 197	N95-19653 #
AIAA PAPER 94-0393	p 211	N95-19776 #
AIAA PAPER 95-0038	p 202	N95-19769 *
ARA-MEMO-390	p 210	N95-19774 #
ARA-MEMO-391	p 188	N95-19772 #
ARA-MEMO-392	p 188	N95-19546 #
ARA-MEMO-399	p 210	N95-19775 #
ARA-MEMO-401	p 211	N95-19776 #
ARA-MEMO-403	p 211	N95-19777 #
ARA-MEMO-406	p 194	N95-19789 #
ARB-R-94/534	p 216	N95-19582 #
ARL-CR-219	p 210	N95-19567 *
ARL-TN-49	p 204	N95-19848
BTN-94-EIX94351108100	p 191	A95-66500
BTN-94-EIX94351143311	p 207	A95-65845
BTN-94-EIX94351143320	p 195	A95-65854
BTN-94-EIX94351143325	p 195	A95-67298
BTN-94-EIX94351143328	p 207	A95-67301
BTN-94-EIX94351143331	p 207	A95-67304
BTN-94-EIX94361122401	p 207	A95-65897
BTN-94-EIX94361133526	p 207	A95-65981
BTN-94-EIX94371347838	p 206	A95-69131
BTN-94-EIX94371347843	p 206	A95-69136
BTN-94-EIX94371347996	p 206	A95-69164
BTN-94-EIX94441380974	p 195	A95-68158
BTN-94-EIX94441380977	p 195	A95-68161
BTN-94-EIX94441380978	p 196	A95-68162
BTN-94-EIX94441380981	p 208	A95-68165
BTN-94-EIX94441380983	p 208	A95-67329
BTN-94-EIX94441385752	p 179	A95-68216
BTN-94-EIX94441385753	p 213	A95-68217

BTN-94-EIX94441385754	p 184	A95-68218
BTN-94-EIX94441385755	p 184	A95-68219
BTN-94-EIX94441385756	p 184	A95-68220
BTN-94-EIX94441386129	p 189	A95-68185
BTN-94-EIX94441386131	p 189	A95-68187
BTN-94-EIX94441386132	p 189	A95-68188
BTN-94-EIX94441386601	p 182	A95-67332
BTN-94-EIX94441386604	p 182	A95-67335
BTN-94-EIX94441386606	p 182	A95-67336
BTN-94-EIX94441386606	p 183	A95-67337
BTN-94-EIX94441386611	p 208	A95-67342
BTN-94-EIX94441386612	p 208	A95-67343
BTN-94-EIX94441386614	p 213	A95-67345
BTN-94-EIX94441386616	p 183	A95-67347
BTN-94-EIX94441386619	p 208	A95-68168
BTN-94-EIX94441386623	p 179	A95-68172
BTN-94-EIX94441386624	p 183	A95-68173
BTN-94-EIX94441386625	p 184	A95-68174
BTN-94-EIX94441386631	p 184	A95-68180
BTN-94-EIX94441386632	p 179	A95-68181
BTN-94-EIX94441386633	p 196	A95-68182 *
BTN-94-EIX94441386682	p 205	A95-68191 *
BTN-94-EIX94441386686	p 184	A95-68195
BTN-95-EIX95031502749	p 217	A95-68256
BTN-95-EIX95031502750	p 196	A95-68257
BTN-95-EIX95031502751	p 179	A95-68258
BTN-95-EIX95031502752	p 209	A95-68259
BTN-95-EIX95031502753	p 188	A95-68260
BTN-95-EIX95041503010	p 192	A95-68313
BTN-95-EIX95041503011	p 213	A95-68314
BTN-95-EIX95041503093	p 184	A95-68353
BTN-95-EIX95041503778	p 210	A95-69209 *
BTN-95-EIX95041503779	p 204	A95-69210 *
BTN-95-EIX95041503780	p 205	A95-69211 *
BTN-95-EIX95041503781	p 205	A95-69212
BTN-95-EIX95041503782	p 193	A95-69213
BTN-95-EIX95041503783	p 193	A95-69214
BTN-95-EIX95041503784	p 180	A95-69215
BTN-95-EIX95041503785	p 180	A95-69216
BTN-95-EIX95041503787	p 205	A95-69218 *
BTN-95-EIX95042474388	p 209	A95-68312
BTN-95-EIX95042474389	p 196	A95-68311
BTN-95-EIX95042474393	p 217	A95-68307 *
BTN-95-EIX95042474398	p 209	A95-68302
BTN-95-EIX95042474400	p 192	A95-68309
BTN-95-EIX95042474401	p 203	A95-68320
BTN-95-EIX95042474409	p 209	A95-68291
BTN-95-EIX95042474413	p 209	A95-68287
BTN-95-EIX95042474418	p 209	A95-68282
BTN-95-EIX95042474624	p 189	A95-68278
BTN-95-EIX95042474626	p 209	A95-68280
BTN-95-EIX95042477108	p 179	A95-68351
BTN-95-EIX95042477109	p 179	A95-68350
BTN-95-EIX95042477110	p 192	A95-68349
BTN-95-EIX95062487521	p 218	A95-69229 *
BTN-95-EIX95062487522	p 180	A95-69230 *
BTN-95-EIX95062487524	p 186	A95-69232 *
BTN-95-EIX95062487525	p 203	A95-69233
BTN-95-EIX95062487526	p 186	A95-69234 *
BTN-95-EIX95062487527	p 186	A95-69235
BTN-95-EIX95062487528	p 204	A95-69236 *
BTN-95-EIX95062487530	p 186	A95-69238
BTN-95-EIX95062487531	p 187	A95-69239
BTN-95-EIX95062487532	p 187	A95-69240
BTN-95-EIX95062487533	p 194	A95-69241 *
BTN-95-EIX95062487534	p 193	A95-69242 *
BTN-95-EIX95062487535	p 190	A95-69243 *
BTN-95-EIX95062487536	p 187	A95-69244
BTN-95-EIX95062487537	p 187	A95-69245
BTN-95-EIX95062487538	p 193	A95-69246
BTN-95-EIX95062487539	p 187	A95-69247
BTN-95-EIX95062487540	p 187	A95-69248
BTN-95-EIX95062487541	p 184	A95-68355
BTN-95-EIX95062487542	p 192	A95-68356
BTN-95-EIX95062487543	p 185	A95-68357
BTN-95-EIX95062487544	p 185	A95-68358
BTN-95-EIX95062487545	p 185	A95-68359
BTN-95-EIX95062487546	p 185	A95-68360
BTN-95-EIX95062487547	p 192	A95-68361
BTN-95-EIX95062487548	p 192	A95-68362 *
BTN-95-EIX95062487550	p 203	A95-68364
BTN-95-EIX95062487551	p 203	A95-68365
BTN-95-EIX95062487552	p 185	A95-68366

BTN-95-EIX95062487553	p 203	A95-68367
BTN-95-EIX95062487554	p 185	A95-68368 *
BTN-95-EIX95062487555	p 186	A95-68369
BTN-95-EIX95062487556	p 193	A95-68370
BTN-95-EIX95062487557	p 203	A95-68371
BTN-95-EIX95062487558	p 186	A95-68372 *
BTN-95-EIX95072419881	p 180	A95-68398
BTN-95-EIX95072419883	p 180	A95-68396
BTN-95-EIX95072498877	p 210	A95-68393
BTN-95-EIX95072498878	p 180	A95-68394
BTN-95-EIX95072498879	p 180	A95-68395
BTN-95-EIX95112522529	p 190	A95-69334
BTN-95-EIX95112522530	p 190	A95-69333
BTN-95-EIX95112522531	p 190	A95-69332
BTN-95-EIX95112522534	p 190	A95-69329
BTN-95-EIX95112522535	p 190	A95-69328
BTN-95-EIX95112523809	p 194	A95-69324
BTN-95-EIX95112523811	p 188	A95-69322
BTN-95-EIX95112524190	p 206	A95-69318
BTN-95-EIX95112524198	p 197	A95-69310 *
BTN-95-EIX95112524199	p 197	A95-69309
BTN-95-EIX95112524200	p 210	A95-69308
BTN-95-EIX95112524204	p 196	A95-69304
BTN-95-EIX95112524205	p 196	A95-69303
BTN-95-EIX95112524206	p 196	A95-69302
BTN-95-EIX95112530749	p 193	A95-69295
CONF-940548-7	p 216	N95-19855 #
DE94-011865	p 216	N95-19855 #
DE94-015351	p 206	N95-19579 #
DODA-AR-008-375	p 204	N95-19848
DOT/FAA/CT-92/13	p 189	N95-19805
DOT/FAA/CT-93/49	p 191	N95-19810
E-9345	p 210	N95-19567 *
E-9393	p 202	N95-19769 *
E-9404	p 211	N95-19794 *
E-9416	p 197	N95-19651 *
F-632	p 211	N95-19809
HTN-95-A0001	p 183	A95-67828
HTN-95-A0002	p 183	A95-67829
HTN-95-A0003	p 183	A95-67830
HTN-95-A0175	p 215	A95-69766
HTN-95-10686	p 214	A95-68845
HTN-95-20631	p 215	A95-69574
HTN-95-40359	p 212	A95-68689
HTN-95-40659	p 215	A95-69803
HTN-95-40689	p 216	A95-69833
HTN-95-60505	p 214	A95-68756
HTN-95-60511	p 214	A95-68762 *
HTN-95-60545	p 205	A95-69854
HTN-95-70139	p 214	A95-69431 *
HTN-95-70250	p 181	A95-66276
HTN-95-80258	p 212	A95-66315
HTN-95-80564	p 218	A95-69658
HTN-95-90356	p 212	A95-66429
HTN-95-90508	p 213	A95-67780 *
HTN-95-90534	p 213	A95-67806 *
HTN-95-90690	p 215	A95-69717
HTN-95-90694	p 215	A95-69721
ISBN-92-836-0005-3	p 197	N95-19653 #
NAS 1.15:104806-VOL-2	p 205	N95-19624 *
NAS 1.15:106840	p 211	N95-19794 *
NAS 1.26:195416	p 210	N95-19567 *
NAS 1.26:195426	p 202	N95-19769 *
NAS 1.26:195429	p 197	N95-19651 *
NAS 1.26:197320	p 204	N95-19576 *
NASA-CR-195416	p 210	N95-19567 *
NASA-CR-195426	p 202	N95-19769 *
NASA-CR-195429	p 197	N95-19651 *
NASA-CR-197320	p 204	N95-19576 *
NASA-TM-104806-VOL-2	p 205	N95-19624 *
NASA-TM-106840	p 211	N95-19794 *

REPORT

NREL/TP-441-7080**REPORT NUMBER INDEX**

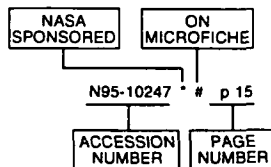
NREL/TP-441-7080	p 216	N95-19855	#
NRL/MR/5710-94-7485	p 188	N95-19863	
NTSB/SIR-94/02	p 188	N95-19793	#
PB94-207610	p 216	N95-19582	#
PB94-217445	p 188	N95-19720	#
PB94-917006	p 188	N95-19793	#
S-786-VOL-2	p 205	N95-19624 *	#
SAND-94-8210	p 206	N95-19579	#
TACOM-13603	p 211	N95-19809	
WL-TR-94-4079	p 194	N95-19517	#

ACCESSION NUMBER INDEX

AERONAUTICAL ENGINEERING / A Continuing Bibliography (Supplement 317)

May 1995

Typical Accession Number Index Listing



Listings in this index are arranged alphanumerically by accession number. The page number indicates the page on which the citation is located. The accession number denotes the number by which the citation is identified. An asterisk (*) indicates that the item is a NASA report. A pound sign (#) indicates that the item is available on microfiche.

A95-65845	p 207	A95-68217	p 213	A95-69210	p 204	N95-19678	# p 201
A95-65854	p 195	A95-68218	p 184	A95-69211	p 205	N95-19679	# p 201
A95-65897	p 207	A95-68219	p 184	A95-69212	p 205	N95-19680	# p 202
A95-65981	p 207	A95-68220	p 184	A95-69213	p 193	N95-19681	# p 202
A95-66276	p 181	A95-68256	p 217	A95-69214	p 193	N95-19683	* p 202
A95-66277	p 181	A95-68257	p 196	A95-69215	p 180	N95-19684	# p 202
A95-66282	p 181	A95-68258	p 179	A95-69216	p 180	N95-19685	# p 216
A95-66285	p 181	A95-68259	p 209	A95-69218	p 205	N95-19688	# p 217
A95-66296	p 181	A95-68260	p 188	A95-69229	p 218	N95-19693	# p 194
A95-66297	p 181	A95-68278	p 189	A95-69230	p 180	N95-19720	# p 188
A95-66300	p 191	A95-68280	p 209	A95-69232	p 186	N95-19730	p 210
A95-66301	p 204	A95-68282	p 209	A95-69233	p 203	N95-19731	p 194
A95-66302	p 191	A95-68287	p 209	A95-69234	p 186	N95-19751	* p 217
A95-66303	p 182	A95-68291	p 209	A95-69235	p 186	N95-19759	* p 217
A95-66304	p 182	A95-68299	p 203	A95-69236	p 204	N95-19767	* p 217
A95-66305	p 191	A95-68300	p 192	A95-69238	p 186	N95-19769	* p 202
A95-66315	p 212	A95-68302	p 209	A95-69239	p 187	N95-19772	# p 188
A95-66429	p 212	A95-68307	p 217	A95-69240	p 187	N95-19774	# p 210
A95-66500	p 191	A95-68311	p 196	A95-69241	p 194	N95-19775	# p 210
A95-66869	p 212	A95-68312	p 209	A95-69242	p 193	N95-19776	# p 211
A95-66949	p 212	A95-68313	p 192	A95-69243	p 190	N95-19777	# p 211
A95-67298	p 195	A95-68314	p 213	A95-69244	p 187	N95-19789	# p 194
A95-67301	p 207	A95-68314	p 213	A95-69245	p 187	N95-19793	# p 188
A95-67304	p 207	A95-68349	p 192	A95-69246	p 193	N95-19794	* p 211
A95-67329	p 208	A95-68350	p 179	A95-69247	p 187	N95-19798	* p 211
A95-67332	p 182	A95-68351	p 179	A95-69248	p 187	N95-19805	p 189
A95-67335	p 182	A95-68353	p 184	A95-69249	p 193	N95-19809	p 211
A95-67336	p 182	A95-68355	p 184	A95-69302	p 196	N95-19810	p 191
A95-67337	p 183	A95-68356	p 192	A95-69303	p 196	N95-19848	p 204
A95-67342	p 208	A95-68357	p 185	A95-69304	p 196	N95-19855	# p 216
A95-67343	p 208	A95-68358	p 185	A95-69308	p 210	N95-19863	p 188
A95-67345	p 213	A95-68359	p 185	A95-69309	p 195	N95-19864	p 203
A95-67347	p 183	A95-68360	p 185	A95-69310	p 197		
A95-67780	p 213	A95-68361	p 192	A95-69318	p 206		
A95-67806	p 213	A95-68362	p 192	A95-69322	p 188		
A95-67828	p 183	A95-68364	p 203	A95-69324	p 194		
A95-67829	p 183	A95-68365	p 203	A95-69328	p 190		
A95-67830	p 183	A95-68366	p 185	A95-69329	p 190		
A95-68158	p 195	A95-68367	p 203	A95-69332	p 190		
A95-68161	p 195	A95-68368	p 185	A95-69333	p 190		
A95-68162	p 196	A95-68369	p 186	A95-69334	p 190		
A95-68165	p 208	A95-68370	p 193	A95-69431	p 214		
A95-68168	p 208	A95-68371	p 203	A95-69574	p 215		
A95-68172	p 179	A95-68372	p 186	A95-69658	p 218		
A95-68173	p 183	A95-68393	p 210	A95-69717	p 215		
A95-68174	p 184	A95-68394	p 180	A95-69721	p 215		
A95-68180	p 184	A95-68395	p 180	A95-69766	p 215		
A95-68181	p 179	A95-68396	p 180	A95-69803	p 215		
A95-68182	p 196	A95-68398	p 180	A95-69833	p 216		
A95-68185	p 189	A95-68756	p 214	A95-69854	p 205		
A95-68187	p 189	A95-68762	p 214				
A95-68188	p 189	A95-68845	p 214	N95-19517	# p 194		
A95-68191	p 205	A95-69131	p 206	N95-19546	# p 188		
A95-68195	p 184	A95-69136	p 206	N95-19567	* p 210		
A95-68216	p 179	A95-69164	p 206	N95-19576	* p 204		
		A95-69209	p 210	N95-19579	# p 206		
				N95-19582	# p 216		
				N95-19595	# p 197		
				N95-19624	* p 205		
				N95-19651	* p 197		
				N95-19653	# p 197		
				N95-19654	# p 198		
				N95-19655	# p 198		
				N95-19656	# p 198		
				N95-19657	# p 198		
				N95-19658	# p 198		
				N95-19659	# p 198		
				N95-19660	# p 199		
				N95-19661	# p 199		
				N95-19662	# p 199		
				N95-19663	# p 199		
				N95-19664	# p 199		
				N95-19665	# p 199		
				N95-19666	# p 200		
				N95-19668	# p 200		
				N95-19669	# p 200		
				N95-19670	# p 200		
				N95-19671	# p 200		
				N95-19672	* p 200		
				N95-19673	# p 201		
				N95-19675	# p 201		
				N95-19676	# p 201		
				N95-19677	# p 201		

ACCESSION

AVAILABILITY OF CITED PUBLICATIONS

OPEN LITERATURE ENTRIES (A95-60000 Series)

Inquiries and requests should be addressed to NASA Center for AeroSpace Information, 800 Elkridge Landing Road, Linthicum Heights, MD 21090-2934. Orders are also taken by telephone, (301) 621-0390, e-mail, help@sti.nasa.gov, and fax, (301) 621-0134. Please refer to the accession number when request-ing publications.

STAR ENTRIES (N95-10000 Series)

One or more sources from which a document announced in *STAR* is available to the public is ordinarily given on the last line of the citation. The most commonly indicated sources and their acronyms or abbreviations are listed below, and their addresses are listed on page APP-3. If the publication is available from a source other than those listed, the publisher and his address will be displayed on the availability line or in combination with the corporate source line.

Avail: CASI. Sold by the NASA Center for AeroSpace Information. Prices for hard copy (HC) and microfiche (MF) are indicated by a price code following the letters HC or MF in the *STAR* citation. Current values for the price codes are given in the tables on page APP-5.

NOTE ON ORDERING DOCUMENTS: When ordering publications from NASA CASI, use the N accession number or other report number. It is also advisable to cite the title and other bibliographic identification.

Avail: SOD (or GPO). Sold by the Superintendent of Documents, U.S. Government Printing Office, in hard copy.

Avail: BLL (formerly NLL): British Library Lending Division, Boston Spa, Wetherby, Yorkshire, England. Photocopies available from this organization at the price shown. (If none is given, inquiry should be addressed to the BLL.)

Avail: DOE Depository Libraries. Organizations in U.S. cities and abroad that maintain collections of Department of Energy reports, usually in microfiche form, are listed in *Energy Research Abstracts*. Services available from the DOE and its depositories are described in a booklet, *DOE Technical Information Center - Its Functions and Services* (TID-4660), which may be obtained without charge from the DOE Technical Information Center.

Avail: ESDU. Pricing information on specific data, computer programs, and details on Engineering Sciences Data Unit (ESDU) topic categories can be obtained from ESDU International Ltd. Requesters in North America should use the Virginia address while all other requesters should use the London address, both of which are on page APP-3.

Avail: Fachinformationszentrum Karlsruhe. Gesellschaft für wissenschaftlich-technische Information mbH 76344 Eggenstein-Leopoldshafen, Germany.

Avail: HMSO. Publications of Her Majesty's Stationery Office are sold in the U.S. by Pendragon House, Inc. (PHI), Redwood City, CA. The U.S. price (including a service and mailing charge) is given, or a conversion table may be obtained from PHI.

Avail: Issuing Activity, or Corporate Author, or no indication of availability. Inquiries as to the availability of these documents should be addressed to the organization shown in the citation as the corporate author of the document.

Avail: NASA Public Document Rooms. Documents so indicated may be examined at or purchased from the National Aeronautics and Space Administration (JBD-4), Public Documents Room (Room 1H23), Washington, DC 20546-0001, or public document rooms located at NASA installations, and the NASA Pasadena Office at the Jet Propulsion Laboratory.

Avail: NTIS. Sold by the National Technical Information Service. Initially distributed microfiche under the NTIS SRIM (Selected Research in Microfiche) are available. For information concerning this service, consult the NTIS Subscription Section, Springfield, VA 22161.

Avail: Univ. Microfilms. Documents so indicated are dissertations selected from *Dissertation Abstracts* and are sold by University Microfilms as xerographic copy (HC) and microfilm. All requests should cite the author and the Order Number as they appear in the citation.

Avail: US Patent and Trademark Office. Sold by Commissioner of Patents and Trademarks, U.S. Patent and Trademark Office, at the standard price of \$1.50 each, postage free.

Avail: (US Sales Only). These foreign documents are available to users within the United States from the National Technical Information Service (NTIS). They are available to users outside the United States through the International Nuclear Information Service (INIS) representative in their country, or by applying directly to the issuing organization.

Avail: USGS. Originals of many reports from the U.S. Geological Survey, which may contain color illustrations, or otherwise may not have the quality of illustrations preserved in the microfiche or facsimile reproduction, may be examined by the public at the libraries of the USGS field offices whose addresses are listed on page APP-3. The libraries may be queried concerning the availability of specific documents and the possible utilization of local copying services, such as color reproduction.

FEDERAL DEPOSITORY LIBRARY PROGRAM

In order to provide the general public with greater access to U.S. Government publications, Congress established the Federal Depository Library Program under the Government Printing Office (GPO), with 53 regional depositories responsible for permanent retention of material, inter-library loan, and reference services. At least one copy of nearly every NASA and NASA-sponsored publication, either in printed or microfiche format, is received and retained by the 53 regional depositories. A list of the regional GPO libraries, arranged alphabetically by state, appears on the inside back cover of this issue. These libraries are *not* sales outlets. A local library can contact a regional depository to help locate specific reports, or direct contact may be made by an individual.

PUBLIC COLLECTION OF NASA DOCUMENTS

An extensive collection of NASA and NASA-sponsored publications is maintained by the British Library Lending Division, Boston Spa, Wetherby, Yorkshire, England for public access. The British Library Lending Division also has available many of the non-NASA publications cited in *STAR*. European requesters may purchase facsimile copy or microfiche of NASA and NASA-sponsored documents, those identified by both the symbols # and * from ESA — Information Retrieval Service European Space Agency, 8-10 rue Mario-Nikis, 75738 CEDEX 15, France.

STANDING ORDER SUBSCRIPTIONS

NASA SP-7037 supplements and annual index are available from the NASA Center for AeroSpace Information (CASI) on standing order subscription. Standing order subscriptions do not terminate at the end of a year, as do regular subscriptions, but continue indefinitely unless specifically terminated by the subscriber.

ADDRESSES OF ORGANIZATIONS

British Library Lending Division
Boston Spa, Wetherby, Yorkshire
England

Commissioner of Patents and Trademarks
U.S. Patent and Trademark Office
Washington, DC 20231

Department of Energy
Technical Information Center
P.O. Box 62
Oak Ridge, TN 37830

European Space Agency-
Information Retrieval Service ESRIN
Via Galileo Galilei
00044 Frascati (Rome) Italy

Engineering Sciences Data Unit International
P.O. Box 1633
Manassas, VA 22110

Engineering Sciences Data Unit
International, Ltd.
251-259 Regent Street
London, W1R 7AD, England

Fachinformationszentrum Karlsruhe
Gesellschaft für wissenschaftlich-technische
Information mbH
76344 Eggenstein-Leopoldshafen, Germany

Her Majesty's Stationery Office
P.O. Box 569, S.E. 1
London, England

NASA Center for AeroSpace Information
800 Elkridge Landing Road
Linthicum Heights, MD 21090-2934

National Aeronautics and Space Administration
Scientific and Technical Information Office
(JT)
Washington, DC 20546-0001

National Technical Information Service
5285 Port Royal Road
Springfield, VA 22161

Pendragon House, Inc.
899 Broadway Avenue
Redwood City, CA 94063

Superintendent of Documents
U.S. Government Printing Office
Washington, DC 20402

University Microfilms
A Xerox Company
300 North Zeeb Road
Ann Arbor, MI 48106

University Microfilms, Ltd.
Tylers Green
London, England

U.S. Geological Survey Library National Center
MS 950
12201 Sunrise Valley Drive
Reston, VA 22092

U.S. Geological Survey Library
2255 North Gemini Drive
Flagstaff, AZ 86001

U.S. Geological Survey
345 Middlefield Road
Menlo Park, CA 94025

U.S. Geological Survey Library
Box 25046
Denver Federal Center, MS914
Denver, CO 80225

NASA CASI PRICE CODE TABLE

(Effective January 1, 1995)

CASI PRICE CODE	NORTH AMERICAN PRICE	FOREIGN PRICE
A01	\$ 6.00	\$ 12.00
A02	9.00	18.00
A03	17.50	35.00
A04-A05	19.50	39.00
A06-A09	27.00	54.00
A10-A13	36.50	73.00
A14-A17	44.50	89.00
A18-A21	52.00	104.00
A22-A25	61.00	122.00
A99	Call For Price	Call For Price

IMPORTANT NOTICE

For users not registered at the NASA CASI, prepayment is required. Additionally, a shipping and handling fee of \$1.00 per document for delivery within the United States and \$9.00 per document for delivery outside the United States is charged.

For users registered at the NASA CASI, document orders may be invoiced at the end of the month, charged against a deposit account, or paid by check or credit card. NASA CASI accepts American Express, Diners' Club, MasterCard, and VISA credit cards. There are no shipping and handling charges. To register at the NASA CASI, please request a registration form through the NASA Access Help Desk at the address or numbers below.

NASA Center for AeroSpace Information
800 Elkridge Landing Road
Linthicum Heights, MD 21090-2934
Telephone: (301) 621-0390
E-mail: help@sti.nasa.gov
Fax: (301) 621-0134

REPORT DOCUMENT PAGE

1. Report No. NASA SP-7037 (317)	2. Government Accession No.	3. Recipient's Catalog No.	
4. Title and Subtitle Aeronautical Engineering A Continuing Bibliography (Supplement 317)		5. Report Date May 1995	
		6. Performing Organization Code JT	
7. Author(s)		8. Performing Organization Report No.	
		10. Work Unit No.	
9. Performing Organization Name and Address NASA Scientific and Technical Information Office		11. Contract or Grant No.	
		13. Type of Report and Period Covered Special Publication	
12. Sponsoring Agency Name and Address National Aeronautics and Space Administration Washington, DC 20546-0001		14. Sponsoring Agency Code	
		15. Supplementary Notes	
16. Abstract This report lists 224 reports, articles and other documents recently announced in the NASA STI Database.			
17. Key Words (Suggested by Author(s)) Aeronautical Engineering Aeronautics Bibliographies		18. Distribution Statement Unclassified - Unlimited Subject Category - 01	
19. Security Classif. (of this report) Unclassified	20. Security Classif. (of this page) Unclassified	21. No. of Pages 92	22. Price A05/HC

FEDERAL REGIONAL DEPOSITORY LIBRARIES

ALABAMA

AUBURN UNIV. AT MONTGOMERY LIBRARY

Documents Dept.
7300 University Dr.
Montgomery, AL 36117-3596
(205) 244-3650 Fax: (205) 244-0678

UNIV. OF ALABAMA

Amelia Gayle Gorgas Library
Govt. Documents
P.O. Box 870266
Tuscaloosa, AL 35487-0266
(205) 348-6046 Fax: (205) 348-0760

ARIZONA

DEPT. OF LIBRARY, ARCHIVES, AND PUBLIC RECORDS

Research Division
Third Floor, State Capitol
1700 West Washington
Phoenix, AZ 85007
(602) 542-3701 Fax: (602) 542-4400

ARKANSAS

ARKANSAS STATE LIBRARY

State Library Service Section
Documents Service Section
One Capitol Mall
Little Rock, AR 72201-1014
(501) 682-2053 Fax: (501) 682-1529

CALIFORNIA

CALIFORNIA STATE LIBRARY

Govt. Publications Section
P.O. Box 942837 - 914 Capitol Mall
Sacramento, CA 94337-0091
(916) 654-0069 Fax: (916) 654-0241

COLORADO

UNIV. OF COLORADO - BOULDER

Libraries - Govt. Publications
Campus Box 184
Boulder, CO 80309-0184
(303) 492-8834 Fax: (303) 492-1881

DENVER PUBLIC LIBRARY

Govt. Publications Dept. BSG
1357 Broadway
Denver, CO 80203-2165
(303) 640-8846 Fax: (303) 640-8817

CONNECTICUT

CONNECTICUT STATE LIBRARY

231 Capitol Avenue
Hartford, CT 06106
(203) 566-4971 Fax: (203) 566-3322

FLORIDA

UNIV. OF FLORIDA LIBRARIES

Documents Dept.
240 Library West
Gainesville, FL 32611-2048
(904) 392-0366 Fax: (904) 392-7251

GEORGIA

UNIV. OF GEORGIA LIBRARIES

Govt. Documents Dept.
Jackson Street
Athens, GA 30602-1645
(706) 542-8949 Fax: (706) 542-4144

HAWAII

UNIV. OF HAWAII

Hamilton Library
Govt. Documents Collection
2550 The Mall
Honolulu, HI 96822
(808) 948-8230 Fax: (808) 956-5968

IDAHO

UNIV. OF IDAHO LIBRARY

Documents Section
Rayburn Street
Moscow, ID 83844-2353
(208) 885-6344 Fax: (208) 885-6817

ILLINOIS

ILLINOIS STATE LIBRARY

Federal Documents Dept.
300 South Second Street
Springfield, IL 62701-1796
(217) 782-7596 Fax: (217) 782-6437

INDIANA

INDIANA STATE LIBRARY

Serials/Documents Section
140 North Senate Avenue
Indianapolis, IN 46204-2296
(317) 232-3679 Fax: (317) 232-3728

IOWA

UNIV. OF IOWA LIBRARIES

Govt. Publications
Washington & Madison Streets
Iowa City, IA 52242-1166
(319) 335-5926 Fax: (319) 335-5900

KANSAS

UNIV. OF KANSAS

Govt. Documents & Maps Library
6001 Malott Hall
Lawrence, KS 66045-2800
(913) 864-4660 Fax: (913) 864-3855

KENTUCKY

UNIV. OF KENTUCKY

King Library South
Govt. Publications/Maps Dept.
Patterson Drive
Lexington, KY 40506-0039
(606) 257-3139 Fax: (606) 257-3139

LOUISIANA

LOUISIANA STATE UNIV.

Middleton Library
Govt. Documents Dept.
Baton Rouge, LA 70803-3312
(504) 388-2570 Fax: (504) 388-6992

LOUISIANA TECHNICAL UNIV.

Prescott Memorial Library
Govt. Documents Dept.
Ruston, LA 71272-0046
(318) 257-4962 Fax: (318) 257-2447

MAINE

UNIV. OF MAINE

Raymond H. Fogler Library
Govt. Documents Dept.
Orono, ME 04469-5729
(207) 581-1673 Fax: (207) 581-1653

MARYLAND

UNIV. OF MARYLAND - COLLEGE PARK

McKeldin Library
Govt. Documents/Maps Unit
College Park, MD 20742
(301) 405-9165 Fax: (301) 314-9416

MASSACHUSETTS

BOSTON PUBLIC LIBRARY

Govt. Documents
666 Boylston Street
Boston, MA 02117-0286
(617) 536-5400, ext. 226
Fax: (617) 536-7758

MICHIGAN

DETROIT PUBLIC LIBRARY

5201 Woodward Avenue
Detroit, MI 48202-4093
(313) 833-1025 Fax: (313) 833-0156

LIBRARY OF MICHIGAN

Govt. Documents Unit
P.O. Box 30007
717 West Allegan Street
Lansing, MI 48909
(517) 373-1300 Fax: (517) 373-3381

MINNESOTA

UNIV. OF MINNESOTA

Govt. Publications
409 Wilson Library
309 19th Avenue South
Minneapolis, MN 55455
(612) 624-5073 Fax: (612) 626-9353

MISSISSIPPI

UNIV. OF MISSISSIPPI

J.D. Williams Library
106 Old Gym Bldg.
University, MS 38677
(601) 232-5857 Fax: (601) 232-7465

MISSOURI

UNIV. OF MISSOURI - COLUMBIA

106B Ellis Library
Govt. Documents Sect.
Columbia, MO 65201-5149
(314) 882-6733 Fax: (314) 882-8044

MONTANA

UNIV. OF MONTANA

Mansfield Library
Documents Division
Missoula, MT 59812-1195
(406) 243-6700 Fax: (406) 243-2060

NEBRASKA

UNIV. OF NEBRASKA - LINCOLN

D.L. Love Memorial Library
Lincoln, NE 68588-0410
(402) 472-2562 Fax: (402) 472-5131

NEVADA

THE UNIV. OF NEVADA LIBRARIES

Business and Govt. Information
Center
Reno, NV 89557-0044
(702) 784-6579 Fax: (702) 784-1751

NEW JERSEY

NEWARK PUBLIC LIBRARY

Science Div. - Public Access
P.O. Box 630
Five Washington Street
Newark, NJ 07101-7812
(201) 733-7782 Fax: (201) 733-5648

NEW MEXICO

UNIV. OF NEW MEXICO

General Library
Govt. Information Dept.
Albuquerque, NM 87131-1466
(505) 277-5441 Fax: (505) 277-6019

NEW MEXICO STATE LIBRARY

325 Don Gaspar Avenue
Santa Fe, NM 87503
(505) 827-3824 Fax: (505) 827-3888

NEW YORK

NEW YORK STATE LIBRARY

Cultural Education Center
Documents/Gift & Exchange Section
Empire State Plaza
Albany, NY 12230-0001
(518) 474-5355 Fax: (518) 474-5786

NORTH CAROLINA

UNIV. OF NORTH CAROLINA - CHAPEL HILL

Walter Royal Davis Library
CB 3912, Reference Dept.
Chapel Hill, NC 27514-8890
(919) 962-1151 Fax: (919) 962-4451

NORTH DAKOTA

NORTH DAKOTA STATE UNIV. LIB.

Documents
P.O. Box 5599
Fargo, ND 58105-5599
(701) 237-8886 Fax: (701) 237-7138

UNIV. OF NORTH DAKOTA

Chester Fritz Library
University Station
P.O. Box 9000 - Centennial and
University Avenue
Grand Forks, ND 58202-9000
(701) 777-4632 Fax: (701) 777-3319

OHIO

STATE LIBRARY OF OHIO

Documents Dept.
65 South Front Street
Columbus, OH 43215-4163
(614) 644-7051 Fax: (614) 752-9178

OKLAHOMA

OKLAHOMA DEPT. OF LIBRARIES

U.S. Govt. Information Division
200 Northeast 18th Street
Oklahoma City, OK 73105-3298
(405) 521-2502, ext. 253
Fax: (405) 525-7804

OKLAHOMA STATE UNIV.

Edmon Low Library
Stillwater, OK 74078-0375
(405) 744-6546 Fax: (405) 744-5183

OREGON

PORTLAND STATE UNIV.

Branford P. Millar Library
934 Southwest Harrison
Portland, OR 97207-1151
(503) 725-4123 Fax: (503) 725-4524

PENNSYLVANIA

STATE LIBRARY OF PENN.

Govt. Publications Section
116 Walnut & Commonwealth Ave.
Harrisburg, PA 17105-1601
(717) 787-3752 Fax: (717) 783-2070

SOUTH CAROLINA

CLEMSON UNIV.

Robert Muldrow Cooper Library
Public Documents Unit
P.O. Box 343001
Clemson, SC 29634-3001
(803) 656-5174 Fax: (803) 656-3025

UNIV. OF SOUTH CAROLINA

Thomas Cooper Library
Green and Sumter Streets
Columbia, SC 29208
(803) 777-4841 Fax: (803) 777-9503

TENNESSEE

UNIV. OF MEMPHIS LIBRARIES

Govt. Publications Dept.
Memphis, TN 38152-0001
(901) 678-2206 Fax: (901) 678-2511

TEXAS

TEXAS STATE LIBRARY

United States Documents
P.O. Box 12927 - 1201 Brazos
Austin, TX 78701-0001
(512) 463-5455 Fax: (512) 463-5436

TEXAS TECH. UNIV. LIBRARIES

Documents Dept.
Lubbock, TX 79409-0002
(806) 742-2282 Fax: (806) 742-1920

UTAH

UTAH STATE UNIV.

Merrill Library Documents Dept.
Logan, UT 84322-3000
(801) 797-2678 Fax: (801) 797-2677

VIRGINIA

UNIV. OF VIRGINIA

Alderman Library
Govt. Documents
University Ave. & McCormick Rd.
Charlottesville, VA 22903-2498
(804) 824-3133 Fax: (804) 924-4337

WASHINGTON

WASHINGTON STATE LIBRARY

Govt. Publications
P.O. Box 42478
16th and Water Streets
Olympia, WA 98504-2478
(206) 753-4027 Fax: (206) 586-7575

WEST VIRGINIA

WEST VIRGINIA UNIV. LIBRARY

Govt. Documents Section
P.O. Box 6069 - 1549 University Ave.
Morgantown, WV 26506-6069
(304) 293-3051 Fax: (304) 293-6638

WISCONSIN

ST. HIST. SOC. OF WISCONSIN LIBRARY

Govt. Publication Section
816 State Street
Madison, WI 53706
(608) 264-6525 Fax: (608) 264-6520

MILWAUKEE PUBLIC LIBRARY

Documents Division
814 West Wisconsin Avenue
Milwaukee, WI 53233
(414) 286-3073 Fax: (414) 286-8074

National Aeronautics and
Space Administration
Code JTT
Washington, DC 20546-0001

7